NASA/CP-2006-214549

Proceedings of the 2006

NASA Laboratory Astrophysics Workshop

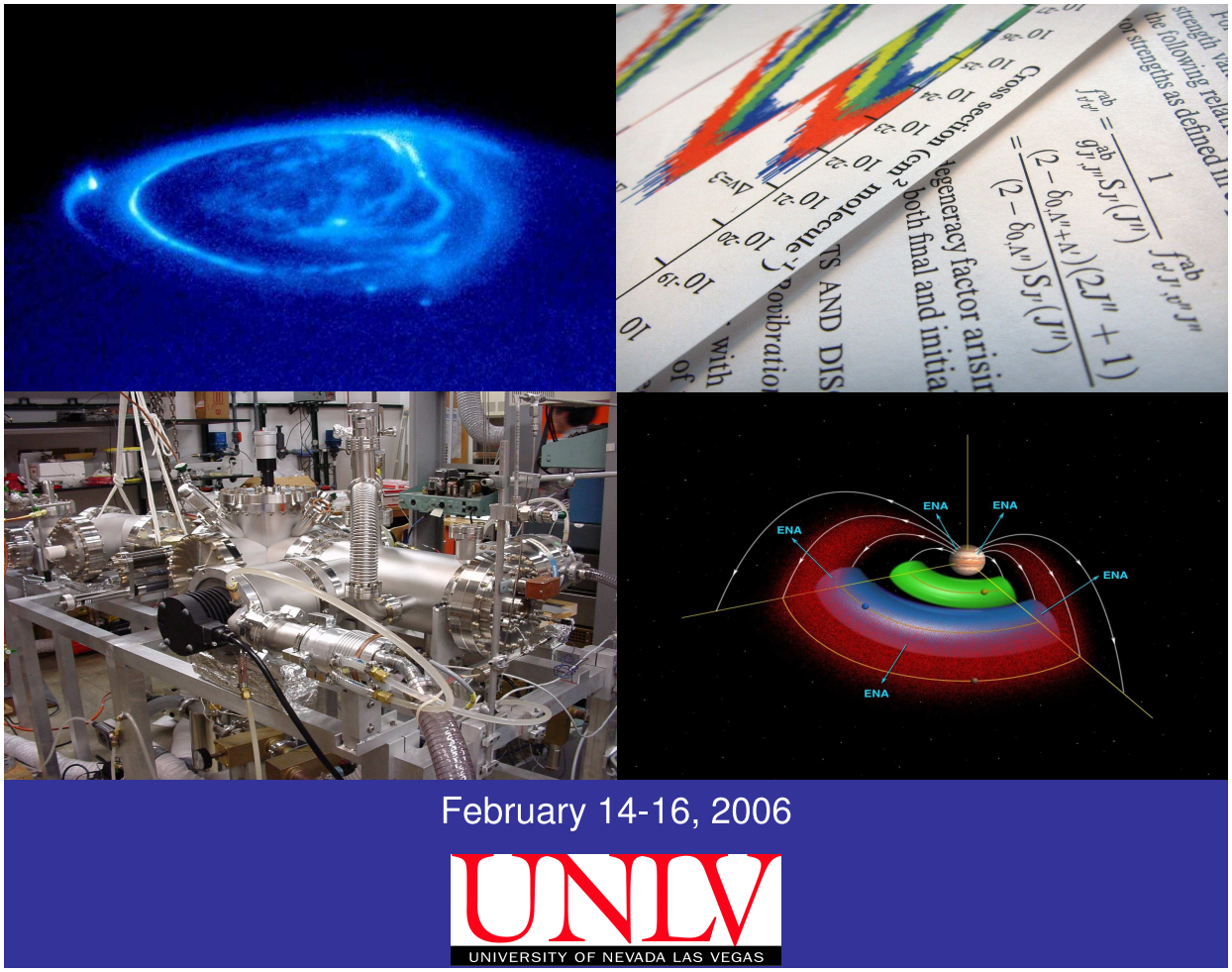

February 14-16, 2006

UNLV
UNIVERSITY OF NEVADA LAS VEGAS

Sponsored by:

National Aeronautics and Space
Administration, Washington, DC 20546-0001

University of Nevada, Las Vegas
Las Vegas, NV 89154-4002

Edited and Coordinated by:

Philippe F. Weck & Victor H. S. Kwong
University of Nevada, Las Vegas

Farid Salama
NASA Ames Research Center

August 2006

The NASA STI Program Office... in Profile

Since its founding, NASA has been dedicated to the advancement of aeronautics and space science. The NASA Scientific and Technical Information (STI) Program Office plays a key part in helping NASA maintain this important role.

The NASA STI Program Office is operated by Langley Research Center, the lead center for NASA's scientific and technical information. The NASA STI Program Office provides access to the NASA STI Database, the largest collection of aeronautical and space science STI in the world. The Program Office is also NASA's institutional mechanism for disseminating the results of its research and development activities. These results are published by NASA in the NASA STI Report Series, which includes the following report types:

- TECHNICAL PUBLICATION. Reports of completed research or a major significant phase of research that present the results of NASA programs and include extensive data or theoretical analysis. Includes compilations of significant scientific and technical data and information deemed to be of continuing reference value. NASA counterpart of peer-reviewed formal professional papers, but having less stringent limitations on manuscript length and extent of graphic presentations.
- TECHNICAL MEMORANDUM. Scientific and technical findings that are preliminary or of specialized interest, e.g., quick release reports, working papers, and bibliographies that contain minimal annotation. Does not contain extensive analysis.
- CONTRACTOR REPORT. Scientific and technical findings by NASA-sponsored contractors and grantees.
- CONFERENCE PUBLICATION. Collected papers from scientific and technical conferences, symposia, seminars, or other meetings sponsored or co-sponsored by NASA.
- SPECIAL PUBLICATION. Scientific, technical, or historical information from NASA programs, projects, and missions, often concerned with subjects having substantial public interest.
- TECHNICAL TRANSLATION. English-language translations of foreign scientific and technical material pertinent to NASA's mission.

Specialized services that complement the STI Program Office's diverse offerings include creating custom thesauri, building customized databases, organizing and publishing research results... even providing videos.

For more information about the NASA STI Program Office, see the following:

- Access the NASA STI Program Home Page at `http://www.sti.nasa.gov`
- E-mail your question via the Internet to help@sti.nasa.gov
- Fax your question to the NASA STI Help Desk at (301) 621-0134
- Telephone the NASA STI Help Desk at (301) 621-0390
- Write to:
  NASA STI Help Desk
  NASA Center for AeroSpace Information
  7121 Standard Drive
  Hanover, MD 21076-1320

Image Credit:
Top left: NASA and the Hubble Heritage Team (STScI/AURA).
Bottom right: NASA/JPL/Johns Hopkins University Applied Physics Laboratory.

NASA/CP-2006-214549

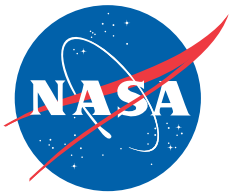

Proceedings of the 2006

NASA Laboratory Astrophysics Workshop

February 14-16, 2006
University of Nevada, Las Vegas
Las Vegas, NV, U.S.A.

Sponsored by:

National Aeronautics and Space
Administration, Washington, DC 20546-0001

University of Nevada, Las Vegas
Las Vegas, NV 89154-4002

Edited and Coordinated by:

Philippe F. Weck & Victor H. S. Kwong
University of Nevada, Las Vegas

Farid Salama
NASA Ames Research Center

August 2006

Acknowledgements

The editors wish to express their appreciation to all the members of the 2006 NASA Laboratory Astrophysics Workshop for their active participation; and especially to the members of the Scientific Organizing Committee and the Local Organizing Committee for their dedication, professional skills, and timeless efforts in making this event a success. The efforts of three people in particular are gratefully acknowledged: John Kilburg for constructing and maintaining a very clear and informative web site, Bill O'Donnell for the smooth operation of the presentations during the meeting, and Cara Loomis for the essential logistic support for the participants in the Workshop. We are also grateful to the support from Carol Harter, President of the University of Nevada, Las Vegas, Richard Lee, Vice Provost on Educational Outreach, Mark Rudin, Associate Vice President on Research Services, and Ron Yasbin, Dean of Sciences.

The editors wish to acknowledge Ames Reproduction Department, code JGS, Ames Research Center, Moffett Field, CA for printing services.

This report is available from:

NASA Center for AeroSpace Information
7121 Standard Drive
Hanover, MD 21076-1320
301-621-0390

National Technical Information Service
5285 Port Royal Road
Springfield, VA 22161
703-605-6000

Complete information on the Workshop and all related documents can also be found at `http://www.physics.unlv.edu/labastro/`. The papers presented at the Workshop will also be published by the NASA Astrophysical Data System at `http://adsabs.harvard.edu/`.

PREFACE

This report is a collection of papers presented at the 2006 NASA Workshop on Laboratory Astrophysics held in the University of Nevada, Las Vegas (UNLV) from February 14 to 16, 2006.

This workshop brings together producers and users of laboratory astrophysics data so that they can understand each other's needs and limitations in the context of the needs for NASA's missions.

The last NASA-sponsored workshop was held in 2002 at Ames Research Center. Recent related meetings include the Topical Session at the AAS meeting and the European workshop at Pillnitz, Germany, both of which were held in June 2005. The former showcased the importance of laboratory astrophysics to the community at large, while the European workshop highlighted a multi-laboratory approach to providing the needed data.

The 2006 NASA Workshop on Laboratory Astrophysics, sponsored by the NASA Astrophysics Division, focused on the current status of the field and its relevance to NASA. This workshop attracted 105 participants and 82 papers of which 19 were invited. A White Paper identifying the key issues in laboratory astrophysics during the break-out sessions was prepared by the Scientific Organizing Committee, and has been forwarded to the Universe Working Group (UWG) at NASA Headquarters. This White Paper, which represented the collective inputs and opinions from experts and stakeholders in the field of astrophysics, should serve as the working document for the future development of NASA's R&A program in laboratory astrophysics.

Philippe F. Weck
Victor H. S. Kwong
Farid Salama

August 2006

TABLE OF CONTENTS

MISSION STATEMENT

Target Audience

Laboratory Astrophysicists and Astrochemists (experimentalists, theorists, and modelers), Astronomers and Astrophysicists (observers, theorists, and modelers), Space Mission Scientists, Instrument Developers and other interested researchers.

Background

The *NASA Universe Working Group* (UWG) has requested that the laboratory astrophysics community put together a White Paper in time for the UWG's next meeting in April 2006. The Laboratory Astrophysics Workshop (LAW) 2006 has been designed to produce the requested report.

Goals and Specific Objectives

The White Paper will be the result of bringing together producers and users of laboratory astrophysics data so that they can understand each other's needs and limitations in the context of NASA's mission needs. Increasing the collaboration and cross fertilization of ideas is important to ensuring that the priorities for Laboratory Astrophysics are determined by NASA's astronomy and astrophysics goals, and that the products of Laboratory Astrophysics feed back to the user community in a timely way.

The desired White Paper should specifically contain science requirement flow down charts that begin with the major science goals as defined in the *2006 NASA Strategic Plan*. The White Paper should also provide details on the critical laboratory astrophysics data requirements which will have to be met, if the desired science results are actually to be achieved. The best means of distributing this critical information to the astronomical community, such as through extensive databases, will be discussed.

Another important item in the White Paper should be a tabulation of recent significant astronomical results where the input from laboratory astrophysics was of critical importance (although the laboratory astrophysics contribution may not have received the credit due it, as is so often the case). The current funding environment, including the very difficult years ahead, will require a certain amount of salesmanship.

There should additionally be a detailed discussion of the specific laboratory astrophysics efforts that will need to be undertaken in direct support of not just past and current missions and programs, but also those on the near horizon. These include specifically Herschel, Stratospheric Observatory for Infrared Astronomy (SOFIA), James Webb Space Telescope (JWST), Constellation-X, and Atacama Large Millimeter Array (ALMA) (of primary concern to NSF).

Lastly, with an eye on the future, a discussion should also be given as to what can be done in order to help foster the creation of new faculty positions and the education and

production of future generations of laboratory astrophysics scientists. See:

- *Letter on this topic from the SOC to the NSF AST Senior Review*
- *AST Senior Review*

Laboratory astrophysics is the foundation for much of astrophysics, and yet its infrastructure may be fragile in the face of declining funds. Investments are needed in order to insure the future vitality and scientific success for astrophysical research.

Weblinks

NASA Universe Working Group (UWG):
`http://www.physics.unlv.edu/labastro/nasa_uwg_memo_sept2005e.pdf`

2006 NASA Strategic Plan:
`http://www.nasa.gov/about/budget`

SEU 2003 Roadmap:
`http://universe.nasa.gov/be/preface.html`

2003 Origins Roadmap:
`http://origins.jpl.nasa.gov/library/roadmap03`

2006 NASA Laboratory Astrophysics Workshop:
`http://www.physics.unlv.edu/labastro`

2002 NASA Laboratory Astrophysics Workshop:
`http://www.astrochemistry.org/nasalaw.html`

1998 NASA Laboratory Astrophysics Workshop:
`http://cfa-www.harvard.edu/amdata/ampdata/law/index.html`

2002 Laboratory Astrophysics White Paper:
`http://www.astrochemistry.org/nasalaw.html`

Letter on this topic from the SOC to the NSF AST Senior Review:
`http://www.physics.unlv.edu/labastro/astseniorreview.html`

AST Senior Review:
`http://www.nsf.gov/mps/ast/ast_senior_review.jsp`

ORGANIZING COMMITTEE

Science Organizing Committee (SOC)

Nancy Brickhouse (Harvard-Smithsonian Center for Astrophysics)
Steve Federman (Chair) (University of Toledo)
Victor Kwong (LOC Chair) (University of Nevada, Las Vegas)
Farid Salama (NASA Ames Research Center)
Daniel Savin (Columbia Astrophysics Laboratory)
Phillip Stancil (University of Georgia)
Joe Weingartner (George Mason University)
Lucy Ziurys (University of Arizona)

Ex-officio SOC Members

Hashima Hasan (NASA)
Pamela Marcum (NASA)
Wilt Sanders (NASA)
Philippe Crane (NASA)
Adolf Witt (University of Toledo & UWG Laboratory Astrophysics)

Local Organizing Committee (LOC)

John Kilburg
Victor Kwong (Chair)
Stephen Lepp
Cara Loomis
Bill O'Donnell
David Shelton
Philippe Weck
Bernard Zygelman

LABORATORY ASTROPHYSICS WHITE PAPER

(BASED ON THE 2006 NASA LABORATORY ASTROPHYSICS WORKSHOP AT THE UNIVERSITY OF NEVADA, LAS VEGAS, 14-16 FEBRUARY, 2006)

Report prepared by the Scientific Organizing Committee:

Nancy Brickhouse, Harvard-Smithsonian Center for Astrophysics,
<bhouse@head.cfa.harvard.edu>
Steve Federman, University of Toledo, <steven.federman@utoledo.edu>, Chair
Victor Kwong, University of Nevada, Las Vegas, <vhs@physics.unlv.edu>, Chair of LOC
Farid Salama, NASA Ames Research Center, <Farid.Salama@nasa.gov>
Daniel Savin, Columbia University, <savin@astro.columbia.edu>
Phillip Stancil, University of Georgia, <stancil@physast.uga.edu>
Joe Weingartner, George Mason University, <joe@physics.gmu.edu>
Lucy Ziurys, University of Arizona, <lziurys@as.arizona.edu>

Reviewers: Ara Chutjian (Jet Propulsion Laboratory), Gary Ferland (University of Kentucky), Steve Manson (Georgia State University), Peter Smith (Harvard-Smithsonian Center for Astrophysics)

1. Preface

Laboratory astrophysics and complementary theoretical calculations are the foundations of astronomical and planetary research and will remain so for many generations to come. From the level of scientific conception to that of the scientific return, it is our understanding of the underlying processes that allows us to address fundamental questions regarding the origins and evolution of galaxies, stars, planetary systems, and life in the cosmos. In this regard, laboratory astrophysics is much like detector and instrument development at NASA and NSF; these efforts are necessary for the astronomical research being funded by the agencies.

The NASA Laboratory Astrophysics Workshop met at the University of Nevada, Las Vegas (UNLV) from 14-16 February, 2006 to identify the current laboratory data needed to support existing and future NASA missions and programs in the Astrophysics Division of the Science Mission Directorate (SMD). Here we refer to both laboratory and theoretical work as laboratory astrophysics unless a distinction is necessary. The format for the Workshop involved invited talks by users of laboratory data, shorter contributed talks and poster presentations by both users and providers that highlighted exciting developments in laboratory astrophysics, and breakout sessions where users and providers discussed each others' needs and limitations. We also note that the members of the Scientific Organizing Committee are users as well as providers of laboratory data. As in previous workshops, the focus was on atomic, molecular, and solid state physics.

The NASA Universe Working Group (UWG) within the SMD requested a White Paper be drawn up outlining the conclusions of the Workshop for presentation at the next UWG meeting in April 2006. Specifically, the request included

1. addressing the major science goals as defined in the 2006 NASA Strategic Plan and then providing details on the critical laboratory astrophysics data requirements that will have to be met, if the desired science results are actually to be achieved,
2. reporting of recent significant astronomical results where the input from laboratory astrophysics was of critical importance, and
3. discussing in detail the specific laboratory astrophysics efforts that will need to be undertaken in direct support of missions and programs that are on the near horizon, specifically *Herschel*, *SOFIA*, *JWST*, *Hubble* servicing, and ALMA (the latter of primary concern to NSF).

These points are addressed in the subsequent sections of this requested White Paper, which also contains a set of recommendations drawn from a consensus view of the Workshop participants.

A number of points figured prominently at the UNLV Workshop, points that were raised in the White Paper from the 2002 NASA Ames Laboratory Astrophysics Workshop. These include: "Laboratory facilities are aging and major funding is required to replace them with modern, state-of-the-art equipment" and "The training of new scientists in laboratory astrophysics is crucial for the future of the field, but the low level of funding is making it more difficult to attract students..."

In the last four years the situation has become even more dire. Laboratory astrophysics has reached a point where it is ceasing to be a viable, productive field. This should be of great concern to NASA and NSF. Without laboratory astrophysics, the scientific return from current and future NASA missions and NSF ground-based observations will diminish significantly. Without laboratory astrophysics the future progress of astronomy and astrophysics is imperiled. Recommendations are provided below that address this issue in a time of limited resources, especially funding.

2. General Findings

- A study of the importance of laboratory astrophysics for all of astronomy under the auspices of the National Research Council and involving NASA, NSF, DOE, and DoC/NIST is long overdue.
- There is a strong requirement for a rich, vibrant laboratory astrophysics community that can respond on a "rapid" time scale to ongoing observations over a wide range in wavelengths and physical conditions.
- There is an urgent need to maintain the infrastructure, in terms of both personnel and facilities.

- Databases of atomic, molecular, and solid state parameters that are complete (e.g., wavelength lists for all stages of ionization) and critically evaluated are a necessity.
- In a number of areas, theory and experiment are converging so that the astrophysics, which depends on such data, is more secure.
- There is significant overlap between data needed to study phenomena beyond the Solar System and within it.
- As missions probe earlier moments in the history of the Universe, phenomena associated with high energies (short wavelengths) are observed with missions having instrumentation designed for low energies (long wavelengths).
- The data requirements for advances in astrophysics from NASA missions are more often than not the same requirements for DOE-sponsored research on plasmas and NSF-sponsored astronomical research; the need for critical evaluations of available data highlights the close connection to DoC/NIST.

3. Recent Successes

Astrophysical discoveries are propelled forward in part by experimental and theoretical advances in atomic, molecular, and solid state physics. Presented below are selected examples of significant astrophysical results that arose from recent laboratory and theoretical efforts on phenomena involving atoms, molecules, and solids. When possible, we also highlight future avenues for the research.

- Abundance determinations for old metal-poor halo stars using the *Hubble Space Telescope* and ground-based observations suggest that two different rapid neutron-capture processes may exist for nucleosynthesis beyond the iron peak (Cowan et al. 2005, ApJ, 627, 238). This insight is the result of new laboratory oscillator strengths for high Z elements (e.g., Ivarsson et al. 2003, A&A, 409, 1141). The new data have also allowed for improvements in radioactive dating using Th/Eu ratios and are yielding reasonable cosmochronometric age estimates for halo stars (Sneden et al. 2003, ApJ, 591, 936).
- X-ray emission from comets is due to charge exchange between solar wind ions and neutrals in cometary comae (e.g., Cravens 2002, Science, 296, 1042; Beiersdorfer et al. 2003, Science, 300, 1558). It is now also predicted that up to half of the diffuse soft X-ray background may not be extra-solar but may actually be due to solar wind charge exchange with geocoronal and interstellar neutrals (Robertson & Cravens 2003, J. Geophys. Res., 108, 8031). These findings suggest that charge exchange involving higher principal quantum numbers and emission at UV/visible wavelengths and involving simple molecules like H2O may be important as well (Greenwood et al. 2001, Phys. Rev., A 63, 062707).
- In the well-studied AGN NGC 3783, the warm absorber density and location have been found, respectively, to be smaller and closer to the central black hole than expected (Krongold et al. 2005, ApJ, 622, 842). This discovery is a major success of theoretical atomic physics, which identified the numerous unknown absorption lines in the high

resolution *Chandra* and XMM-*Newton* spectra of warm absorbers. These lines were shown to be inner-shell absorption transitions for the low charge states of Fe and were also used as a powerful new plasma diagnostic (Behar et al. 2001, ApJ, 563, 497).

- Measuring the atmospheric temperature of the extra-solar planets TrES-1 (Charbonneau et al. 2005, ApJ, 626, 523) and HD 209458b (Deming et al. 2005, Nature, 434, 740) with the *Spitzer Space Telescope* is partly a success of stellar atmosphere spectral synthesis and laboratory studies of molecular opacities. Transit searches for extra-solar planets also use synthetic stellar spectra as templates against which to correlate measured radial velocities (Konacki et al. 2003, Nature, 421, 507), a method which is at the core of NASA's future *Kepler Mission*. For these and other cases, the increasing completeness of the calculated line lists and opacities (Bautista 2004, A&A, 420, 763) has been a critical factor.
- Using the *Kuiper Airborne Observatory (KAO)*, important molecules have been detected in the interstellar medium (ISM) whose emission had been inaccessible by ground-based astronomy. Of particular note are H_2D^+, a cornerstone species in the ion-molecule theory of interstellar chemistry, HCl, a fundamental hydride, and H_3O^+, a direct tracer of the water abundance (e.g., Zmuidzinas et al. 1995, ASP Conf. Ser., 73, 555; Timmermann et al. 1996, ApJ, 463, L109), as well as the pure rotational lines of NH_3, OH, and CH (e.g., Stacey et al. 1987, ApJ, 313, 859). The *KAO* has also been invaluable in detecting ro-vibrational transitions of heavier species such as C_3 in molecular clouds (e.g., Giesen et al. 2001, ApJ, 551, L181). Studies of these species have led to breakthroughs in our understanding of the molecular component of the interstellar medium. These discoveries were only made possible by preceding high resolution, laboratory spectroscopy (e.g., Brown et al. 1993, ApJ, 414, L125; Harrison et al. 2006, ApJ, 637, 1143). Such laboratory measurements are needed for the sensitive spectral-line surveys proposed for *Herschel*.
- High rotational lines of CO (up to $J = 45$) have been discovered in the Orion-KL Nebula using the *KAO* and the *Infrared Space Observatory* (Gonzalez-Alfonso et al. 2002, A&A, 386, 1074). These spectral lines gave the first early glimpses of the process of high mass star formation with associated shocks and high velocity outflows (e.g., Hollenbach et al. 1995, ASP Conf. Ser., 73, 243; Ceccarelli et al. 1996, ApJ, 471, 400). These studies would not have been possible without previous high resolution laboratory spectroscopic work; the understanding of the dynamics in this environment rests on past investigations of collisional excitation. This and the preceding example reveal the exciting results anticipated at sub- millimeter wavelengths with *SOFIA* and *Herschel* and from new approaches to molecular synthesis on grains in shock-heated regions (Madzunkov et al. 2006, Phys. Rev., A 73, 020901(R)).
- *FUSE* observed UV absorption of H_2 and HD in the ISM from a range of excited rotational levels (Snow et al. 2000, ApJ, 538, L65; Ferlet et al. 2000, ApJ, 538, L69), providing new insights into the physics and chemistry of translucent clouds and a tool to evaluate the ISM deuterium abundance. These observations and their interpretations

were made possible by laboratory studies of the electronic transitions and processes relevant to the formation of H_2.

- Aromatic infrared bands (AIBs), commonly dubbed "PAH bands", are now routinely observed with the *Spitzer Space Telescope* and used to probe dust in extragalactic environments (Hogg et al. 2005, ApJ, 624, 162; Wu et al. 2006, ApJ, 639, 157) and to measure redshift (Yan et al. 2005, ApJ, 628, 604; Weedman et al. 2006, ApJ, 638, 613). Such emission measured in a recent *Spitzer* survey of elliptical galaxies indicates that the carriers, attributed to polycyclic aromatic hydrocarbons (PAHs) and their derivatives, are a probe of recent merger activity in these galaxies (Kaneda et al. 2005, ApJ, 632, L83). It certainly looks like the AIB emission is correlated with star formation (Lutz et al. 2005, ApJ, 625, L83; Wu et al. 2005, ApJ, 632, L79). This progress has only been possible thanks to laboratory emission and absorption spectra of PAH-type species, including ions. Furthermore, the signature of individual PAH-like molecules can now be sought in astronomical spectra at UV and visible wavelengths, making it possible, for the first time, to detect specific aromatic compounds in space.
- The analysis of the first cometary and interstellar sample return from the Stardust mission will provide key information on grain formation and processing in space. Observations with *ISO* and *Spitzer* have revealed the presence of specific minerals (e.g., crystalline silicates) in a variety of Galactic environments, including outflows from evolved stars and protoplanetary disks (Waelkens et al. 1996, A&A, 315, L245; Waters et al. 1996, A&A, 315, L361). This work is critical to understanding dust processing during its lifetime, and is only possible thanks to laboratory measurements of the infrared spectra for candidate grain materials (Begemann et al. 1994, ApJ, 423, L71; Jäger et al. 2003, J. Quant. Spectr. Rad. Transf., 79-80, 765).
- Studies of dust and ice provide a clear connection between astronomy within and beyond the solar system (Strazzulla et al. 2005, Icarus 174, 31). Planetary surface temperatures are derived from ice measurements in the NIR (Grundy et al. 2002, Icarus, 155, 486), while planetary atmospheres (Europa, Ganymede,...) are explained by laboratory studies of ices (Hansen et al. 2005, Icarus, 176, 305).

While examples listed above demonstrate the rich astrophysics enabled by laboratory astrophysics, they are by no means the only notable advances. We are limited here only by the constraints of space.

4. Current and Future Needs

We now turn our attention to the needs to reach the next level of understanding of the Universe, near and far. The discussion is guided by the 2006 NASA Strategic Plan. Of most relevance to laboratory astrophysics are items in Strategic Goal 3, sub-goals 3B, 3C, and 3D. Particular areas of research include (1) the origin, structure, evolution, and destiny of the Universe, (2) the potential for life elsewhere, and (3) the nature of solar activity and its effect on the solar system.

4.1 Atoms and Ions in Astrophysics

Astrophysics needs vast quantities of atomic data. Data are needed for all the cosmically abundant elements as well as for the rarer elements in order to tease out the chemical evolution of the Universe. We discuss in general the atomic data needs of the astrophysics community and give some specific, but not exclusive, examples.

Analyzing and modeling cosmic spectra begin with identifying the observed lines which may be seen in emission or absorption. This requires **accurate and complete wavelengths across the electromagnetic spectrum** for spectral line identification, wind velocity determinations, and investigating variations in the fine structure constant over the age of the Universe. The need includes bandpasses that are commonly considered the realm of ground-based observations. For example, the *James Webb Space Telescope* will observe many objects whose ultraviolet and visible lines have been redshifted into the IR.

The next step toward understanding the properties of an observed cosmic source depends on accurate knowledge of the underlying atomic processes producing the observed lines. **Oscillator strengths and transition probabilities** are critical to a wide variety of temperature and abundance studies from infrared to X-ray wavelengths. Many existing data for the heavier elements are still notoriously unreliable. These current limitations on the atomic data available for mid-Z elements make it difficult to determine the nature of the r-process. For example, non-LTE spectral analysis of the prototypical super-soft source Cal 83 provides stellar parameters indicating a massive hot white dwarf. This is of great interest as such sources are the likely progenitors of Type Ia supernovae. But a detailed chemical analysis of Cal 83 is not possible with currently available data in the soft X-ray domain. **Inner shell photoabsorption and fluorescence yields** are needed for studies of X-ray photoionized plasmas such as AGN and X-ray binary winds, and for finding the hot interstellar and intergalactic gas. *Chandra* searches for the "missing baryons" in the warm hot intergalactic medium (WHIM) have been enabled by new laboratory studies of inner-shell transitions; however, many line identification issues remain. Rate coefficients for **electron impact excitation** approaching 10% accuracy are necessary for the most important line ratio diagnostics yielding temperature, optical depth, density, and abundance. Recent theoretical and laboratory studies of the important ion Fe XVII suggest for the first time that this is possible, confirming the quantitative analysis of resonance scattering in the elliptical galaxy NGC 4636 and suggesting that conventional chemical-enrichment models for ellipticals are not correct. **Proton impact excitation** is important because ions in hot post-shock material decouple from radiatively cooling electrons and may remain hot enough to produce line emission through collisional impact, as seen in SN 1006. Atomic data for these processes also appear to be important for our understanding of colliding winds in hot star binaries. There is a crucial need for **state specific cross sections for dielectronic and radiative recombination and for charge exchange**. Complete spectral models require accurate predictions for the line emission from all recombination processes. Temperature and abundance determinations in a wide range of cosmic sources make use of this line emission. Observations of the WHIM are contaminated by X-ray emission from the

heliosphere, requiring accurate data for X-ray line emission due to charge exchange. These data will be needed to analyze X-ray emission from stellar winds within astrospheres, which if detected would provide a diagnostic of the stellar wind composition.

Turning the observed line strengths into elemental abundances requires accurate ionization balance calculations. Cosmic plasmas can be divided into two broad classes: photoionized and electron-ionized. Photoionized gas is formed in objects such as AGNs, X-ray binaries, planetary nebulae (PNe), H II regions, the intergalactic medium, Wolf- Rayet nebulae, and luminous blue variable nebulae. Electron ionized gas is formed in objects such as stellar coronae, supernova remnants, the interstellar medium, and gas in galaxies or in clusters of galaxies.

Modeling the ionization structure of each class of plasma requires accurate data on many processes. Photoionized gas requires reliable low temperature **dielectronic recombination** (DR) and electron ionized gas high temperature DR. Calculating reliable low temperature DR is theoretically challenging and for some systems laboratory measurements are the only way to produce reliable data. For high temperature DR, few benchmark measurements exist for L-shell and M-shell ions. Density dependent DR rate coefficients are needed for dense plasmas but are sorely lacking. For decades astrophysicists have had to rely on theoretical **photoionization** calculations of varying degrees of sophistication. The development of third generation synchrotron light sources has opened up the possibility of measuring photoionization cross sections for many astrophysically important ions. High energy electrons or photons can lead to the production of an inner shell hole which then decays via the sequential emission of single or multiple electrons (most often) and/or photons (less often); past data sets have used inaccurate approximations for the **Auger yield**. Some modern theoretical work has been carried out for K-shell vacancies, but more work remains, especially for L-shell vacancies. **Charge exchange (CX) recombination** with H and He and **CX ionization** with H^+ and He^+ have been shown to be important for many systems, but few modern calculations or laboratory measurements exist at the relevant temperatures. Data are also needed for low charge states of elements such as Se and Kr in order to study nucleosynthesis in PN progenitor stars. The recommended **electron impact ionization** (EII) data are highly suspect. Recommended data derived from the same scant set of measurements and calculations can differ by factors of 2 to 3. Much of the published experimental data include contributions from an unknown metastable fraction in the ion beams used. The recommended EII data have not undergone any significant revision or laboratory benchmarking since around 1990. Little data also exist for **three-body recombination**, the time reverse of EII, which is important in high density plasmas.

Implicitly included in all the above data needs is the potential for developing new plasma diagnostics. One particularly exciting possibility is that of an X-ray line diagnostic for magnetic field strength. It may also be possible to measure the equation of state of neutron stars using a simultaneous measurement of the gravitational redshift and pressure broadening of atomic absorption lines. This will require accurate Stark profile data for highly charged heavy ions in very dense plasma (10^{19} to 10^{23} cm^{-3}). Experimental and theoretical work

such as this offers the potential to open up new areas of astrophysical research.

To conclude, the above discussion brings to the fore two important issues. First, interpreting astrophysical spectra from neutral to highly charged ions generally requires large modeling codes (e.g., radiative transfer codes, photoionization codes, collisional ionization codes). Many of these are publicly available. These codes incorporate vast amounts of theoretical atomic data, which themselves often come from large atomic codes, as well as data derived from laboratory measurements. A collaboration among astrophysicists (observers, theorists, and modelers) and atomic physicists (theorists, and experimentalists) has proven highly successful not just in the examples highlighted here but for many other cases. Such collaborations are vital for maximizing the scientific output of past, present, and future NASA spectroscopic missions. Second, the need for closer coordination with other agencies and departments is clearly evident. A significant body of atomic research has been funded by NSF and DOE in the past, but the scope and accuracy required for today's research in astrophysics and fusion physics demands a renewed effort. Many studies on stellar abundances and atmospheres are conducted at ground-based observatories. With respect to ground-based observations, NSF is the most appropriate source for funding work on the necessary laboratory data for wavelengths, oscillator strengths, and collision cross sections. Moreover, reliable results require critically evaluated compilations, which have been accomplished with great success in the past by DoC/NIST and DOE laboratories, especially Oak Ridge National Laboratory. This must continue with NASA and NSF support.

4.2 Molecular Astrophysics

Over the past 30 years, space-based and ground-based astronomy have shown that the Universe is highly molecular in nature. In fact, half of the mass in the inner 10 kpc of our Galaxy is thought to be composed of molecular material. The discovery of over 130 different chemical compounds in interstellar gas, with the vast majority organic molecules, reveals the complexity of interstellar chemistry. Protogalaxies and the first stars are predicted to have formed from primordial clouds where H_2 and HD controlled the cooling and collapse of these clouds. Subsequent stars and planetary systems are known to form out of the most complex molecular environments; therefore, it is inevitable that interstellar chemistry is intimately connected to the origins of life.

An understanding of the molecular component of the Universe requires a two-fold approach. First, the chemical compounds, their abundances, and how they are distributed in astronomical sources need to be determined. Second, molecular formation mechanisms including reaction pathways and dynamics need to be understood. Attaining these goals is crucial in guiding future missions designed to observe molecules and to interpret results from past and current missions. We now discuss the needs for laboratory data.

High resolution laboratory spectroscopy is absolutely essential in establishing the identity and abundances of molecules observed in astronomical data. It is extremely important for laboratory measurements to have a resolving power higher than the astronomical

instruments at sub-millimeter and terahertz wavelengths, namely, 1 part in 10^7 to 10^8. Given the advancements in detector technologies, astronomical spectra obtained in this frequency region will be extremely complex. Such will be the case for spectra obtained toward star-forming regions with *Herschel*. Furthermore, all the main functional groups known to organic chemists have now been observed in interstellar molecules, suggesting that interstellar chemistry contains the organic complexity seen on Earth. This result indicates that the origin of life may have begun in the gas phase chemistry of interstellar clouds. Laboratory spectroscopy is crucial in making the link between interstellar molecules and simple biological compounds that could seed life. It is also crucial in making the link between interstellar molecules (gas phase) and dust (solid phase) that is discussed in the following section.

For molecular data obtained from NASA missions to be of practical use, **accurate assignments of observed spectral features** are essential. The problem here is two-fold. First, the transitions of known molecules need to be assigned in these spectra, including higher energy levels and new isotopic species. Second, the spectra of undiscovered species that promise to serve as important new probes of astronomical sources need to be identified, such as the following. **Hydrides**, including metal hydrides and their ion counterparts, have transitions unique to the sub-mm/IR, and hence are excellent targets for space astronomy. **Organic ions and radicals**, including large aromatic species, serve as molecular probes and key intermediaries in chemical reactions that lead to more complex molecules. The simplest, and most fundamental, of these molecules also have important transitions in the sub-mm/IR. **Biogenic compounds**, including possible radical intermediates, directly tie into questions of the origin of life.

The spectroscopic study of such molecules, many of which cannot be produced in large abundance in the laboratory, **requires the development and application of state-of-the- art ultra-sensitive spectroscopic instruments** (e.g., velocity modulation, cw and pulsed cavity ringdown, time-of-flight mass spectrometers). Construction and implementation of these instruments is costly and time-consuming, and data production from these devices cannot be turned on and off at will. Efficient utilization requires continued support.

Detecting the possible presence of a species, however, is not sufficient since it must be reconciled with other physical properties of the medium. Even the steps leading to formation of simple species, such as CH^+ and H_3^+, have not been fully resolved. To understand the chemical composition of these environments and to direct future molecular searches in the framework of future NASA missions, it is important to **untangle the detailed chemical reactions and processes** leading to the formation of new molecules in extraterrestrial environments. The data necessary to understand ion- molecule and neutral-neutral reactions leading to carbon-bearing and hence biologically relevant molecules in the interstellar medium and in planetary and cool stellar atmospheres involve the use of ion storage rings, flowing afterglow and selected ion flow tubes, crossed beams machines, and setups establishing low temperature kinetics. Data are urgently needed for (1) **products** of bimolecular reactions, (2) **intermediates of these reactions** that can be stabilized by three-body reactions in denser media such as cometary, planetary, and stellar atmospheres and gravitationally-

collapsing gas of protostellar objects, and (3) reactive/inelastic **rate coefficients, with pressure and temperature dependent branching ratios**. These data will establish credible chemical models of interstellar, planetary, and stellar environments. The chemical models in turn are imperative to predict the existence of distinct molecules in extraterrestrial environments, thus guiding future astronomical searches of hitherto unobserved molecular species. Even for the simplest of molecules, H_2, many uncertainties remain in its formation and destruction mechanisms, from primordial to solar-metallicity gas. The former may limit our ability to understand protogalaxy and structure formation at high redshift, a major scientific goal of *JWST*.

Quantum mechanical calculations are an integral tool in laboratory astrophysical studies. There are many examples where calculations aided in the **interpretation of high-resolution spectra**, provided key **collisional excitation cross sections and the most accurate thermo-chemical data**, and delineated **important reaction pathways**. Input from quantum chemical/molecular physics studies are vital, particularly for extra-solar planets, cool stars, star forming regions, and primordial chemistry. As spectral observations of these sources continue to become available, at ever increasing resolutions, models will be necessary to interpret the spectra for information such as temperature, atmospheric composition, etc.

Critical needs in this area include **line lists, excitation rates, and mechanisms for forming and destroying molecules**. Ro-vibrational and/or electronic line lists for CrH, FeH, H_2O, CH_4, and NH_3 and accompanying molecular structure data are woefully incomplete. NH_3 and methanol, which are widely observed in various astronomical environments, are of particular interest since these molecules possess large amplitude motions and their spectra are highly sensitive to their physical environment. Collisional excitation rates of CO, H_2O, TiO, and hydrides are required to obtain abundance data from line intensities. Alkali broadening profiles due to collisions by H_2 are needed to deduce gravity and effective temperatures in brown dwarfs. Electronic and vibrational spectra of large polyatomic molecular structures (PAHs, other aromatic carbon compounds, carbon chains,...) and oscillator strengths are required to interpret ubiquitous interstellar spectral features such as the IR emission bands (AIBs) and diffuse interstellar bands (DIBs). Molecular formation/destruction mechanisms, such as UV and X-ray photodissociation of molecules, are essential ingredients for the development of non- chemical equilibrium models.

4.3 Dust and Ices in Astrophysics

The formation of stars and planetary systems takes place deep inside cold gas and dust clouds, often obscured by hundreds of visual magnitudes of extinction. At high redshifts, the assembly of galaxies through the merging of smaller units is accompanied by large amounts of obscuring dust. In order to properly decipher the mechanisms that occur in these environments, laboratory studies of silicate and carbonaceous dust precursor molecules (in the gas phase) and grains (solid phase) are required as are studies of the interaction between dust

and its environment (including radiation and gas). These interactions play critical roles in the gas physics and dust processing. Astronomical observations and supporting laboratory experiments over a wavelength region that extends from the X-ray domain to the ultraviolet, infrared, and sub-millimeter regions are of paramount importance for studies of the molecular and dusty universe. It is here where stars and planets form and where most of the chemistry of the Universe occurs. Observations at infrared and sub-millimeter wavelengths penetrate the dusty regions and probe the processes occurring deep within them. Moreover, these wavelengths provide detailed profiles of molecular transitions associated with dust. Because of its importance, NASA has launched or will launch and participate in a number of missions centered on this wavelength region (*Spitzer*, *SOFIA*, *Herschel*, and *JWST*), which will chart the star formation history of the Universe, star and planet formation in the Milky Way, the galactic life cycle of the elements, and the molecular and dusty universe. Together these span most of the key questions in modern astronomy.

The ensemble of current (*Spitzer*) and planned (*SOFIA*, *Herschel*, *JWST*) IR/sub-mm missions will bring in enormous quantities of data in spectral regions where little is known. Laboratory studies are essential in order to support the analyses of these data. Understanding the interaction of cosmic dust with its environment requires the laboratory study of the formation and destruction mechanisms of interstellar grains from their molecular precursors. **Determination of the physical properties of grains** is also critical. These include the nature of atomic and molecular binding sites on the surface, the photoelectric yield, probabilities that incident particles (including electrons and ions) stick to the grain, and ionization potentials.

Mid-IR spectra of individual objects such as H II regions, reflection nebulae, and planetary nebulae as well as the general interstellar medium of galaxies as a whole are dominated by a set of **emission features due to large aromatic molecules**. Studies of the IR characteristics of such molecules and their dependence on molecular structure and charge state are of key importance for our understanding of this ubiquitous molecular component of the ISM.

At long wavelengths, the continuum dust opacity is uncertain by an order of magnitude. IR spectral features of interstellar dust grains are used to determine their specific mineral composition, hence their opacities, which determine inferred grain temperatures and the masses of dusty objects, including the interstellar medium of entire galaxies. Emission bands from warm astronomical environments such as circumstellar regions, planetary nebulae, and star-forming clouds lead to the determination of the composition and physical conditions in regions where stars and planets form. The laboratory data essential for investigations of dust include measurements of the **optical properties of candidate grain materials** (including carbonaceous and silicate materials, as well as metallic carbides, sulfides, and oxides) as a function of temperature. For abundant materials (e.g., forms of carbon such as PAHs), the **measurements should range from gas-phase molecules to nanoparticles to bulk materials**. The IR spectral region is critical for the identification of grain composition, but results are also required for shorter wavelengths (i.e., UV), which heat the grains. Previous

studies in the UV have focused on the only identified spectral feature (at 2200 Å), but all materials should show UV spectral signatures. This need will become all the more important with the return of data from COS/*HST*. COS will be searching for the spectral signatures of specific individual aromatics, which provide a link between simpler gas phase species and solids, in the UV and near UV (NUV).

The UV spectral region contains features of important large interstellar molecules, such as organic species that carry the IR emission bands (AIBs) and diffuse interstellar bands (DIBs) and that may be related to the origin of life. Studies of the UV characteristics of such molecules and their dependence on molecular structure and charge state are of key importance for our understanding of this molecular component of the ISM. Identification of UV spectra of large aromatics is especially important to address these issues and represents one of the key science goals of *HST* (COS) and *FUSE*. We draw attention to the far-UV spectral region where *FUSE* operates. Here special coatings and detectors are needed, with the result that laboratory data are lagging far behind the astronomical data. The lack of experimental data in this spectral region has hampered progress in theoretical studies as well as the interpretation of astronomical data. **UV spectra are uniquely capable of identifying specific molecules**, in contrast with the less specific transitions observed in the IR. Laboratory studies provide spectroscopy of large organic molecules (such as PAHs) and their ions in the solid and in the gas phases. This work must be **complemented by quantum theory calculations** so that the laboratory data are properly interpreted.

The UV wavelength region, often used in conjunction with other wavelengths, provides an understanding of the fundamental processes (and especially the energy balance) associated with emissions from planetary atmospheres and magnetospheres, including planetary aurora and dayglow emissions (relevant for all planets and satellites with atmospheres and magnetospheres), as well as comets. Laboratory data on polyatomic molecules and dust grains are needed for modeling planetary atmospheres (a typical recent example is the Cassini-Huygens mission with the return of in-situ measurements from the hazy atmosphere of Titan). Lack of reflectance spectra (UV-visible-NIR) of low temperature frosts/volatile ices has inhibited interpretation of the Galileo data. Unless something is done in the near future, the situation will be similar for Saturn Cassini data. Water is reasonably well studied, and the mid- and far-IR has been done for astrophysical ices, although not at the 50 to 150 K temperatures relevant for solar system objects. **Optical constants/properties** of organic solids (important for most "red" solid bodies in the outer solar system) and of solid sulfur are needed.

New results from *Chandra* and XMM-*Newton* suggest additional areas in need of laboratory astrophysics. Recent astrophysical observations have tentatively identified X- ray absorption by molecules and solids, a new area for laboratory measurements of photoabsorption physics that can lead to differentiation between gas and dust in diffuse media. Detailed examination of **X-ray absorption edges** can, in fact, reveal which specific minerals are present in the ISM.

X-rays detected in the laboratory from olivine and augite surfaces bombarded by highly charged ions (HCIs) indicate that one should be able to detect mineral components when

HCIs collide with a comet or planetary surface (from, for example, the solar wind) and provide wavelengths at which X-ray observations should be made. Such work opens up the possibility of doing **"mineral prospecting" by X-ray spectroscopy** using remote spectrometers.

5. Recommendations

Recommendation 1: Conduct a study of the importance and need of laboratory astrophysics for all of astronomy under the auspices of the National Research Council and involving the principal funding sources for astronomical research, NASA and NSF, as well as DOE and DoC/NIST, whose activities encompass similar areas of study. This is an exciting time for astrophysics, but further progress requires improved atomic, molecular, and solid state data. Laboratory astrophysics, including the related theoretical effort, has reached a point where the field is becoming extinct; the impact on current and future missions will undoubtedly be catastrophic. The report from the NRC should include how the agencies and departments can best work together to maintain this important national resource. Specific items to address include:

1. how to support the development and maintenance of laboratories and their unique instrumentation for ground-breaking research;
2. how to encourage and retain faculty in this area, in terms of ensuring the future supply of laboratory astrophysicists and in maintaining/revitalizing infrastructure in the field;
3. how to foster graduate student participation and PhD theses in these areas, in order to revitalize an aging discipline;
4. how to coordinate the activities of the agencies and departments that benefit from a robust effort in laboratory astrophysics; and
5. how to combine interdisciplinary teams and/or centers, such as present in NASA's Astrobiology Institute, focused on solving specific complex problems and generating comprehensive data to address mission related needs, while continuing a fully funded Astronomy and Physics Research and Analysis (APRA) program to support ground-breaking ideas of individual researchers that could potentially revolutionize aspects of astrophysics and increase the scientific return from expensive NASA missions.

Recommendation 2: Ongoing missions (e.g., *Chandra*, *HST*, and *Spitzer*) and missions that will be initiated in the near future (e.g., *SOFIA*, *Herschel*, *JWST*, and *Beyond Einstein*) suggest a natural ranking for the observational bandpasses of 1) far infrared/sub- millimeter, 2) X-ray and infrared, and 3) UV/visible. This suggests a similar ranking for laboratory and theoretical efforts over the next few years. However, it is important to keep in mind that there is not always a 1-to-1 correspondence between these observational bandpasses and the needed laboratory astrophysics data. For example, standard UV/visible diagnostics for probing astrophysical environments are redshifted to longer wavelengths in high z objects. Also, models of chemical

processes involving photons at one wavelength are used to understand environments observed at other wavelengths. Funding should be based on projects considered the most meritorious by peers, as has been done in the past. The highest priority should be given to research most strongly coupled to the needs of NASA missions. Representative examples of laboratory needs coming from the Workshop include the following:

1. far infrared/sub-millimeter spectroscopy of simple hydrides and larger organic molecules; collision cross sections; chemical reaction rates; photoabsorption cross sections; optical constants of solids
2. X-ray and infrared dielectronic recombination, charge exchange, and electron impact ionization data; photoionization cross sections; spectroscopy of solids and ices; surface reactions; particle and radiative bombardment of solids and ices; optical constants of solids
3. UV/visible atomic and molecular spectroscopy, including DIB candidates; oscillator strengths; photoabsorption cross sections; chemical reaction rates; collision cross sections; optical constants of solids

It is important to note that many of the needs cross wavelengths and disciplines: laboratory work on N_2 and hydrocarbons, for example, has proven relevant to the ISM, the atmospheres of Titan and Triton, and the atmosphere of Earth.

Recommendation 3: Provide higher visibility within astronomical community. This can be accomplished through the establishment of a Working Group on Laboratory Astrophysics in the AAS. Its Bylaws should include close interaction with IAU Commission 14 on Atomic and Molecular Data. The Working Group can organize sessions at AAS meetings that build upon the success of the recent Topical Session during the Minneapolis Meeting.

Recommendation 4: Increase support for the NASA Astronomy and Physics Research and Analysis (APRA) program. The health and vitality of the laboratory astrophysics community depends on continued APRA support. It is important to maintain the core competency of the community and ensure the development of future generations of laboratory astrophysicists. If the current program is cut any further, significant research capabilities will be lost and NASA may not be able to get optimum scientific return from its future, very expensive missions. A viable level of support should be restored for this program.

Recommendation 5: Mission support of laboratory astrophysics. Current APRA funding is insufficient to produce all the data needed to ensure successful scientific return from NASA missions. Mission support of laboratory astrophysics through competitively run three year grants would make a significant positive impact on the production of the needed data. Support arising from 1-year grants from observing cycles (e.g., *Chandra* and *Spitzer*) does not address the long-term nature of laboratory work.

Recommendation 6: Provide adequate funding for databases. Critically evaluated data are needed by those analyzing astronomical measurements and modeling the

associated environments. True understanding is only possible when collections of the highest quality data on atoms, molecules, and solids are utilized. Here, too, the relevant agencies and departments need to coordinate their efforts. Database compilation and the associated, vital critical compilation, is a skill that is developed over decades in many cases. Long term commitment of funds is essential. In the past, funding of databases and their development was provided as part of the Applied Information System Research Program (AISRP); NASA should consider reestablishing AISRP support for databases. Such a distinction would reduce the conflict reviewers for the ARPA program have in choosing between newly acquired data and compilations of existing data.

Recommendation 7: Another laboratory astrophysics workshop should take place in 4 years. Given the fundamental importance of laboratory astrophysics, it is important to monitor the health of the field and to ensure that the laboratory astrophysics community is adequately supporting NASA's space missions. While NASA should continue to be the lead agency, the other agencies and departments (NSF, DOE, DoC/NIST) should be active partners in this workshop.

INVITED TALK *NASA LAW*, February 14-16, 2006, UNLV, Las Vegas

NASA Laboratory Astrophysics Workshop 2006 Introductory Remarks

Hashima Hasan

Astrophysics Division, NASA Headquarters, Washington DC 20546

hhasan@nasa.gov

1. Introduction

NASA Laboratory Astrophysics Workshop 2006, is the fourth in a series of workshops held at four year intervals, to assess the laboratory needs of NASA's astrophysics missions - past, current and future. Investigators who need laboratory data to interpret their observations from space missions, theorists and modelers, experimentalists who produce the data, and scientists who compile databases have an opportunity to exchange ideas and understand each other's needs and limitations. The multi-wavelength character of these workshops allows cross-fertilization of ideas, raises awareness in the scientific community of the rapid advances in other fields, and the challenges it faces in prioritizing its laboratory needs in a tight budget environment.

Currently, we are in the golden age of Space Astronomy, with three of NASA's Great Observatories, Hubble Space Telescope (HST), Chandra X-Ray Observatory (CXO), and Spitzer Space Telescope (SST), in operation and providing astronomers and opportunity to perform synergistic observations. In addition, the Far Ultraviolet Spectroscopic Explorer (FUSE), XMM-Newton, HETE-2, Galaxy Evolution Explorer (GALEX), INTEGRAL and Wilkinson Microwave Anisotropy Probe (WMAP), are operating in an extended phase, while Swift and Suzaku are in their prime phase of operations. The wealth of data from these missions is stretching the Laboratory Astrophysics program to its limits. Missions in the future, which also need such data include the James Webb Space Telescope (JWST), Space Interferometry Mission (SIM), Constellation-X (Con-X), Herschel, and Planck. The interpretation of spectroscopic data from these missions requires knowledge of atomic and molecular parameters such as transition probabilities, f-values, oscillator strengths, excitation cross sections, collision strengths, which have either to be measured in the laboratory by simulating space plasma and interactions therein, or by theoretical calculations and modeling. Once the laboratory data are obtained, a key step to making them available to the observer is the creation and maintenance of critically compiled databases. Other areas of study, that are important for understanding planet formation, and for detection of molecules that are indicators of life, are also supported by the Laboratory Astrophysics program. Some examples are: studies of

ices and dust grains in a space environment; nature and evolution of interstellar carbon-rich dust; and polycyclic aromatic hydrocarbons. In addition, the program provides an opportunity for the investigation of novel ideas, such as simulating radiative shock instabilities in plasmas, in order to understand jets observed in space.

A snapshot of the currently funded program, mission needs, and relevance of laboratory data to interpreting observations, will be obtained at this workshop through invited and contributed talks and poster papers. These will form the basis for discussions in splinter groups. The Science Organization Committee will integrate the results of the discussions into a coherent White Paper, which will provide guidance to NASA in structuring the Laboratory Astrophysics program in subsequent years, and also to the scientific community in submitting research proposals to NASA for funding.

2. NASA's Laboratory Astrophysics Landscape

Proposals for the Laboratory Astrophysics Program are solicited through the Science Mission Directorate's omnibus solicitation, Research Opportunities in Earth and Space Science (ROSES). The program element in ROSES that the Laboratory Astrophysics Program is a sub-element of is the Astronomy and Physics Research and Analysis (APRA) Program. The solicitation is open to all investigators and proposals are competitively selected through a peer review process. A typical investigation is funded for three years, so that approximately one third of the program is reviewed every year. Programmatic balance between different Laboratory Astrophysics research areas is achieved by the Selection Official by reviewing all the selectable proposals, investigations in the second and third year of funding, and aligning them with NASA's strategic priorities.

In Fiscal Year (FY) 2006, 33 investigations were funded for a total of ∼$3.8M. Of these, 4 could be broadly categorized as infrared investigations, 9 as those supporting interstellar medium (ISM) studies, 5 in the area of submillimeter spectroscopy, 8 in the area of UV/Optical atomic processes, 2 in the area of UV/Optical molecular and dust formation processes, and 5 in the support of X-ray missions. Given below are extracts from the abstracts of the proposals submitted by investigators. Full abstracts can be found through links on the NASA web page for research solicitations, the url for which is http://nspires.nasaprs.com/external/

2.1. Infrared Investigations

Peter Bernath (University of Arizona) is analyzing laboratory spectra of astrophysically-relevant molecules using a Fourier transform spectrometer, FTS. Molecules of interest include hot water and transition metal-containing diatomics. The laboratory spectra of water, CaH,

MgH, FeH, TiH, VO, CN and C_2 molecules will be analyzed to provide improved spectroscopic parameters and molecular opacities. This work is required in order to calculate the spectral energy distributions of cool stellar and sub-stellar objects. The next generation of NASA missions in the submillimeter, infrared and near infrared regions will provide spectra of exquisite sensitivity but (generally) moderate resolution. Interpretation of these spectra will require simulations based on data supplied by this investigation.

Benjamin McCall (University of Illinois at Urbana-Champaign) proposes to obtain laboratory spectra of buckminsterfullerene, C_{60}, and its positive ion C_{60}^+ in the gas phase, using continuous-wave cavity ringdown spectroscopy with infrared lasers. The laboratory spectroscopy of C_{60} will directly enable a sensitive search for interstellar and circumstellar C_{60} using TEXES at NASA's IRTF and eventually using EXES on the Stratospheric Observatory for Infrared Astronomy (SOFIA). The laboratory spectroscopy of C_{60}^+ will enable us to test the controversial hypothesis that C_{60}^+ is the carrier of two of the enigmatic Diffuse Interstellar Bands (DIBs) in the near-infrared. Together, this work will enable the first census of the fraction of cosmic carbon that is tied up in the form of fullerenes. Mc Call will also develop an ultrasensitive new technique (SCRIBES: Sensitive, Cooled, Resolved Ion BEam Spectroscopy) that will allow us to record the spectra of molecular ions with a sensitivity approaching the limit of single molecule absorption spectroscopy.

Anne Hofmeister's (Washington University) work is focused on distinguishing grain-size and temperature effects on the infrared fingerprints of astrominerals. Characterizing dust properties will further our understanding of many aspects of astrophysics, since it is an essential part of star formation processes; is key to understanding mass loss from aging stars; and contributes to interstellar processes such as gas heating and the formation of molecules. Improved laboratory data will be obtained, and an analysis performed of available astronomical databases using the new information. The results will be applied against available ISO data and up-coming Spitzer data. One goal is to identify Al_2O_3, which is known to exist in pre-solar grains in meteorites, but the astronomical evidence is equivocal and interpretations are controversial. As the data are published, the information would be disseminated though websites maintained by the participating universities.

Perry Gerakines (University of Alabama at Birmingham) is producing a database of laboratory infrared spectra of ice mixtures containing carbon dioxide. Mixtures representative of solid CO_2 in interstellar icy grain mantles in a wide variety of environments will be studied. These spectra will be used primarily in the analyses of IR data obtained with the Spitzer Space Telescope We will draw upon existing knowledge of interstellar solid CO_2 as obtained in the analyses of data from the Infrared Space Observatory, with which we have extensive experience. Existing databases will be refined to include a more systematic study of ice compositions and effects of ice thermal history. Optical constants, of wide use to the general astronomical community, will be calculated from the IR transmission spectra for use in scattering calculations. Data will be distributed via the Internet to the general community.

2.2. Interstellar Medium Processes

Theodore Snow (University of Colorado) is continuing his program to measure chemical reaction rates involving large molecular ions with astrophysically common reactants. The motivation for this work is two pronged - the identification of diffuse interstellar bands, and the study of reactions that may be relevant to dense interstellar clouds, such as: reactions with anions of polycyclic aromatic hydrocarbons (PAHs), which may be chemically and energetically important in dense clouds. In a parallel collaborative effort chemical models relevant to the reactions and products measured in the laboratory, will be developed. The research will have impact on the interpretation of data from Spitzer, SOFIA, JWST, Herschel and the HST instrument, Cosmic Origins Spectrograph (COS).

Vidali Gianfranco (Syracuse University) plans to investigate the formation of molecular hydrogen in different simulated astrophysical environments. Knowledge of surface science techniques will be applied to obtain information on the mechanisms and efficiency of formation of H_2 in different conditions of composition and morphology of grains. Measurements done in the past will be extended to amorphous silicates of various composition (from Fe-to Mg-rich) and to carbonaceous materials obtained using various methods. The new information obtained will be used in models of H_2 formation in various ISM environments. An understanding of H_2 formation routes and degree of internal excitation following its formation on grains is needed for the analysis of data of H_2 transitions obtained in space-based observations using, for example, ISO, HST, and FUSE. It also impacts analyses of observations of molecules in dense clouds using infrared space observatories (ISO, Spitzer, SOFIA, Herschel).

Gary Ferland (University of Kentucky) is computing rovibrational excitation and dissociation cross sections and rate coefficients for collisions of H, H_2 and He with H_2 and HD for all transitions between all bound rovibrational levels of the target molecules. The results of this proposal will then enable models, such as the very widely used and tested computer code CLOUDY, to reliably simulate astrophysical environments, leading to deeper examination and understanding of their physical properties, such as cooling processes, molecular emission, and nonequilibrium effects in molecular gaseous nebulae and other molecular environments. Thus, it will be possible to extract the maximum scientific return from the significantly improved observations of such environments from NASA's Spitzer Infrared Telescope Facility, and other upcoming infrared astrophysics missions such as SOFIA, the James Webb Space Telescope, Herschel, and Astro-F.

Phillip Stancil (University of Georgia) is performing theoretical investigations of atomic and molecular processes for applications to M, magnetic white, and cool white dwarfs are proposed. In addition, collision processes relevant to the ejecta of Type II supernovae will be computed. The data will be provided to stellar and nebula modelers for testing of the resulting calculations, as existing experimental or theoretical data are lacking in most cases, and for predicting of spectra for comparison to observations. All data will also be made

available on the WWW. The results from this work are critical to development of advanced non-thermal and non-chemical equilibrium models which will aid in the analysis of observations from the current and next generations of space- and ground-based telescopes enhancing the scientific return from NASA astrophysics missions.

Swaraj Tayal (Clark Atlanta University) aims to provide accurate extensive radiative and collisional atomic data for astrophysically important ions for analysis and interpretation of spectroscopic observations from the International Ultraviolet Explorer (IUE), HST, Astro-1,2, Extreme Ultraviolet Explorer (EUVE), and FUSE. The UV and visible lines provide powerful diagnostic tools to advance the understanding of the physical and chemical conditions of a variety of astrophysical environments such as atmospheres of stars.

Thomas Gorczyca (Western Michigan University) is focusing his efforts towards obtaining improved simulations of astrophysical plasmas through the computation of new atomic data. Calculations of dielectronic recombination (DR) and fluorescence and Auger yields due to a 1s vacancy, needed for modeling shocked gas in supernova remnants and X-ray photoionized plasmas are being performed. The new atomic data will be disseminated to the astrophysics community via the web page http://homepages.wmich.edu/∼gorczyca/atomicdata and will be used by the authors in the non-equilibrium plasma simulation code CLOUDY to enable more accurate interpretations of ionized emission/absorption line gas. This work will be relevant to the interpretation of spectroscopic data from a range of past, present, and future satellite observatories including IUE, HST, EUVE, ISO, HUT, ORFEUS, Einstein, EXOSAT, ROSAT, ASCA, FUSE, GALEX, Chandra, XMM, JWST, Spitzer, Suzaku, and Constellation-X.

Hantao Ji (Princeton Plasma Physics Laboratory) is performing a laboratory study of Magnetorotational Instability (MRI) in a Gallium disk. The goal is to demonstrate MRI, study its properties, and compare experiments with numerical and analytical modeling. The astrophysical importance of MRI is that it is now believed that it drives accretion in disks ranging from quasars and X-ray binaries to cataclysmic variables and perhaps even protoplanetary disks.

John Laming (Naval Research Laboratory) is studying instabilities of radiative shocks. Shocks will be launched by high power laser irradiation of a target either in a shock tube to study ID instabilities or in a gas cell to study multi D instabilities of blast waves. The results are expected to be of importance to astrophysical fields ranging from stellar wind and interstellar medium shocks, to those occurring in accreting objects such as T Tauri stars, white dwarfs and other compact accretors, as well as core-collapse supernovae.

Mark Bannister (Oak Ridge National Laboratory) is performing a series of laboratory measurements and theoretical calculations of electron-impact ionization (EII) in support of a wide range of past, present, and future NASA flight missions. EII is the dominant ionization mechanism in supernova remnants, galaxies, clusters of galaxies, and stellar atmospheres. These measurements will provide new EII rate coefficients with uncertainties of less than

15%. The new atomic data will be used to benchmark state-of-the-art EII calculations using time-dependent close-coupling, R-matrix with pseudostates, and distorted-wave techniques. Once the theoretical and experimental results converge, calculations will be made for the needed EII rate coefficients for the remaining unmeasured ions in the relevant isoelectronic sequences. These data will be fit with the standard fitting formulae used by the astrophysics community for ionization balance calculation. Results will be widely disseminated.

2.3. Submillimeter/THz Studies

In anticipation of the launch of SOFIA and Herschel, several investigators are producing laboratory data in the submillimeter and THz regime. Eric Herbst's (Ohio State University investigations are aimed at enriching the database of laboratory submillimeter-wave spectra so that assignment and analysis of astronomical spectra in this wavelength region can become more routine. The submillimeter-wave spectra of a wide variety of molecules will be measured and analyzed. Geoffrey Blake (California Institute of Technology) is continuing his laboratory studies to characterize the rotational spectra of key hydrides (especially water, ammonia, and their isotopologues) and the rotation-torsion interactions in complex species known to exist in star-forming cores. Lucy Ziurys (University of Arizona) is assembling a complete database of highly accurate rotational rest frequencies for metal hydride molecules of astrophysical interest. John Pearson (Jet Propulsion Laboratory) is obtaining precise laboratory data on the rotation spectrum of CH^+ and its $^{13}CH^+$ and CD^+ isotopomers. His group will also improve the accuracy of the known transitions of ^{13}CH and CD from approximately 10MHz to 100kHz. Brian Drouin (Jet Propulsion Laboratory) is measuring the state-to-state collision rates and pressure broadening of water with dihydrogen as a function of temperature for the lowest ortho and para rotational transitions of water. This data is central to interpretation of SWAS and Herschel water spectra.

2.4. UV/Optical Atomic Studies

James Lawler (University of Wisconsin, Madison) is developing a Spatial Heterodyne Spectrometer (SHS) in the vacuum ultraviolet (VUV) and using it in the 300 nm to 100 nm wavelength range for the measurement of basic atomic data including atomic transition probabilities, hyperfine structure constants, and isotope shifts of lines from singly and multiply ionized iron group ions. This laboratory project supports VUV astronomy with Hubble Space Telescope and other missions at low red shift, and supports future research with the James Webb Space Telescope at high red shift.

James Babb (Harvard-Smithsonian Center for Astrophysics) is studying the pressure-broadening of alkali atom resonance lines for modeling atmospheres of extrasolar giant planets and white dwarfs.

Steven Federman (University of Toledo) is determining oscillator strengths of ultraviolet atomic and molecular transitions. Laboratory data on lifetimes, branching fractions, and oscillator strengths will be acquired through beam-foil techniques and absorption studies with synchrotron light source; these data will be interpreted using appropriate theoretical tools. Relevant to analysis of data from HST, FUSE, SOFIA, Spitzer, Herschel.

Steven Manson (Georgia State University) is calculating photoabsorption and recombination rates for astrophysically important species over a broad range of wavelengths from the UV/Visible to the X-ray using a variety of state-of-the-art methodologies to augment the existing atomic database in this area. This work will support HST, FUSE, Chandra, XMM, CHIPS and future space missions.

Sultana Nahar (Ohio State University) is computing large-scale radiative data mainly for Fe ions using the state-of-the-art relativistic R-matrix method. The calculations will constitute a multi-wavelength database useful across a wide spectral range and will be made available electronically to the astrophysical community for analysis of observations from a number of space missions ranging from far-infrared to X-ray.

Ara Chutjian (Jet Propulsion Laboratory) is using the JPL Highly Charged Ion Facility to measure absolute electron-impact cross sections (collision strengths) in those highly charged ions that are detected in stars, quasars, planetary nebulae, and the shock-heated ISM. Emphasis includes ions emitting in the EUV through X-ray regions to accommodate the enormous data returns from HST, FUSE, and EUVE; and from the high-resolution X-ray spectrometers aboard Chandra and XMM-Newton. There is a concomitant need for laboratory measurements and benchmarking of the various theoretical calculations in distorted-wave, multistate R-matrix, Breit-Pauli, etc. approximations. The JPL measurements will include ions/charge/states/transitions that are numerators or denominators in electron temperature and density diagnostics of the emitting plasma. Work will continue on excitation cross-sections for the He-like C V, N VI, and O VII X-ray triplets. First measurements anywhere were published by JPL on absolute excitation cross sections for the Fe X coronal red line. Work will continue on absolute measurements on Fe XII - Fe XVI, including the coronal green line in Fe XIV. All measurements are compared to the latest theoretical results in distorted-wave or R-matrix calculations. This work supports the many spacecraft data streams described above, as well as new missions such as Suzaku and Constellation X.

Peter Beiersdorfer (Lawrence Livermore National Laboratory) , in response to observations of stellar coronae by Chandra and XMM in the extreme ultraviolet region, which have found numerous emission lines that are absent from the spectral models, is performing systematic laboratory measurements of the L-shell line emission spectra of the intermediate ionization stages of magnesium (Mg III - Mg X), aluminum (Al IV - Al XI), calcium (Ca XI - Ca XVIII), and nickel (Ni IX - Ni XXVI). These measurements will establish a complete emission line catalogue of these ions in the 25 to 200 Å region under well controlled laboratory conditions and densities comparable to coronal plasmas ($< 10^{12}$ cm^{-3}), providing line

identification, wavelengths, and relative line intensities for specific electron temperatures, adding to the catalogue of silicon, sulfur, argon, and iron lines established earlier. The possibility of using specific Mg III, Si V, S VII, Ar IX, and Ca XI lines as diagnostics of the magnetic field strength in the range of about 0.5 to 10 kG, i.e., in a range comparable to that of classical T Tauri stars, will also be addressed in the measurements. The intensity of the relevant spectral lines for a range of magnetic field strengths will be studied in order to firmly establish the diagnostic utility of these spectra for such novel measurements.

Joseph Reader (National Institute of Standards and Technology) will expand and refine the NIST database on atomic transition probabilities, wavelengths, and energy levels, responding to current and anticipated needs of space astronomy. Results of the critical compilations will be made available through the online NIST Atomic Spectra Database and in hardcopy publications.

2.5. UV/Optical Molecular and Dust Studies

Martin Head-Gordon (University of California Berkeley) is developing a theoretical model of the electronic spectroscopy of PAHs that can play an important role in complementing, focusing and guiding laboratory PAH research in two directions. First, this modeling can help to identify general classes of PAH molecules that have particularly distinctive spectral signatures, that can cause them to be particularly promising as carriers of the DIBs. Second, theoretical modeling will help to enable specific identification of molecules that are believed to be isolated in laboratory spectroscopy experiments.

Farid Salama (NASA Ames Research Center) will provide laboratory data that will permit the analysis of astronomical data for the presence of specific complex organic molecules through their unique electronic spectrum in the ultraviolet, visible and NIR range. He will measure the absorption spectra of selected PAH and fullerene ions for the first time in the gas phase thus allowing a conclusive test for the presence of specific species in the interstellar medium. He will also measure in the laboratory the changes induced in samples exposed to space environment on board the international space station to provide a fundamental diagnostic on the evolution of organic matter. The ultimate goal is to conclusively determine whether or not these large carbon-containing molecules and ions contribute to the interstellar extinction curve, including the DIBs see in absorption.

2.6. High Energy Studies

Steven Kahn (Stanford University) is continuing his program of X-ray spectroscopic laboratory astrophysics measurements using the electron beam ion trap (EBIT) facility at the Lawrence Livermore National Laboratory and the X-ray microcalorimeter detec-

tor developed at the Goddard Space Flight Center. Scott Porter (GSFC) is using the EBIT/microcalorimeter to measure absolute cross sections for both direct electron impact excitation and dielectronic recombination, identify spectral signatures of plasmas which are not in ionization equilibrium, measure the composite X-ray emission from plasmas at a specified Maxwellian temperature, and measure X-ray emission from low energy charge exchange collisions. The results will be used to both verify and complement atomic data used in spectral modeling packages that are heavily used in the astrophysics community

Bradford Wargelin (Smithsonian Astrophysical Observatory) is using an EBIT to continue his study of X-ray emission from charge exchange (CX) of highly-charged ions with neutral hydrogen and helium. The primary results of the research will be high-resolution emission spectra and state-specific relative cross sections as a function of ion energy and temperature.

Timothy Kallman (Goddard Space Flight Center) aims to calculate the yet unknown atomic quantities needed for modeling and interpreting data for an important class of cosmic X-ray sources: those in which photoionization dominates the ionization and heating of gas. These include inner shell photoionization cross-sections and line parameters, recombination cascade rates and branching ratios, and data for the element, Ni.

Daniel Savin (Columbia University) is continuing his program to measure low temperature dielectric recombination rate coefficients for photoionized cosmic plasmas such as are formed in active galactic nuclei, X-ray binaries, the intergalactic medium, planetary nebulae, and HII regions.

I would like to acknowledge Doug Hudgins' analysis of NASA's Laboratory Astrophysics Program, which I have used in preparing the last section of this paper.

INVITED TALK *NASA LAW*, February 14-16, 2006, UNLV, Las Vegas

Laboratory Astrophysics: Enabling Scientific Discovery and Understanding

K. Kirby

Harvard-Smithsonian Center for Astrophysics, Cambridge, MA

kkirby@cfa.harvard.edu

ABSTRACT

NASA's Science Strategic Roadmap for Universe Exploration lays out a series of science objectives on a grand scale and discusses the various missions, over a wide range of wavelengths, which will enable discovery. Astronomical spectroscopy is arguably the most powerful tool we have for exploring the Universe. Experimental and theoretical studies in Laboratory Astrophysics convert "hard-won data into scientific understanding". However, the development of instruments with increasingly high spectroscopic resolution demands atomic and molecular data of unprecedented accuracy and completeness. How to meet these needs, in a time of severe budgetary constraints, poses a significant challenge both to NASA, the astronomical observers and model-builders, and the laboratory astrophysics community. I will discuss these issues, together with some recent examples of productive astronomy/ lab astro collaborations.

1. Introduction

As demonstrated by the many invited and contributed papers at this meeting, the field of Laboratory Astrophysics is incredibly diverse and fascinating. Whether one considers the Cold Universe or the Hot Universe, Laboratory Astrophysics plays a pivotal role in both discovery and understanding.

This is an exciting but extremely challenging time for our field. The NASA Science Strategic Roadmap, released in May, 2005, articulated a grand vision of Universe Exploration, consisting of two major program elements: Beyond Einstein – exploring extreme conditions in the Universe; and Pathways to Life – focusing on the formation and evolution of galaxies, stars and planets. As new missions develop better capabilities for spectroscopy with improved photon sensitivities and higher spectroscopic resolution, exciting new phenomena in our universe will be revealed. Laboratory Astrophysics will be a necessary element in making these discoveries. It is a challenging time because the funding to sustain this field

is so small, and has in fact declined in this program over the last year. In addition, the research itself is often very difficult, requiring the fastest computer facilities available and laboratory instruments which may be unique or may not even exist in the United States.

The plenary speaker of four years ago (NASA LAW, May 2002), Martin Harwit, ended his talk: "Without laboratory astrophysics there can be no astronomical science!" The science examples which I have chosen to discuss in this talk will illustrate this point. Whereas this quote is generally accepted in the LabAstro community, it needs to be more widely recognized throughout the Astronomy community. The potential for LabAstro to really challenge the astrophysics can only be realized once the uncertainties in the atomic, molecular and solid state parameters have been reduced to a negligible level. Astronomers need to be more critical of the LabAstro data that they use and more aware of how issues such as accuracy, outdated cross sections, and old approximations can seriously corrupt the interpretations of their observations and lead to false astrophysical conclusions.

2. Sustainability Concerns

The sustainability of the Laboratory Astrophysics enterprise is greatly threatened. Although NASA is to be congratulated for having a program in LabAstro (no other agency does), this program is small and getting smaller. Ground-based astronomy needs LabAstro just as much as space astronomy, so there need to be additional sources of funding beyond NASA for this field.

The reason that Laboratory Astrophysics is so poorly funded at this point is due to the historical fact that much of the research in atomic and molecular collisions and spectroscopy (the vast majority of the LabAstro research) used to be funded by the Atomic and Molecular Physics programs at the National Science Foundation (NSF) and Department of Energy (DOE). Astronomy benefited, but did not have to fund this work from astronomy programs. Now, however, the funding priorities for Atomic, Molecular and Optical (AMO) Physics programs have changed and new forefront areas of AMO Physics, such as the study of Bose-Einstein Condensation, generation of ultra-fast light pulses, quantum control, and quantum information science have commanded most of the resources in these programs.

Now is the time to argue for new sources of funding for LabAstro at NSF (Astronomy), DOE and NIST – the agencies singled out for significant budgetary increases in the recent State of the Union address (January, 2006). Although these agencies have very different missions, each could play a unique role in support of LabAstro. Not only would the field be strengthened by a diversity of funding sources, but also the NASA Laboratory Astrophysics program would benefit from the synergism.

There are other sustainability issues as well – but each concern can be traced back to lack of funding. The training of students and postdocs in Laboratory Astrophysics research is absolutely essential if the field is to continue. Young people are the "life-blood" of the field. There are almost no faculty or research staff appointments in the field of LabAstro – either

in physics, chemistry, or astronomy departments. New positions are usually not created in areas of research that are extremely under-funded. Finally laboratory research facilities are aging and need to be updated and maintained, with funds for new instrumentation and equipment. Despite these very serious issues, the science itself continues to be as compelling as ever.

3. Scientific Examples

There are so many examples I could have chosen to highlight from the broad array of scientific papers submitted to this workshop. From spectroscopic studies of PAHs and laboratory simulations in ices and minerals, to astrochemistry in the interstellar medium and in sites of star formation, to measurements of spectral lines and oscillator strengths of heavy elements such as Samarium in order to better understand nucleosynthesis scenarios, the work is of exceptional quality and value to the field of astronomy.

3.1. Understanding the Origin of Cometary X-rays

While the cometary x-ray story is not new, the reason to re-tell it in this setting is to emphasize that the solution to the origin of the x-rays rests exclusively with an atomic collision process, and that as astronomers and laboratory astrophysicists study this in more detail this process is proving to be the explanation for the x-rays seen in a variety of solar system settings, and potentially even beyond.

In 1996 Lisse and collaborators reported on observations of x-ray and EUV emissions from the comet Hyakutake, as it approached the sun. Observations were made using ROSAT and the Rossi X-ray Timing Explorer, with such low resolution that essentially no lines were discernible. Subsequently a number of other comets were found to exhibit x-ray emission as well. The source of these x-rays was a mystery.

Without an adequate spectrum several possible mechanisms for x-ray production were proposed and dismissed. Thermal bremsstrahlung was ruled out because the flux of energetic electrons was not high enough, by several orders of magnitude, to account for the detected intensity. Fluorescent scattering of solar x-rays by material in the comet's coma was rejected because generally x-rays do not scatter strongly. It was Cravens in 1997 who suggested that highly-charged ions in the solar wind were colliding with neutral molecules in the cometary atmosphere, capturing electrons in a process known as "charge exchange". A valence electron is captured from the neutral species into a highly excited level of the ion, and as the electron decays to the lowest available energy level the ion emits radiation at x-ray and EUV wavelengths. Because this radiation is characteristic of the emitting ion, the spectrum contains valuable information about the original ions present in the solar wind.

The Chandra satellite has afforded the opportunity to resolve a number of spectral fea-

tures. Figure 1 shows a Chandra x-ray spectrum of Comet McNaught-Hartley (open circles) and a model of the emission over the range from 0.5 to 1.0 keV. The narrow dark lines are the spectral lines from theoretical calculations and experimental measurements. When the model spectra are convolved with the Chandra spectroscopic resolution, and the abundances of the solar wind ions are included as adjustable parameters, an excellent fit to the Chandra data can be obtained, as shown by the red line in Figure 1. Theorists were also able to predict the presence of a line of Ne^{8+} which the astronomers were able to identify subsequently.

The charge exchange mechanism is thought to be the major contributor to the heliospheric diffuse soft x-ray background, as well as explaining many of the x-ray observations of planets such as Jupiter, Mars and Saturn. This mechanism is not confined to solar system objects, however. Charge exchange may occur wherever there is the interaction of a highly-ionized plasma with a surrounding gas of neutral material, such as might be found close to the center of Active Galactic Nuclei.

In the future, with increasingly high resolution spectra available with new and planned x-ray telescope facilities, better experiment and theoretical calculations, it is anticipated that cometary x-ray spectra could be used as important diagnostics of the solar wind composition.

3.2. Fe XVII: Diagnostic of Collisionally-ionized Plasmas

The topic of collisionally-ionized plasmas is large, so I will just focus on one important but powerful diagnostic, the 3C/3D line ratio in Fe XVII. Recent work on this line ratio exemplifies the productive way that astrophysical modelers, laboratory experimenters and theorists can work together to determine critical data with high accuracy.

Stellar coronae and supernova remnants are among the many x-ray sources that are thought to be collisionally-ionized plasmas. The collisional models require a detailed understanding of atomic collision processes over a wide range of temperatures, as well as large amounts of data including: line identifications, line strengths, electron impact ionization and excitation cross sections, dielectronic and radiative recombination cross sections, and proton impact excitation and ionization cross sections. The challenges for both the modelers and the labastro scientists are the completeness and consistency of the atomic data, as well as the accuracy.

Line intensity ratios can be powerful diagnostics of astrophysical plasmas, allowing one to deduce temperature, electron density, ion abundances and opacity from the observations of spectral lines. Neon-like iron is a very abundant ion in objects with temperatures in the range of $2-6\times10^6$K. In particular, the 3C resonance line at 15.01 A is the strongest line in the solar x-ray spectrum. The 3C line is due to a dipole-allowed transition ($2p^5 3d\,^1P_1^o \rightarrow 2p^6\,^1S_o$) and the 3D at 15.26 A is a spin- forbidden intercombination line ($2p^5 3d\,^3D_1^o \rightarrow 2p^6\,^1S_o$).

Historically there has been a problem with the 3C/3D line ratio, in that solar observations gave values considerably smaller than the early theoretical calculations by factors of 2 to 5. To account for these discrepancies, astrophysical effects, such as opacity and resonant

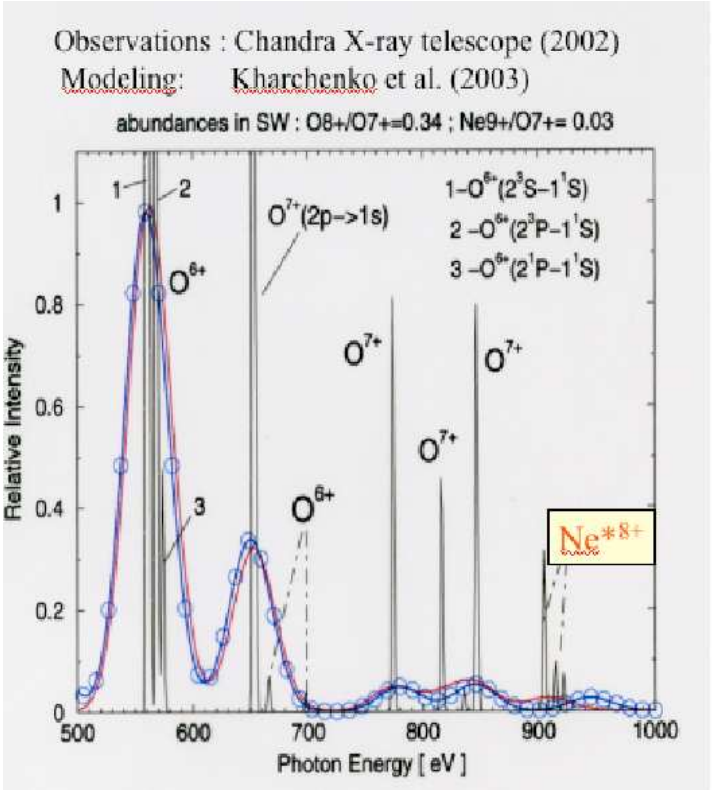

Fig. 1.— Chandra X-ray observations (open circles) of Comet McNaught-Hartley together with model spectra obtained from theory and experiment convolved at the spectral resolution of Chandra, using solar wind (SW) abundance ratios as listed at the top of the figure. (Courtesy of V. Kharchenko)

scattering, were posited as being responsible. It should be noted however that the early theoretical calculations used the distorted wave approximation that neglects channel coupling and resonances. It is known that forbidden and intercombination transitions, such as 3D, are more sensitive to the neglect of resonances than the dipole-allowed transitions.

Fortunately, experimental measurements of these transitions were made. The group at the LLNL EBIT (Brown, Beiersdorfer et al.) measured 3C/3D at several selected beam energies and obtained values more in harmony with the solar observations. Similar values were also reported by the NIST EBIT group (Laming et al.) in 2001. The laboratory measurements were absolutely critical in motivating theorists to look again at this problem. Chen and Pradhan (2002) carried out large-scale relativistic close-coupling calculations using the Breit-Pauli R-matrix method, including atomic levels up through n=4. They demonstrated the significant enhancement of the 3D collision strength due to the inclusion of resonances, bringing their 3C/3D ratio into better agreement with the EBIT measurements. They estimated the accuracy of their calculation to be at the 15-20% level.

Recently Chen (2006) has significantly improved on the calculation of Chen and Prad-

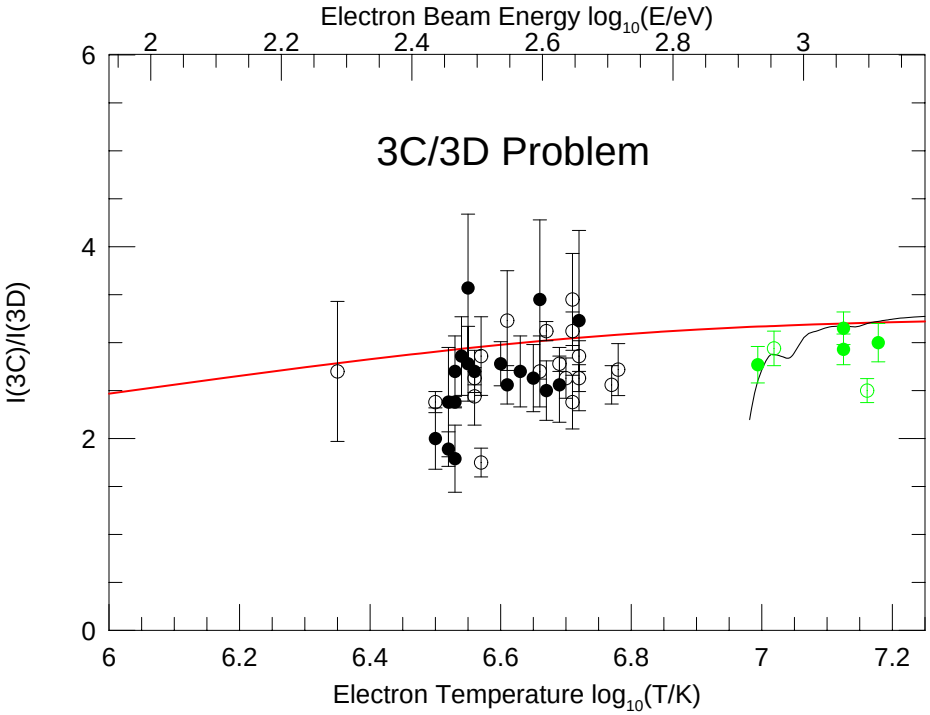

Fig. 2.— The Fe XVII 3C/3D line ratio as a function of electron temperature. The filled and open circles in the center of the figure are Chandra and XMM Newton observations for various stellar and cosmic sources. The EBIT measurements appear as filled and open circles at the far right-hand side of the graph. The Maxwellian-averaged theoretical calculations appear as the solid line, and a Gaussian average of the theoretical calculations (FWHM = 30 eV) is the wavy solid line going through the EBIT points. (Courtesy of G.X.Chen)

han by using a fully relativistic multi-configuration Dirac Fock R-matrix method, including levels up through n=5. He has demonstrated convergence in his calculations, and estimates an error of about 5% in the calculated line ratio. When the new theoretical results are Maxwellian-averaged, the solid line in Figure 2 is obtained. If, however, a Gaussian average of these same theoretical values is performed, using a full-width half maximum (FWHM) of 30 eV, the wavy curve lying on top of the EBIT measurements is obtained. (The EBIT measurements are the filled and open circles on the right-hand side of the graph; a Gaussian average is most appropriate for describing the EBIT electron distribution function.)

It is clear from Figure 2, that if one needs a Maxwellian average, the theoretical calculations are absolutely essential, as the EBIT experiments are best described by a Gaussian averaged electron distribution function, and the line ratios obtained for each kind of average are quite different. More discussion of the electron impact excitation cross sections of Fe

XVII at the Livermore EBIT are being reported (E9[1]) at this meeting (Brown et al.). The NIST EBIT group (E33) is extending its work on Fe XVII to other neon-like ions (J. Tan et al.) Also in these Proceedings, N. Brickhouse (M1) will discuss why the 3C/3D line ratio has been so low in solar observations.

3.3. Line-broadening Diagnostics of Brown Dwarfs and Extrasolar Planets

Over the last ten years, the continuing discovery and the increasingly accurate characterization of brown dwarfs and extrasolar giant planets have created an exciting frontier in stellar and planetary astronomy. Brown dwarfs and extrasolar giant planets can be grouped together as substellar mass objects (SSMOs) in that they have significant overlap in terms of the parameter space of atmospheric temperatures, densities, and thus similar chemistries as well. The development of accurate spectral diagnostics and the refinement of the theoretical models to describe these objects are among the most important challenges for the future.

In the optical and near-infrared spectra of L-dwarfs and T-dwarfs the resonance lines of sodium (at 589 nm) and potassium (at 770 nm) appear as prominent absorption features, profoundly broadened due to collisions with the most abundant neutral species in the atmospheres of these objects: molecular hydrogen and He. The broadening is such that the line wings extend as much as 100 nm either side of line core. Although no full spectrum of an extrasolar planet has yet been observed, theoretical models of certain classes of exoplanets also predict these broadened absorption resonance lines to be prominent features in the visible and near-infrared.

At the Harvard-Smithsonian Center for Astrophysics we have a joint theoretical and experimental program to provide accurate line profiles for the resonance lines of K and Na, broadened by collisions with H_2 and He. We have found it advantageous to benchmark theory at particular temperatures and pressures obtainable in the laboratory, and then theory can be used to explore other parameter spaces. In brief, the double-beam absorption spectroscopy experiment features a Mach-Zehnder interferometer which provides the optical arrangement for the double-beam absorption paths, and a 3 m Czerny-Turner grating spectrograph, fitted with an array detector which disperses and records the spectra from 360 nm to 900 nm. The theoretical calculations focus on the line wings of the alkali-perturber systems, which are sensitive to the details of the interaction potentials. Densities are low enough that we can use the binary approximation. The line-broadening results from the change in transition energy of the system during the course of the collision, as described by the energy difference between the 4s- and 4p-type potential curves. Of particular interest are "satellite" features which arise at extrema of the difference potentials, and can be very sensitive to the temperature. Thus satellites can be very useful diagnostics.

A paper in this Proceedings will give more details regarding the theoretical calculations

[1]Editorial note: Presentation codes are given in Appendix B, p. 306

and experimental details (Shindo et al., E6) on this work. Another paper by Lillestolen and Hinde (T3) reports on independent theoretical calculations of the line-broadening of K and Na by collisions with He.

4. Concluding Remarks

The close-coupling of Astronomy and Laboratory Astrophysics is particularly important in times of severe budgetary constraints. Astrophysics must help set the priorities regarding the LabAstro research that is needed, but astronomers must understand the necessity of testing new theoretical methods and experimental techniques on systems which are most tractable, before larger, more complex systems can be treated with confidence.

There is room for considerable improvement at the interfaces between the LabAstro researchers ("data providers") and the databases, the modelers and the observers. Much can be lost at each of these interfaces. The lack of support for the development, updating and maintaining of databases is very serious. In addition, there is a tremendous need for critically evaluated data, which can help to identify areas in which new LabAstro research is necessary.

Finally, there are a number of challenges for the Astronomy community. The first is understanding the accuracy (or lack thereof) of LabAstro "data", and appreciating how this impacts the astrophysical interpretations. The second is addressing the question as to whether LabAstro databases should become part of the National Virtual Observatory (NVO). And ultimately, it is essential that astrophysicists, realizing the importance of LabAstro to their science, support more funding for this research from within Astronomy programs, particularly at NASA and at NSF.

Some of this material is based upon work supported by NASA under Grant NAG5-12751. I thank J. Babb, N. Brickhouse, G.X. Chen, V. Kharchenko, and A. Dalgarno for valuable discussions.

REFERENCES

Brown, G.V., Beiersdorfer, P., Liedahl, D.A., Widmann, K., & Kahn, S.M. 1998, ApJ, 502, 1015

Chen, G.X. & Pradhan, A.K. 2002, Phys. Rev. Lett., 89, 013202

Chen, G.X. 2006, *private communication*

Cravens, T.E. 1997, Geophys. Res. Letters, 24, 105

Laming, J.M. *et al.* 2000, ApJ, 545, L161

Lisse, C.M. *et al.* 1996, Science, 274, 205

INVITED TALK *NASA LAW*, February 14-16, 2006, UNLV, Las Vegas

The Gaseous Disks of Young Stellar Objects

A. E. Glassgold

Astronomy Department, University of California, Berkeley, CA 94720

aglassgold@astron.berkeley.edu

ABSTRACT

Disks represent a crucial stage in the formation of stars and planets. They are novel astrophysical systems with attributes intermediate between the interstellar medium and stars. Their physical properties are inhomogeneous and are affected by hard stellar radiation and by dynamical evolution. Observing disk structure is difficult because of the small sizes, ranging from as little as 0.05 AU at the inner edge to 100-1000 AU at large radial distances. Nonetheless, substantial progress has been made by observing the radiation emitted by the dust from near infrared to mm wavelengths, i.e., the spectral energy distribution of an unresolved disk. Many fewer results are available for the gas, which is the main mass component of disks over much of their lifetime. The inner disk gas of young stellar objects (henceforth YSOs) have been studied using the near infrared rovibrational transitions of CO and a few other molecules, while the outer regions have been explored with the mm and sub-mm lines of CO and other species. Further progress can be expected in understanding the physical properties of disks from observations with sub-mm arrays like SMA, CARMA and ALMA, with mid infrared measurements using *Spitzer*, and near infrared spectroscopy with large ground-based telescopes. Intense efforts are also being made to model the observations using complex thermal-chemical models. After a brief review of the existing observations and modeling results, some of the weaknesses of the models will be discussed, including the absence of good laboratory and theoretical calculations for essential microscopic processes.

1. Introduction

Understanding how stars form is a natural development of several decades of study of molecular clouds, the birthplace of stars. A crucial stage in the process is the accretion phase, which involves several steps: the collapse of the nascent *molecular cloud core* (typical size about 0.1 pc), the formation of the *accretion disk* (extending in some cases from 0.05 AU to

1000 AU), and the development of *accretion flows* from the disk to the star and accompanied by outflows or winds from the inner regions of the disk. Starting from core collapse, the buildup of a low-mass star takes only a few million years, and the major accretion phase much less. Accretion is difficult to study because of the intrinsically inhomogeneous and dynamical nature of the dusty gas involved in the process. The observations require a multi-wavelength approach that runs the gamut from X-ray to mm wavelength bands. The biggest observational obstacle to progress is the very small size of star-forming regions. Resolving a region of the size of our own planetary system (35 AU) at the distance of the nearby star-forming cluster in Taurus (140 pc) requires a resolution of 0.25″. Although such observations are possible in some of the relevant wavelength bands, imaging the most dynamic parts of the accretion process requires improvements in angular resolution of 1-2 orders of magnitude.

Theoretical modeling of accretion disks around low-mass stars in the process of formation presents its own challenges. Many of the simplifications used in interstellar cloud chemistry do not apply. For example, a common procedure in interstellar chemistry is to calculate the temporal evolution of hundreds of species at constant density under the assumption of complete photon shielding. This makes no sense for disks around YSOs because it is the irradiated surface regions that are usually observed. Not only is the assumption of complete shielding invalid for these regions, but account has to be taken of both the stellar and the interstellar radiation fields, each with its own spectral distribution. Even for an axi-symmetric disk, the physical properties vary in both the radial and the vertical direction, so the assumption of a uniform medium is also invalid. In the rest of this report, After a brief review of the observations, I will try to give the flavor of the current state of theoretical modeling of the disks around low-mass YSOs, emphasizing some of the barriers to future progress, especially those involving the incompleteness of the underlying microscopic data.

2. Observations of Disks

Most information about YSO disks comes from the spectral energy distribution (SED) which is dominated by emission from dust. SEDs are usually obtained by spatially-unresolved low-spectral resolution observations across the spectrum from near-infrared through mm wavelengths (made with several telescopes). A particularly interesting example (Lahuis et al. 2006) shown in Figure 1 includes *Spitzer* mid-infrared spectra as well as data from five other systems, 2MASS, VLT, ISO, SCUBA and IRAM. This is a rare case of a disk seen nearly edge on, so the silicate feature near 10μm and various molecular features, both solid and gas phase, are seen in absorption.

Molecules are more often observed in emission from the optically thin surface regions of YSO disks, as reviewed at Protostars and Planets V (PPV, Najita, Carr, Glassgold & Valenti 2006; Dullemond et al. 2006). The main tool has been the ro-vibrational transitions of the abundant and robust CO molecule, although OH and H_2O have also been detected in

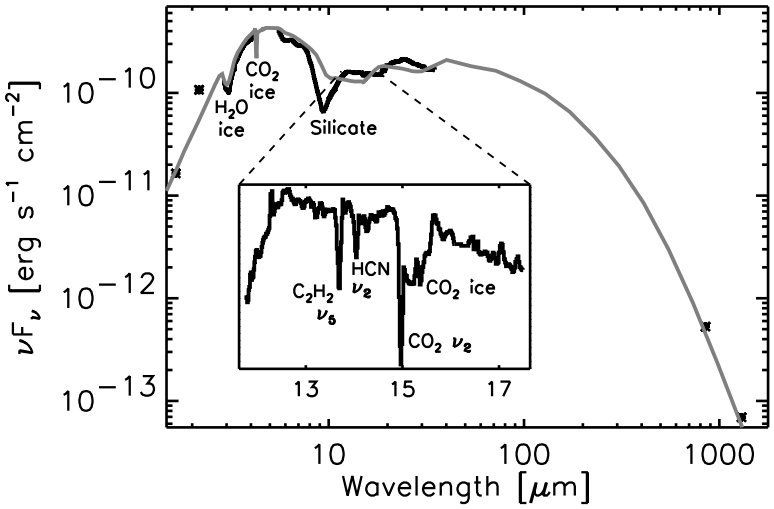

Fig. 1.— Composite SED of the edge-on disk around IRS 46 (Lahuis et al. 2006) from 1.25 μm to 1,3 mm including the full *Spitzer* spectrum from 10-37 μm (dark line). The light line is a theoretical model; the insert shows gas and solid molecular features.

the NIR. The absorption lines ascribed to C_2H_2, HCN, and CO_2 in Figure 1 represent the first detection of polyatomic species in these disks, and much attention can be expected to be given to such species in the near future.

The most important result of the NIR observations of both the fundamental and overtone bands of CO (4.6 μm and 2.3 μm, respectively) is that the emission lines arise from warm gas (1000-1500 K) down to considerable depth ($10^{21}-10^{22}$cm^{-2}) in the inner disk (0.05−2.0 AU). Although well known for more massive YSOs (e.g., Najita et al. 1996 and references therein), Najita et al. (1993) have confirmed that they are a ubiquitous presence in the low-mass YSOs known as T-Tauri stars. The presence of the warm gas is confirmed by the detection of UV fluorescence from Ly-α pumped H_2 (e.g., Herczeg et al. 2002), also seen in many sources (reviewed by Najita et al. 2006 at PPV). The observation of the H_2 fluorescence provides a direct demonstration of the existence of vibrationally excited H_2 because the threshold for the excitation of the Lyman and Werner band electronic transitions from the ground state occurs at a shorter wavelength than Lyα.

The gas in disks can also be probed by mm and sub-mm transitions of CO, as has been demonstrated persuasively by observations with the IRAM Plateau de Bure interferometer and more recently at the SMA (reviewed at PPV by Guilloteau, Dutrey & Ho 2006). The difficulty here is that the available spatial resolution had been limited to about 1″, but significant progress will be possible with the new generation interferometric arrays, such as SMA and CARMA, and eventually ALMA.

3. Thermal-Chemical Modeling

The goals and methodology of theoretical modeling of YSO disks are basically the same as for any astrophysical system: The abundance of the diagnostic species and the excitation of the upper level of a relevant spectral line need to be calculated. But this requires a knowledge of the physical properties, i.e., the density, temperature, and ionization fraction. For disks the physical properties themselves depend on the abundances, i.e, on the chemistry. Thus one needs to calculate the temperature and the abundances simultaneously in a self-consistent manner. This kind of calculation is particularly challenging for disks because they are basically inhomogeneous with the physical properties varying over very wide ranges. An additional complication is that radiation fields of quite different character are involved, e.g., far ultraviolet (FUV) just below the H Lyman limit and X-rays with photon energies well above the ionization potential of H. For studying the inner disk, e.g., within 10 AU, the main source of the radiation is the young star itself, or from it's close environment such as the magnetosphere.

It is ironic that the X-ray properties of YSOs are better known than the FUV. The former has been studied with a series of X-ray observatories, such as ROSAT, *Chandra* and XMM-NEWTON, that are sensitive to the main band of YSO emission from 0.1 to 10 keV. On the other hand, HST cuts off at just before the crucial FUV band from 91 to 110 nm. Utilizing FUSE has helped, although there are problems (e.g., Bergin et al. 2003). Figure 2 shows an example of the X-ray spectrum of a YSO in the Orion Nebula Cluster observed with the *Chandra* COUP project (Getman et al. 2005). It shows how measured YSO spectra (highlighted by the solid line) are typically fit by two thermal components (lighter lines) with temperatures of order 1 keV and 3 keV. The hard component is responsible for the wide-ranging effects of X-rays incident on disks, e.g., the absorption length of a 3-keV X-ray photon is $\sim 10^{23}\,\mathrm{cm}^{-2}$. By way of contrast, a 100 nm FUV photon is absorbed over a column that is 200 times smaller. A significant fraction of the total luminosity of a low-mass YSO is emitted in X-rays, i.e., $L_{\rm X}/L_{\rm bol} \sim 10^{-4} - 10^{-3}$. Thus for the nearby T-Tauri star TW Hya, only 56 pc distant, $L_{\rm X} \sim 10^{30}\,\mathrm{erg\ s}^{-1}$. The luminosity in FUV band from 91 to 110 nm is about the same (Bergin et al. 2003), but it is of course absorbed over a much smaller column. Another aspect of the UV emission of YSOs is the presence of a strong Lyα line, discussed above in the context of its role in exciting H_2 flourescence; it's flux is typically 10% of the FUV flux from 91 to 110 nm. In principle, both X-ray and FUV radiation should be included in thermal-chemical modeling of YSO disks, but many of the papers in the literature tend to emphasize just one or the other.

Figure 3 shows vertical temperature profiles obtained by Glassgold, Najita, and Igea (2004; henceforth GNI04) with a thermal-chemical model based on the dust model of D'Alessio et al. (1999) for a generic T-Tauri star. The accretion rate is $10^{-8}\,M_\odot$ and the radial distance is 1 AU. The gas temperature is plotted against perpendicular column density measured from the top of the atmosphere. The dashed line at the bottom shows the dust temperature rising above its midplane value due to the increase in illumination with height of small dust grains

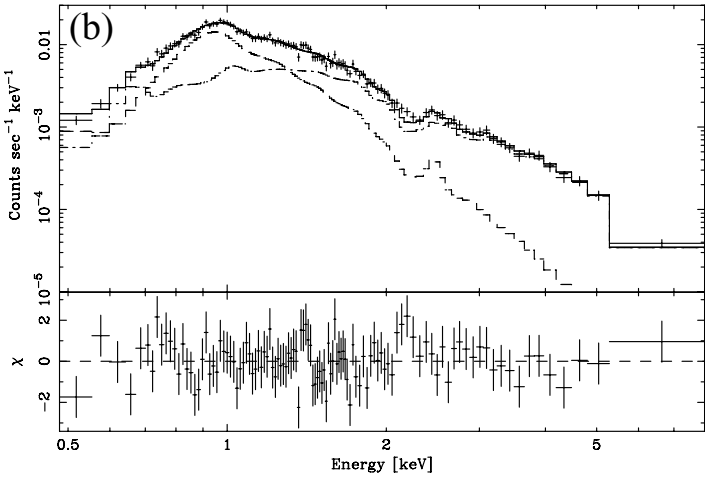

Fig. 2.— X-ray energy spectrum of COUP source # 567 from Fig. 6b of Getman *et al.* (2005). The spectrum is fit (heavy solid line) by a conventional two-temperature model with $kT_1 = 0.8\,\mathrm{keV}$ and $kT_2 = 3.1\,\mathrm{keV}$ (lighter lines). The residuals present evidence of Ne-Fe anomalies often seen in strong flares. The sub-keV emission is absorbed out by intervening material with a column density, $N_\mathrm{H} = 2 \times 10^{21}\mathrm{cm}^{-2}$.

by the stellar radiation field. The dust undergoes a modest temperature inversion, going from about 140 K at midplane to 450 K at the top of the disk. Above a vertical column density $\sim 10^{22}\mathrm{cm}^{-2}$, the gas temperature begins to depart from that of the dust and, due to strong surface heating, eventually manifests a very large temperature inversion high up in the atmosphere.

The figure contains several curves because GNI04 considered the possibility that the surface layers of protoplanetary disks are heated by the dissipation of mechanical energy as well as by stellar photons. This might arise through the interaction of a wind with the upper layers of the disk or through the effects of viscous dissipation associated with outward angular momentum transport. Since the theoretical understanding of these processes is incomplete, GNI04 adopted a phenomenological approach. The currently most widely accepted mechanism for viscous accretion is the magneto-rotational instability (Balbus and Hawley 1991; Stone et al. 2000), which leads to the local heating formula,

$$\Gamma_\mathrm{acc} = \frac{9}{4}\alpha_h \rho c^2 \Omega, \tag{1}$$

where ρ is the mass density, c is the isothermal sound speed, Ω is the angular rotation speed, and α_h is a phenomenological parameter that depends on how the turbulence dissipates. For example, one can argue, on the basis of simulations by Miller and Stone (2000), that midplane turbulence generates waves which, on reaching the diffuse surface regions, produce shocks and heating. Wind-disk heating can be represented by a similar expression on the basis of dimensional arguments. Equation 1 is essentially an adaptation of the expression

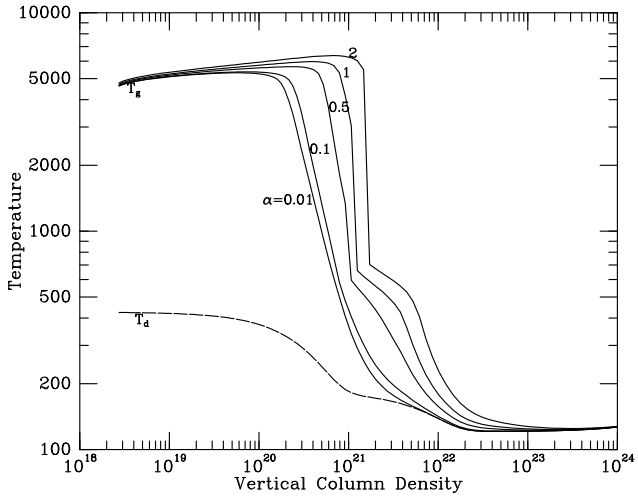

Fig. 3.— Temperature profiles from GNI04 for the surface of the protoplanetary disk atmosphere discussed in §3.1 of the text. The radial distance is 1 AU, and the mass-loss rate is $10^{-8} M_{\odot} \mathrm{yr}^{-1}$. The dashed line is the dust temperature of D'Alessio *et al.* (1999). The solid curves are gas temperature profiles labeled by the coefficient α in Eq. 1. The choice $\alpha = 0.01$ closely follows the limiting case of pure X-ray heating. The abscissa is vertical column density in cm^{-2}, and the ordinate is temperature in degrees K.

for the volumetric heating in an α-disk model, where α in general can depend on position. GNI04 used the notation α_h to distinguish its role for heating the disk atmosphere with the phenomenological formula in Equation 1 (unfortunately, the subscript has been dropped from the figure).

The top layers of the atmosphere are fully exposed to X-rays, and the temperature there at 1 AU is ∼5000 K. Further down, there is a warm transition region (500–2000 K), composed mainly of atomic hydrogen but with carbon fully associated into CO. The complete conversion from atomic H to H_2 is reached at a column density of $6 \times 10^{21}\,\mathrm{cm}^{-2}$, with more complex molecules such as water predicted to form deeper in the disk. The location and thickness of the warm molecular region depends on the strength of the surface heating. Thus X-ray heating dominates the transition region for $\alpha_h < 0.01$, whereas mechanical heating dominates when $\alpha_h > 0.1$. This result, that the warm transition region is mainly atomic hydrogen but has carbon fully associated into molecules, has the important consequence that CO rotation-vibration transitions are easily excited because of the large collisional excitation cross sections for H + CO inelastic scattering (much larger than for molecular hydrogen).

Gas temperature inversions can also be produced by UV radiation operating on small dust grains and PAHs, as demonstrated by the thermal-chemical models of Jonkheid et al. (2004), Kamp and Dullemond (2004) and Nomura and Millar (2005). Jonkheid et al. use the D'Alessio et al. (1999) model and focus on the disk beyond 50 AU. At this radius, the

gas temperature can rise to 800 K or 200 K, depending on whether small grains are well mixed or settled. For a thin disk and a high stellar UV flux, Kamp and Dullemond obtain temperatures that asymptote to several 1000 K inside 50 AU. Of course these results are subject to assumptions made about the stellar UV, the abundance of PAHs, and the growth and settling of dust grains. Nomura and Millar (2005) made a detailed thermal model of a disk that includes the formation of H_2 on grains, destruction via FUV lines, and excitation by Lyα photons. The gas at the surface is heated primarily by the photoelectric effect on dust grains and PAHs (with a dust model appropriate for interstellar clouds, i.e., one showing little grain growth). Both interstellar and stellar UV radiation are included, the latter based on observations of TW Hya. The gas temperature at the surface of their flaring disk model reaches 1500 K at 1 AU. Their model partially accounta for the H_2 fluorescence measurements of Herczeg et al. (2002), although the theoretical fluxes fall short by a factor of five or so. A possible defect in their model is that the calculated temperature of the disk surface may be too low, a problem that might be remedied by reducing the UV attenuation by dust and by including X-ray or other surface heating processes. Disk chemistry was reviewed extensively at Protostars and Planets V by Bergin et al. (2006), Dullemond et al. (2006) and Najita et al. (2006)

4. Challenges for Laboratory Astrophysics

The initial attempts to model gaseous disks have had some success in understanding the warm atmospheric gas inferred from observations of CO and H_2. Many other modeling challenges and opportunities await future observations of these and more complex species. The discussion in the previous sections shows that theoretical modeling is complicated. It is also fraught with uncertainties and ambiguities characteristic of our limited understanding of YSO disks. Much of the uncertainty comes from the unknown (and time-dependent) gas distribution and from our poor understanding of how disks are heated. Rather than focusing here on these astrophysical issues, we highlight the gaps in the microphysical basis of thermal-chemical modeling. Although we mainly referred to our own calculations in §3 for purposes of illustration, there is almost universal agreement on the laboratory astrophysics needs of modelers of YSO disks.

4.1. Gas Phase Reactions

The occurence of a chemically active transition zone between hot and cold gas layers clearly indicates that, at least in the inner regions of disks, neutral radical reactions are essential for understanding disk chemistry. Modeling of disks involves temperatures that range below 500 K. Since most neutral reactions have activation energies, their rate coeffcients are small in this temperature range, and they are difficult to measure, especially radical-

radical reactions. A good example is the well-studied reaction, $O + H_2 \rightarrow OH + H$, important for the synthsesis of CO and H_2O. Most modelers agree on the rate coefficent above 500 K, but disagree at lower temperatures. The experiments in this temperature range are typically 30 years old. Two other consideration are relevant. First, the inverse reaction, $OH + H \rightarrow O + H_2$, is also important, but its rate coeffcient has not been measured and has to be calculated from detailed balance; again, there is considerable uncertainty in its value at low tempertaure. Second, the fine structure of the O atom becomes important in this temperature range. Sims et al. (2006) have taken up this challenge in a number of interesting cases. Similar considerations apply to S atom reactions, for which measurements are badly needed.

Another class of poorly known reactions affecting disk chemistry is low-energy (< 1 eV) charge exchange. Mutiply-charged heavy ions are produced by hard ($\gtrsim 1$ KeV) X-rays via the Auger effect. Disk gas is incompletely ionized, and the abundance of atomic hydrogen is large in the atmosphere exposed to X-rays. The higher ions rapidly charge transfer to H, but the rate coeffcients for low ions are poorly known at low temperatures. The case of S was discussed at the last workshop (Glassgold 2002). The ions S^{q+} with $q = 3 - 6$ are produced by keV stellar X-rays. The high-level calculation of Stancil et al. (2001) shows that $S^{4+} + H \rightarrow S^{3+} + H^+$ is fast down to low temperatures, but the situation for S^{3+} and S^{2+} remains problematic. Early calcuations of $S^{2+} + H \rightarrow S^+ + H^+$ (Butler & Dalgarno 1980, Christensen & Watson 1981) suggest that the rate coeffcient is small at low tempertaures. Calculations of S^{3+} charge exchange (Bacchus-Montabonel 1998; Labuda et al. 2004) are restricted to keV energies. The recent study of $H^+ + S \rightarrow S^+ + H$ by Zhao et al. (2005) sheds new light on the temperature variation of this important reaction. Theoretical and experimental studies of S^{2+} and S^{3+} charge transfer with H at low energies are badly needed. These essentially unknown rates affect the abundance ratio S II/S I and thus the intensities of both optical/infrared forbidden and mid-infrared fine structure transitions from disks and jets. Similar gaps in low-energy charge exchange rate coeffcients are commmon among the ions of other heavy elements.

Many if not most of the reactions needed by chemical modelers have not been studied experimentally or theoretically. This is a serious problem since literally thousands of reactions are potentially important. In the case of ion-molecule reactions, approximate rules hold in many cases, at least when the reactions are highly exothermic. But general rules are more difficult to obtain for neutral reactions, especially at very low tempertaures. A similar statement applies to charge transfer reactions below 1 eV, as just discussed. A useful response to this situation is to identify the handful of reactions that are truly critical in a particular problem and to then make the case for experimental measurement. Of course some modelers have always chosen to work with small selected sets of reactions. More recently, several groups have attempted to determine the crucial reactions for particular problems by objective criteria and to assess the effect of rate coefficent uncertainties on modeling results (e.g., Wiebe, Semenov, & Henning 2003; Semenov, Wiebe, & Henning 2004; Wakelam et al. 2005).

The Munich group has focused on the implications for disk modeling (Semenov, Wiebe, & Henning 2004; Semenov, Henning, & Vasyunin 2006, private communication). They find that the largest effects of uncertainties in rate coeffcients are radical-radical reactions near the midplane and radiative-association reactions above the midplane.

4.2. Dust and PAHs

Grain surface chemistry almost certainly plays a critical role in disks because of the high density and the low temperatures near the midplane. Not too close to the star, the temperature are low enough to condense volatile species, even those with small dipole moments such as CO. Granted that freeze-out is likely to occur, we need to understand what kinds of reactions occur on grain surfaces and how the products are removed. It is generally assumed that a one result of grain surface chemistry is the hydrogenation of heavy atoms and radicals, leading for example to the production of ammonia and methane. More complex reactions occur that are crucial for understanding the chemical environment of disks in the region of planet formation. All of the disk modelers contacted for this review agree that laboratory experiments and theoretical simulations of adsorption and desorption processes (especially photodesorption) as well as surface reactivity are among the most important needs of disk chemistry. Further studies of molecular hydrogen formation on surfaces would also be of great interest, e.g., by going to higher temperatures and including deuterium reactions.

A similar consensus recommendation applies to PAHs, which have been observed in disks. If their abundance turns out to be similar to that found in the interstellar medium ($\sim 10^{-7}$ relative to total hydrogen), then PAHs obviously have a role to play in the ionization and chemistry of YSO disks. The role of PAHs in the heating of disks is clearly demonstrated by the calculations of Nomura & Millar (2005), referred to in §3. Another aspect of PAHs in disks that merits laboratory study is the effect of X-rays on their chemical structure and abundance. Among the basic chemical processes of PAHs that need further investigation are electron attachment, photoionization and neutralization.

5. Conclusion

We have tried to show that improving observational capabilities will soon begin to reveal the distribution of the gas in the disks of YSOs, and that this will contribute significantly to our understanding of how low-mass stars form. Detailed thermal-chemical modeling of the physical properties of the disks will be required to interpret the observations. But the astrophysics of the disks calls for complex models and, to obtain meaningful results, significant uncertainties in the underlying physical and chemical processes need to be reduced by theoretical and laboratory studies. Work is particularly needed on the following topics:

1. Dust surface chemistry
2. PAH structure, spectroscopy and chemical kinetics
3. Gas phase neutral radical reactions and radiative association
4. Ionic reactions of atoms and radicals, including charge exchange of 1st and 2nd ions
5. Photo processes, including photodissociation and especially photodesorption from grains
6. X-ray interactions with dust grains and PAHs
7. Collisional excitation rates
8. Critical evaluation and maintenance of reaction rate data bases

This work was supported in part by a grant from the National Science Foundation. The author would like to acknowledge with thanks the comments of many colleagues on the needs of Laboratory Astrophysics for disk modeling: Yuri Aikawa, Thomas Henning, David Hollenbach, Inga Kamp, Dmitri Semenov, Ewine van Dishoeck and Karen Willacy. He would also like to thank Phil Stancil for continuing advice on the status of charge-exchange reactions.

REFERENCES

Bacchus-Montabonel, M.-C. 1998, Chem. Phys. 228, 181

Balbus, S. A. & Hawley J. F. 1991, ApJ, 376, 214

Bergin, E. A., Aikawa, Y., Blake, G. A. & van Dishoeck, E. F. 2006, Protostars and Planets V, B. Reipurth, San Francisco: ASP, in press

Bergin, E., Calvet, N., D'Alessio, P., & Herczeg, G. J. 2003, ApJ, 591, L159

Butler, S. & Dalgarno, A. 1980, ApJ, 241, 838

Christensen & Watson, W. D. 1981, Phys. Rev. A24, 1331

Dullemond, C., Hollenbach, D., Kamp, I. & D'Alessio 2006, Protostars and Planets V, B. Reipurth, San Francisco: ASP, in press

D'Alessio, P., Calvet, N., and Hartmann, L., Lizano, S., and Cantoó, J. 1999, ApJ, 527, 893

Getman, K. V., Flaccomio, E., Broos, P. S., Grosso, N., Tsujimoto, M., Townsley, L. K., *et al.* 2005, ApJS, 160, 319

Glassgold, A. E. 2002, NASA Laboratory Astrophysics Workshop, F. Salama, NASA/CP-2002-21186, 56

Glassgold, A. R., Najita, J. & Igea, J. 2004, ApJ, 615, 972

Guilloteau, S., Dutrey, A. & Ho. P 2006, Protstars and Planets V, B. Reipurth, San Francisco: ASP, in press

Herczeg, G. J., Linsky, J. L., Valenti, J. A., Johns-Krull, C. M. & Wood, B. E. 2002, ApJ, 572, 310

Jonkheid, B., Fass, F. G. A., van Zadelhoff, G.-J. & van Dishoeck 2004, A&A, 428, 511

Kamp, I. & Dullemond, C. P. 2004, ApJ, 615, 991

Labuda, M., Tergiman, Y. S., Bacchus-Montabonel, M.-C. & Sienkiewicz, J. E. 2004, Chem. Phys. Letts. 394, 446

Lahuis, F., van Dishoeck, E., Boogert, A. C. A. et al. 2006, ApJ, 636, L145

Miller, K. A. & Stone, J. M. 2000, ApJ, 534, 298

Najita, J. R. , Carr, J. S., Glassgold, A. E. and Valenti, J. A. 2006, Protostars and Planets V, B. Reipurth, San Francisco: ASP, in press

Najita, J., Carr, J. S., Glassgold, A. E., Shu, F. H. & Tokunaga, A. T. 1996, ApJ, 462, 919

Najita, J., Carr, J. S. & Mathieu, R. D. 2003, ApJ, 589, 931

Nomura H. & Millar T. J. 2005, A&A, 438, 923

Sims, I. R. 2006, Astrochemistry: Recent Successes and Current Challenges, D. C. Lis, G. A. Blake & E. Herbst, Cambridge : Cambridge, 97

Semenov, D., Wiebe, D. & Henning, Th. 2004, A&A, 417, 93

Stancil. P. C., Turner, A. R., Cooper, D. L., Schultz, D. R., Raković, M. J., Fritsch, W. & Zygelman, B. 2001, J. Phys. B 34. 2481

Stone, J. M., Gammie, C. F., Balbus, S. A., and Hawley, J. F. (2000), Protostars and Planets IV, V. Mannings, A. P. Boss & S. S. Russell, Tucson : Univ. Arizona Press), 589

Wakelam, V., Selsis, F., Herbst, E. & Caselli, P. 2005, A&A, 444, 833

Wiebe D., Semenov, D. & Henning, Th. 2003, A&A, 399, 177

Zhao, L. B., Stancil, P. C., Gu, J.-P., Liebermann, H.-P., Funke, P., Buenker, R. J. & Kimura, M. 2005. Phys. Rev. A71

INVITED TALK *NASA LAW*, February 14-16, 2006, UNLV, Las Vegas

Astrochemistry and the Role of Laboratory and Theoretical Support

E. Herbst[1]

Department of Physics,The Ohio State University, Columbus, OH 43210

herbst@mps.ohio-state.edu

ABSTRACT

We emphasize some current needs of astrochemists for laboratory data. The data are urgently required both to detect molecules in assorted regions and to produce robust models of these regions. Three areas of laboratory-based research are particularly crucial and yet are not being studied in the United States: (i) reactions more complex than the formation of molecular hydrogen occurring on interstellar grain analogs, (ii) molecular spectroscopy in the THz (far-infrared) region of the electromagnetic spectrum, and (iii) gas-phase kinetics of reactions leading to complex molecules. Without solid knowledge of many unstudied but key reactions, both in the gas and on grains, astrochemists will not be in position to keep up with the large amount of new information expected to come from the next generation of telescopes.

1. Introduction: the Role of Spectroscopy

There would exist no astrochemistry, and very little astronomy, if there were no atomic and molecular spectroscopy. Spectroscopy, the study of the interaction of matter and radiation, lies at the heart of any detailed research concerning material in the heavens. In the interstellar medium of our galaxy and others, the rich molecular nature of the gas phase of dense objects has been discovered and studied mainly through the rotational spectroscopy of molecules, typically detected in the microwave, millimeter-, and submillimeter-wave regions. But, in order to use spectroscopy for remote sensing, one must know the spectra thoroughly from laboratory studies. The current generation of millimeter-wave and submillimeter-wave telescopes are useful for molecular research only because of relevant laboratory studies by

[1]Also: Departments of Chemistry and Astronomy

groups such as our own, which pioneered the movement from the microwave to higher frequency regions.

In recent years, we have used our ultra-fast ("FASSST") spectrometer, most often in the frequency range 100-400 GHz, to study organic molecules somewhat larger than those currently known to be in interstellar clouds in an attempt to help astronomers find these species in space. Typically located in warm regions associated with protostars, known as hot cores or hot corinos, the molecules are interesting in an astrobiological sense as prebiotic species and tell us infomation concerning the physical conditions of the sources. Although these molecules had been studied before at lower frequencies, it is very difficult to predict a higher-frequency spectrum from lower-frequency data because of the non-rigidity of the molecules. And yet it is the higher frequencies that are often associated with molecules in warm star-forming regions, since the higher temperatures allow excitation to higher molecular energy levels, which are typically separated more widely than the lower-lying rotational levels. Some of the species recently studied in our laboratory are the alcohols *n*-propanol ($CH_3CH_2CH_2OH$ and *iso*-propanol ($(CH_3)_2CHOH$), the ethers ethyl methyl ether ($C_2H_5OCH_3$) and diethyl ether ($C_2H_5OC_2H_5$), the ester ethyl formate ($HCOOC_2H_5$), and the pre-biotic species oxiranecarbonitrile (c-$H_2COC(H)CN$) and cyanoformamide ($NCCONH_2$) (Maeda et al. 2006; Fuchs et al. 2003; Medvedev et al. 2003; Behnke et al. 2004; Winnewisser et al. 2005). In addition to these studies, we have collaborated with the group at the University of Cologne in Germany to study molecular spectra in the 1-2 THz region for a small number of species, most importantly the radical methylene (CH_2), which was subsequently detected in the galactic center based on our measurements (Michael et al. 2003; Bruenken et al. 2004; Polehampton et al. 2005).

Although the Cologne group does study some molecules in the THz region, this group has lost both its long-term funding and its leader, Gisbert Winnewisser, who has retired. Moreover, it is probably the only group in the world that specializes in this arcane area of spectroscopy. Yet, with the advent in the near future of telescopes operating in the THz, or far-infrared, region of the electromagnetic spectrum, much more laboratory spectroscopic information will be required to make sense of the huge amounts of data to be taken. Both SOFIA, an airborne project developed by NASA in collaboration with the German Space Agency, and Herschel, a space telescope developed by ESA with the help of NASA, will operate in regions where little laboratory information has been obtained. Without a crash program in laboratory THz studies, a catastrophe may be in the making.

Since most rotational spectral lines in the interstellar medium are detected in emission, it is often necessary to understand the details of molecular excitation via rotationally inelastic collisions in order to convert a line of a given intensity into a column density. The laboratory study of rotational excitation is very difficult, and most of the needs of astronomers have been met by theoretical chemists. Since the death of the late Sheldon Green, the US has seen very little if anything in the way of such theoretical studies, which are performed mainly by groups in the United Kingdom and France.

2. Astrochemistry and Star Formation

By the analysis of molecular spectra and continua from dust particles, astrochemists have succeeded in understanding much of the evolution of cold cores of dense interstellar clouds into stellar and planetary systems. Each of the sources along the way, however, is likely to be heterogeneous and to have a complex history. In order to understand the sources in some detail, one must study the chemical processes that create and destroy molecules and use these processes in large simulations in which both chemistry and possibly dynamical changes take place. If the chemistry is to be used to try to unravel the history and heterogeneity of the sources, a secure knowledge of all of the chemical processes occurring is needed.

The evolutionary path to low-mass star formation goes through the following stages (Herbst 2005a): (i) *cold cores*, defined as stable regions characterized by a rich gas-phase chemistry, a density of 10^4 cm^{-3} chiefly composed of H_2, and a temperature of 10 K; (ii) *prestellar cores*, which are collapsing regions maintaining a near constant temperature of 10 K but developing a central condensation of density$10^{\ 5-6}$ cm^{-3} where gas-phase species heavier than hydrogen and helium are strongly accreted onto the dust particles, (iii) *protostars*, observed as regions in which the central condensation has started to heat up, a disk of gas and dust has formed in the equatorial plane, violent jets flow out along the poles, and the envelope warms to a temperature of 100-300 K, constituting what is now known as a "hot corino"; (iv) *protoplanetary disks and T Tauri stars* in which adolescent stars have formed surrounded by dense disks of gas and dust.

All of the objects along the path to low-mass star formation have been modeled using large chemical networks, mainly consisting of gas-phase processes. State-of-the-art gas-phase networks contain about 4000 reactions and 400 species. These networks include the UMIST collection (http://www.udfa.net/) and the Ohio State compendium (http://www.physics.ohio-state.edu/ eric/research.html), both of which are available for use by astrochemists. Use of these networks, however, is afflicted by the following four classes of chemical problems:

- uncertain rate coefficients
- incomplete chemistry (missing reactions, missing temperature ranges)
- incorrect chemistry or rate coefficients
- non-thermal chemistry (e.g. ortho/para effects).

Let us consider these problems in turn. The effect of uncertain rate coefficients can be quantified by a Monte Carlo analysis in which each rate coefficient and its uncertainty is treated as a log-normal distribution Wakelam et al. (2005). For any given simulation, each rate coefficient in the set of approximately 4000 is chosen randomly according to its distribution. The simulation is rerun many times, until good statistics are obtained. Unless non-linear effects occur, the calculated concentration for each molecule at any given time

is a distribution of values with a Gaussian or near-Gaussian shape. Thus, the output of the model calculation is an abundance and its uncertainty at all times for each species. Moreover, the important reactions leading to the uncertainties can be elucidated, so that improved measurements can be made.

The effect of incomplete chemistry is hard to deduce, since it is difficult to prove that a large model is incomplete. For temperatures higher than 300 K, however, it should be realized that many endothermic reactions and exothermic reactions with barriers will start to become competitive. The use of standard databases designed more for low temperatures can be fraught with error, although the UMIST data base makes some allowance for endothermic processes. In our view, two types of additional calculations can be considered. First, one can consider inclusion of the backwards reactions for all reactions in the networks, using a thermal equilibrium argument to deduce the rate coefficients for the reverse processes. If there is a significant difference in the results, other processes may also have to be taken into account. If there is no difference in the results, it is likely that the network is still valid. Secondly, at still higher temperatures one can consider the use of a true thermodynamic approach in which the global free energy is minimized.

Incorrect chemical processes or those with incorrect rates in the networks can only be discovered by laboratory or theoretical studies. Four examples to be considered are the three specific processes:

$$CH_3^+ + H_2O \longrightarrow CH_3OH_2^+ + h\nu, \tag{1}$$

$$H_2D^+ + H_2CO \longrightarrow H_2DCO^+ + H_2, \tag{2}$$

$$CH_3OH_2^+ + H_2CO \longrightarrow HC(OH)OCH_3^+ + H_2, \tag{3}$$

and the general case of dissociative recombination reactions. Reaction (1), a radiative association, has recently been measured to proceed orders of magnitude more slowly than predicted at temperatures under 100 K (Luca et al. 2002). This reaction was supposed to lead to the formation of methanol in cold cores by the dissociative recombination of protonated methanol with electrons. Reaction (2) was supposed to start the deuteration of formaldehyde, eventually leading to the isotopologs HDCO and D_2CO by cycles of deuteration and dissociative recombination reactions. It has been calculated, however, that the reaction proceeds to make the deuterated ion H_2COD^+, with the deuteron on the opposite side of the molecule from the two protons (Osamura et al. 2005). The ensuing dissociative recombination produces H_2CO + D and possibly HCOD + H, neither of which set of products contains HDCO. The third reaction was supposed to lead to the production of protonated methyl formate in hot cores, starting from methanol that had earlier evaporated from grain mantles due to rising temperatures. The reaction does not occur because of a large activation energy barrier (Horn et al. 2004). Finally, storage-ring results indicate that a class of dissociative recombination reactions involving hydrogen-rich ions, designated AH^+, tend to fragment strongly rather than to give off a single H atom to product the species A (Geppert et al. 2006). Examples include the $CH_3OH_2^+ + e^-$ reaction, in which the methanol

+ H channel is only 6%, and the $CH_3OHCH_3^+ + e^-$ reaction, in which no dimethyl ether + H is found. The latter reaction was considered to be critical in forming dimethyl ether in hot cores at temperatures of 100-300 K. New methods of synthesizing this and other complex hydrogen-rich species thought to form in hot cores via dissociative recombination will have to be studied. One possibility is to consider the chemistry occurring on warming grain surfaces (Garrod & Herbst 2006). Other possibilities involve high-energy processes such as irradiation on grain surfaces. Clearly, more work is needed to understand the formation of organic molecules in warm environments.

Non-thermal effects can strongly affect rates of reaction. Consider the reaction system

$$H_3^+ + HD \rightleftharpoons H_2D^+ + H_2, \tag{4}$$

which is exothermic in the left-to-right direction by 230 K. In a 10 K cloud, the backwards, endothermic reaction is exceedingly slow and the equilibrium lies far to the right, so that H_2D^+ becomes highly abundant compared with H_3^+, a process known as fractionation (Herbst 1982). Indeed, the equilibrium constant is larger than 10^9. But, suppose that the system is not strictly thermal, and that a small portion of ortho-H_2 in its $J = 1$ state exists. This state can collide with H_2D^+ to exothermically excite that ion to its lowest ortho state, designated 1_{11}. The reaction between the lowest ortho states of H_2 and H_2D^+ to form H_3^+ + HD is exothermic rather than endothermic, so is much faster than the thermal value. This non-thermal effect can possibly be quantified by actual measurements of deuteration in cold sources as a function of temperature (Maret 2006).

3. Grain-Surface Chemistry

Much of the chemistry that occurs in cold regions of the interstellar medium occurs on the surfaces of dust particles, probably by the well-known Langmuir-Hinshelwood, or diffusive, mechanism. The most important reaction, the production of molecular hydrogen from the surface recombination of two hydrogen atoms, has drawn the most attention, both theoretically and in the laboratory. Although other processes have received some study, much more work remains to fully quantify them. Among the most important reactions are those involving atomic hydrogen, since this atom is bound particularly weakly to surfaces and so diffuses readily, and is also quite reactive. Consider, for example, what happens to an oxygen atom that lands on and sticks to a grain surface. When a hydrogen atom lands on the same grain, it diffuses readily and eventually finds the rather stationary oxygen atom. Like the situation in the gas phase, an OH complex is formed. But, unlike the situation in the gas phase, the grain acts as a third body to remove sufficient energy from the complex to stabilize it. The newly formed OH radical is as reactive as its precursor, and associates with the next diffusing hydrogen atom to form water. Unlike the case of H_2, which is weakly bound to the grain and so eventually desorbs back into the gas, water is strongly bound and remains on the surface. In cold regions, this conversion of O into H_2O continues and eventually

forms a sizable mantle of water ice, which is detected through infrared absorption. Similar processes result in the hydrogenation of carbon atoms into methane and of nitrogen atoms into ammonia, although competing reactions in the gas phase lower the amount of C and N available for accretion. As the cold cloud ages, copious amounts of carbon monoxide are produced in the gas, and some accretes onto grain surfaces. Despite the fact that the reaction possesses some activation energy, the hydrogenation of surface CO, designated CO(s), into HCO:

$$\mathrm{CO(s) + H(s) \longrightarrow HCO(s)} \tag{5}$$

occurs. Once the radical HCO is formed, a second hydrogenation occurs facilely to form formaldehyde, H_2CO. Subsequent hydrogenation to form the methoxy radical and finally methanol has been detected in one laboratory but not in others (Hidaka et al. 2004). The sequence of reactions is important because no mechanism is known to produce methanol efficiently in the gas. More work is clearly needed.

Not only are few surface reactions understood in any degree of detail, but the desorption of molecules back into the gas is also poorly understood. In the absence of star formation, the cloud remains cold so that no species heavier than hydrogen and helium can evaporate into the gas. Yet, to account for the gas-phase abundance of methanol in cold sources, there must be some non-thermal desorption mechanisms. Possible mechanisms considered are cosmic ray heating of the grains, photodesorption, and desorption via the energy generated in exothermic chemical reactions, but none has been studied in the degree of detail needed to understand fully what occurs in interstellar clouds. Once again, more work is clearly required.

So far, almost all experiments on analogs of interstellar dust particles have been undertaken with large surfaces rather than with actual dust particles. It has been shown that there are severe differences in the reaction mechanisms for processes on small particles and those on larger surfaces, especially when in the former case, there is on average less than one reactive surface species per grain (Herbst 2005b). Consequently, experiments that probe surface chemistry on and desorption from tiny particles would be most desirable.

4. Summary

Laboratory astrophysics has been and still is crucial for understanding star formation and other processes in the interstellar medium. At this time, some key projects can be identified, including the following:

1. the sustained study of molecular spectroscopy in the THz regime,

2. the calculation and measurement of rotationally inelastic rate coefficients,

3. the improvement of gas-phase chemical networks by (i) the reduction of uncertainties in rate coefficients, (ii) the correction of errors, and (iii) the inclusion of non-thermal processes when necessary,

4. the study of grain-surface chemistry, especially involving products more complex than molecular hydrogen.

This work was supported in part by grants from NASA for laboratory astrophysics and the National Science Foundation for astrochemistry.

REFERENCES

Behnke, M., Medvedev, I. R., Winnewisser, M., De Lucia, F. C., & Herbst, E. 2004, ApJS, 152, 97

Bruenken, S., Michael, E. A., Lewen, F., Giesen, Th., Ozeki, H., Winnewisser, G., Jensen, P., & Herbst, E. 2004, Can. J. Chem., 82, 676

Fuchs, U., Winnewisser, G., Groner, P., De Lucia, F. C., & Herbst, E. 2003, ApJS, 144, 277

Garrod, R. T., & Herbst, E. 2006, A&A, submitted

Geppert, W. et al. 2006, Faraday Discuss., in press

Herbst, E. 1982, A&A, 111, 76

Herbst, E. 2005a, J. Phys. Chem., 109A, 4017

Herbst, E. 2005b, J. Phys. Conf. Ser., 6, 18

Hidaka, H., Watanabek, N., Shiraki, T., Nagaoka, A., & Kouchi, A. 2004, ApJ, 614, 1124

Horn, A., Møllendal, H., Sekiguich, O., Uggerud, E., Roberts, H., Herbst, E., Viggiano, A. A., & Fridgen, T. D. 2004, ApJ, 611, 605

Luca, A., Voulot, D., & Gerlich, D. 2002, WDS'02(Prague) Proceedings of Contributed Papers, Part II, 294

Madea, A., De Lucia, F. C., Herbst, E., Pearson, J. C., Riccobono, J., Trosell, E., & Bohn, R. 2006, ApJS, 162, 428

Maret, S. 2006, at a talk given at the Symposium "Molecules in Space" at the 231st meeting of the American Chemical Society.

Medvedev, I. R. et al. 2003, ApJS, 148, 593

Michael, E. A., Lewen, F., Winnewisser, G., Ozeki, H., Habara, H., & Herbst, E. 2003, ApJ, 596, 1356

Osamura, Y., Roberts, H., & Herbst, E. 2005, ApJ, 621, 348

Polehampton, E. T., Menten, K. M., Bruenken, S., Winnewisser, G., & Baluteau, J.-P. 2005, A&A, 431, 203

Wakelam, V., Selsis, F., Herbst, E., & Caselli, P. 2005, A&A, 444, 883

Winnewisser, M., Medvedev, I. R., De Lucia, F. C., Herbst, E., Koput, J., Sastry, K. V. L. N., & Butler, R. A. H. 2005, ApJS, 159, 189

INVITED TALK *NASA LAW*, February 14-16, 2006, UNLV, Las Vegas

Herschel and the Molecular Universe

A. G. G. M. Tielens[1]

Kapteyn Astronomical Institute, PO Box 800, 9700 AV Groningen, The Netherlands & MS 245-3, NASA Ames Research center, Moffett Field, CA 94035-1000

atielens@mail.arc.nasa.gov

F. P. Helmich[2]

SRON Netherlands Institute for Space Research & Kapteyn Astronomical Institute, PO Box 800, 9700 AV Groningen, The Netherlands

F.P.Helmich@sron.rug.nl

ABSTRACT

Over the next decade, space-based missions will open up the universe to high spatial and spectral resolution studies at infrared and submillimeter wavelengths. This will allow us to study, in much greater detail, the composition and the origin and evolution of molecules in space. Moreover, molecular transitions in these spectral ranges provide a sensitive probe of the dynamics and the physical and chemical conditions in a wide range of objects at scales ranging from budding planetary systems to galactic and extragalactic sizes. Hence, these missions provide us with the tools to study key astrophysical and astrochemical processes involved in the formation and evolution of planets, stars, and galaxies. These new missions can be expected to lead to the detection of many thousands of new spectral features. Identification, analysis and interpretation of these features in terms of the physical and chemical characteristics of the astronomical sources will require detailed astronomical modeling tools supported by laboratory measurements and theoretical studies of chemical reactions and collisional excitation rates on species of astrophysical relevance. These data will have to be made easily accessible to the scientific community through web-based data archives. In this paper, we will review the Herschel mission and its expected impact on our understanding of the molecular universe.

---

[1]Herschel-HIFI Project scientist, SOFIA project scientist, and Network Coordinator of the Molecular Universe

[2]Calibration scientist of HIFI and Administrative Coordinator of the Molecular Universe

Europe has recognized the challenge in analyzing and interpreting the multitude of data that will become available and has has started a closely knit but wide ranging scientific network in the area of molecular astrophysics. This "Molecular Universe" network combines 21 institutes in 9 countries and is funded through the Marie Curie program of the European Union. The network will support training of some 15-20 young graduate students and postdocs. The scientific emphasis of the network will be on a deeply interwoven research program on molecular complexity in space and chemistry in regions of star formation. The results of this network will be made widely available through data bases and web interfaces. This network will be described in some detail and the challenges of research in this highly interdisciplinary research area will be discussed.

1. Herschel

The Herschel Space Observatory (Originally called Far InfraRed and Submillimeter Telescope (FIRST)), the European Space Agency's 4^{th} cornerstone mission, is designed for observations in the far-infrared/sub-millimeter wavelength region. Herschel is equipped with a 3.5 meter diameter reflecting telescope and instruments cooled to close to absolute zero. Herschel will be launched together with Planck on an Ariane 5 with an expected launch date of mid-2008. After a four-month journey from Earth, Herschel will spend a nominal mission lifetime of three years in orbit around the second Lagrange point of the Sun-Earth system (L2). The ESA Science Center is located at ESTEC Noordwijk, The Netherlands (http://www.rssd.esa.int/herschel). NASA is a minor partner providing hardware for HIFI (mixers and local oscillator chains for bands 5 and 6) and SPIRE (spider web detectors) as well as sofware support. The US Herschel Science Center is located at IPAC, Caltech (http://www.ipac.caltech.edu/Herschel/). Details on the Herschel mission are provided in Pilbratt (2004).

Herschel has three instruments, HIFI, PACS and SPIRE, which cover the $\sim 60-600$ μm with imaging and and medium-to-high resolution spectroscopy capabilities. These instruments are optimized to address key questions in astronomy: "the origin and evolution of galaxies in the early universe", "the origin and evolution of stars and their interaction with the interstellar medium", and "the composition and evolution of the molecular universe". Many of the key objects and evolutionary stages of the universe – including protostars, protoplanetary systems, dying stars and their ejecta, and starburst and massive black hole activity in the centers of galactic nuclei – are hidden from view by copious amounts of cold dust and gas. Most of the energy emitted by these objects escapes therefore in the far-infrared and sub-millimeter spectral windows. Conversely, this implies that Herschel will provide a unique handle on the physical and chemical conditions and the processes taking place in these environments.

1.1. HIFI

The Heterodyne Instrument for the Far-Infrared (HIFI) is a high resolution heterodyne spectrometer with 6 bands covering almost completely the 150 to 600 μm range. The mixer bands use SIS (Superconductor-Insulator-Superconductor) mixers in bands 1-5 and HEB (Hot Electron Bolometer) mixers in band 6. Instantaneous Intermediate Frequency bandwidth is 4 GHz in Bands 1-5 and 2.4 GHz in Band 6. The resolving power can be as high as $\nu/\Delta\nu = 10^7$ or 0.3 km/s. Specifically, two available backends, the wide band spectrometer (dual acousto-optical) and the high resolution spectrometer (autocorrelator), provide frequency resolutions of 140 kHz, 280 kHz, and 1 MHz. HIFI is being designed by a large consortium spread over 13 countries led by Thijs de Graauw, SRON Groningen, The Netherlands. Details on HIFI and its science program can be found in de Graauw et al. (2004).

Table 1: HIFI characteristics

Band	1	2	3	4	5	6
Frequency coverage	480-640	640-800	800-960	960-1120	1120-1250	1410-1910
FWHM [arcsec]	41	29	25	21	18.5	14.5, 12.5
Sensitivity[a][10^{-18} W m^{-2}	1.3	2.9	4.9	8.1	24	34

[a] [5σ in 1 hr at $R = 10^4$]

1.2. PACS

The Photodetector Array Camera and Spectrometer (PACS) is a bolometer array photometer and a photoconductor array imaging spectrometer operating at a wavelenght range between 60 and 210 μm. The characteristics of the three band imaging photometer are summarized in Table 2. Observations are made simultaneously in two bands: the 170 μm band and either the 75 or 110 μm band. The two filled bolometer arrays consist of 32×16 (red) and 64×32 (blue) pixels covering the same field of view (1.75×3.5 arc minutes). The point source detection limit is approximately 3 mJy (5σ in 1 hr).

In addition, PACS has an integral field spectrometer which covers simultaneously the spectral bands from 57 to 105 and 105 to 210 μm. The $47'' \times 47''$ field of view (5×5 pixel array) is rearranged via an image slicer on two 16×25 stressed Ge:Ga detector arrays. The spectral resolution is ~ 1500 and the line sensitivity is $\sim 5 \times 10^{-18}$ W m^{-2} 5σ in 1 hr. PACS is being designed and built by a consortium of institutes and university departments from across Europe under the leadership of Principal Investigator Albrecht Poglitsch located at

Table 2: PACS imaging characteristics

Central wavelength [μm]	75	110	170
Band range [μm]	60-85	85-130	130-210
FWHM [arcsec]	6	8	12
Spectral resolution, $\lambda/\Delta\lambda$	2.5	2.8	2.1

Note. — Observations are simultaneously in two bands: the red band (170 μm) and either of the two blue bands (75/110 μm).

Max-Planck-Institute for Extraterrestrial Physics (MPE), Garching, Germany. Details on PACS and its science program can be found in Poglitsch et al. (2004).

1.3. SPIRE

The Spectral and Photometric Imaging Receiver (SPIRE) consists of a 3-band imaging photometer and a Imaging Fourier Transform Spectrometer and will operate at wavelengths between 200 and 670 μm. The imaging photometer array on SPIRE consists of hexagonally packed spider-web bolometer arrays, which observe simultaneously in three bands (Table 3). The field of view is 4×8 arc minutes but requires jiggling or scanning for full spatial coverage. The point source sensitivity is ~ 3.5 mJy 5σ in 1 hr.

Table 3: SPIRE imaging characteristics

Central wavelength [μm]	250	360	520
FWHM [arcsec]	18	25	36
Spectral resolution, $\lambda/\Delta\lambda$	~ 3	~ 3.2	~ 3

Note. — Observations are simultaneously in three bands.

The Fourier Transform Spectrometer has a field of view of 2.6 arc minutes diameter. The two bolometer arrays cover 200-325 and 315-670 μm with 37 and 19 hexagonally close-packed detector arrays, respectively. The FWHM will vary between approximately 20 to 25 and 30 to 50 $''$ in the short wavelength and long wavelength band, respectively. The spectral resolution can be adjusted between 0.04 and 2 cm^{-1}, corresponding to a resolution of 1000 to 20 at 200 μm. SPIRE is being developed by a consortium of European and American institutes, led by Matt Griffin at the Physics and Astronomy Department of Cardiff University. Details on

SPIRE and its science program can be found in Griffin et al. (2004).

1.4. The Herschel science program

About 7000 hours of science time will be available per year. About one-third of the total observing time is reserved for the consortia which build the three instruments. The other two-third is open to the world-wide science community. While Herschel builds upon the legacy of the Infrared Astronomical Satellite (IRAS), the Infrared Space Observatory (ISO) and the Spitzer Space Telescope in the far-infrared, the sub-millimeter sky is largely unexplored and hence Herschel is often called *its own precursor mission*. To accomodate this sub-millimeter survey aspect, a considerable portion of the total science time (> 50 %) on Herschel is envisioned to be part of large scale coherent programs, so-called Key Programs. These Key Programs should exploit unique Herschel capabilities to address (an) important scientific issue(s) in a comprehensive manner, require a large amount of observing time to be used in a uniform and coherent fashion, and produce a resulting, well-characterized dataset of high archival value. Indeed, much of the instrument teams guaranteed time is expected to be devoted to Key Programs. The large format arrays of PACS and SPIRE are designed for sensitive large scale mapping programs and the PACS and SPIRE guaranteed time Key Programs are centered on large scale, unbiased surveys of the high redshift universe and of star forming regions. For HIFI, the guaranteed time Key Programs focus on unbiased spectral surveys of the molecular universe and on studies of the many rotational transitions of water. In addition, many open time Key Programs are also expected. These Key programs will be selected before launch – first, the guaranteed time and then the open time. After launch and the science verification phase, a call for normal (guaranteed time followed by open time) programs will be issued.

2. HIFI preparatory science

Interpretation and analysis of the data obtained by the Herschel instruments will require careful science preparation. Requirements for preparatory science are summarized in the Herschel preparatory science white paper available at the links section of http://www.sron.nl/hifiscience/. Here, we will focus on the data required for HIFI. The unbiased spectral surveys – central to the HIFI Key Program – will return 1000's of spectral lines for selected sources while the water studies will bring line intensities of rotational transitions in broad samples of sources. The goal of these observations are to understand the physics and chemistry of these regions, including the physical conditions, dynamics, the molecular inventory, and the underlying chemical processes.

Molecular astrophysics is a highly interdisciplinary field of research as schematically illustrated in figure 1. The identication of species in space requires direct comparison of

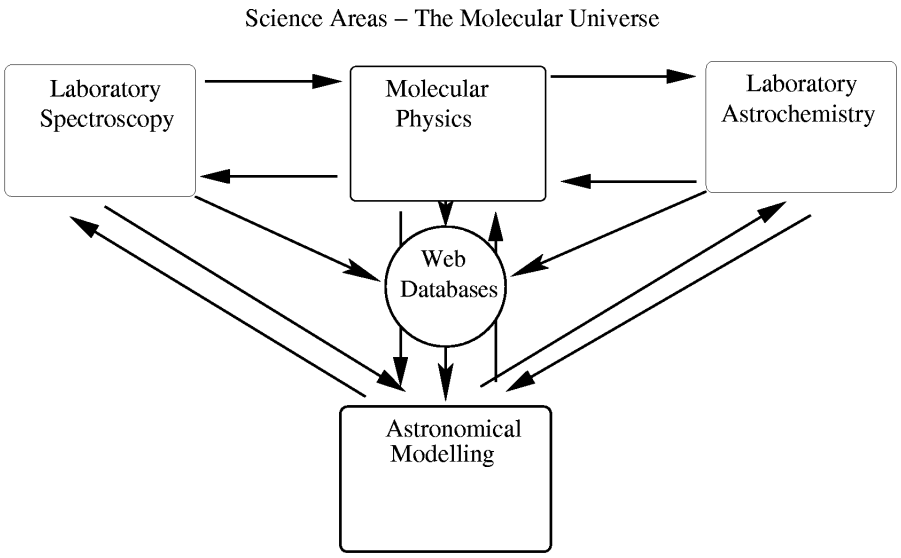

Fig. 1.— Schematic figure illustrating the multidisciplinary aspect of the field of molecular astrophysics. The four different science areas involved in molecular astrophysics are characterized by the use of different techniques and methods. In addition, the results of studies will have to be made available to the whole science community through data bases accessible through special webportals.

the particular frequencies of emission or absorption lines observed in interstellar space with spectroscopic measurements of known species in a controlled laboratory experiment. In order to interpret the measured laboratory spectra in terms of the properties of the molecule (ie., assign lines to specific transitions), supporting molecular physics quantum chemical calculations are required. The intensities of lines observed in space depend directly on the collisional excitation rates of the molecules with the predominant collision partners, atomic or molecular hydrogen and helium. These rates will have to be calculated using quantum chemical methods or measured in the laboratory by molecular physicists. Such rates can then be used by astronomers to determine the physical conditions and the abundances of the molecules involved in the interstellar regions where the emission or absorption arises. The abundances of interstellar molecules are the result of a balance between formation and destruction reactions. The rate coefficients and products of relevant reactions will have to be measured under astrophysically relevant conditions (eg., low temperature, low pressure) or quantum chemically calculated. These rates can then be used by astronomical modelers to calculate the abundances of interstellar species. For example, when specific reaction routes have been proposed and the relevant reaction rate coefficients measured, abundances of new species can be predicted. Laboratory spectroscopists can then measure their transition frequencies while molecular physicists can calculate their excitation rate coefficients. All of these data together can then be used by astronomical modelers to predict the expected line intensities of new species which can then be targeted in specific searches.

It is clear that action in all of these four science areas has to be strongly interwoven in studies of the molecular universe. However, in general, no single group, institute, or often even nation has expertize or experience in all relevant areas. Thus, support for the analysis and interpretation of space-based data requires large scale, global efforts involving many scientists at different institutes and in different countries collaborating together on interdisciplinary projects, each contributing only a subset of the solution. This requires a new structure for astronomy, resembling the structure in science areas such as particle physics where much of the research effort has, for decades, been organized in large scale projects connected to, for example, CERN.

The other challenging aspect is that, while these areas serve great needs for the astronomical community, research on frequencies or oscillator strength of molecular transitions is not forefront science within molecular physics. Likewise, chemical reactions involving astronomically relevant species is not central to modern chemistry. Funding support for activities in these areas is therefore not high priority within these communities. As a result, national space agencies will have to take the lead in organizing, coordinating, and funding these scientific activities.

2.1. The Molecular Universe

In Europe, the importance of a proper preparation for Herschel and ALMA in this area is well recognized and a consortium "The Molecular Universe" has been formed, consisting of 21 institutes in 9 European countries all active in various aspects of molecular astrophysics. The coordinator and co-coordinator of this consortium are Xander Tielens and Marie-Lise Dubernet. This consortium has been funded by the European Union as a Marie Curie Research and Training Network through the 6^{th} Frame Work Program (FP6). More details on teh network can be found at http://molecular-universe.obspm.fr/.

One main activity of the Molecular Universe network is to train the next generation of researchers in this field. The Marie Curie program provides specific support for this and the network has obligated itself to provide 444 person months of training. This will include training of 9 Early Stage Researcher (ESR; eg., graduate students) and 5 (joint) Experienced Researchers (ER; eg., postdocs). These researchers are spread over the different institutes involved in the network. In addition, through the liberal use of secondments, all students and postdocs will spend part of their training at other institutes where they will acquire complementary skills required for productive research in this field. The training is also supplemented by a yearly summerschool where the different science aspects of the field of molecular astrophysics are covered at a level suitable for such an interdisciplinary mix of young researchers. Finally, the students and postdocs are offered an opportunity to present their scientific research at network meetings and workshops.

The other main activity of the network centers on an active and deeply interwoven

research program. These are focussed in the area of molecular complexity in space – comprising studies on water in the universe, carbon chemistry, and deuterium chemistry – and of chemistry in regions of star formation – including ionization along the star formation trail, nitrogen chemistry as tracer of protostellar condensations, and molecular tracers of shocks. We will highlight two topics here. 1) Within the "water in the Universe" theme, a wide range of studies are coordinated on the physics and chemistry of H_2O in astrophysical environments, including spectroscopy of high excitation levels, theoretical ro-vibrational excitation cross sections, experimental excitation cross sections, the astrochemistry of H_2O, and radiative transfer models of H_2O in astrophysical environments. 2) Similarly, the "carbon chemistry" theme organizes a range of investigations on the physics and chemistry of hydrocarbons in astrophysical environments such as experimental studies of reaction rate coefficients of hydrocarbons, spectroscopy of PAHs and carbon chains, excitation models for PAHs and carbon chains, and astrochemistry of PAHs and carbon chains.

2.2. Data bases and web interfaces

A wide dissemination of the fundamental data acquired within this field to the wider astronomical community is of key importance to the success of the planned space missions. The best tool for this is provided by data bases made accessible through special web-interfaces. Data bases exists in all relevant areas. For spectroscopy there is the JPL data base (http://spec.jpl.nasa.gov/ftp/pub/catalog/catdir.html), the Cologne data base (http://www.ph1.unikoeln.de/vorhersagen/), and the HITRAN data base at Harvard (http://www.cfa.harvard.edu/HITRAN/). In molecular physics, there are the data bases at Meudon (http://amdpo.obspm.fr/basecol/) and Goddard (http://data.giss.nasa.gov/mcrates/). Several astrochemistry databases exist, including UMIST (http://www.udfa.net), Ohio State (http://www.physics.ohio-state.edu/∼eric/research.html), and SWRI (http://amop.space.swri.edu). The cassis group in Toulouse has developed special tools for fitting pure rotational spectra (http://www.cesr.fr/∼walters/web_cassis/).

Despite this wide array of data bases, access by the community is still of great concern. First, the data that is included in these data bases require carefull and critical evaluation and validation. Preferably, this validation should be delegated to a small board of experts in the field who are qualified to carefully balance any conflicting experimental measurements and/or calculations. Such evaluation structures have been set up already in related fields such as combustion chemistry research community (eg., the PrIMe network). However, this requires man power and support and validation of data is presently generally not standard in these data bases. Second, many of these data base activities are performed as unheralded services to the community driven by personal conviction and commitment and are hardly or not supported by funding agencies. For example, the JPL spectroscopy data base has not been funded for several years, the Cologne data base has just lost its funding from the German equivalent of the national science foundation, the Goddard data base on molecular physics

has not been maintained since the untimely death of Sheldon Greene, and the astrochemistry data base at SWRI is no longer maintained after the retirement of Walter Huebner. Third, maintenance of data bases is not an area of growth – scientific growth, personal growth, or funding growth – and young scientists are not steered in this direction – and rightfully so ! The absence of funding, the loss of key scientists, and the lack of young influx threatens these endeavors right at the time when they are needed the most.

3. Conclusion

Analysis and interpretation of space missions require fundamental data on atomic, ionic and molecular species. Specifically, Spitzer, Herschel and SOFIA, as well as JWST need experimental and theoretical data on frequencies and oscillator strength of transitions of astrophysical relevance. This is a highly interdisciplinary field where physics and chemistry meet astronomy. The US has many researchers who are at the forefronts of these discisplines. However, typically, no single group or institute has the required expertize and experience to address all the relevant aspects and instead progress will have to come from large scale consortia where multiple partners bridge this gap. Astronomy will have to organize itself much like other branches of physics and chemistry have done earlier. NASA as well as other space agencies will have to take the lead in supporting such endeavors. Such funding support will also go a long way to convince young researchers to step into this field and provide these essential support studies. In addition, NASA and other agencies will have to start supporting efforts in the area of data bases and web interfaces. These will be key to make the results of such studies widely available to the astronomical "customer". Only when these challenges are met, will we be able to reap the full science benefit of the large money and manpower investments in space projects.

Europe has recognized the importance of organization and collaboration in this multidisciplinary field and has started such a concerted effort funded by the European Union. The US has to quickly follow suit if its science community does not want to lag behind in this effort. Initial steps have been taken by a group centered around Ben McCall (University of Illionois, Urbana) and Eric Herbst (The Ohio State University) with additional centers at, among others, the University of Colorado, Boulder (V. Bierbaum), the University of Georgia (N. Adams), and the University of Toledo (S. Federman). Additional centers of expertize in the area of molecular astrophysics are located at University of Arizona (L. Ziurys), Caltech (G. Blake), and Harvard (P. Thaddeus). There are also very active groups at NASA Centers including NASA Ames Research Center (L. Allamandola; F. Salama), JPL (J. Pearson), and Goddard Space Flight Center (J. Nuth). Together, these groups cover all the relevant expertize in molecular astrophysics. Compared to the total costs of NASA science missions, a modest investment of funding by NASA – covering joint students and postdocs as well as the networking aspects – will be able to crosslink the scientific efforts of these different groups and mold an integrated science area to the benefit of space sciences. This is a clear

case where the whole will be more than the sum of the parts.

This study is supported in part by the European Community's human potential Programme under contract MCRTN 512302, Molecular Universe.

REFERENCES

Poglitsch, A., et al., 2004, The dusty and molecular universe: a prelude to Herschel and ALMA, A. Wilson, ESA SP-577, p11

de Graauw, et al., 2004, The dusty and molecular universe: a prelude to Herschel and ALMA, A. Wilson, ESA SP-577, p23

Griffin, M., et al., 2004, The dusty and molecular universe: a prelude to Herschel and ALMA, A. Wilson, ESA SP-577, p17

Pilbratt, G., 2004, The dusty and molecular universe: a prelude to Herschel and ALMA, A. Wilson, ESA SP-577, p3

INVITED TALK *NASA LAW*, February 14-16, 2006, UNLV, Las Vegas

Comets

P. D. Feldman

Department of Physics and Astronomy, Johns Hopkins University, Baltimore, MD 21218

pdf@pha.jhu.edu

ABSTRACT

Spectroscopy of comets, in the X-ray and far-ultraviolet from space, and in the near infrared and millimeter from the ground, have revealed a wealth of new information, particularly about the molecular constituents that make up the volatile fraction of the comet's nucleus. Interpretation of these data requires not only proper wavelengths for identification but also information about the photolytic and excitation processes at temperatures typical of the inner coma (70–100 K) that lead to the observed spectral signatures. Several examples, mainly from *Far Ultraviolet Spectroscopic Explorer* and *Hubble Space Telescope* spectra of comets observed during the last few years, will be given to illustrate some of the current issues.

1. Introduction

Cometary spectroscopy has long had a synergistic relationship with laboratory spectroscopy, particularly concerning free radicals that are unstable in the laboratory environment. Historical examples include the discovery of C_3 before its identification in terrestrial laboratories (recounted by Herzberg 1971), and the identification of H_2O^+ in the plasma tail of comet Kohoutek (Wehinger et al. 1974). Beginning in the 1970s, the window of the electromagnetic spectrum began to open, extending to the identification of parent molecules in the infrared and microwave (Bockelée-Morvan et al. 2004) and to the final atomic dissociation products in the ultraviolet (Feldman et al. 2004). Following the fortuitous apparitions of two bright comets, C/1996 B2 (Hyakutake) and C/1995 O1 (Hale-Bopp) in 1996 and 1997, more than two dozen parent molecules have been identified (Crovisier & Bockelée-Morvan 1999; Crovisier et al. 2004). Isotope ratios, particularly the D/H ratio, in molecules such as HDO have been determined from millimeter observations (Bockelée-Morvan et al. 2004). The same period saw the unexpected detection of soft X-ray emission from comets, followed by intense laboratory and theoretical activity to explain the features of the observed emission (Krasnopolsky et al. 2004).

In this brief overview, I will summarize some of the recent results that illustrate the importance of laboratory and theoretical data in interpreting a broad range of cometary observations. I will give these examples in order of increasing wavelength, with a bit more emphasis on the far ultraviolet with which I am most familiar. The references cited will be largely recent reviews, rather than the original papers. For a comprehensive bibliography, the reader is referred to the recently published *Comets II* book (Festou et al. 2004) and the relevant chapters therein.

2. X-Rays

Prior to 1996, X-rays had not been detected in comets and the conventional wisdom was that they were unlikely to be produced in the cold, rather thin cometary atmosphere. The discovery of soft X-ray emission ($E < 2$ keV) from comet C/1996 B2 (Hyakutake) by the *Röntgen Satellite* (*ROSAT*) thus came as a surprise. Since then, X-ray emission has been detected from over a dozen comets using *ROSAT* and four other space observatories, the *Extreme Ultraviolet Explorer*, *BeppoSAX*, the *Chandra X-ray Observatory* (*CXO*), and *Newton-XMM* (Krasnopolsky et al. 2004). The earliest observations were at very low spectral resolution making it difficult to select amongst the possible excitation mechanisms: charge exchange, scattering of solar photons by attogram dust particles, energetic electron impact and bremsstrahlung, collisions between cometary and interplanetary dust, and solar X-ray scattering and fluorescence. The more recent *CXO* observations, at somewhat higher spectral resolution, favor the charge exchange of energetic minor solar wind ions such as O^{6+}, O^{7+}, C^{5+}, C^{6+}, and others, with cometary gas, principally H_2O, CO, and CO_2, as the primary mechanism. This mechanism would explain why the X-ray intensity appears to be independent of the gas production rate of the comet and that the peak emission is offset from the location of the comet's nucleus. This conclusion is also supported by recent laboratory work on the charge transfer of highly ionized species with cometary molecules (Beiersdorfer et al. 2003) and by theoretical calculations of state specific cascades (Kharchenko & Dalgarno 2001). The X-ray emission thus tells us more about the solar wind than about the gaseous composition of comets. Nevertheless, cometary X-rays provide an excellent example of how laboratory astrophysics, in both laboratory experiments and theoretical modeling, were brought to bear on an unexpected observational phenomenon.

3. Far-Ultraviolet

The *Far Ultraviolet Spectroscopic Explorer* (*FUSE*), launched in 1999, has provided access to the spectral region between 900 and 1200 Å at very high spectral resolving power (up to 20,000) although for comets, because of their extended nature, only a spectral resolution of ∼0.25 Å has been achieved. Four comets have been observed by *FUSE* and their spectra

in this region are unexpectedly rich, dominated by three Hopfield-Birge band systems of CO and atomic O and H lines. In addition, H_2 fluorescence pumped by solar Lyman-β has been detected (Feldman et al. 2002) as well as some three dozen unidentified emission lines (Weaver et al. 2002). However, only upper limits on Ar I, N_2, and O VI were obtained, the latter despite the prediction of strong doublet emission at 1031.9 and 1037.6 Å from the X-ray model of Kharchenko & Dalgarno (2001). Emission of the 1031.9 Å line was initially detected in comet C/2000 WM1 (LINEAR), but increased signal-to-noise ratio in the spectra of comet C/2001 Q4 (NEAT), observed in 2004, enabled an accurate determination of the wavelength of this feature and identified it as the H_2 (1,1) Q(3) Werner band line, fluorescently pumped by solar O VI (Feldman 2005). The corresponding Q(3) lines of the (1,3) band at 1119.1 Å and the (1,4) band at 1163.8 Å are also detected.

The problem with this interpretation was that a large population of H_2 molecules in the $v = 1$ vibrational level was required. It was also noticed that there was a broad satellite feature centered near the position of the P(40) line of the $C\,^1\Sigma^+ – X\,^1\Sigma^+$(0,0) band at 1087.9 Å that implied the presence of a hot, non-thermal population of CO rotational levels (Feldman et al., in preparation). Both populations result from the photodissociation of formaldehyde, the dynamics of which has been intensively studied, both experimentally and theoretically, for many decades (see, for example van Zee et al. 1993; Zhang et al. 2005, and references therein). The "molecular channel," leading to CO and H_2 as products, leaves the CO rotationally hot and the H_2 in several excited vibrational levels, the exact populations depending on the energy of the incident photon. H_2CO is also a minor comet species and has been detected in a number of recent comets both in the infrared and millimeter (Mumma et al. 2003; Biver et al. 2002, 2006) and its known abundance is able to account for the brightness of the observed CO and H_2 emissions. Moreover, the shape of the observed P-branch (the R-branch is at wavelengths below the detector cutoff) closely matches the population of J-levels seen in the laboratory spectra. A large population of higher H_2 vibrational levels can also account for some of the other unidentified features in the *FUSE* spectrum. As an example, pumping from the ground state $v = 2$ level of H_2 by solar Lyman-α photons can lead to a rich cascade spectrum from the $v = 1$ level of the excited B state (Lupu et al. 2006). The solar Lyman-β pumped lines described above require the H_2 to be in the ground vibrational level and these molecules are most likely produced in the secondary H_2O photodissociation branch to H_2 + O(^{1}D) (Slanger & Black 1982).

One of the initially unidentified features seen in the spectrum of comet C/2001 A2 (LINEAR) is at 1026.5 Å. This feature, together with a weaker feature at 1028.9 Å, appears as a satellite to the O I $2p^3 3d\ ^3D^o – 2p^4\ ^3P$ multiplet. It is identified as the O I intercombination multiplet $2p^3 3d\ ^5D^o – 2p^4\ ^3P$ (Feldman 2005). This multiplet does not appear at all in any of the terrestrial dayglow spectra recorded by *FUSE*, implying that electron impact excitation of atomic oxygen is negligible, and does not appear to have been reported in any astrophysical source to date. The $^5D^o$ state has two decay paths, the observed intercombination transition to the ground state, and cascade through allowed multiplets at 9261–9266 Å and 7772–

7775 Å to the $^5S^o$ level followed by the 1356 Å intercombination transition to the ground state. Recent calculations suggest that the branching ratio of the intercombination lines to the cascade lines is of the order 10^{-5} (Tachiev & Froese Fischer 2002), which would make observation of this multiplet extremely unlikely, contrary to this observation. This discrepancy remains to be resolved. We note that two lines of the cascade ^5P – $^5S^o$ multiplet at 7771.9 and 7774.2 Å appear (the third is blended), listed as unidentified, in the high resolution spectral atlas of comet 122P/de Vico (Cochran & Cochran 2002). The source of the $^5D^o$ excitation remains unknown, although charge exchange of oxygen ions degraded through successive charge transfers is a possibility that warrants further investigation.

4. Atomic Deuterium

Isotope ratios, particularly the abundance of D relative to H in water, are relevant to planetary formation scenarios and to the question of the delivery of water to the Earth's oceans (Owen & Bar-Nun 2002). The ratio of HDO to H_2O has been measured in only three very active comets; in 1P/Halley by *in situ* mass spectrometry, and by microwave spectroscopy in comets C/1996 B2 (Hyakutake) and C/1995 O1 (Hale-Bopp) (Bockelée-Morvan et al. 2004). The value of this ratio was found to be about twice that of terrestrial sea water for these three comets, but this represents a very small, biased sample. Except for a marginal detection of DCN, no other deuterated molecules have been detected in comets.

Weaver et al. (2004) reported the first direct detection of D I Lyman-α in comet C/2001 Q4 (NEAT) using the echelle mode of the Space Telescope Imaging Spectrograph (STIS) on *HST*. This line, ∼0.3 Å to the blue of the H I line, is clearly separated from both the cometary and geocoronal H I lines and appears at the correct geocentric velocity of the comet. One difficulty in interpreting the observed brightness is that the OD/OH branching ratio in HDO photodissociation varies with the energy of the incident photon (Vander Wal et al. 1991). OD was searched for but not found in longer wavelength STIS spectra. However, using a mean branching ratio there are still difficulties in modeling both the spectral and spatial profiles of the D I line. These difficulties may be related to the excess velocity of the D photofragment and suggest a closer look at the photodissociation dynamics of HDO.

5. Infrared and Microwave

We have already noted the direct detection of two dozen parent molecules, all but S_2 by means of infrared and radio frequency spectroscopy (Bockelée-Morvan et al. 2004; Crovisier et al. 2004). S_2 was first detected in the ultraviolet (A'Hearn et al. 1983) (its origin remains uncertain) while CO is the only parent observable in both the ultraviolet, infrared, and millimeter. This number of molecules is small compared with the known inventory of molecules in interstellar clouds. Upper limits for an additional two dozen species searched

for in comet Hale-Bopp have been given by Crovisier et al. (2004). Many of these are likely to be detected when a new facility, the *Atacama Large Millimeter Array* (*ALMA*) becomes operational. Crovisier et al. also list 16 unidentified radio lines in this comet.

Microwave spectroscopy has also provided measurements of a number of isotope ratios of molecules containing C, N, O and S atoms (Bockelée-Morvan et al. 2004). These measurements are complemented by very high resolution ground-based spectroscopy of visible band systems of CN and C_2. Another recent measurement is that of the ortho-to-para population ratios in the ground states of H_2O and NH_3, all of which seem to be lower than the statistical values, implying spin temperatures in the range of 25–35 K (Kawakita et al. 2004). The spin temperatures, which appear to be similar for all comets observed to date, are interpreted in terms of the temperature of the comet formation region in the protosolar nebula.

6. Outlook

Traditional cometary spectroscopy has expanded in recent years to include the spectral domains of X-rays, far-ultraviolet, infrared and millimeter. Significant contributions to cometary science have been made by orbiting observatories spanning this spectral range: *CXO*, *FUSE*, *HST*, *SWAS*, and *Odin*, amongst others. Recent (*Stardust, Deep Impact*) and current (*Rosetta*) comet missions will provide ground truth for the interpretation of spectroscopic data. New facilities, such as *ALMA*, will greatly enhance our ability to determine the volatile composition of comets and to trace their evolution from interstellar matter. There are still significant challenges in understanding the atomic and molecular physics of the cometary atmosphere, a long term issue being the identification of the large number of unidentified lines seen in high resolution spectra across the entire electromagnetic spectrum.

This work was supported in part by grants from NASA and from the Space Telescope Science Institute.

REFERENCES

A'Hearn, M. F., Schleicher, D. G., & Feldman, P. D. 1983, ApJ, 274, L99
Beiersdorfer, P., et al. 2003, Science, 300, 1558
Biver, N., et al. 2002, Earth Moon and Planets, 90, 323
Biver, N., et al. 2006, A&A, 449, 1255
Bockelée-Morvan, D., Crovisier, J., Mumma, M. J., & Weaver, H. A. 2004, in Comets II, ed. M. C. Festou, H. A. Weaver, & H. U. Keller (Tucson: Univ. of Arizona), 391
Cochran, A. L., & Cochran, W. D. 2002, Icarus, 157, 297
Crovisier, J., & Bockelée-Morvan, D. 1999, Space Science Reviews, 90, 19

Crovisier, J., Bockelée-Morvan, D., Colom, P., Biver, N., Despois, D., & Lis, D. C. 2004, A&A, 418, 1141

Feldman, P. D. 2005, Physica Scripta, T119, 7

Feldman, P. D., Cochran, A. L., & Combi, M. R. 2004, in Comets II, ed. M. C. Festou, H. A. Weaver, & H. U. Keller (Tucson: Univ. of Arizona), 425

Feldman, P. D., Weaver, H. A., & Burgh, E. B. 2002, ApJ, 576, L91

Festou, M. C., Keller, H. U., & Weaver, H. A. 2004, Comets II (Tucson: Univ. of Arizona)

Herzberg, G. 1971, The spectra and structures of simple free radicals. an introduction to molecular spectroscopy (Ithaca: Cornell University Press)

Kawakita, H., Watanabe, J.-I., Furusho, R., Fuse, T., Capria, M. T., De Sanctis, M. C., & Cremonese, G. 2004, ApJ, 601, 1152

Kharchenko, V., & Dalgarno, A. 2001, ApJ, 554, L99

Krasnopolsky, V. A., Greenwood, J. B., & Stancil, P. C. 2004, Space Science Reviews, 113, 271

Lupu, R. E., France, K., & McCandliss, S. R. 2006, ApJ, in press

Mumma, M. J., Disanti, M. A., dello Russo, N., Magee-Sauer, K., Gibb, E., & Novak, R. 2003, Advances in Space Research, 31, 2563

Owen, T. C., & Bar-Nun, A. 2002, in ASP Conf. Ser. 269: The Evolving Sun and its Influence on Planetary Environments, ed. B. Montesinos, A. Gimenez, & E. F. Guinan, 163

Slanger, T. G., & Black, G. 1982, J. Chem. Phys., 77, 2432

Tachiev, G. I., & Froese Fischer, C. 2002, A&A, 385, 716

van Zee, R. D., Foltz, M. F., & Moore, C. B. 1993, J. Chem. Phys., 99, 1664

Vander Wal, R. L., Scott, J. L., Crim, F. F., Weide, K., & Schinke, R. 1991, J. Chem. Phys., 94, 3548

Weaver, H. A., A'Hearn, M. F., Arpigny, C., Combi, M. R., Feldman, P. D., Festou, M. C., & Tozzi, G.-P. 2004, BAAS, 36, 1120

Weaver, H. A., Feldman, P. D., Combi, M. R., Krasnopolsky, V., Lisse, C. M., & Shemansky, D. E. 2002, ApJ, 576, L95

Wehinger, P. A., Wyckoff, S., Herbig, G. H., Herzberg, G., & Lew, H. 1974, ApJ, 190, L43

Zhang, X., Rheinecker, J. L., & Bowman, J. M. 2005, J. Chem. Phys., 122, 4313

NASA LAW, February 14-16, 2006, UNLV, Las Vegas

Laboratory Studies on the Formation of Carbon-Bearing Molecules in Extraterrestrial Environments: From the Gas Phase to the Solid State

C. S. Jamieson, Y. Guo, X. Gu, F. Zhang, C. J. Bennett, & R. I. Kaiser

Department of Chemistry, University of Hawaii at Manoa, Honolulu, HI 96822

kaiser@gold.chem.hawaii.edu

1. Introduction

A detailed knowledge of the formation of carbon-bearing molecules in interstellar ices and in the gas phase of the interstellar medium is of paramount interest to understand the astrochemical evolution of extraterrestrial environments (1). This research also holds strong implications to comprehend the chemical processing of Solar System environments such as icy planets and their moons together with the atmospheres of planets and their satellites (2). Since the present composition of each interstellar and Solar System environment reflects the matter from which it was formed and the processes which have changed the chemical nature since the origin (solar wind, planetary magnetospheres, cosmic ray exposure, photolysis, chemical reactions), a detailed investigation of the physicochemical mechanisms altering the pristine environment is of paramount importance to grasp the contemporary composition. Once these underlying processes have been unraveled, we can identify those molecules, which belonged to the nascent setting, distinguish molecular species synthesized in a later stage, and predict the imminent chemical evolution of, for instance, molecular clouds.

Laboratory experiments under controlled physicochemical conditions (temperature, pressure, chemical composition, high energy components) present ideal tools for simulating the chemical evolution of interstellar and Solar System environments. Here, laboratory experiments can predict where and how (reaction mechanisms; chemicals necessary) in extraterrestrial environments and in the interstellar medium complex, carbon bearing molecules can be formed on interstellar grains and in the gas phase. This paper overviews the experimental setups utilized in our laboratory to mimic the chemical processing of gas phase and solid state (ices) environments. These are a crossed molecular beams machine (3) and a surface scattering setup (4). We also present typical results of each setup (formation of amino acids, aldehydes, epoxides; synthesis of hydrogen terminated carbon chains as precursors to complex PAHs and to carbonaceous dust grains in general; nitriles as precursor to amino acids).

2. Surface scattering machine

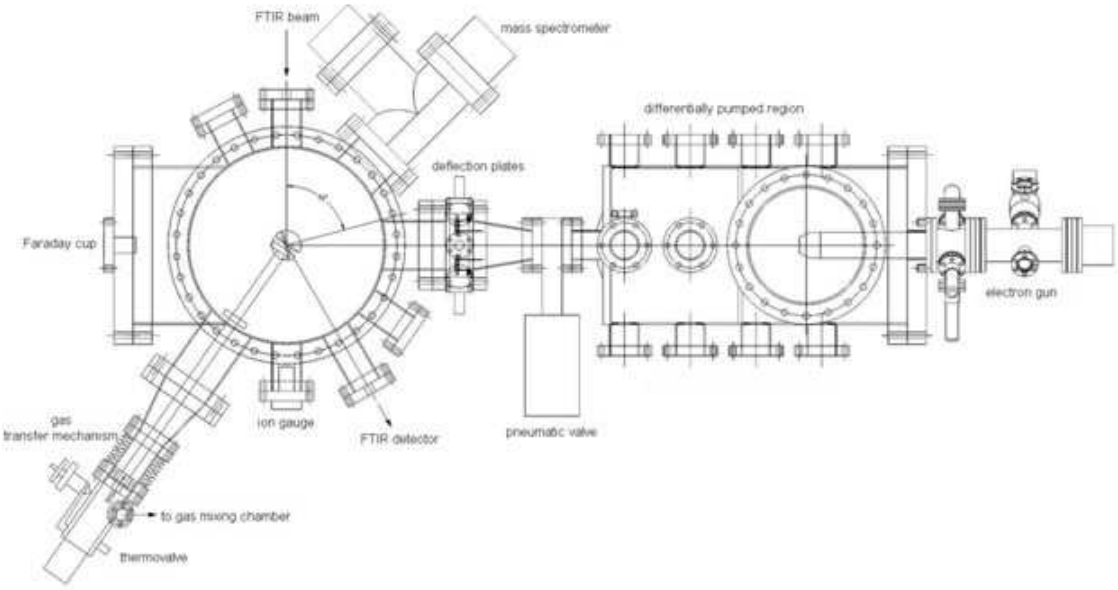

Fig. 1.— Schematic top view of the surface scattering machine.

To investigate the formation of astrochemically and astrobiologically relevant molecules in low temperature, extraterrestrial ice analog samples, we carry out radiolysis experiments in a contamination free ultra high vacuum stainless steel chamber (Fig. 1) (5). The chamber can reach pressures down to 5×10^{-11} torr by use of a magnetically suspended turbo molecular pump that is backed by a scroll pump. All pumps used are oil-free to ensure no hydrocarbon contaminants enter the system. Temperatures of 10 K are reached using a two-stage closed-cycle helium refrigerator that is interfaced directly to a polished single crystal silver mirror onto which the gases are condensed. The silver substrate is suspended by a differentially pumped rotatable feedthrough, which aligns the wafer in the center of the main chamber. Gas condensation is carried out at 10 K and generally at a pressure of 1.0×10^{-7} torr to a total thickness of about 200 nm. The experiment proceeds by irradiating the ice samples isothermally with 5 keV electrons for one hour to simulate the radiation effects in the aforementioned environments. The progress of the reaction is monitored using a Fourier Transform Infrared Spectrometer (FTIR). The spectrometer has a wavenumber range of 10,000-500 cm^{-1} and operates in absorption-reflection-absorption mode with a reflection angle of 75 deg from the normal relative to the mirror surface. The infrared spectra of the ice were recorded online and in situ at an integrated time of 2.5 minutes and at a resolution of 2 cm^{-1}. After irradiation the sample is left at 10 K to check the stability of the resulting molecules. In the final phase of the experiment, the sample is warmed at a rate of 0.5 K min^{-1} in an attempt to observed reaction, dissociation, and/or sublimation of the molecular species. Molecules that have sublimed may then be observed with the mass spectrometer that is directly attached to the reaction chamber. This procedure allows us to get

information on i) newly formed molecules in the gas phase (QMS) and solid state (FTIR), ii) the production rates, iii) the kinetics and dynamics involved, and iv) the underlying reaction mechanisms.

3. Crossed beams machine

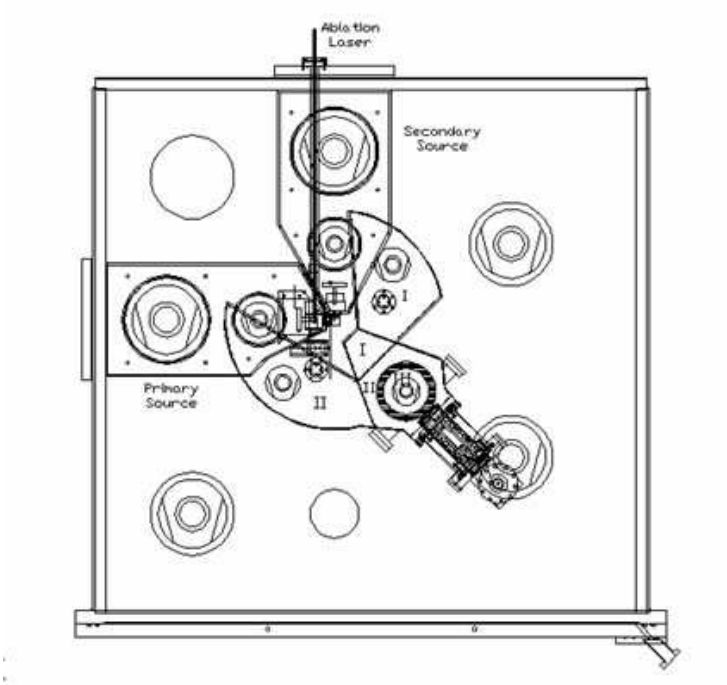

Fig. 2.— Schematic top view of the crossed beams machine.

The crossed molecular beams technique represents the most versatile approach in the elucidation of the energetics and chemical dynamics of elementary reactions relevant to astrochemistry (1). In contrast to bulk experiments, where the reactants are mixed, the main advantage of a crossed beams approach is the capability to form the reactants in separate, supersonic beams. In principle, both reactant beams like carbon atoms (C), cyano radicals (CN), ethynyl radicals (C_2H), carbon clusters (C_2, C_3) can be prepared in well-defined quantum states before they cross at a well-defined collision energy under single collision conditions. The species of each beam are made to collide only with the molecules of the other beam, and the products formed fly undisturbed toward the detector. These features provide an unprecedented approach to observe the consequences of a single collision event, preventing secondary collisions and wall effects. Crossed beams experiments can also help to infer those intermediates involved and provide reaction products together with their branching ratios critical input parameters in chemical reaction models of interstellar environments and of atmospheres of planets and their moons. Briefly, the main chamber of the crossed beams

machine consists of a stainless steel box and is evacuated to the low 10^{-8} torr region (Fig. 2). The source regions, in which the supersonic reactant beams are generated, are located inside the main chamber. In the primary source, we generate the reactive, open shell species like carbon atoms (C), cyano radicals (CN), ethynyl radicals (C_2H), or carbon clusters (C_2, C_3) via laser ablation techniques (1; 2). The ablated species are then seeded in a helium carrier gas released by a pulsed valve. A chopper wheel situated after the skimmer selects a part of the ablation beam of a well-defined peak velocity and velocity spread. Both beams pass through skimmers and cross perpendicularly in the interaction region. The reactively scattered products are monitored in the collision plane using a triply differentially pumped quadrupole mass spectrometer with an electron-impact ionizer in the time-of-flight (TOF) mode, i.e. recording the time-dependent intensity of ions at distinct m/z-ratios at different laboratory scattering angles. To extract information on the reaction dynamics, intermediates involved, energetics, and reaction products, we finally transform the laboratory data into the center-of-mass (CM) system.

4. Results

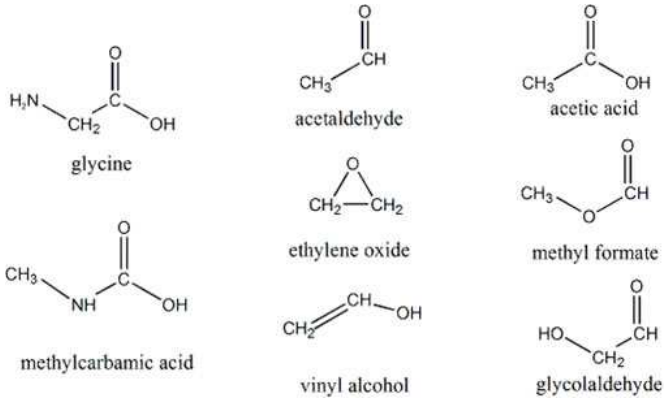

Fig. 3.— Structures of astrobiologically relevant species identified by our laboratory (7).

Our experimental setups are well suited for investigating chemistry that occurs in cold extraterrestrial ices (Figure 3), in cold molecular clouds, circumstellar envelopes, and in hydrocarbon-rich atmospheres of planets and their satellites (Figure 4). For example, in solid state experiments, identified species have obvious relevance in attempting to understand the abiotic synthesis of, for instance, amino acids and their isomers. Acetaldehyde and ethylene oxide have also been detected and have been suggested to play an important function in amino acid formation and in early metabolic pathways, respectively. The presence of ethylene oxide demonstrates the stability and the presence of formation routes to ring structures suggesting that sugars may also be easily formed. Currently work is being done to understand the synthesis of the $C_2H_4O_2$ isomers, acetic acid (CH_3COOH), methyl

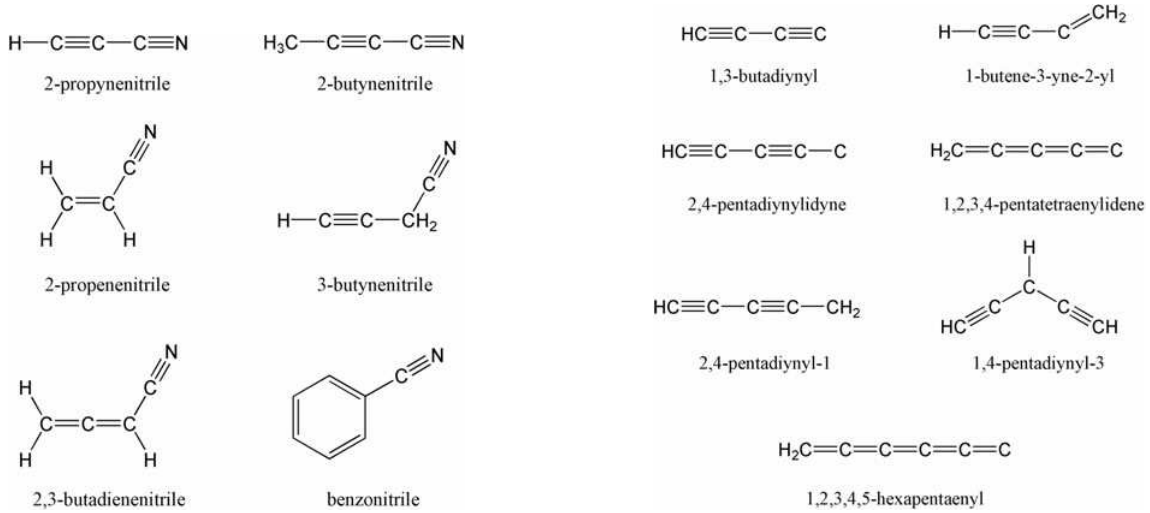

Fig. 4.— Left: Structures of nitriles relevant to the organic chemistry in Titan's atmosphere and of cold clouds. Right: Structures of carbon-bearing molecules identified by our laboratory.

formate ($HCOOCH_3$), and the simplest carbohydrate glycolaldehyde ($HCOCH_2OH$) in interstellar and solar system ices. Through these and future experiments we can elucidate the reaction pathways relevant to a variety of environments and applications, including astrobiology. The gas phase experiments proposed various formation routes to nitriles in the interstellar medium and in Titan's atmosphere (Figure 4, left panel) (2). The carbon bearing species synthesized via reactions of dicarbon and tricarbon molecules with unsaturated hydrocarbons provide vital building blocks to form polycyclic aromatic hydrocarbons (PAHs) and also precursors to more complex, carbon-based nanoparticles (interstellar grains) in the outflow of carbon rich stars as in IRC+10216 (6).

REFERENCES

R.I. Kaiser, Chem. Rev., 102, 1309 (2002)
R.I. Kaiser, 34, 699 (2001)
X. Gu, Y.Guo, R.I. Kaiser, Int. J. Mass Spectr. Ion. Processes 246, 29 (2005)
C.J. Bennett, C. Jamieson, A.M. Mebel, R.I. Kaiser, Phys. Chem. Chem. Phys. 6, 735 (2004)
C.J. Bennett, Y. Osamura, R.I. Kaiser, ApJ 624, 1097 (2005)
X. Gu, Y. Guo, F. Zhang, A.M. Mebel, R.I. Kaiser, Reaction Dynamics of Carbon-Bearing Radicals in Circumstellar Envelopes of Carbon Stars. Faraday Discussion 133: Chemical Evolution of the Universe (in press 2006)
P. D. Holtom, C. J. Bennett, Y. Osamura, N. J. Mason, R. I. Kaiser, ApJ 626, 940 (2005). J. Bennett, Y. Osamura, M. D. Lebar, R. I. Kaiser, ApJ 634, 698 (2005). C.J. Bennett, R.I. Kaiser, ApJ 635, 1362 (2005)

NASA LAW, February 14-16, 2006, UNLV, Las Vegas

Laboratory experiments on interstellar ice analogs: The sticking and desorption of small physisorbed molecules

G. W. Fuchs[1], K. Acharyya[2], S. E. Bisschop[1], K. I. Öberg[1], F. A. van Broekhuizen[1],H. J. Fraser[3], S. Schlemmer[4], E. F. van Dishoeck[1], & H. Linnartz[1]

[1]*Raymond and Beverly Sackler Laboratory for Astrophysics at Leiden Observatory, The Netherlands,* [2]*Center For Space Physics, Kolkata, India,* [3] *Department of Physics, University of Strathclyde, Scotland,* [4] *I.Physikalisches Institut, University of Cologne, Germany*

fuchs@strw.leidenuniv.nl

ABSTRACT

Molecular oxygen and nitrogen are difficult to observe since they are infrared inactive and radio quiet. The low O_2 abundances found so far combined with general considerations of dense cloud conditions suggest molecular oxygen is frozen out at low temperatures (< 20 K) in the shielded inner regions of cloud cores. In solid form O_2 and N_2 can only be observed as adjuncts within other ice constituents, like CO. In this work we focus on fundamental properties of N_2 and O_2 in CO ice-gas systems, e.g. desorption characteristics and sticking probabilities at low temperatures for different ice morphologies.

1. Introduction

The understanding of dense cloud and pre-stellar core chemistry depends strongly on the available molecule budget and distribution. This is particularly true for oxygen and nitrogen. Since O_2 nor N_2 has an electric dipole moment direct observations of these species in cold environments are difficult and abundances are uncertain. Nevertheless, the low values that have been derived from SWAS and ODIN observations of the order $N(O_2)/N(H_2) \approx 10^{-7}$ - 10^{-8} for gas phase O_2 raise questions on the total oxygen budget, especially when compared with atomic oxygen abundances observed towards diffuse clouds. It is believed that at high enough densities ($n(H_2)$=10^6-10^8 cm^{-3}) and low enough temperatures (10-30

[1]Correspondence to: G. W. Fuchs

K) even volatile molecules like CO, N_2 and O_2 are removed from the gas-phase by freeze-out processes on grains, thus building interstellar ices. These freeze-out processes can also significantly influence the chemistry. For example, since CO is one of the main destroyers of N_2H^+ a different freeze-out temperature of CO and N_2 would alter any subsequent reaction of N_2H^+. An anti-correlation between $C^{18}O$ and N_2H^+ can be observed towards the B68 pre-stellar cloud and it has been suggested that different sticking probabilities or binding energies between CO and N_2 (the parent molecule of N_2H^+) are responsible for this effect (Flower *et al.* 2005; Bergin *et al.* 2002). Experiments in the laboratory help clarifying the situation by measuring key properties of ice-gas interactions, like the sticking probability, desorption kinetics and binding energies of the species.

2. Experiment

Experiments have been performed using the CRYOPAD ultra-high vacuum set-up previously described in van Broekhuizen 2005 and Fuchs *et al.* 2006. CO, N_2 and O_2 have been deposited on a poly-crystalline gold surface at 14 K in mixed and layered structures forming amorphous ices. For astrophysical relevance, ices between 10 and 160 mono-layer thickness have been investigated using TPD (Temperature Programmed Desorption) techniques. The TPD spectra are used to determine the binding energies and desorption kinetics of these species under various conditions. They also give insight into the underlying intermolecular interactions. The TPD were taken by a controlled linear warm up ($dT/dt = 0.1$ K/min) of the ices between 14 and 80 K during which the evaporated molecules have been monitored by a quadrupole mass spectrometer. Simultaneously reflection absorption infrared (RAIR) spectra have been recorded using a Fourier Transform infrared spectrometer to investigate changes in the ice structure. The RAIR data have been discussed in Fuchs *et al.* 2006 and aid the modeling of the TPD data.

3. Results

The experiments have been discussed in Fuchs *et al.* 2006 and Öberg *et al.* 2005, Bisschop *et al.* 2006, Acharyya *et al.* 2006. To elucidate the anti-correlation problem between CO and N_2H^+ and also to confirm whether O_2 might be frozen out on grains the sticking coefficients S for CO sticking on CO, N_2 on CO, O_2 on O_2, etc. have been determined It has been found that all sticking coefficients at 15 K have similar values and that their lower limit value is around 0.9, thus verifying the assumption S=1 made by most modelers. Hence, O_2 can easily freeze out below 20 K in dense cores and the anti-correlation between CO and N_2H^+ is not due to different sticking coefficients of N_2 and CO.
TPD spectra have been recorded for pure O_2, CO and N_2 and analyzed using Polanyi-Wigner type rate equations, e.g. to determine the desorption energies E_d. It has been found that

$E_d(O_2) > E_d(CO) > E_d(N_2)$, with $E_d(O_2)\approx$ 925 K, $E_d(CO)\approx$855 K and $E_d(N_2)\approx$ 790 K using 0^{th}-order desorption kinetics. Layered and mixed CO-O_2 ices reveal similar TPD spectra with respect to pure ices but the desorption energies of the O_2 in these cases are lowered by 10 K whereas the E_d for CO is increased by 15 K. No significant co-desorption of CO with O_2 can be observed (Acharyya *et al.* 2006). In contrast, CO-N_2 ices show co-desorption of N_2 with CO for layered and mixed ices. Thus, the CO-N_2 ice system reveals a two-step desorption process for the N_2 molecule involving 0^{th}- and 1^{st}-order kinetics due to diffusion and a sufficiently large E_d energy separation between the N_2-N_2 binding sites and the N_2-CO type binding sites (Bisschop *et al.* 2006).
Both N_2 and O_2 interact with CO mainly due to quadrupole interaction with quadrupole moments of $Q(N_2) \lesssim Q(CO)$ and $Q(O_2) \ll Q(N_2)$. Furthermore, CO and N_2 have the same crystalline structure below 30 K whereas O_2 possesses a different crystalline architecture. Thus, N_2 can interact well with CO, i.e. stick, mix and co-desorb, whereas O_2 cannot. This follows the more general idea that desorption processes can be classified according to their intermolecular interaction pattern and crystalline structures. For example, CO, N_2 and O_2 in water ice behave differently (Collings *et al.* 2004 , see their Fig. 3) causing CO to desorb at higher temperatures than O_2 (around 30-50 K)

4. Astrophysical implications

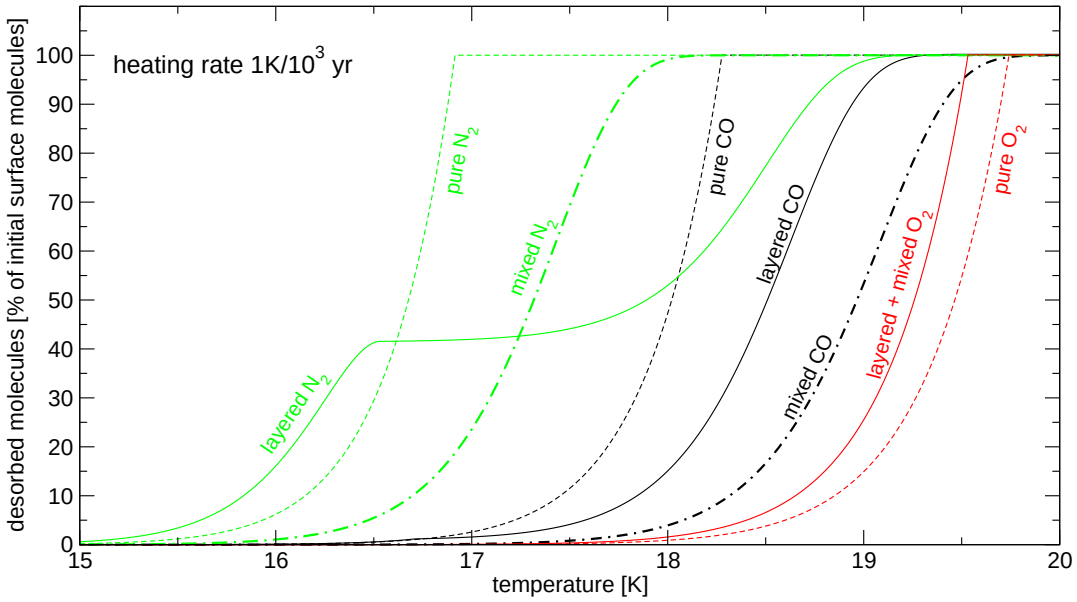

Fig. 1.— Desorption on astrophysical timescales (1 K/10^3 yr) starting at 10 K and assuming 40 monolayer of pure, mixed or layered O_2, CO, N_2 ice (i.e. no accretion has been considered).

The experimental data have been incorporated in an empirical kinetic model to predict desorption rates at a typical warm up rate ($dT/dt = 1\mathrm{K}/10^3$ yr) for a newly born star (Fig. 1). N_2 desorbs first, then CO followed by O_2 at the highest temperatures. Independent of the ice morphology, oxygen molecules desorb mainly between 18.5 and 20 K. CO is more volatile and also has a wider desorption temperature range showing larger differences between pure, mixed and layered CO ices. Most remarkably is N_2 which in its layered CO-N_2 form desorbs in two steps covering a desorption range of 4 K between 15 and 19 K. Overall the desorption takes place within 5 K for all species, i.e. equivalent to only 5000 yr of the evolutionary stage of the star, and can thus hardly make up for the observed anti-correlation between CO and N_2H^+. Although O_2 can well be frozen out in dense cores it has not been seen in the later stages of star formation, e.g. in hot cores, probably due to beam dilution effects. Future deep searches for O_2 with the HERSCHEL Space Observatory will be able to put stringent limits on the gaseous O_2 abundance.

This work has been supported by NOVA and a NWO Spinoza grant.

REFERENCES

Acharyya *et al.* 2006, Astron.&Astrophys., in prep.
Bergin *et al.* 2002, Astrophys.J., 570, L101
Bisschop *et al.*, 2006, Astron.&Astrophys., in press, (see astro-ph/0601082)
Collings *et al.* 2004, Mon.Not.R.Astron.Soc., 354, 1133
Flower *et al.* 2005, Astron.&Astrophys., 436, 933
Fuchs *et al.* 2006, Faraday Discuss., in press (DOI:10.1039/B517262B)
Öberg *et al.* 2005, Astrophys.J.Lett. 621, L33.
van Broekhuizen 2005, PhD thesis, Leiden University

NASA LAW, February 14-16, 2006, UNLV, Las Vegas

Use of Laboratory Data to Model Interstellar Chemistry

Gianfranco Vidali [1], J. E. Roser [2], E. Congiu [3] & L. Li

201 Physics Bldg., Syracuse University, Syracuse, NY 13244-1130

gvidali@syr.edu, jroser@mail.arc.nasa.gov, e.congiu@ca.astro.it, lli03@mailbox.syr.edu

G. Manicò & V. Pirronello

Università di Catania, DMFCI, 95125 Catania, Sicily, Italy

gmanico@dmfci.unict.it; pirronello@dmfci.unict.it

ABSTRACT

Our laboratory research program is about the formation of molecules on dust grains analogues in conditions mimicking interstellar medium environments. Using surface science techniques, in the last ten years we have investigated the formation of molecular hydrogen and other molecules on different types of dust grain analogues. We analyzed the results to extract quantitative information on the processes of molecule formation on and ejection from dust grain analogues. The usefulness of these data lies in the fact that these results have been employed by theoreticians in models of the chemical evolution of ISM environments.

1. Introduction

It is well known that gas-phase formation of H_2 doesn't occur with the rate necessary to explain its abundance in the ISM. More than thirty years ago Hollenbach and Salpeter (1971) proposed that H_2 formation occurs on the surfaces of dust grains. They calculated that the migration of H atoms on the grain via tunneling was so fast that, if two atoms happened to be on a grain at a given time, they would encounter and bond before leaving the grain. For

[1]Corresponding author

[2]Present address: NASA Ames, Mail Stop 245-6, Moffett Field, CA, 94035

[3]Permanent address: INAF -Osservatorio Astronomico di Cagliari, Sardinia, Italy

this rate of formation to match the observed destruction rate in diffuse clouds, thus achieving steady-state conditions, the sticking probability of H on a grain has to about 0.3, a number close to what they obtained in semiclassical calculations of sticking of H atoms on model surfaces. Smoluchowski (1981) reasoned that, if interstellar ice is amorphous, the diffusion by tunneling would be greatly limited; in his calculation he obtained a recombination rate much smaller than the one necessary to explain observations.

In the late 90's we initiated a program to measure in the laboratory the formation on surfaces of H_2 and other key molecules in conditions as close to actual interstellar environments as technically feasible. The first measurement of H_2 formation on a surface at low temperature was performed by our group using a telluric polycrystalline sample of olivine as a proxy of a dust grain (Pirronello et al. 1997a). Since then we extended our measurements to samples of amorphous carbon and amorphous water ice (Vidali et al. 2006a). Besides the formation efficiency, to be defined below, we characterized the kinetics of the reaction in order to learn about the mechanisms of H_2 formation. In this presentation, we summarize our latest results of the determination of the mechanisms of H_2 formation on amorphous water ice.

2. Experimental Methods

The apparatus consists of two triply differentially pumped atomic beam lines, a sample chamber, and a time-of-flight section (Vidali et al. 2006a). The experiment is done in two stages. In the first, or irradiation stage, we send *low flux* beams of H and D atoms onto the surface of a dust grain analogue held at 5 to 30 K. The HD yield that comes off the sample during irradiation with H and D atoms is collected by a quadrupole mass spectrometer. In the second stage, or TPD - Thermal Programmed Desorption, in order to set H and D atoms in motion so they can react, or to remove HD molecules that formed on the surface during irradiation, the temperature of the surface is rapidly raised and the HD molecules coming off the surface are detected . The sum of the yields collected during the irradiation and the thermal desorption experiment is then divided by half of the number of atoms that are detected striking the surface during the irradiation phase. Corrections are applied for the detection geometry and sensitivity, and for the different reaction paths. The number obtained (between 0 and 1) is the recombination efficiency. From an analysis of the shape of the TPD traces information on the kinetics of the reaction and on the mechanisms of reaction can be obtained (Vidali et al. 2006b).

3. Results

In Fig. 1 we show the recombination efficiency of H_2 obtained on surfaces of polycrystalline olivine, amorphous carbon, and amorphous water ice (Vidali et al. 2006a).

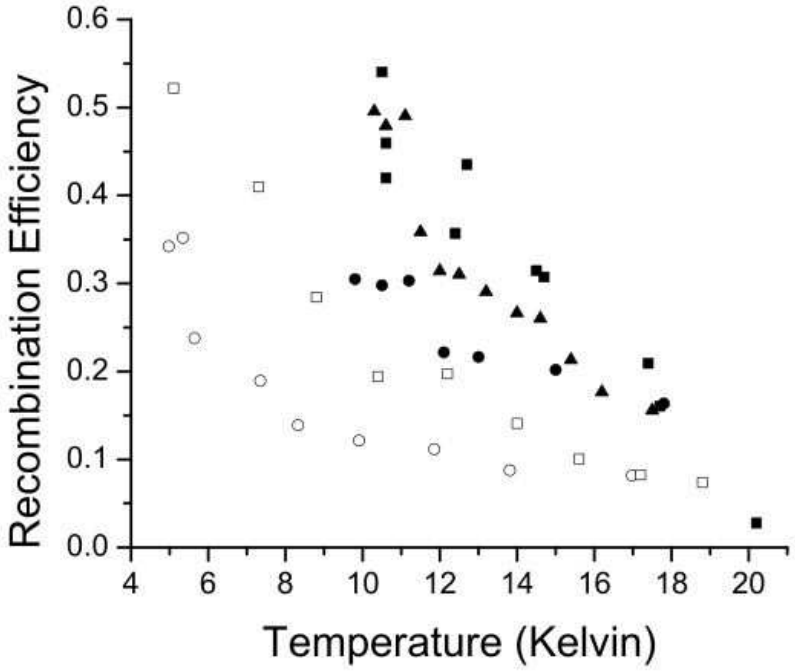

Fig. 1.— Recombination efficiency of molecular hydrogen vs. temperature of the sample at irradiation. High-density amorphous water ice: filled circles; low-density amorphous water: filled square; water vapor-deposited low-density amorphous ice: filled triangles; polycrystalline olivine: empty circles; amorphous carbon: empty squares. From Vidali et al. (2006a).

In Fig. 2 we plot the results of experiments designed to probe the mechanisms of reaction. We prepared an amorphous water ice sample (see Roser et al. (2003) for details) and deposited molecular HD at 10 K followed by a TPD (see trace with ∘). After cleaning the surface, we sent H and D atoms and then we did a TPD that produced HD molecules. If HD molecules formed rapidly during the irradiation phase and stayed on the surface, then the TPD trace should have the same shape as the one in the experiment in which molecular HD was deposited and then made to leave the surface via a TPD. Clearly the two traces are different. Specifically, the figure shows that a good fraction of HD in the experiment of molecular deposition comes off at a lower temperature than in the experiment of deposition of H and D atoms. We conclude, as we did about the experiments of HD formation on polycrystalline olivine *at low irradiation doses* (Pirronello et al. 1997a), that H and D atoms remain on the surface as atoms until a thermal pulse is given. Thus, the formation of molecular hydrogen *is primarily initiated by thermal energy.*

In another experiment, see (Roser et al. 2003), we measured the time-of-flight of HD

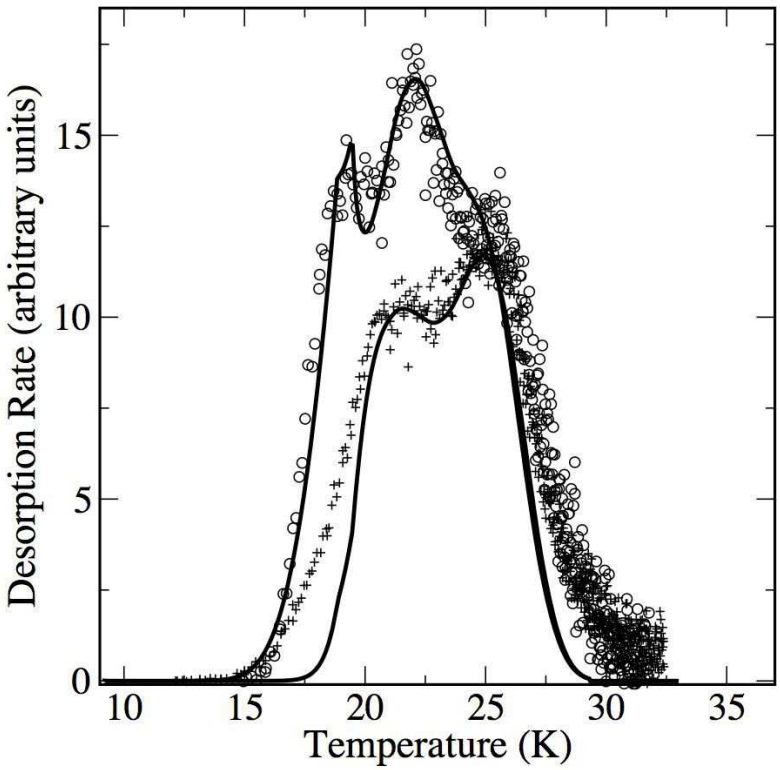

Fig. 2.— TPD traces of HD desorption after irradiation with HD molecules (∘) and H+D atoms (+) on amorphous low density water ice. The solid lines are fits obtained by a rate equations model. (Perets et al. (2005)).

molecules flying off the surface after the formation process. The velocity distribution of the molecules was fit with a Maxwell-Boltzmann distribution with a translational speed around 20 K, depending on the conditions of the experiment. A similar result was obtained independently by Hornekaer et al. (2003). Recently, the ro-vibrational excitation of HD leaving a graphitic surface was measured (Creighan et al. 2006) giving a rotational energy of about 250 to 280 K.

4. Discussion

Our experiments are designed to measure the formation efficiency and mechanisms of reactions in conditions as close as possible to ISM conditions. In order to use our results in models of the chemistry of ISM environments, theorists (Katz et al. 1999; Cazaux and Tielens 2004; Perets et al. 2005; Cuppen and Herbst 2005) have used models with rate or stochastic equations to fit our data and then to predict the formation of molecular hydrogen in ISM conditions and on grains with a distribution of sizes. From the analysis

of experimental data and the results of the models, one gets the following picture. The recombination efficiency is higher on amorphous surfaces, indicating that morphology plays a role. The efficiency is high in a narrow temperature range on polycrystalline olivine, but this range is wider on amorphous analogues. H atoms experience weak physisorption forces and thermal activation is needed to promote diffusion. The reaction proceeds either by the Langmuir-Hinshelwood or the hot atom mechanism, depending on the conditions (see Vidali et. al. 2006a,b for details).

5. Conclusion

Our work shows that through laboratory research and in close collaboration with theoreticians and modelers precious information can be obtained on the catalytic activity of surfaces, on the mechanisms of reaction and on the energy released in the reaction. This knowledge is useful for understanding the formation of hydrogen in the ISM and the role that dust grains play in the formation of molecules. Experiments on H_2 formation on other analogues (such as silicates) are in progress.

This work was supported in part by NASA through grants NAG5-9093 and NAG5-11438 (G.V) and by the Italian Ministry for University and Scientific Research through grant 21043088 (V.P).

REFERENCES

Creighan, S., Perry, J. S. A., & Price, S. D. 2006 J. Chem. Phys., 124, 114701
Cazaux, S. & Tielens, A. G. G. M. 2004 Astrophys.J., 604, 222
Cuppen, H. M. & Herbst, E. 2005, Mon. Not. Royal Astron. Soc., 361, 565
Hollenbach, D. & Salpeter, E. E. 1971, Astrphys. J., 163, 155; ibid., 163, 165
Hornekaer, L., Baurichter, A., Petrunin, V. V., Field, D., & Luntz, A. C. 2003, Science, 302, 1943
Katz, N., Furman, I., Biham, O., Pirronello, V., & Vidali, G. 1999, Astrophys. J., 522, 305
Roser, J. E., Swords, S., Vidali, G., Manicò, G., and Pirronello, V. 2003, Astrphys. J., 596, L55
Perets, H.B., Biham, O., Manicò, G., Pirronello, V., Roser, J., Swords, S., & Vidali, G. 2005, Astropys. J., 627, 850
Pirronello, V., Liu, C., Shen, L., & Vidali, G. 1997 Astrphys. J., 475, L69
Smoluchowski, R. 1981, Astrophys. and Space Sci., 75, 353
Vidali, G., Roser, J. E., Manicò, G., & Pirronello, V. 2006a, Proceedings IAU Symposium, No. 231, D. C. Lis, G. A. Blake & E. Herbst, eds., 355
Vidali, G., Roser, J. E., Li, L., Congiu, E., Manicò, G., & Pirronello, V. 2006b, Faraday Discussion, 133, in press

INVITED TALK *NASA LAW*, February 14-16, 2006, UNLV, Las Vegas

Nucleosynthesis: Stellar and Solar Abundances and Atomic Data

John J. Cowan,[1] James E. Lawler,[2] Christopher Sneden,[3] E. A. Den Hartog,[2] and Jason Collier[1]

ABSTRACT

Abundance observations indicate the presence of often surprisingly large amounts of neutron capture (*i.e.*, *s*- and *r*-process) elements in old Galactic halo and globular cluster stars. These observations provide insight into the nature of the earliest generations of stars in the Galaxy – the progenitors of the halo stars – responsible for neutron-capture synthesis. Comparisons of abundance trends can be used to understand the chemical evolution of the Galaxy and the nature of heavy element nucleosynthesis. In addition age determinations, based upon long-lived radioactive nuclei abundances, can now be obtained. These stellar abundance determinations depend critically upon atomic data. Improved laboratory transition probabilities have been recently obtained for a number of elements. These new gf values have been used to greatly refine the abundances of neutron-capture elemental abundances in the solar photosphere and in very metal-poor Galactic halo stars. The newly determined stellar abundances are surprisingly consistent with a (relative) Solar System *r*-process pattern, and are also consistent with abundance predictions expected from such neutron-capture nucleosynthesis.

1. Stellar Abundances and New Atomic Data

Abundance studies of heavy elements and isotopes in Galactic halo stars are providing important clues and insights into the nature of, and sites for, nucleosynthesis early in the history of the Galaxy (Sneden & Cowan 2003; Cowan & Thielemann 2004; Cowan & Sneden

[1]Homer L. Dodge Department of Physics and Astronomy, University of Oklahoma, Norman, OK 73019; cowan@nhn.ou.edu, collier@nhn.ou.edu

[2]Department of Physics, University of Wisconsin, Madison, Madison, WI 53706; jelawler@wisc.edu, eadenhar@wisc.edu

[3]Department of Astronomy and McDonald Observatory, University of Texas, Austin, Texas 78712; chris@verdi.as.utexas.edu

2006). Observations of heavy neutron-capture elements (*i.e.*, those produced in the slow (s) or rapid (r)-process) in both old (low iron, or metallicity) stars and younger (more metal-rich) stars are also providing clear indications of the nature of the Galactic chemical evolution. In addition the detection of the long-lived radioactive n-capture elements, such as thorium and uranium, are allowing direct age determinations for the oldest stars in the Galaxy - thus, providing lower limits on both the age of the Galaxy and the Universe.

All of these abundance determinations and studies depend critically upon atomic data, particularly transition probabilities. During the past few years there have been dramatic improvements in the experimental determinations of these transition probabilities for a number of rare earth elements: these include improved laboratory values for the elements Ce (Palmeri et al. 2000), Nd (Den Hartog et al. 2003), Ho (Lawler et al. 2004), Pt (Den Hartog et al. 2005), and Sm (Lawler et al. 2006). New values for the element Gd have also recently been obtained (Den Hartog et al. 2006), but Gd abundances in the current paper do not reflect these new data. These improved data sets have been employed to determine elemental abundances in three metal-poor Galactic halo stars. In addition new (refined) solar photospheric abundances have been obtained for Nd, Ho and Sm - this was not possible, however, for Pt. We show in Figure 1 the abundances from Ba-Er (normalized at the r-process element Eu) in CS 22892-052 (Sneden et al. 2003), BD +17°3248 (Cowan et al. 2002), HD 115444 (Westin et al. 2000) and the Sun (Lodders 2003). We focus in the left panel on abundance determinations for Nd, Sm and Ho in these four stars based upon published atomic data. The abundances for those same three elements, employing the newer laboratory atomic data, is shown in the right panel of this figure. It is clear, that as a result of employing the new atomic data, the star-to-star scatter among the three metal-poor Galactic halo stars is markedly reduced, and there is good agreement between the elemental values in these stars and the solar system r-process value (indicated by the horizontal line).

2. Discussion

Employing the new atomic data, we have updated several of the abundance values from Sneden et al. (2003) for CS 22892-052. We show those values in Figure 2 (top panel) compared to an s-only (dashed line) and an r-only (solid line) solar system elemental abundance curve. These solar system elemental abundance curves from Simmerer et al. (2004) are the sums of individual isotopic contributions from the s and r-process and are tabulated in table 1. Using the so called "classical model" approximation in conjunction with measured neutron capture cross-sections, the individual s-process contributions are first determined. Subtracting these s-process isotopic contributions from the total solar abundances predicts the residual r-process contributions. These individual s- and r-process isotopic solar system abundances (based upon the Si = 10^6 scale) that are listed in table 1, are derived from the work of Käppeler et al. 1989, Wisshak et al. 1998 and O'Brien et al. 2003, and can be used for future isotopic studies.

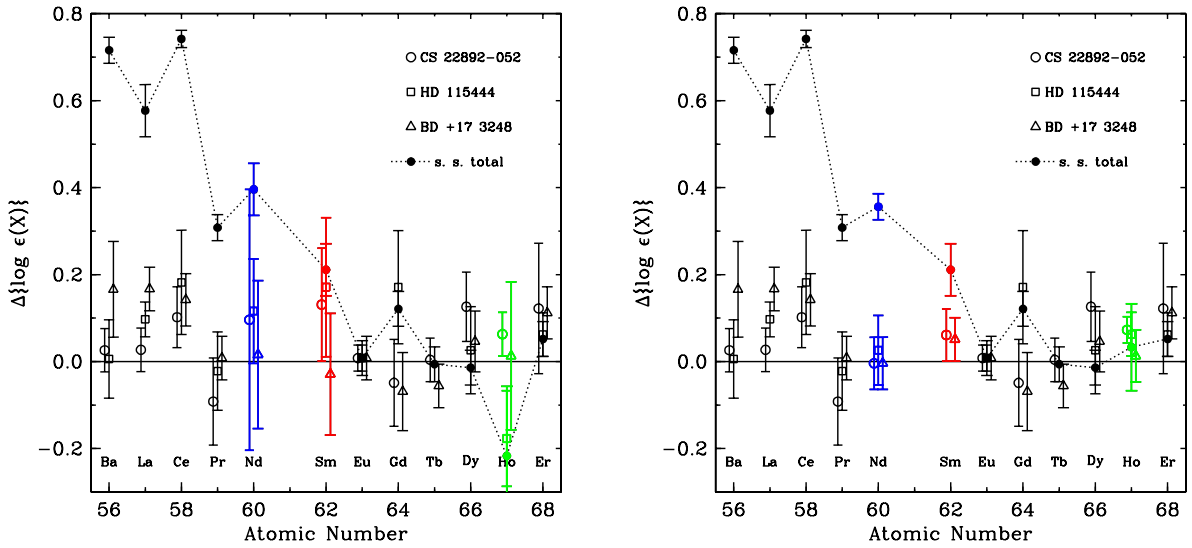

Fig. 1.— (left) Abundance values (scaled at the element Eu) for selected elements in the stars CS 22892-052 (open circles), HD 115444 (squares), BD +17°3248 (triangles) and the Sun (filled circles), based upon previously published atomic data. (right) Newly derived abundance values based upon recent experimental lab data (after Lawler et al. 2006).

It is clear in both the top and bottom panels of Figure 2 that the abundances of the stable elements Ba and above are consistent with the scaled solar system elemental r-process distribution. This agreement has been seen in other r-process-rich stars and strongly suggests that the r-process is robust over the history of the Galaxy. It further demonstrates that early in the history of the Galaxy, all of the n-capture elements were synthesized in the r-process, and not the s-process. Additional comparisons in the figure, however, suggest the lighter elements do not fall on this same curve that fits the heavier n-capture elements. The upper limit on Ge, for example, falls far below the scaled solar system r-process curve. Recent analyses of this element indicates its abundance is tied to the iron level in metal-poor halo stars (Cowan et al. 2005), and thus suggests Ge synthesis in some type of charged-particle reactions, or other primary process, in massive stars and supernovae in the early Galaxy (see discussion in Cowan & Sneden 2006). We also note that the abundances of the n-capture elements from Z = 40–50 in CS 22892-052, in general, fall below the solar r-process curve. This has been interpreted as suggesting perhaps a second r-process synthesis site in nature (see discussion in Kratz et al. 2006 and Cowan & Sneden 2006). Interestingly, new abundances studies of the star HD 221170 show better agreement with the scaled solar system curve for the elements from Z = 40-50 than CS 22892-052 does (Ivans et al. 2006).

In spite of the good overall match between the scaled-solar r-process abundances and

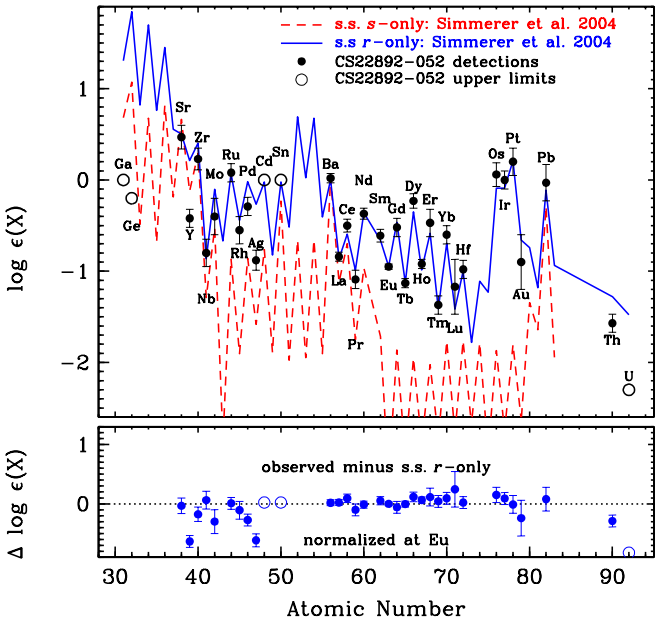

Fig. 2.— (top) Abundance values for CS 22892-052 compared to a scaled solar system s-process (dashed line) and r-process distribution (solid line, Simmerer et al. 2004). (bottom) Differences between observed abundances in CS 22892-052 and the scaled solar system r-process abundances (after Cowan & Sneden 2006).

those of very metal-poor stars, some small deviations are becoming apparent, as shown in Figures 1 and 2. The increasingly accurate stellar abundance determinations, resulting in large part from the more accurate laboratory atomic data, are helping to constrain, and ultimately could predict, the actual values of the solar system r-process abundances. Thus, the current differences might suggest that some of those solar system r-process elemental predictions need to be reassessed. Recall that the elemental r-process curve is based upon the isotopic r-process residuals, resulting from the subtraction of the s-process isotopic contributions from the total solar system abundances. Thus, a reanalysis of some of the s-process contributions, and new neutron-capture cross sections measurements, might be in order.

3. Conclusions

Abundance observations of metal-poor (very old) Galactic halo stars indicate the presence of n-capture elements. New laboratory atomic data is dramatically reducing the stellar abundance uncertainties in these stars and increasingly improving the Solar System abun-

dances. Recently determined abundances, based upon the new laboratory data, indicate that the elemental patterns in the old halo stars are consistent with each other and with a scaled solar system r-process abundance distribution – demonstrating that all of these elements (even s-process ones like Ba) were synthesized in the r-process early in the history of the Galaxy. These more accurate abundance determinations, based upon more precise laboratory atomic data, might be employed to constrain predictions for the solar system r-process abundances. In the future additional (and improved) lab data will have implications for a number of synthesis studies, including providing evidence regarding the possibility of two astrophysical r-process sites. Such new experimental data will also help in understanding the Galactic chemical evolution of the elements, and could have an impact on chronometric age estimates of the Galaxy and the Universe. New stellar and atomic data in both the UV and IR wavelength regimes may also allow the detection of never before seen elements in these stars, and will aid in new determinations of isotopic abundance mixtures for elements such as Sm.

We thank our colleagues for valuable insights and contributions. This work has been supported in part by NSF grants AST 03-07279 (J.J.C.), AST 05-06324 (J.E.L.), AST 03-07495 (C.S.), and by STScI.

REFERENCES

Cowan, J. J., et al. 2002, ApJ, 572, 861
Cowan, J. J., et al. 2005, ApJ, 627, 238
Cowan, J. J., & Sneden, C. 2006, Nature, in press
Cowan, J. J., & Thielemann, F.-K., 2004, Phys. Today, 57, 47
Den Hartog, E. A., Lawler, J. E., Sneden, C., & Cowan, J. J. 2003, ApJS, 148, 543
Den Hartog, E. A., Herd, T. M., Lawler, J. E., Sneden, C., Cowan, J. J., & Beers, T. C. 2005, ApJ, in press
Den Hartog, E. A., Lawler, J. E., Sneden, C., & Cowan, J. J. 2006, ApJ, to be submitted
Ivans, I. I., et al. 2006, ApJ, in press
Käppeler, F., Beer, H. & Wisshak, K. 1989, Rep. Prog. Phys., 52, 945
Kratz, K.-L., Farouqi, K., Pfeiffer, B., Truran, J. W., Sneden, C., & Cowan, J. J. 2006, ApJ, in preparation
Lawler, J. E., Den Hartog, E. A., Sneden, C., & Cowan, J. J. 2005, ApJ, in press
Lawler, J. E., Sneden, C., & Cowan, J. J. 2004, ApJ, 604, 850
Lodders, K. 2003, ApJ, 591, 1220
O'Brien, S., et al. 2003, Pys. Rev. C, 68, 035801
Palmeri, P., Quinet, P., Wyart, J.-F., & Biémont, E. 2000, Physica Scripta, 61, 323
Simmerer, J., Sneden, C., Cowan, J. J., Collier, J., Woolf, V. M., & Lawler, J. E. 2004, ApJ, 617, 1091
Sneden, C., et al. 2003, ApJ, 591, 936

Sneden, C., & Cowan, J. J. 2003, Science, 299, 70
Westin, J., Sneden, C., Gustafsson, B., & Cowan, J.J. 2000, ApJ, 530, 783
Wisshak, K., Voss, F., Käppeler, F., Kazakov, L., & Reffo, G. 1998, Phys. Rev. C, 57, 391

Table 1. *s*- AND *r*-PROCESS ISOTOPIC SOLAR SYSTEM ABUNDANCES

Element	Z	Isotope	N[s]	N[r]	Element	Z	Isotope	N[s]	N[r]
Ga	31	69	11.137	11.600	Pd	46	104	0.165	0.000
		71	10.413	4.700			105	0.040	0.269
Ge	32	70	15.000	0.000			106	0.186	0.193
		72	18.323	14.000			108	0.226	0.145
		73	3.531	5.670			110	0.000	0.163
		74	15.733	27.300	Ag	47	107	0.058	0.239
		76	0.000	9.200			109	0.059	0.196
As	33	75	1.456	5.330	Cd	48	110	0.178	0.000
Se	34	76	4.656	0.000			111	0.042	0.165
		77	1.679	3.040			112	0.198	0.196
		78	7.402	7.210			113	0.060	0.139
		80	7.446	24.300			114	0.287	0.140
		82	0.000	5.710			116	0.000	0.121
Br	35	79	0.450	0.000	In	49	115	0.057	0.121
		81	0.479	4.640	Sn	50	116	0.511	0.000
Kr	36	80	1.021	0.000			117	0.146	0.128
		82	6.207	0.000			118	0.706	0.137
		83	1.989	3.750			119	0.155	0.065
		84	10.575	18.000			120	1.099	0.078
		86	9.481	0.930			122	0.000	0.154
Rb	37	85	0.690	2.790			124	0.000	0.199
		87	2.214	0.100	Sb	51	121	0.047	0.113
Sr	38	86	2.111	0.000			123	0.000	0.132
		87	1.443	0.000	Te	52	122	0.133	0.000
		88	16.986	2.550			123	0.047	0.000
Y	39	89	3.344	1.310			124	0.248	0.000
Zr	40	90	4.529	0.990			125	0.088	0.267
		91	1.158	0.040			126	0.450	0.525
		92	1.289	0.540			128	0.000	1.526
		94	1.687	0.170			130	0.000	1.634
		96	0.000	0.300	I	53	127	0.050	0.851
Nb	41	95	0.229	0.110	Xe	54	128	0.126	0.000
Mo	42	95	0.189	0.213			129	0.066	1.240
		96	0.475	0.000			130	0.199	0.000
		97	0.156	0.087			131	0.087	0.954
		98	0.514	0.093			132	0.498	0.800
		100	0.000	0.242			134	0.000	0.449
Tc	43	99	0.006	0.172			136	0.000	0.373
Ru	44	99	0.049	0.000	Cs	55	133	0.056	0.315
		100	0.242	0.000	Ba	56	134	0.178	0.000
		101	0.050	0.266			135	0.068	0.298
		102	0.261	0.327			136	0.500	0.000
		104	0.000	0.348			137	0.372	0.283
Rh	45	103	0.055	0.289			138	3.546	0.225
La	57	139	0.337	0.110	Lu	71	175	0.006	0.031
Ce	58	140	0.894	0.089			176	0.002	0.000
		142	0.000	0.115	Hf	72	176	0.008	0.000
Pr	59	141	0.079	0.082			177	0.005	0.024
Nd	60	142	0.227	0.000			178	0.021	0.022
		143	0.037	0.065			179	0.007	0.015
		144	0.105	0.094			180	0.035	0.020
		145	0.020	0.049	Ta	73	181	0.009	0.013

Table 1—Continued

Element	Z	Isotope	N[s]	N[r]	Element	Z	Isotope	N[s]	N[r]
		146	0.091	0.053	W	74	182	0.024	0.012
		148	0.004	0.044			183	0.013	0.007
		150	0.000	0.047			184	0.029	0.013
Sm	62	147	0.003	0.031			186	0.006	0.031
		148	0.038	0.000	Re	75	185	0.004	0.014
		149	0.005	0.031			187	0.001	0.033
		150	0.022	0.000	Os	76	186	0.012	0.000
		152	0.018	0.053			187	0.006	0.000
		154	0.000	0.059			188	0.016	0.079
Eu	63	151	0.000	0.042			189	0.004	0.111
		153	0.002	0.048			190	0.021	0.168
Gd	64	152	0.001	0.000			192	0.001	0.293
		154	0.009	0.000	Ir	77	191	0.005	0.241
		155	0.003	0.045			193	0.003	0.408
		156	0.015	0.055	Pt	78	192	0.010	0.000
		157	0.007	0.046			194	0.020	0.431
		158	0.027	0.058			195	0.006	0.457
		160	0.000	0.072			196	0.035	0.312
Tb	65	159	0.004	0.060			198	0.000	0.099
Dy	66	160	0.009	0.000	Au	79	197	0.010	0.176
		161	0.004	0.075	Hg	80	198	0.035	0.000
		162	0.016	0.101			199	0.016	0.043
		163	0.002	0.093			200	0.051	0.030
		164	0.018	0.091			201	0.020	0.027
Ho	67	165	0.006	0.083			202	0.079	0.026
Er	68	164	0.004	0.000			204	0.000	0.020
		166	0.012	0.072	Tl	81	203	0.042	0.012
		167	0.005	0.053			205	0.060	0.041
		168	0.020	0.047	Pb	82	204	0.057	0.000
		170	0.001	0.037			206	0.326	0.223
Tm	69	169	0.006	0.031			207	0.313	0.280
Yb	70	170	0.006	0.000			208	1.587	0.118
		171	0.004	0.029	Bi	83	209	0.051	0.093
		172	0.018	0.036	Th	90	232	0.000	0.042
		173	0.008	0.031	U	92	235	0.000	0.006
		174	0.040	0.037			238	0.000	0.020
		176	0.000	0.030					

INVITED TALK *NASA LAW*, February 14-16, 2006, UNLV, Las Vegas

Data needs for stellar atmosphere and spectrum modeling

C. I. Short

Department of Astronomy & Physics and Institute for Computational Astrophysics, Saint Mary's University, Halifax, NS, Canada, B3H 3C3

ishort@ap.smu.ca

ABSTRACT

The main data need for stellar atmosphere and spectrum modeling remains atomic and molecular transition data, particularly energy levels and transition cross-sections. We emphasize that data is needed for bound-free ($b-f$) as well as bound-bound ($b-b$), and *collisional* as well as radiative transitions. Data is now needed for polyatomic molecules as well as atoms, ions, and diatomic molecules. In addition, data for the formation of, and extinction due to, liquid and solid phase dust grains is needed. A prioritization of species and data types is presented, and gives emphasis to Fe group elements, and elements important for the investigation of nucleosynthesis and Galactic chemical evolution, such as the α-elements and n-capture elements. Special data needs for topical problems in the modeling of cool stars and brown dwarfs are described.

1. Introduction

It has long been known that the radiative extinction of gas plays a major role in determining both the structure of a stellar atmosphere and the emergent spectral energy distribution. Accurate knowledge of the extinction requires accurate knowledge of transition wavelengths, λ, and of transition cross sections, σ_ν (or, equivalently, for bound-bound ($b-b$) transitions, oscillator strengths (gf values)), which in turn requires accurate knowledge of the energy level (E-level) structure of atoms, ions, and molecules. With the discovery and classification of an increasing number of brown dwarfs, for which atmospheric temperatures are lower than that of the coolest objects that are traditionally regarded as stars, there is now a need for molecular data for polyatomic molecules, in addition to that for diatomic molecules (Allard *et al.* 2003).

The importance of the $b - b$ transitions, which give rise to spectral lines, has been well documented. However, bound-free ($b - f$) transitions also significantly determine the atmospheric structure and spectral energy distribution of stars, and accurate knowledge of the corresponding cross-sections, σ_ν, is crucial. The importance of radiative transitions has been long recognized because they contribute directly to extinction. However, for realistic treatments, collisional transitions also play a central role in determining the equilibrium state of the gas, and thus, through the physics of radiative transfer, the emergent spectrum.

As a point of general motivation, we note that there is a long tradition, still being practiced, in quantitative stellar spectroscopy of "tuning" atomic parameters so that solar atmospheric models match solar spectral features of interest. This approach is based on the assumption that we have a correct model of the solar atmospheric structure and correct solar abundances. Therefore, it is particularly disconcerting to note that the solar abundances of C, N, and O have recently been revised downward by factors of two to three on the basis of including turbulent hydrodynamic structure in the atmospheric model (Asplund 2000). Furthermore, the solar abundance of Fe is still in dispute by a factor of 1.5 (Kostik *et al.* 1996). Clearly, it would be helpful to remove the atomic data as a "variable" from this process.

In addition to atomic and molecular data, extinction cross sections for liquid and crystalline aerosols of all types are needed. Again, it is in the cool brown dwarf objects that aerosols play a significant role in the atmospheric structure and emergent spectrum (Allard *et al.* 2003).

2. Atomic data

2.1. Prioritization

One way to rank the chemical elements in urgency is to weight them by the product of their relative abundance in stellar atmospheres and the richness of the line spectrum that they contribute. With this ranking, iron (Fe) and the Fe group elements have the highest priority. Another prioritization is to weight the elements by their importance to particular problems in nucleosynthesis and Galactic chemical evolution. By this criterion, the α-process and neutron capture (n-capture) elements deserve urgent consideration.

2.2. Fe group

Fig. 1 shows the E-level diagrams for atomic models of Fe I and II that are based on laboratory and semi-empirical atomic data of Kurucz (1994) and Kurucz & Bell (1995). From

the energy gap between the highest included bound E-levels and the ionization limit, we conclude that the atomic models are not complete. In addition to the E-levels and transitions displayed in Fig. 1, Kurucz (1992) has also made available data for hundreds of levels and thousands of lines on the basis of theoretical quantum mechanical calculations. Kurucz (1992) has demonstrated that inclusion of these additional theoretical lines in solar atmospheric modeling reduces the predicted solar flux in the UV band, thus allowing theoretical solar atmospheric models to fit the observed UV band flux much more closely than was previously possible. However, when high resolution synthetic spectra computed with the theoretical lines are compared to the observed solar spectrum, the match is *worse* than when the theoretical lines are omitted from the calculation (Bell *et al.* (1996), Short & Lester (1996)). This is due to the pervasiveness of significant errors in the E-level values (and, hence, transition λ values) and in the gf values. It should be noted that Kurucz (1992) himself acknowledged at the outset that the theoretical lines should only be used for stellar atmospheric structure and broad-band flux level calculations. This points to the need for more reliable and complete measurements of E-levels and gf values for Fe.

Need for completeness: It is worth noting that although many of the Fe transitions seen in Fig. 1 give rise to very weak lines, it has been long understood that thousands of weak lines of a particular element concentrated in a particular band, such as the near UV, act collectively as a broad-band pseudo-continuous veiling opacity that can significantly affect the atmospheric structure and the emergent flux level (the "iron curtain" effect) (Rutten 1986). Furthermore, in non-local thermodynamic equilibrium calculations (non-LTE), high lying E-levels can act as an important channel of ionization to the ground state of the next higher stage, and their neglect in the atomic model can lead to erroneous results for the ionization equilibrium (see, for example, Short & Hauschildt (2005)).

There is a particular dearth of atomic data for Fe ionization stages greater than II, especially for $b - b$ transitions of $\lambda < 2000$ Å (ie. vacuum UV and far UV (FUV) band transitions). Stages III and IV, and UV transitions thereof, are important for the study of hot stars (spectral class O and B), and the chromospheres and transition regions between the chromospheres and coronae, of solar type and relatively cool stars. Stages XII through XIV are useful for modeling the X-ray band spectra of stellar coronae.

LS coupling: Another area of concern is the lack of atomic data from quantum mechanical calculations for transitions that are not predicted under the assumption of LS coupling. For example, Fe III has been detected outside the H II regions around hot stars, yet of the 64 terms of Fe II, as predicted by LS coupling, none have transitions to Fe III of $\lambda < 911$ where photo-ionizing flux may escape from the H II region. This indicates that non-LS coupling transitions may be important, and the data for them should be measured.

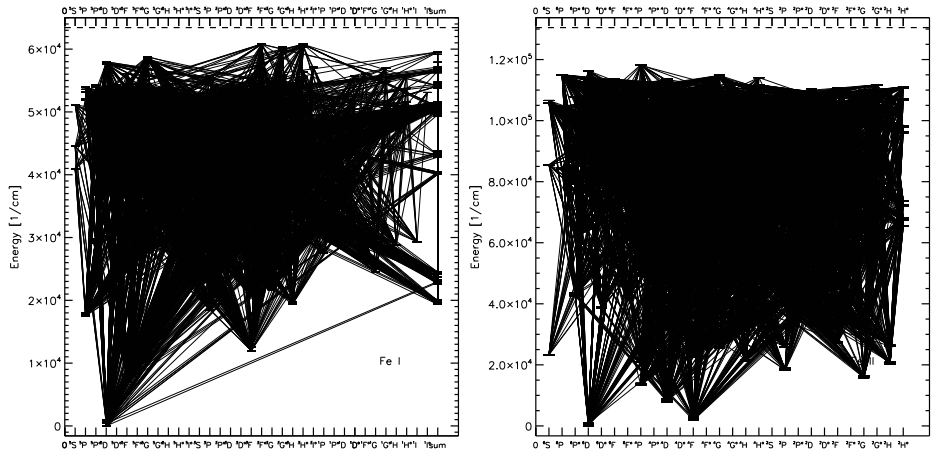

Fig. 1.— Grotrian diagrams of the models of Fe I (left) and II (right) based on the laboratory and semi-empirical data compiled by Kurucz (1994) and Kurucz & Bell (1995).

2.3. Nucleosynthesis and Galactic chemical evolution

α-process elements: There is a particularly urgent need for improved data, or any data at all, for the following elements associated with He fusion and the α-process: 1) gf values for $b - b$ transitions of Mg I and Si II; 2) σ_ν values for $b - f$ transitions of C I and II, Mg I and II, and Ca I and II; 3) low E (0-5 eV) e^- and H collisional σ_ν values for O I, Mg I, Al I, and Ca I.

n-capture elements: The advent of 8-m class telescopes has allowed the acquisition of spectra of faint Galactic halo red giant stars of sufficient quality to allow quantitative analysis. This includes the extremely metal poor (XMP) stars, in which $[\frac{\mathrm{Fe}}{\mathrm{H}}]$ is less than -3, and can be as low as -5. In these stars, the "iron curtain" referred to in Section 2 is relatively transparent. As a result, investigators have detected spectral lines of relatively heavy elements that are formed by the n-capture process (both the rapid (r-process) and slow (s-process)). The spectroscopic determination of the abundances of these elements is important for the investigation of the astrophysical sites of nucleosynthesis, the formation of the Galaxy, and the nature of the first stars. However, quantitative analysis will require accurate and complete atomic data of the sort that has been long called for in traditional light element analysis.

2.4. General atomic considerations

Bound-bound transitions: Given the constraints on measuring (or calculating) atomic parameters, there has been a tendency for stellar spectroscopists to prioritize by emphasiz-

ing those transitions that give rise to spectral lines that are useful abundance diagnostics. However, we note that extinction due to *all* transitions contributes to determining the radiative equilibrium (RE) structure of a stellar atmosphere. Furthermore, in non-LTE modeling determination of the excitation and ionization equilibria is a non-local problem such that the rate of *any* transition may affect the rate of any other (multi-level non-LTE effects). Worse, to the extent that different chemical species may have transitions that overlap in wavelength, the computed strength of a spectral line of one chemical species may depend on the equilibrium state of other species (multi-*species* non-LTE effects) (see Short & Hauschildt (2006) for examples of the non-LTE effect of Fe group elements on Sr and Ba lines). Therefore, accurate modeling of any spectral feature can depend on accurate atomic data for many transitions, not just the transition that directly corresponds to that spectral feature.

Bound-free transitions: Bound-bound transitions receive much attention because of the obvious importance of spectral lines. However, photo-ionization and recombination rates are also of central importance to calculating the equilibrium state of a gas and radiation field in non-LTE, and the emergent spectrum in any case. Therefore, measured values of $b-f$ σ_ν values are very useful. We note that auto-ionizing resonances can greatly complicate the dependence of σ_ν on λ, and cause values computed with simple analytic formulae to be significantly inaccurate (see, for example, Bautista *et al.* (1998)).

Collisional transitions: Cross-sections for excitations and ionizations due to inelastic collisions, mainly with e^-'s and H I, have become increasingly important as a result of the increase in non-LTE modeling. In non-LTE models, the excitation and ionization equilibria of chemical species are calculated by solving a statistical equilibrium among all the processes that populate and de-populate E-levels and ionization states, including *collisional* processes. Therefore, collisional rates have a much more central importance than they do in LTE modeling, and are particularly crucial when collisional transition rates are similar in magnitude to radiative rates. In turn, the calculated opacity, and hence spectral line strength, depends on the computed equilibria. As a result of current uncertainty in collisional σ_ν values, the results of non-LTE modeling must be carefully qualified by laborious perturbation analyses. We note that collisional σ_ν values are needed for dipole-*forbidden* as well as permitted transitions.

Excited states: We note that for realistic modeling, σ_ν values are needed for $b-f$ and collisional transitions arising from *excited* states as well as from the ground state.

3. Special problems requiring improved physical data

3.1. Brown dwarf and Jovian planetary atmospheres

Polyatomic molecular bands: As a result of their low temperatures ($T_{\rm eff} < 3000$ K), brown dwarf atmosphere chemistry admits significant polyatomic molecule formation. Molecular bands that form in the visible and near UV spectral regions (ie. "hot" bands) have a significant effect on both the atmospheric structure and the emergent spectral energy distribution. However, there is a dearth of molecular data for especially important bands of methane (CH_4), water (H_2O), ammonia (NH_3), and iron hydride (FeH). For completely accurate extinction modeling, there is also a need for data for metal hydrides in addition to FeH. See Leggett *et al.* (2001) for examples of observed spectra with molecular bands identified.

With the discovery of an increasing number of extra-solar "hot Jupiter" planets, brown dwarf modeling has been extended downward in temperature to the regime of hot gas giant planets. For these models there is a need for σ_ν values for excitation of H_2 by inelastic collisions.

Atomic resonance line damping: Because the gas pressure in brown dwarf atmospheres is relatively large, the resonance lines of some atomic species, most notably Na I and K I, have Lorentzian damping wings that span over 1000 Å (see Allard *et al.* (2003)). As a result, the wing of a single spectral line acts as a broad-band pseudo-continuous opacity source that significantly affects both the atmospheric structure and the emergent spectral energy distribution. Therefore, it is especially important to accurately model the line profile and to have accurate knowledge of the atomic line broadening parameters.

Aerosols: The low temperatures of brown dwarf atmospheres also allow for the condensation of a large variety of liquid droplet and crystalline grain aerosols. Data is needed for the extinction versus λ for these. Again, their extinction affects both the atmospheric structure and the emergent spectrum (see Allard *et al.* (2003) for example). Important examples for which data is needed are NH_3 and NH_4SH.

3.2. Stars: solar type and cool

CO collisional excitation: The fundamental vibrational ($\Delta\nu = 1$) band of CO at 5μm has been found generally to be stronger than expected in the spectra of solar type and relatively cool stars. The most compelling explanation that has been put forward is that the outer atmospheres of cool stars are thermally bifurcated, with the CO band forming in clouds

of cool gas that are embedded in warmer gas at altitudes that are considered to be purely chromospheric in traditional $1D$ models (Ayres & Wiedemann 1989). If valid, then this interpretation represents a major advance in moving beyond one of the main restrictions of classical stellar spectrum interpretation, namely horizontal homogeneity. However, as noted in Section 2.4, the true excitation equilibrium of a chemical species may depend on collisional transition rates. Therefore, the correct interpretation of the strength of the $\Delta\nu = 1$ band depends on the adopted value of σ_ν for the excitation of CO by inelastic collisions with H I. Currently, these σ_ν values are estimated by scaling σ_ν values for collisional excitation by H_2, and are uncertain by a factor of approximately 100. The large uncertainty limits the ability to model the atmospheric structure on the basis of the $\Delta\nu = 1$ band with certainty.

SiO collisional excitation: Similarly, more accurate knowledge of the σ_ν value for collisional excitation by H I of SiO would be helpful for modeling maser emission in the vicinity of very large cool stars. Masing occurs in an extreme non-LTE equilibrium, thus collisional transition rates are important.

Silicate dust in winds: In cool stars with dusty winds the measured density of silicate dust grains is greater than expected on the basis of the gas density in the wind. One explanation is that the physical data relevant to silicate grain nucleation and condensation is inadequate. Silicate grain formation has not been as well studied as that of carbon grains.

REFERENCES

Allard, N.F., Allard, F., Hauschildt, P.H., Kielkopf, J.F., Machin, L., 2003, A&A, 411, 473
Asplund, M., 2000, A&A, 359, 755
Ayres, T.R & Wiedemann, G.R, 1989, ApJ, 338, 1033
Bautista, M.A., Romano, P., & Pradhan, A.K., 1998, ApJS, 118, 259
Bell R.A., Paltoglou G. & Tripicco M.J., 1994, MNRAS, 268, 771
Kostik, R.I., Shchukina, N.G. & Rutten, R.J., 1996, A&A, 305, 325
Kurucz R.L., 1994, CD-ROM No 22, Atomic Data for Fe and Ni (Cambridge: SAO)
Kurucz, R.L., 1992, Rev. Mex. Astron. Astrofis., 23, 181
Kurucz, R.L., & Bell, B. 1995, CD-ROM 23, Atomic Line List (Cambridge: SAO)
Leggett, S.K., Allard, F., Geballe, T.R, Hauschildt, P.H., Schweitzer, A., 2001, ApJ, 548, 908
Rutten, R.J., 1986, in IAU Colloquium 94, Physics of Formation of Fe II lines outside LTE, ed. R Viotti (Dordrecht: Reidel)
Short, C.I. & Hauschildt, P.H., 2006, ApJ, too appear in April
Short, C.I. & Hauschildt, P.H., 2005, ApJ, 618, 926
Short, C.I. & Lester, J.B., 1996, ApJ, 469, 898

NASA LAW, February 14-16, 2006, UNLV, Las Vegas

Laboratory Spectroscopy of CH^+ and isotopic CH

J. C. Pearson & B. J. Drouin

Jet Propulsion Laboratory, California Institute of Technology, Mail Stop 301-429, Pasadena, CA 91109

John.C.Pearson@jpl.nasa.gov, Brian.J.Drouin@jpl.nasa.gov

ABSTRACT

The $A^1\Pi - X^1\Sigma$ electronic band of the CH^+ ion has been used as a probe of the physical and dynamical conditions of the ISM for 65 years. In spite of being one of the first molecular species observed in the ISM and the very large number of subsequent observations with large derived column densities, the pure rotational spectra of CH^+ has remained elusive in both the laboratory and in the ISM as well. We report the first laboratory measurement of the pure rotation of the CH^+ ion and discuss the detection of $^{13}CH^+$ in the ISM. Also reported are the somewhat unexpected chemical conditions that resulted in laboratory production.

1. Introduction

The $A^1\Pi - X^1\Sigma^+$ system of CH^+ was first observed by Douglas & Herzberg (1941) and later the 0-0 1-0 and 2-0 vibrational sub-bands were analyzed (Douglas & Herzberg 1942). The laboratory spectrum confirmed CH^+ as a major constituent in interstellar clouds (Adams 1942). In spite of the astronomical significance, subsequent laboratory work on CH^+ has been relatively limited. The original data was extended to include the 0-1, 1-1, 2-1, 3-1 and 4-1 bands and Douglas & Morton (1960) extended the previous analysis to include the 0-1, 1-1, 2-1, 3-1 and 4-1 vibrational sub-bands. Later the 3-0 and 4-0 vibrational sub-bands of the $A^1\Pi - X^1\Sigma^+$ system and the $^1\Delta - ^1\Pi$ system and the $^3\Sigma - ^3\Pi$ systems were observed by Carre (1968). The 0-0, 0-1, 1-0, 1-1, 1-2, 1-3, 2-1 and 3-1 vibrational bands of the $A^1\Pi - X^1\Sigma^+$ system were remeasured at higher resolution and a complete set of molecular constants for the ground state of CH^+ were determined (Carrington & Ramsay 1981)

Laboratory investigations of isotopic CH^+ have been similarly limited with all the available data coming from the electronic bands. The $A^1\Pi - X^1\Sigma^+$ system was first tentatively identified on the basis of interstellar spectra (Bortolot & Thaddeus 1969), which led to a

laboratory investigation of the 0-0, 1-0, 1-0, 2-1, 2-0 and 3-1 vibrational sub-bands (Antić-Jovanović et al. 1983) confirming the identification. The spectrum of $^{13}CH^+$ in the 0-0, 0-1, 1-0, 1-1, 2-0 and 2-1 bands $A^1\Pi - X^1\Sigma^+$ system was revisited and recorded to higher J values (Bembenek 1997a). The $A^1\Pi - X^1\Sigma^+$ system of CD^+ was first observed by Cisak & Rytel (1971). The initial study was extended to the 0-0, 1-0, 2-0, 0-1, 2-1 and 3-1 vibrational sub-bands (Antić-Jovanović et al. 1979). The 0-0 and 2-1 bands of CD^+ were also measured by Grieman et al. (1981). The most complete analysis of the $A^1\Pi - X^1\Sigma^+$ system of CD^+ including the 0-0, 1-0, 2-0, 0-1, 2-1, 3-1, 1-2 and 1-3 vibrational sub-bands was reported by Bembenek et al. (1987). There is only one reported investigation of the $A^1\Pi - X^1\Sigma^+$ system in $^{13}CD^+$ where the 0-0 and 1-0 vibrational sub-bands were recorded (Bembenek 1997b).

Reconciling the observed CH^+ abundance in the interstellar medium with a chemical production mechanism has been a long standing problem (e.g. Bates & Spitzer (1951); Black & Dalgarno (1973); Black et al. (1975); Black (1998)). CH^+ requires H_2 for formation, but is quickly destroyed by H_2 as well. Radiative association of C^+ with H_2 is to slow to account for the destruction (Black et al. 1978) and the direct formation is endothermic and therefore inconsistent with the cold gas optical line widths (Crane et al. 1995; Gredel 1997). Heterodyne observations would clearly determine the origin of the CH^+ in the interstellar medium and would constrain the variety of mechanisms invoked to produce the large observed column densities.

The $J = 1 - 0$ transition of CH^+ is unfortunately close to the $J = 5 - 3$ Oxygen line at 834.1 GHz. As a result, it cannot be directly observed from the ground and the only astronomical detection was from ISO at too low spectral resolution to address the chemical origins questions (Cernicharo et al. 1997). However, the $^{13}CH^+$ $J = 1-0$ transition is shifted far enough away from the oxygen line to facilitate detection.

2. Astronomical Detection of $^{13}CH^+$

A search for $^{13}CH^+$ based on the optical constants was carried out from the Caltech Submillimeter Observatory towards the bright star forming region G10.6-0.4. Two features were subsequently detected one in emission and one in absorption. In this source there are three gas phase components along the line of site. The Star forming region G10.6-0.4, an extended CO emission region and a deep HI self absorption region without CO have velocities (v_{LSR}) of -2 km/s, +29 km/s and +7 km/s, respectively. The emission line was assigned to A state methanol $7_2^+ - 6_1^+$ in the star forming region. However, the candidate $^{13}CH^+$ line could have a frequency of 830107, 830193 or 830132 MHz depending on the component of the ISM where it originated (Falgarone et al. 2005). An analysis of the $^{13}CH^+$ optical spectrum (Bembenek 1997a) resulted in a predicted frequency of 830150 GHz but the error bars did not preclude any of the possibilities.

3. Laboratory detection of CH^+

Laboratory studies of CH^+ have been problematic due to uncertainty in the chemical production mechanism and technical challenges in generating microwaves at 835 GHz. The microwave challenge was addressed by constructing a new direct synthesis spectrometer (Drouin et al. 2005). Next, a new magnetically enhanced (De Lucia et al. 1983), variable temperature discharge cell was constructed. As a commissioning experiment four transitions of HCO^+ in the ground and first excited vibrational were observed between 800 and 900 GHz. This data is listed on Table 1 and compared to the frequencies in the JPL and CDMS line catalogs. We had previously believed that HCO^+ was sufficiently well studied for Herschel, SOFIA and ALMA, but this is clearly not the case and it will be the subject of a separate investigation.

Table 1: HCO^+ transitions from this study, catalog entries and other experiments.

Ju-Jl	V	Measured	JPL Catalog	Cologne Database
9-8	0	802458.217(50)	802458.329(400)[a]	802457.970(133)[b]
10-9	0	891557.340(50)	891557.924(272)[b]	891557.038(203)[b]
9-8	1	802039.104(75)	802939.079(400)[c]	802038.613(413)[b]
9-8	1	805845.625(75)	805845.788(400)[c]	805845.545(464)[b]

[a] van den Heuvel & Dymanus (1982)

[b] Calculated

[c] Blake et al. (1987)

The initial series CH^+ experiment started with acetylene and argon, but the only line detected was from CH_3CCH. A second series of experiment with improved cell cooling and helium and argon was carried out. CH^+ was discovered at 835078.950(75) GHz in a clean cold cell with slow pumping speed at the start of the experiment. If the cell warmed up, the $12_{0,12} - 11_{0,11}$ line of $H_2^{13}CO$ would appear at 835085.16 GHz and the CH^+ line would disappear. The axial magnetic field and some helium were required for CH^+ production. Additionally the CH^+ signal degraded as the experiment ran and coated the walls with hydrocarbons. CH^+ was also produced in a methane discharge under similar conditions but at a lower methane flow rate since methane does not freeze out at the 90K cell wall temperature. The best signal-to-noise always came from the highest voltage discharge that was stable.

4. The Astronomical Origins of $^{13}CH^+$

In order to determine the origin of the $^{13}CH^+$ line two analyses of the new laboratory frequency were carried out. First, the data from Carrington & Ramsay (1981) and Cernicharo et al. (1997) were combined with the new laboratory frequency and a complete set of Dunham constants (Dunham 1932) determined for CH^+. Table 2 gives the constants for

CH^+ determined from this analysis. The 3-1 band was excluded from the analysis since it shows systematic deviations consistent with a perturbation of the upper state. The analysis improved by a tiny amount when the laboratory frequency was included. From these parameters for $^{13}CH^+$ were derived using isotopic ratios. This resulted in a 830131.4(2.4) MHz frequency without accounting for Born-Oppenheimer breakdown (Watson 1973). A second analysis was performed by fitting all the isotopic data including the Born-Oppenheimer breakdown terms. This resulted in a 830166 MHz frequency with a large uncertainty. The magnitude of the Born-Oppenheimer breakdown correction is known for CO (Wappelhorst et al. 1997) and equates to +1.5 MHz. The correction from CH (Davidson et al. 2004) was estimated on the basis of the B constant, which does not properly account for the vibrational dependence and therefore over estimates the correction at +20 MHz. This leads to the conclusion that the correction is small and positive. The only viable candidate from the ISM is deep HI component without CO where the rest frequency is 830132(3) MHz.

Table 2: Derived Dunham constants for $^{12}CH^+$.

Parameter	Value (MHz)
$Y_{10}/2$	42833117.(83)
$Y_{20}/4$	-444387.7(244)
$Y_{30}/8$	829.43(204)
Y_{01}	425007.05(79)
Y_{02}	-41.3855(250)
$Y_{03}x10^3$	1.923(215)
$Y_{11}/2$	-7402.04(88)
$Y_{12}/2$	0.3426(38)
$Y_{21}/4$	16.544(93)
n_{lines}	211
σ_{red}	1.518
σ_{red}[a]	1.521

[a] σ_{red} without the laboratory line.

5. Conclusions

The rotational spectrum of CH^+ has been observed for the first time in the laboratory facilitating heterodyne astronomical observations from Herschel to constrain the chemical origins of CH^+. The $^{13}CH^+$ frequency and observation should facilitate follow up work along more lines of sight to confirm $^{13}CH^+$ in the diffuse ISM and illuminate the non thermal component that leads to its production. The very large A coefficient of CH^+ 5.9 x $10^{-3}s^{-1}$ should make it a major factor in the energy balance of the diffuse ISM providing an interesting window into this still poorly understood gas phase.

This work was carried out by the Jet Propulsion Laboratory, California Institute of

Technology, under contract with the National Aeronautics and Space Administration. The authors gratefully acknowledge the support of a NASA Astrophysics Research and Analysis Program (APRA) grant

REFERENCES

Douglas, A.E., & Herzberg, G 1941, ApJ, 93, 381
Douglas, A.E., & Herzberg, G 1942, Canad. J. Res. A, 20, 71
Adams, W.S. 1941, ApJ, 93, 11
Douglas A.E., & Morton, J.R. 1960, ApJ, 131, 1
Carre, M. 1968, Physica, 41, 63
Carrington, A., & Ramsay, D.A. 1981, Phys. Scripta, 25, 272
Bortolot, V.J., Jr., & Thaddeus, P. 1969, ApJ, 155, L17
Antić-Jovanović, A., Bojovic, V., Pešic, D.S., & Weniger, S., 1983, Spectrosc. Lett. 16, 11
Bembenek, Z., 1997a, J. Mol. Spectrosc., 181, 136
Cisak, H., & Rytel, M., 1971, Acta Phys. Polon A 39, 627
Antić-Jovanović, A., Bojovic, V., Pešic, D.S., & Weniger S., 1979, J. Mol. Spectosc., 75, 197
Grieman, F.J., Mahan, B.H., O'Keefe, A., & Winn, J.S., 1981, J. Chem. Soc. Faraday Discuss. 71, 191
Bembenek, Z., Cisak, H., & Kepa, R., 1987, J. Phys. B 20, 6197
Bembenek, Z, 1997b, J. Mol. Spectrosc. 182, 439
Bates, D.R., & Spitzer, L., Jr. 1951, ApJ, 113, 441
Black, J.H., & Dalgarno, A., 1973, Astrophys. Lett., 15, 79
Black, J.H., Dalgarno, A., & Oppenheimer, M., 1975, ApJ, 199, 633
Black, J.H., 1998, Faraday Discussions, 109, 257
Black, J.H., Hartquist, T.W., & Dalgarno, A., 1978, ApJ, 224, 448
Crane, P., Lambert, D.L., & Sheffer, Y., 1995, ApJ Supp. 99, 107
Gredel, R., 1997, A&A 320, 929
Cernicharo, J., Liu, X.-W., Cox, P., Barlow, M.J., Lim, T., & Swinyard, B.M., 1997, ApJ 483, L65
Falgarone, E., Phillips, T.G., & Pearson, J.C., 2005, ApJ 634, L149
Drouin, B.J., Maiwald, F.W., & Pearson J.C., 2005, Rev. Sci. Inst., 76, 093113
De Lucia, F.C., Herbst, E., & Plummer, G.M., 1983, J. Chem. Phys. 78, 2312
Dunham, J.L., 1932, Phys. Rev., 41, 721
Watson, J.K.G., 1973, J. Mol. Spectrosc., 45, 99
Wappelhorst, M.W., Saupe, S., Meyer, B., George, T., Urban, W., & LeFloch, A., 1997, J. Mol. Spectrosc. 181, 357
Davidson, S.A., Evenson, K.M., & Brown, J.M., 2004, J. Mol. Spectrosc. 223, 20
van den Heuvel, F.C., & Dymanus, A., 1982, Chem. Phys. Lett., 92, 21
Blake, G.A., Laughlin, K.B., Cohen, R.C., Busarow, K.L., & Saykally, R.J., 1987, ApJ 316, L45.

NASA LAW, February 14-16, 2006, UNLV, Las Vegas

Recent Selected Ion Flow Tube (SIFT) Studies Concerning the Formation of Amino Acids in the Gas Phase

Douglas M. Jackson, Nigel G. Adams, & Lucia M. Babcock

Department of Chemistry, University of Georgia, Athens, GA 30602

ABSTRACT

Recently the simplest amino acid, glycine, has been detected in interstellar clouds, ISC, although this has since been contested. In order to substantiate either of these claims, plausible routes to amino acids need to be investigated. For gas phase synthesis, the SIFT technique has been employed to study simple amino acids via ion-molecule reactions of several ions of interstellar interest with methylamine, ethylamine, formic acid, acetic acid, and methyl formate. Carboxylic acid type ions were considered in the reactions involving the amines. In reactions where the carboxylic acid and methyl formate neutrals were studied, the reactant ions were primarily amine ion fragments. It was observed that the amines and acids preferentially fragment or accept a proton whenever energetically possible. NH_3^+, however, uniquely reacted with the neutrals via atom abstraction to form NH_4^+. These studies yielded a body of data relevant to astrochemistry, supplementing the available literature. However, the search for gas phase routes to amino acids using conventional molecules has been frustrated. Our most recent research investigates the fragmentation patterns of several amino acids and several possible routes have been suggested for future study.

1. Introduction

Astrochemical models have given insight into the formation of ions and molecules in interstellar clouds (ISC)(Chyba & Sagan 1992; Delsemme 2000) and are of much importance today in the interpretation of data from several NASA missions. Deep Impact and Stardust are directly interested in the composition of comets and what their composition might mean concerning interstellar molecules. Amino acids may very well be detected in either mission and have been detected on meteorites in the past (Chyba 1990); they are a class of molecules which may be essential to the formation of life. The origin of amino acids on meteorites is not entirely understood. One explanation is that asteroids and comets collect amino acids and other organic molecules from the ISC as they travel through space (Chyba et al. 1990;

Delsemme 2000). If this is the case, astrochemical models may play an important role in determining the origin of amino acids in these ISC. Recently the simplest amino acid, glycine, has been detected in ISC (Kuan et al. 2003) although this report has since been contested (Snyder et al. 2005). In order to substantiate either of these possibilities, plausible routes to amino acids need to be investigated in the laboratory. Indeed such studies, coupled with detailed modeling, may be the only way that the gas phase existence of prebiotic molecules can be established. For gas phase synthesis, the SIFT technique is useful to study possible routes to simple amino acids via ion-molecule reactions. Neutral molecules, which have been detected in the ISC, include methylamine, formic acid, acetic acid, and methyl formate (Wooten 2002). This paper reports attempts to investigate reactions of these and similar molecules with ions, many of which have been observed in the ISC as well. Carboxylic acid type ions were studied in the reactions involving the amines (Jackson et al. 2005a). In reactions where the carboxylic acid and methyl formate neutrals were studied, the reactant ions were primarily amine ion fragments (Jackson et al. 2005b). Reaction rate coefficients and product distributions of the reactions studied supplement theoretical models of the ISC.

2. Experimental

An overview of the SIFT technique, described in detail elsewhere (Adams & Smith 1976), will be given as it pertains to this particular study. A source gas is introduced into a microwave cavity, MC, ionization source. Ions are drawn into a quadrupole mass filter where the primary reactant ion is selected from the various possible ions via its mass to charge ratio. The primary ion is then introduced into a He carrier gas flow at a total pressure of ~ 0.5 Torr. A neutral reactant gas is added to the flow at one of three ports allowing for varying reaction times. The detection system is composed of a nose cone sampling orifice at a small negative potential followed by a series of focusing lens elements and a second quadrupole mass filter with an electron multiplier. For the introduction of sticky gases such as carboxylic acid vapors, which dimerize, a special procedure was employed (Jackson, et al. 2005b).

3. Results and Discussion

For a complete listing of all reactions studied including data for product distributions and rate coefficients refer to Jackson et al. 2005a, 2005b. Many of the reactions studied resulted in dissociative charge transfer fragmentation of the neutral. These reactions though not necessarily intended to produce amino acids, e.g. Ar^+ reactions, do reveal which fragments form in greatest abundance and thus the connectivity on the reaction potential surface. The preferred fragment for each amine is $H_2CNH_2^+$, and the acids (RCOOH) fragment into RCO^+ and $COOH^+$ solely with RCO^+ in greatest abundance. Methyl formate fragments

into H_3CO^+, HCO^+, and CH_3^+ in descending order of abundance. Reactions which result in proton transfer can be predicted by observing relative proton affinities; however, the reaction of NH_3^+ with the neutrals results in H atom abstraction to form NH_4^+ since proton transfer is endothermic. The reactions of NH_3^+ with the neutrals may play a role in the ISC since NH_3^+ reacts slowly with molecular hydrogen.(Smith & Adams 1980) If this is the case, the abstraction reactions of NH_3^+ with the neutrals may form radical species, which could possibly participate in a further reaction especially if assisted catalytically by molecular dust grains to form more complex species. NH_4^+ does not react with molecular hydrogen and is therefore available for further reaction. Previous studies have indicated that NH_4^+ tends to associate with molecules such as acetic acid. Upon electron-ion recombination, it is possible that glycine could be formed. Blagojevic et al. report ion-molecule reactions that produce glycine and β-alanine using the primary ions $NH_{2,3}OH^+$ (Blagojevic, Petrie, & Bohme 2003). These reactions reportedly undergo "condensation" ejecting water and attaching the amine group to the proper carbon of acetic acid and propanoic acid. However, the interstellar importance of $NH_{2,3}OH^+$ is not known. These molecules have not been observed in the ISC nor has their reactivity with molecular hydrogen been investigated (Blagojevic et al. 2003). Even so, the chemistry indicates that similar reaction pathways involving "condensation" reactions may be possible. For example, reactions of certain neutrals with NH_4^+ may undergo a similar process condensing molecular hydrogen.

4. Conclusion

The present studies reveal that current efforts to synthesize amino acids in the gas phase using conventional molecules have limited success. Many plausible pathways result in proton transfer or fragmentation stifling a progressive synthesis of more complex organics. Though many possible gas phase routes to amino acids through ion-molecule reactions have not yielded amino acids, there has been some success, and a great deal of useful data has been collected. The success of Blagojevic et al. indicates that so-called condensation reactions with NH_4^+ type species with certain neutrals are successful to some degree. Also, as indicated by the reactions of NH_3^+, abstraction of H produces complex neutral radicals, which may react with other radicals or ions to produce more complex species. These kinds of reactions are difficult to study and have not been investigated. Finally, the electron-ion recombination of species such as acetic acid associated with NH_4^+ may yield a product of interest. Little is known about the structure and bonding of these associated products, and further investigation in both theory and experiment is needed. As we have shown, there are many possible routes to amino acids in the ISC that have not been investigated yet. These must be examined to verify the possible existence of glycine and other amino acids in the ISC.

Funding by NASA grant NAG5-8951 and by NSF grant 0212368 are gratefully acknowl-

edged. DMJ also recognizes the continued support of Dr. Pamela Kleiber and the UGA CURO program.

REFERENCES

Adams, N. G., & Smith, D. 1976, Int.J.Mass Spectrom.Ion Phys., 21, 349
Blagojevic, V., Petrie, S., & Bohme , D. K. 2003, Mon. Not. R. Astr. Soc., 339, L7
Chyba, C. F. 1990, Nature, 348, 113
Chyba, C. F., & Sagan, C. 1992, Nature, 355, 125
Chyba, C. F., Thomas, P. J., Brookshaw, L., & Sagan, C. 1990, Science, 249, 366
Delsemme, A. H. 2000, Icarus, 146, 313
Jackson, D. M., Stibrich, N. J., Adams, N. G., & Babcock , L. M. 2005a, Int J. Mass Spectrom., 243, 115
Jackson, D. M., Stibrich, N. J., McLain, J. L., Fondren, L. D., Adams, N. G., & Babcock , L. M. 2005b, Int J. Mass Spectrom., 247, 155
Kuan, Y.-J., Charnley, S. B., Huang, H.-C., Tseng, W.-L., & Lisiel, Z. 2003, Ap. J., 593, 848
Smith, D., & Adams, N. G. 1980, Chem.Phys.Letts., 76, 418
Snyder, L. E., et al. 2005, Astrophys. J., 619, 914
Wooten, H. A. 2002, www.cv.nrao.edu/∼awooten/allmols.html

NASA LAW, February 14-16, 2006, UNLV, Las Vegas

Laboratory Study of Magnetorotational Instability and Hydrodynamic Stability at Large Reynolds Numbers

H. Ji, M. Burin, E. Schartman, J. Goodman, & W. Liu

Plasma Physics Laboratory and Department of Astrophysical Sciences, Princeton University, Princeton, NJ 08540

hji@pppl.gov

ABSTRACT

Two plausible mechanisms have been proposed to explain rapid angular momentum transport during accretion processes in astrophysical disks: nonlinear hydrodynamic instabilities and magnetorotational instability (MRI). A laboratory experiment in a short Taylor-Couette flow geometry has been constructed in Princeton to study both mechanisms, with novel features for better controls of the boundary-driven secondary flows (Ekman circulation). Initial results on hydrodynamic stability have shown negligible angular momentum transport in Keplerian-like flows with Reynolds numbers approaching one million, casting strong doubt on the viability of nonlinear hydrodynamic instability as a source for accretion disk turbulence.

1. Introduction

Accretion disks are the most efficient energy source known to astrophysics. Whereas hydrogen fusion has a maximum efficiency for converting rest-mass to radiation $\lesssim 1\%$, black-hole or neutron-star accretion can achieve $\sim 5-40\%$. Accretion disks power many of the most luminous and violent astrophysical sources, including X-ray binaries, quasars, and perhaps gamma-ray bursts. Protostellar accretion disks, though energetically much less efficient, are nevertheless of great interest as sites of planet formation.

To support the rapid accretion process, an efficient mechanism to transport angular momentum outward is required. Molecular viscosity is completely inadequate. Since Keplerian flow profiles are linearly stable in hydrodynamics, there exist two plausible mechanisms for turbulent transition: nonlinear hydrodynamic instability or linear magnetorotational instability (MRI). The latter is favored for ionized accretion disks ranging from quasars to cataclysmic variables (Balbus & Hawley 1998). Protoplanetary disks, which may be too resistive for MRI, may require the former.

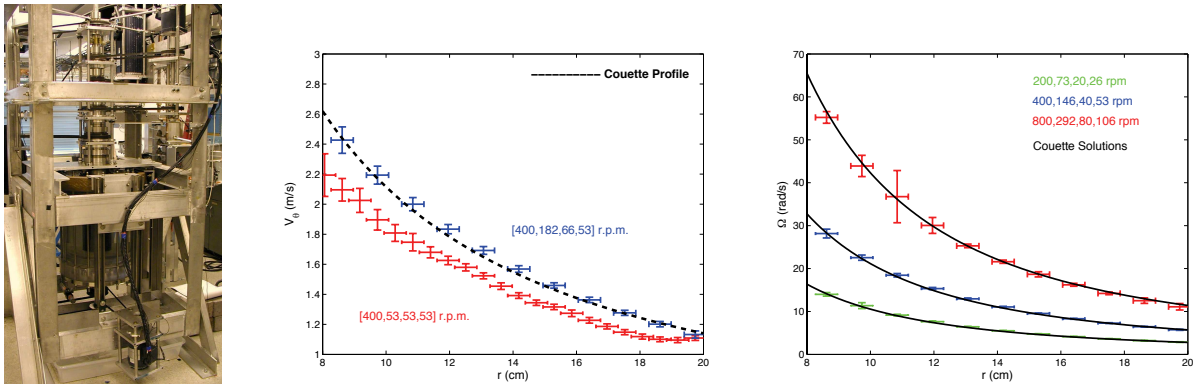

Fig. 1.— *(Left)* A photograph of the assembled apparatus. *(Center)* Flow profiles measured by Laser Doppler Velocimetry with (upper symbols, $\Omega_1 > \Omega_3 > \Omega_4 > \Omega_2$) and without (lower symbols, $\Omega_1 > \Omega_3 = \Omega_4 = \Omega_2$) differentially rotating endcaps. *(Right)* MRI-favorable profiles are produced at 3 different overall speeds at fixed ratios $\Omega_1 : \Omega_3 : \Omega_4 : \Omega_2$.

Linear MRI is simple and robust. MRI saturation and turbulence, however, are known only from simulations, which differ in 2D and 3D; none resolve all active lengthscales [see Balbus & Hawley (1998) and references therein]. Nonrotating hydrodynamic shear flows are typically turbulent at $Re \gtrsim 10^3$. (Richard & Zahn 1999, (RZ)) argue for hydrodynamic turbulence in disks based on old Couette-flow experiments (Wendt 1933; Taylor 1936), where at large enough Re, the flow became turbulent with the inner cylinder at rest—a strongly Rayleigh-stable case. RZ deduce a turbulent viscosity for disks of the form

$$\nu_{\rm T} = -\beta r^3 \frac{\partial \Omega}{\partial r} \ , \qquad \beta = (1-2) \times 10^{-5}, \qquad Re_{\rm crit} \sim \beta^{-1}. \tag{1}$$

The minimum Re for turbulence is sensitive to gap width $[(r_2 - r_1)/r_2]$ and probably to the ratio $R_\Omega \equiv 2(d \ln \Omega / dr)^{-1}$ of rotation to shear. There have been very few experiments relevant to RZ's hypothesis for disk-like R_Ω (Richard 2001). Local 3D simulations find purely hydrodynamic flows to be stable for angular-momentum gradients as strongly positive as in disks [see e.g., Balbus et al. (1996); Lesur & Longaretti (2005)].

To study these proposed mechanisms, a novel laboratory apparatus in a short Taylor-Couette flow geometry has been built in Princeton (Ji et al. 2001; Goodman and Ji 2002), among other proposed or existing experiments (Noguchi et al. 2002; Sisan et al. 2004; Hollerbach & Rüdiger 2005). We briefly describe the apparatus in the next Section, followed by initial hydrodynamic results. A short summary will be given in the last Section.

2. The Apparatus

To minimize Ekman circulation, differentially rotating endcaps are used (Kageyama et al. 2004). The annular area between the inner and outer cylinders has been modified to

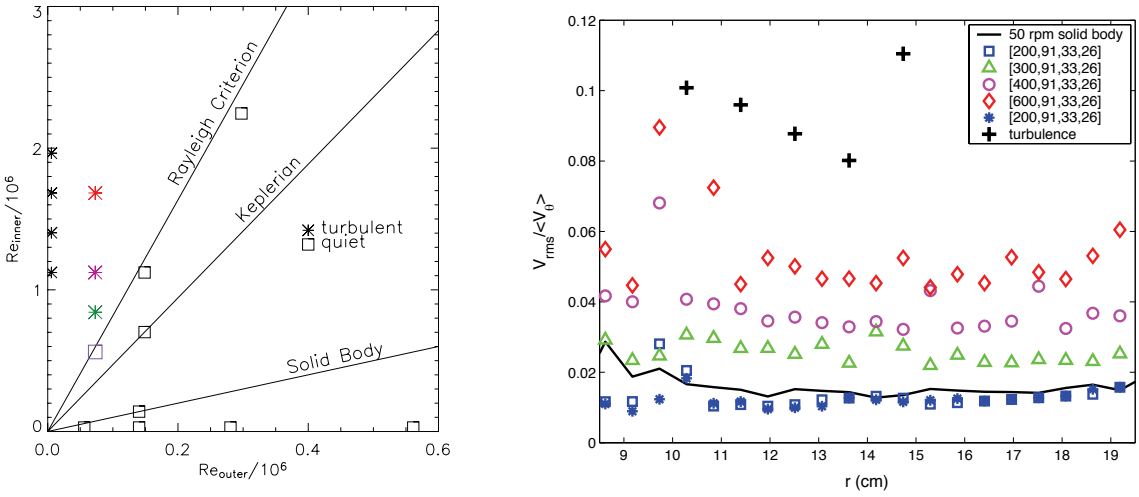

Fig. 2.— *(Left)* A diagram of initial experiments on hydrodynamic stability in the plane of $(Re_{\rm outer}, Re_{\rm inner})$. Square symbols indicate quiet flows (fluctuations $\lesssim 1\%$) while stars indicate fluctuations $> 2\%$. *(Right)* The measured fluctuation level. Triangles, circles, and diamonds correspond to the three points above the Rayleigh line, from bottom to top, at $Re_{\rm outer} \approx 0.05 \times 10^6$ in the left panel; squares and asterisks both correspond to the point just below the Rayleigh line at same $Re_{\rm outer}$. Solid-body ($\Omega_1 = \Omega_3 = \Omega_4 = \Omega_2$) and Rayleigh-unstable ($\Omega_2 = 0$) cases are shown for reference.

accommodate two intermediary rings at both endcaps (Burin et al. 2006). The dimensions are $r_1 = 7.06$cm, $r_2 = 20.30$cm, and $h = 27.86$cm. All dimensions are accurate to ± 0.02cm. A picture of the apparatus is shown in Fig. 1(left).

The suppression of Ekman circulation has been demonstrated using water. Figure 1 shows radial profiles of angular velocity measured by Laser Doppler Velocimetry (LDV). When the rings corotate with the outer cylinder, the flow deviates substantially from the ideal Couette profile. When the rings are activated, the Couette profile is accurately restored [Fig. 1(left)]. Furthermore, the Couette profiles are consistently reproduced at different speeds with the same speed ratios between rotating components [Fig. 1 (right)]. This is especially encouraging because MRI-favorable profiles can be produced at a range of speeds with confidence (Burin et al. 2006).

3. Initial Results of Hydrodynamic Stability at Large Reynolds Numbers

With the newly available apparatus, some initial results on hydrodynamic stability have been obtained using the LDV technique. These are summarized in Fig. 2, where the data are plotted in the plane of $Re_{\rm outer} \equiv \Omega_2 r_2 (r_2 - r_1)/\nu$ and $Re_{\rm inner} \equiv \Omega_1 r_2 (r_2 - r_1)/\nu$. Note that the Reynolds numbers achieved so far are already larger by a factor of 30 than those in the

Richard's experiment; also our gap is much wider ($r_2/r_1 \approx 2.9$ *vs.* 1.3). (Richard also used split endcaps, but with rings affixed to the inner and outer cylinders.) Solid-body rotation, which should be laminar, serves to calibrate systematic offsets in the velocity measurements and their statistical errors, $\sim 1\%$ per sample.

Three types of experiments have been performed to study flow stability at large Reynolds numbers. Those with the outer cylinder at rest ($\Omega_2 = 0$) are highly turbulent with fluctuation levels as large as 10% (see Fig. 2). Those with the *inner* cylinder at rest ($\Omega_1 = 0$) are as quiescent as solid-body rotation ($\Omega_1 = \Omega_2$), with fluctuations much smaller than those reported by Richard. The third type have $1 < \Omega_1/\Omega_2 < (r_2/r_1)^2$ as in keplerian disks. The latter flows are robustly quiet, showing maximum fluctuations indistinguishable from the solid-body case. Hysteresis, a hallmark of subcritical instability, was reported by Richard. A series of experiments was performed to test this. Ω_1 was raised (at constant $\Omega_2, \Omega_3, \Omega_4$) into the linearly unstable regime, then returned to the original linearly stable value. Significant fluctuations were found only in the linearly unstable regime (Fig. 2); no hysteresis was detected.

This results are further supported by direct measurements of Reynolds stress by a dual LDV, and it is found (Ji et al. 2006) that the measured transport coefficients (β) are below the proposed values by 3σ, and in addition, they are almost identical to those measured in solid-body rotation, which has no free energy to support turbulence. Thus these results have shown, for the first time, that purely hydrodynamic instabilities are unlikely to explain rapid accretion in cold disks.

4. Summary

Mechanisms for efficient angular momentum transport in accretion disks are studied in a laboratory experiment in a short Taylor-Couette flow using water and liquid gallium. Initial results on hydrodynamic stability at large Reynolds numbers show, for the first time, that the nonlinear pure hydrodynamic instabilities are very unlikely to sustain the required turbulence. Experiments using liquid gallium to study MRI are planned for the near future.

This work was supported in part by grants from NASA (APRA04-0000-0152) and DoE (DE-AC02-76-CH03073).

REFERENCES

Balbus, S.A., & Hawley, J.F. 1998, Rev. Mod. Phys., 70, 1
Richard, D. & Zahn, J.-P. 1999, Astron. Astrophys., 347, 734
Wendt, F. 1933, Ing. Arch., 4, 577

Taylor, G.I. 1936, Proc. Roy. Soc. London A, 157, 546

Richard, D. 2001, *Instabilités Hydrodynamiques dans les Ecoulements en Rotation Différentielle*. PhD thesis, Université Paris.

Balbus, S.A., Hawley, J.F., & Stone, J.M. 1996, Astrophys. J., 467, 76

Ji, H., Goodman, J., & Kageyama, A. 2001, Mon. Not. Astron. Soc., 325, L1

Goodman, J., & Ji, H. 2002, J. Fluid Mech., 462, 365

Noguchi, K., Pariev, V.I., Colgate, S.A., Beckley, H.F., & Nordhaus, J. 2002, Astrophys. J., 575, 1151

Sisan, D.R., Mujica, N., Tillotson, W.A., Huang, Y., Dorland, W., Hassam, A. B., Antonsen, T. M., & Lathrop, D. P. 2004, Phys. Rev. Lett., 93, 114502,

Hollerbach, R. & Rüdiger, G. 2005, Phys. Rev. Lett., 95, 124501

Kageyama, A., Ji, H., Goodman, J., Chen, F., & Shoshan, E., 2004, J. Phys. Soc. Jpn., 73, 2434

Burin, M.J., Schartman, E., Ji, H., Cutler, R., Heitzenroeder, P., Liu, W., Morris, L., & Raftopolous, S. 2006 in press, Experiments in Fluids

Ji, H., Burin, M., Schartman, E., & Goodman, J. 2006, in preparation.

Lesur, G. & Longaretti, P.-Y. 2005, A&A, 444, 25.

NASA LAW, February 14-16, 2006, UNLV, Las Vegas

Targeting inaccurate atomic data in the η Car ejecta absorption

K. E. Nielsen[1], G. Vieira Kober, & T. R. Gull

NASA Goddard Space Flight Center, Code 667, Greenbelt, MD 20771

nielsen@milkyway.gsfc.nasa.gov, gkober@milkyway.gsfc.nasa.gov, gull@milkyway.gsfc.nasa.gov

R. Blackwell-Whitehead

Imperial Collage, Blackett Laboratory, Prince Consort Rd., London, UK W2 4DX

r.blackwell@imperial.ac.uk

H. Nilsson

Lund Observatory, SE–221 00 Lund, Sweden

hampus.nilsson@astro.lu.se

ABSTRACT

The input from the laboratory spectroscopist community has on many occasions helped the analysis of the η Car spectrum. Our analysis has targeted spectra where improved wavelengths and oscillator strengths are needed. We will demonstrate how experimentally derived atomic data have improved our spectral analysis, and illuminate where more work still is needed.

1. Introduction

Eta Carinae (η Car) is one of the most massive and luminous known objects. It is a star in its late evolutionary stage and is targeted, for example, to gain better understanding of the preliminary stages before becoming a supernova, and possibly to give insight about other extreme objects such as hypernovaes and supernova impostors. Furthermore, it has recently been discovered that the absorption spectrum of η Car shows similar characteristics as observed in gamma ray burster (GRB) progenitors (Chen 2005). The knowledge of the

[1]Catholic University of America, Washington DC 20064

η Car ejecta will serve as platform for future studies of the currently not well known GRBs.

η Car's past is characterized by events in the 1840s and 1890s. The major outburst in the 1840s created the 18″ bipolar Homunculus and an intervening disk (Davidson et al. 2001), while a second less dramatic event in the 1890s is responsible for the interior Little Homunculus and the Weigelt blobs (Ishibashi et al. 2003). For more information about η Car's geometry, see Gull & Nielsen in these proceedings.

The spectrum of η Car displays a great variety of spectral features ranging from emission originating from the surrounding of the star to molecular and atomic absorption formed in the ejecta in the line-of-sight toward the star. The absorption spectrum has been analyzed (Gull et al. 2005; Nielsen et al. 2005; Gull et al. 2006) and used to characterize the ejecta. The Homunculus and the Little Homunculus have different characteristics ranging from a 760 K environment consisting of molecules and neutral elements to a 6400 K inner ejecta observed in predominantly singly-ionized iron-group elements. The Homunculus and the Little Homunculus are measured to have different heliocentric velocities at -513 and -146 km s^{-1}, respectively. Analysis of the η Car ejecta has been impeded by the lack of accurate atomic wavelengths and oscillator strengths. Collaborations with laboratory spectroscopists have provided improved atomic data, utilizing a better understanding of the physical processes of these gaseous and dusty environments.

2. Data and Analysis

The analysis presented in this paper is based on data obtained with (*HST*/STIS) during GTO program 9242 and GO programs 9083 and 9973. The data is obtained with the E230H grating and a 0.″2×0.″3 aperture setting providing a spectral resolving power of $R \sim$110,000. The angular resolving power of *HST* STIS ($\sim$0.″060 FWHM) has been invaluable and utilized the use of a 0.″088 subset of the aperture to avoid contamination from the nebula.

The analysis of the ejecta was performed with a standard curve-of-growth in combination with CLOUDY photo-ionization modeling. Physical parameters such as the excitation temperature, electron density and distance from the ionizing source were derived based on measured atomic level populations in the ejecta.

The analysis has repeatedly been challenged by errors that can be attributed the measurements and/or inaccurate atomic data. By estimating the measurement errors we have been able to target where there is a need for more accurate atomic data. Collaboration with the laboratory spectroscopy community has been very fruitful. New experimental atomic data has improved the accuracy of the derived radial velocities and column densities. Figure 1 shows an attempt to derive expansion velocity for the Homunculus using V II transitions from the lowest energy states. New experimental data (Johansson 2003; Arvidsson 2003) removed the major scatter in the plot and was the base for a single value heliocentric velocity.

The CLOUDY photo-ionizing modeling require input parameter defining the radiative source as well as well as the chemical structure of the ejecta. Therefore, it is essential

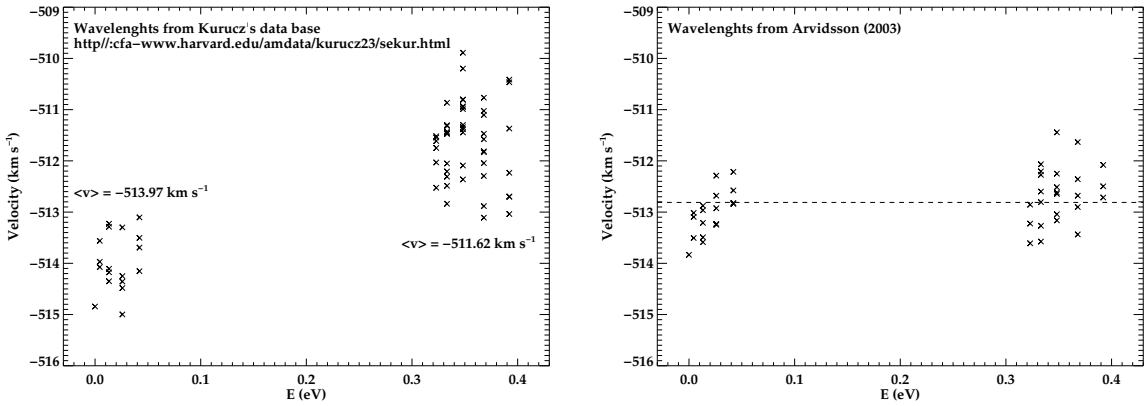

Fig. 1.— Radial velocity measurements for the Homunculus using lines from the lowest configurations in V II.

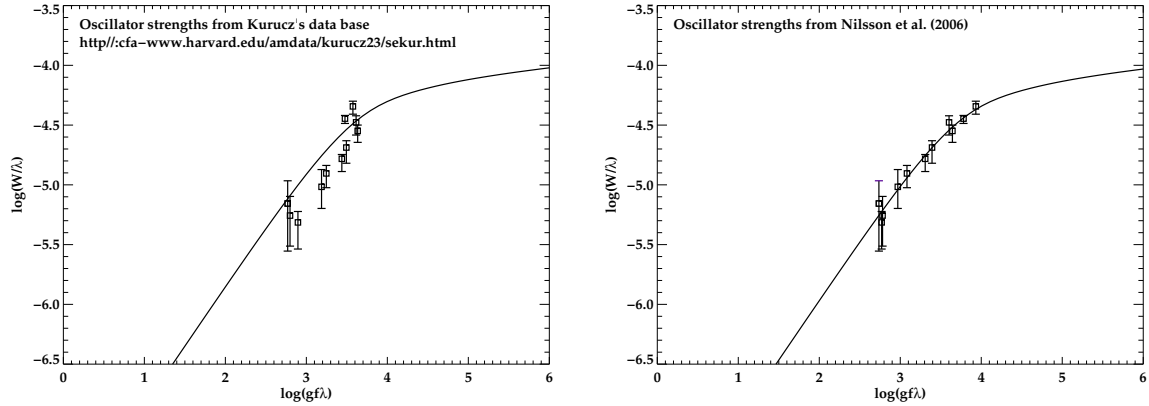

Fig. 2.— Column density measurements using a standard curve-of-growth, presented for the Cr II 4s a^{4}D term. The scatter was dramatically decreased when improved experimental loggf values were used.

to investigate the level populations for as many atoms/ions/molecules as possible. The modeling is highly dependent on the derived column densities and, hence the accuracy of the measurements as well as the available atomic data. Figure 2 present a curve-of-growth for one of the lower energy states in Cr II and how the new set of transition probabilities (Nilsson et al. 2006) has improved the fit of the theoretical curve-of-growth.

3. Summary

The variety of emission and absorption features, together with the angular resolving capabilities of *HST*/STIS, have utilized investigations of low and high density plasmas in the

vicinity of η Car. The spectral analysis is highly dependent on accurate atomic data, whereas collaboration with the laboratory spectroscopy community is essential. We have targeted atomic data requirements, exemplified by V II and Cr II but important for other iron-group atoms/ions, and shown how the new laboratory data have helped improve the astrophysical analysis. The prevailing problems are, especially, oscillator strengths for the some of the neutral light elements, such as C I , N I and O I, but large scatter in Fe I curve-of-growth is also observed. Currently, we can not blame the inaccuracy of the latter on bad atomic data, since the excitation conditions in the analyzed gas may not be fully understood. Progress in the analysis of the η Car ejecta and the future understanding of the GRB progenitor spectra will depend on contributions from the laboratory spectroscopist.

This work is based upon observations made with the NASA/ESA *HST*, obtained at the Space Telescope Science Institute, under NASA contract NAS 5−26555.

REFERENCES

Arvidsson K. 2003, Masters Thesis, Lund University
Chen H. W. et al. 2005, ApJ 634, L25
Davidson K. et al. 2001, AJ 121, 1569
Ishibashi K. et al. 2003, AJ 125, 3222
Gull T. R. et al. 2005, ApJ 620, 442
Gull T. R., Kober G. V. & Nielsen K. E. 2005, ApJS 163, 173
Johansson S. 2003, private communication
Nilsson H. et al. 2006, A&A 445, 1165
Nielsen K. E., Gull T. R. & Kober G. V. 2005, ApJS 157, 138

NASA LAW, February 14-16, 2006, UNLV, Las Vegas

A Spatial Heterodyne Spectrometer for Laboratory Astrophysics; First Interferogram

J. E. Lawler, Z. E. Labby, & F. L. Roesler

Dept. of Physics, Univ. of Wisconsin, Madison, WI 53706

jelawler@wisc.edu, zelabby@wisc.edu, roesler@physics.wisc.edu

J. Harlander

Dept. of Physics, Astronomy, and Engineering Science, St. Cloud State Univ., St. Cloud, MN 56301

harlander@stcloudstate.edu

ABSTRACT

A Spatial Heterodyne Spectrometer with broad spectral coverage across the VUV - UV region and with a high (> 500,000) spectral resolving power is being built for laboratory measurements of spectroscopic data including emission branching fractions, improved level energies, and hyperfine/isotopic parameters.

1. Introduction

Fourier Transform Spectrometers (FTS's) are important to Laboratory Astrophysics programs including the Univ. of Wisconsin effort on atomic transition probabilities. Instruments such as the McMath 1 m FTS at the National Solar Observatory on Kitt Peak have many advantages. They provide a very high spectral resolving power, broad UV to IR wavelength coverage, exceptional wavenumber accuracy and precision, a large etendue, and a high data collection rate. There is an additional advantage of a FTS for measurements of emission branching fractions over large spectra ranges; an interferogram is a simultaneous measurement of all spectral resolution elements. This last advantage makes a FTS insensitive to source intensity drifts during branching fraction measurements. Although the McMath 1 m FTS has been extraordinarily successful in the UV-visible-IR regions for approximately 3 decades, there is critical need for an equally productive instrument in the VUV.

The need for basic spectroscopic data in the VUV arises in part from local Universe observations, such as studies of the Interstellar Medium (ISM) and chemically peculiar stars

of our Galaxy, and from high redshift studies of the ISM of distant, young Galaxies. Quantitative spectroscopy yields most of the detailed physics and chemistry of such studies. The opportunities for high redshift observations will be dramatically improved with the launch of the James Webb Space Telescope.

We are building a new type of FTS called a Spatial Heterodyne Spectrometer (SHS) to meet the needs of Laboratory Astrophysics in the VUV (Harlander and Roesler 1990). The availability of large format, 2 dimensional detector arrays makes it possible to build high performance SHS's. In a traditional FTS based on a Michelson interferometer, at least one mirror is moved to record an interferogram as a function of mirror position (or time) using a single channel detector. In a SHS the interferogram is spread out in space and is projected onto a detector array. The lack of moving parts in SHS instruments simplifies their design and construction and makes these instruments compatible with transient, low duty cycle sources. Furthermore, a SHS is somewhat more tolerant of optical imperfection than a traditional FTS based on a Michelson interferometer. These advantages, and the prospects of building an all reflection SHS for VUV operation, have inspired us to design and build a broadband, very high resolution SHS for the VUV. This paper is a progress report on our project.

2. The Mark 1 SHS

Figure 1 is a schematic of our Mark 1 SHS which is built around a CaF_2 beamsplitter and a matched pair of very coarse (23.2 groove/mm) echelle diffraction gratings. Our Mark 1 SHS will have VUV capability, but it is limited to wavelengths above the CaF_2 transmission cutoff. Order separation, scattered light, and phase stability issues in broadband, high resolution SHS instruments are being addressed using our Mark 1 SHS. Lenses are shown in Figure 1 as the collimating and imaging optics only to simplify the figure. Off-axis mirrors are actually being used.

Essential features of the Mark 1 SHS are easy to understand since its geometry is similar to a Michelson interferometer. The flat phase fronts in Fig. 1 coming from both gratings at the exact Littrow condition recombine at the beamsplitter to form a broad light or dark fringe. This fringe is a Fizeau fringe localized near the projected crossing point of one grating with the virtual image of the other. Phase fronts for a wavelength above or below the Littrow wavelength are tipped, and these cross each other to form Fizeau fringes running perpendicular to the plane of the figure. The fringe frequency is proportional to wavelength separation from Littrow. The ambiguity of equal fringe frequencies above and below Littrow, and the ambiguity of different grating orders, can both be resolved by tipping one of the gratings about an axis in the plane of the figure and parallel to the Littrow phase fronts. Detailed equations for the SHS fringe frequency and desired cross tip angle have been published (Harlander and Roesler 1990). We will focus in subsequent paragraphs on design

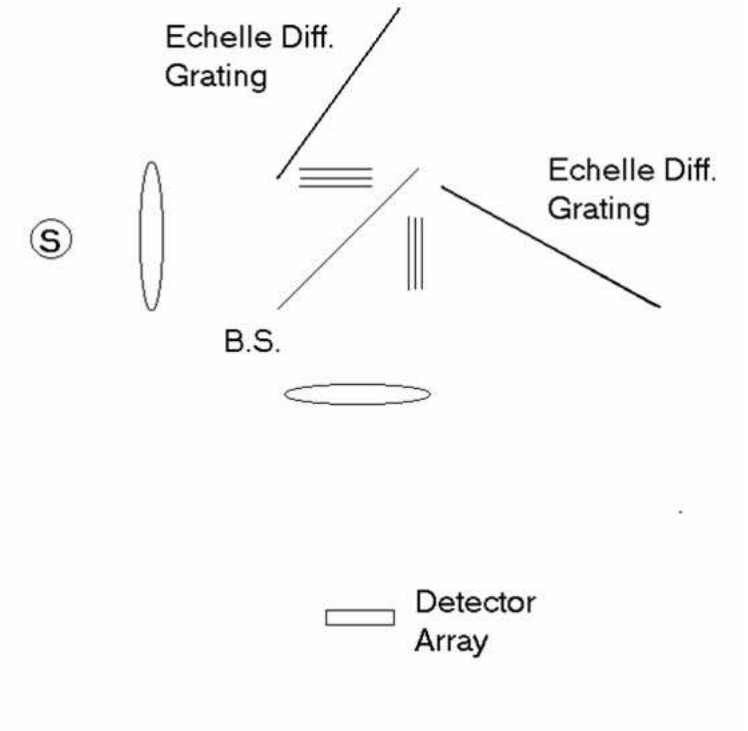

Fig. 1.— Schematic of a SHS with a transmitting beamsplitter.

issues specific to a broadband, high resolution SHS in the VUV.

A very coarse grating is needed to efficiently exploit the square or nearly square format of a CCD camera. We chose replicas of an existing echelle master grating. Our 23.2 groove/mm, 63.5 degree blaze gratings operate in 511^{th} order for wavelengths near 151 nm. The separation of adjacent order (horizontal) fringes in a symmetric interferogram requires at least 4x511 pixels. Our choice of diffraction grating is thus compatible with 2048x2048 pixel CCD camera for wavelengths down to 151 nm. We chose the Princeton Instruments "Pixus" 2K by 2K VUV CCD camera.

The echelle gratings of our Mark 1 SHS have ruled areas of 46 mm x 96 mm. This size grating yields a theoretical limit of resolution of 0.058cm^{-1} (the inverse of the maximum path difference of 2 x 9.6 cm x sin 63.5°) with a symmetric interferogram and a smaller limit with an asymmetric interferogram. The theoretical resolving power at 151 nm is thus $>$ 1,000,000, and is $>$ 500,000 with an entrance aperture opened to maximize the luminosity-resolution product.

In order to approach these very high resolving powers over large spectral ranges, it is essential that the imaging of fringes onto the CCD be nearly free of aberrations. Interferometric quality mirrors are essential. Astigmatism is the most serious Seidel aberration and it arises both from the beamsplitter and from the off axis mirror(s) used to image the fringes

onto the CCD. Mirror astigmatism must be controlled by limiting the mirror tip angle, by using non spherical mirror, or by compensating with more than one mirror. Aberrations have been calculated and included in our design. The highest fringe frequencies occur $\frac{1}{2}$ way between echelle grating orders. We are anticipating some loss of fringe contrast and thus sensitivity at the highest fringe frequency due to residual aberrations and "blooming" between CCD pixels. It is possible that some of the resolving power of our Mark 1 SHS will be sacrificed in order to reduce the sensitivity roll-off between orders. This can be done by modifying the image size on the CCD to over-sample the interferogram as needed.

Traditional phase correction as well as phase distortion issues in SHS instruments were discussed by Englert et al. (2004). Optical imperfections including distortion of the image on the CCD, a lack of perfectly flat grating surfaces, and a lack of a perfectly flat or homogeneous beamsplitter all lead to phase distortion errors in the interferogram. One of the advantages of SHS's is that fringes, curved by optical defects, can be straightened using software. Although software corrections can be convenient and cost effective in an SHS instrument with a narrow spectral coverage, much more effort will be required to map the phase errors of a broadband SHS. For that reason, we have devoted substantial effort and resources to minimizing phase errors (eg. with very high quality optics and proper optical mounts) and to maximizing phase stability of the Mark 1 SHS. Long term phase stability of the SHS is essential if the phase distortion map is to be used for correction of interferograms over an extended period of time. An all Invar, vacuum compatible, custom optical breadboard provides the base of the Mark 1 SHS. Additional Invar "sandwich" plates secure the top and bottom of the beamsplitter and diffraction grating mounts. The remaining aluminum parts of the beam splitter mount and grating mounts have been temperature compensated. Vacuum compatible "picomotors" are used to adjust the critical optics during operation.

Figure 2 is one the first interferograms recorded with the Mark 1 SHS using a monochromatic source. The straight and equally spaced fringes are encouraging. Figure 3 is a plot of every 4 row of a 2 dimensional Fourier transform from one of the Mark 1 SHS interferograms. The fidelity of the instrument is confirmed by the sharp (1 pixel wide) peak of the transformed spectrum.

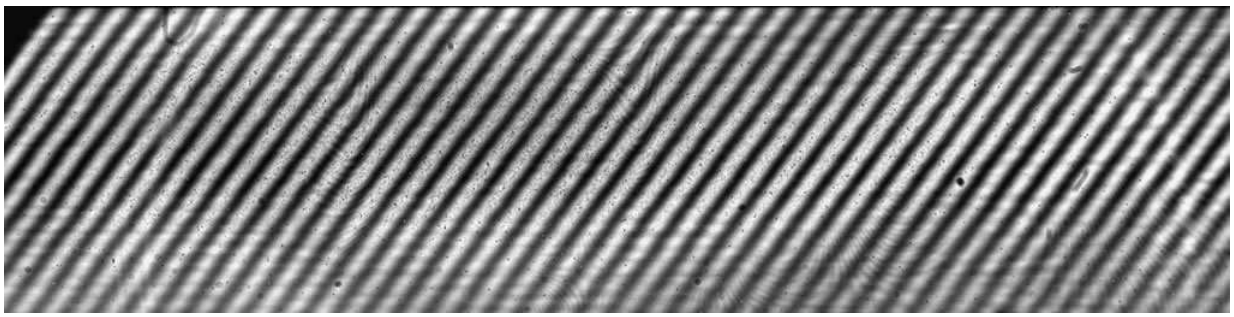

Fig. 2.— Interferogram of a monochromatic source from the Mark 1 SHS.

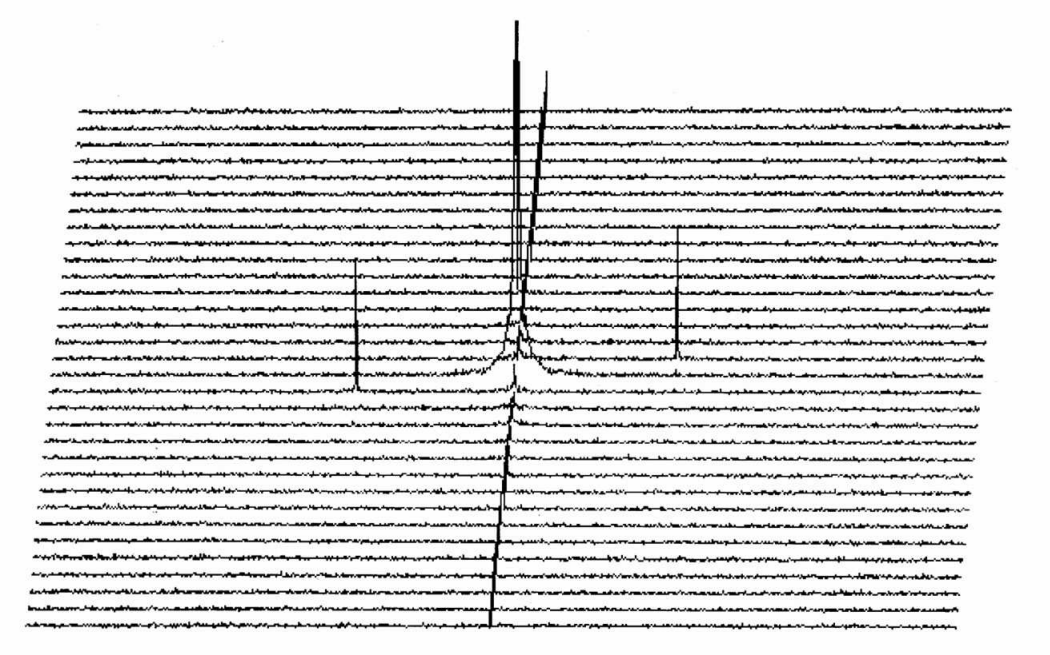

Fig. 3.— Transformed spectrum of a monochromatic source from the Mark 1 SHS.

3. The Mark 2 SHS

All reflection SHS instruments use a diffraction grating as a beam splitter and combiner (Harlander and Roesler 1990). The robust "ring" design is very stable due to the common path (Harlander and Roesler 1990). Several all reflection SHS's have been built and are now being used, but a very broadband instrument of this type has not yet been built. A special coarse diffraction grating with a symmetric blaze at low angle is needed to construct an all reflection, high resolution SHS with very broad spectral coverage. This will require a new master ruling.

Supported by NASA Grant NNG05GD48G.

REFERENCES

Harlander, J. & Roesler, F. L. 1990, "Spatial heterodyne spectroscopy: A novel interferometric technique for ground based and space astronomy", Instrumentation in Astronomy VIII, ed. D. L. Crawford (Proc. SPIE, 1235), 622

Englert, C. R., Harlander, J. M., Cardon, J. G., & Roesler, F. L. 2004, Appl. Opts., 43, 6680

NASA LAW, February 14-16, 2006, UNLV, Las Vegas

Magnetic-Field Sensitive Line Ratios in EUV and Soft X-ray Spectra

P. Beiersdorfer, J. Scofield, G. V. Brown, H. Chen, E. Träbert

High Temperature and Astrophysics Division, Lawrence Livermore National Laboratory, Livermore, CA 94550

beiersdorfer@llnl.gov, scofield1@llnl.gov, brown86@llnl.gov, chen33@llnl.gov, trabert1@llnl.gov

J. K. Lepson

Space Sciences Laboratory, University of California, Berkeley, CA 94720

lepson@ssl.berkeley.edu

ABSTRACT

We discovered a class of lines that are sensitive to the strength of the ambient magnetic field, and present a measurement of such a line in Ar IX near 49 Å. Calculations show that the magnitude of field strengths that can be measured ranges from a few hundred gauss to several tens of kilogauss depending on the particular ion emitting the line.

1. Introduction

The emission from high-temperature plasmas, such as stellar coronae, is dominated by spectral lines in the EUV and soft X-ray range. These lines provide accurate information on temperature, density, and emission volume. So far, none of the lines has provided information on the strength of the ambient magnetic field, even though the fields may be quite high. Magnetic field measurements using the Zeeman effect in optical lines (Zeeman 1897) from neutrals or singly charged ions reveal kilogauss fields in certain types of stars, and magnetospheric accretion models predict fields in excess of 10,000 gauss (Johns-Krull et al. 1999). Fields in cataclysmic variables may even achieve values of several megagauss. Instead of direct measurements, magnetic fields in high-temperature plasmas, which may play an important role for constraining evolutionary models of astrophysical objects, must be estimated rather imprecisely from equipartition arguments.

During the past years we have been engaged in laboratory measurements at the University of California Lawrence Livermore National Laboratory EBIT-I and SuperEBIT electron beam ion trap facility, which systematically have established catalogues of astrophysically relevant lines in the extreme ultraviolet. Our measurements, for example, have produced line lists of the $n \geq 3 \rightarrow 2$ L-shell transitions of Ar, S, and Si (Lepson et al. 2003, 2005; Lepson & Beiersdorfer 2005). These measurements have included a class of lines that are sensitive to the strength of the ambient magnetic field. In particular, the intensity of these lines increases as the magnetic field strength increases. As a result, the ratio of the intensity of this line to those of neighboring lines represents a diagnostic of the magnetic field strength.

The principle of our magnetic field diagnostic is based on the fact that the presence of a magnetic field spoils the spherical symmetry of the Coulomb potential, thereby removing the degeneracy of the magnetic sublevels and allowing mixing among sublevels associated with levels of different total angular momentum as long as they have the same magnetic quantum number and parity. Such mixing in many cases is irrelevant, as it typically is weak, and both levels are likely to have strong radiative decay channels. In other words, a few parts per million change in the radiative decay rates will hardly be noticeable given the present accuracy of calculations and measurements. However, if one of the levels has no or only a very weak radiative channel while the other has a strong channel, magnetic field mixing can result in the apportioning of a finite radiative rate and thus the appearance of a line that would otherwise not exist. The intensity of the new line depends on the mixing and thus on the magnetic field.

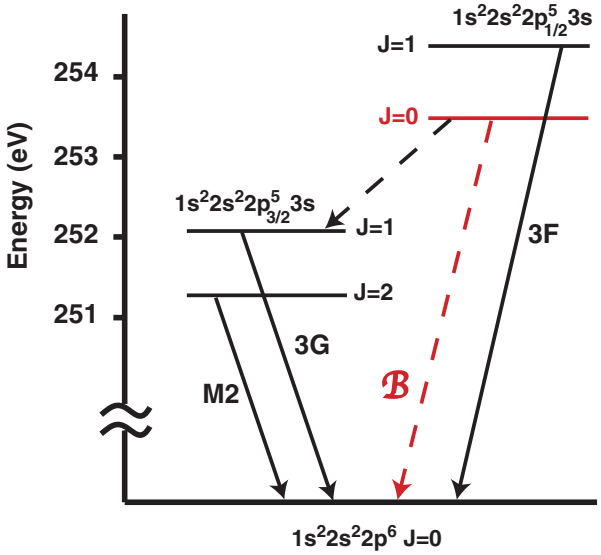

Fig. 1.— Grotrian diagram showing the lowest four excited levels in Ar IX. Transitions are labeled in common notation; the magnetic field sensitive line is labeled $\mathcal{B}$.

Levels with total angular momentum $J = 0$ are strictly forbidden to decay to another

level with zero total angular momentum (in the absence of hyperfine structure). These levels, therefore, represent an ideal case to study magnetic-field induced transitions. A diagram of the four lowest levels in neonlike Ar IX is shown in Fig. 1. The two levels that are best suited for magnetic-field mixing are the $(1s^2 2s^2 2p^5_{1/2} 3s)_{J=0}\ ^3P_0$ level and the close-by $(1s^2 2s^2 2p^5_{1/2} 3s_{1/2})_{J=1}\ ^1P_1$ level. In the absence of an external field, the $^3P_0$ level exclusively decays via a magnetic dipole (M1) transition to the $(1s^2 2s^2 2p^5_{3/2})_{J=1}\ ^3P_1$ level, but because of the small energy separation does so only very weakly with a rate of 58 1/s. By contrast, the neighboring $(1s^2 2s^2 2p^5_{1/2} 3s_{1/2})_{J=1}\ ^1P_1$ level rapidly decays to the ground state via an electric-dipole transition, commonly labeled $3F$, at a rate of 1.4×10^{11} 1/s. Mixing with the $^1P_1$ level allows the $^3P_0$ level to decay to the $^1S_0$ ground state with a finite, albeit small, radiative rate. Although closeness is a prerequisite for mixing, the two levels are sufficiently far apart so that the presence of a line resulting from the magnetic field induced decay of the $^3P_0$ level can be observed and resolved from the decay of the neighboring $^1P_1$ level. We note that in strict LS-coupling such mixing would not be possible. However, mixing occurs because the triplet and singlet levels themselves are not pure states.

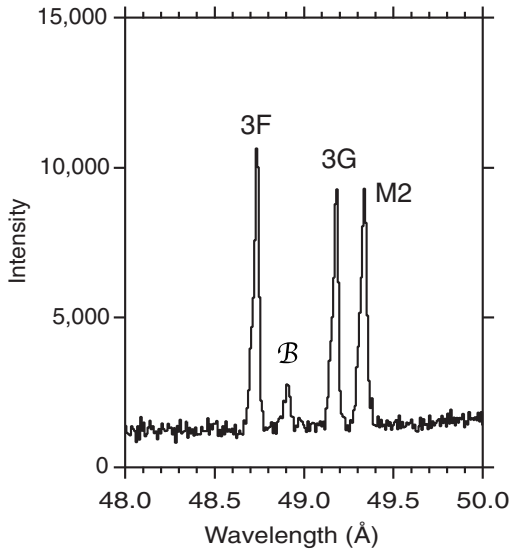

Fig. 2.— Spectrum of the Ar^{8+} $3s \rightarrow 2p$ emission obtained with the new high-resolution grating spectrometer. Lines are labeled in the same notation as in Fig. 1.

Our measurements were performed using the EBIT-I electron beam ion trap at the University of California Lawrence Livermore National Laboratory. Initial measurements utilized a broadband grazing-incidence spectrometer (Beiersdorfer et al. 2003). We have since implemented a very high-resolution grazing-incidence spectrometer based on a 44 m variable line spacing reflective grating (Beiersdorfer et al. 2004). This improved the resolving power by a factor of eight and clearly isolates the line produced by the presence of the magnetic field, as illustrated in Fig. 2.

The variation of the intensity of the field-induced line with magnetic field strength is shown in Fig. 3 for the three neonlike ions Si V, Ar IX, and Fe XVII. The figure shows that the line reaches 20 % of its final strength at 500 G in Si V, at 2500 G in Ar IX, and at about 25,000 G in Fe XVII. These ions thus cover a wide range of magnetic field strengths.

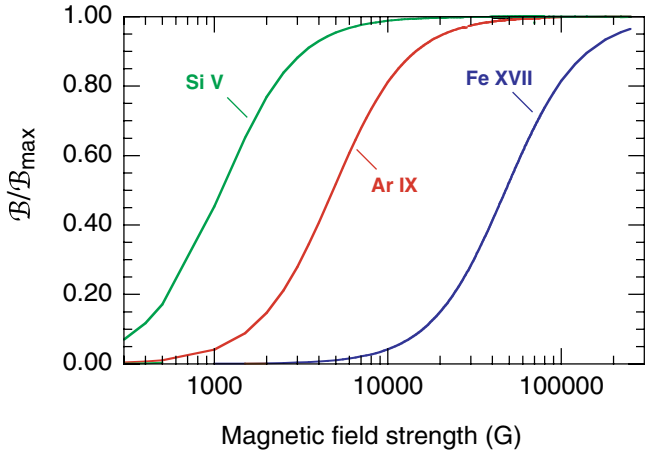

Fig. 3.— Intensity variation of the B line as a function of magnetic field strength in three astrophysically abundant neonlike ions.

This work was supported by NASA Astronomy and Physics Research and Analysis program work order NNH04AA751, and was performed under the auspices of the Department of Energy by the University of California Lawrence Livermore National Laboratory under Contract No. W-7405-ENG-48.

REFERENCES

Beiersdorfer, P., Magee, E. W., Träbert, E., Chen, H., Lepson, J. K., Gu, M.-F., & Schmidt, M. 2004, Rev. Sci. Instrum., 75, 3723

Beiersdorfer, P., Scofield, J. H., & Osterheld, A. L. 2003, Phys. Rev. Lett., 90, 235003

Johns-Krull, C. M., Valenti, J. A., & Koresko, C. 1999, Astrophys. J., 516, 900

Kochukhov, O. P., Piskunov, N. E., Valenti, J. A., & Johns-Krull, C. M. 2001, in *Cool Stars, Stellar Systems and the Sun, Eleventh Cambridge Workshop*, Astronomical Society of the Pacific Conference Series Vol. 223, ed. by R. J. García López, R. Rebolo, and M. R. Zapatero Osorio (ASP, San Francisco, 2001), p. CD-985

Lepson, J. K. & Beiersdorfer, P. 2005, Phys. Scripta, T120, 62

Lepson, J. K., Beiersdorfer, P., Behar, E., & Kahn, S. M. 2003, Astrophys. J., 590, 604

—. 2005, Astrophys. J., 625, 1045

Zeeman, P. 1897, Phil. Mag., 43, 226

NASA LAW, February 14-16, 2006, UNLV, Las Vegas

Sensitivity Analysis Applied to Atomic Data Used for X-ray Spectrum Synthesis

T. Kallman

NASA/GSFC, Code 662, Greenbelt, MD 20771

1. Introduction

A great deal of work has been devoted to the accumulation of accurate quantities describing atomic processes for use in analysis of astrophysical spectra. But in many situations of interest the interpretation of a quantity which is observed, such as a line flux, depends on the results of a modeling- or spectrum synthesis code. The results of such a code depends in turn on many atomic rates or cross sections, and the sensitivity of the observable quantity on the various rates and cross sections may be non-linear and if so cannot easily be derived analytically. This paper describes simple numerical experiments designed to examine some of these issues. Similar studies have been carried out previously in the context of solar UV lines by Gianetti et al. (2000); Savin & Laming (2002) and in the context of the iron M shell UTA in NGC 3783 by Netzer (2004).

We perturb the dielectronic recombination (DR) rates according to the prescription:

$$\log(\mathrm{Rate}') = \gamma \log(\mathrm{Rate}) \tag{1}$$

where the constant γ is a randomly distributed quantity in the range $0.9 \leq \gamma \leq 1.1$. It is randomly chosen for each ion, but is the same for a given ion at all temperatures. The remainder of this paper is devoted to exploring the results of this experiment for gases in both coronal and photoionization equilibrium, and the consequences for the results derived from fitting to recent data from the Chandra X-ray telescope. In addition, we also examine briefly the effects of factor $\sim$2 changes in the rates of ionization by the Auger mechanism, for photoionized plasmas.

2. Coronal ionization balance

Figure (1) shows the ionization balance for gas assuming coronal equilibrium. The left panel shows the ionization balance of iron calculated using the rates equivalent to the rates compiled by Arnaud & Raymond (1992) for dielectronic recombination (DR) and electron

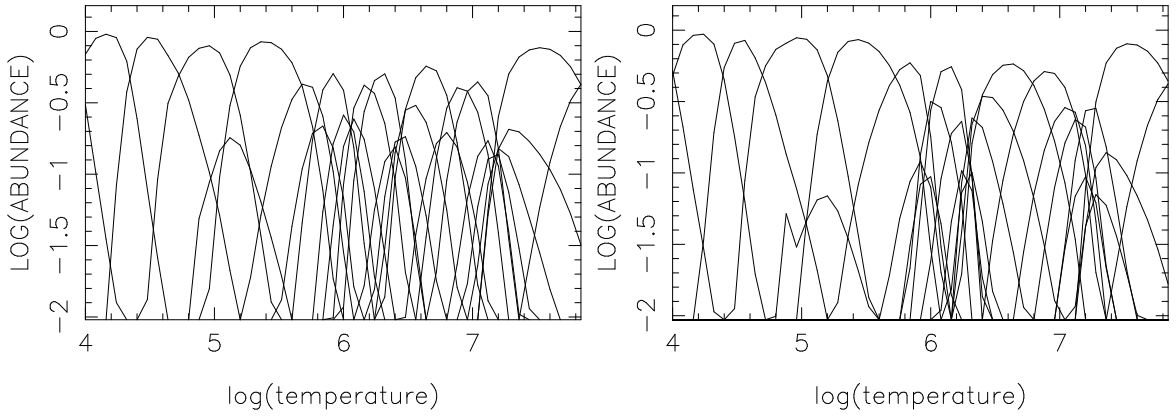

Fig. 1.— Coronal ionization balance for iron using baseline (left) and perturbed (right) recombination rates

impact collisional ionization. The right panel shows the ionization balance obtained when the same DR rates are randomly perturbed using the prescription given in the previous section. This shows that perturbing the DR rates by the amount chosen here leads to a change in the temperature where the abundance of a given ion peaks of Δ log(T)=0.1 for some ions, and less for stable ions such as Fe^{16+}.

3. Coronal Fitting Results

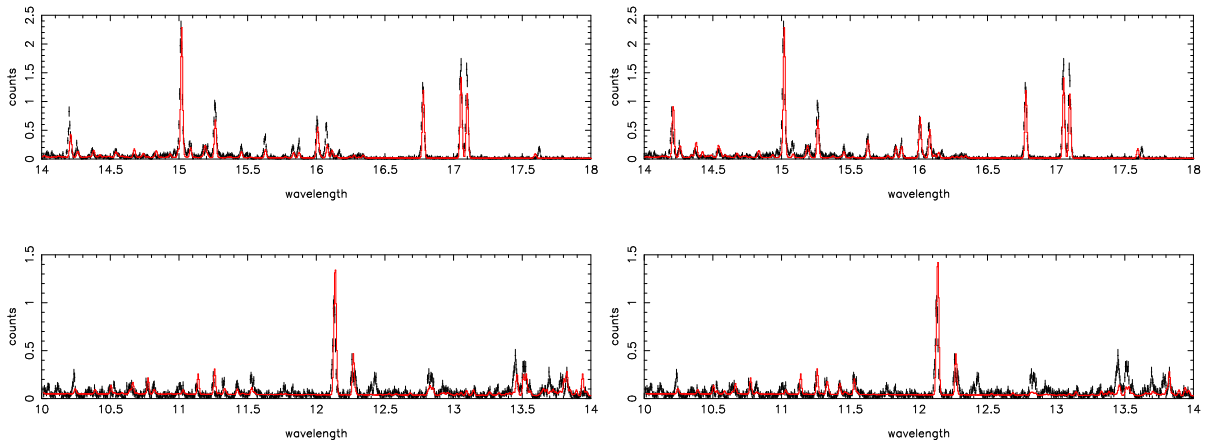

Fig. 2.— Fit to HETG Capella Spectrum using baseline ionization balance (left) and perturbed ionization balance (right)

Figure (2) shows a fit of coronal emission model to a 60 ksec Chandra HETG observation of the active star Capella, similar to that reported by Canizares et al. (2000). The left panels show a fit of the Chandra data to a model calculated using the baseline ionization

balance from Figure (1). The solid (red) curve shows a fit of 2 component model, with log(T)=6.9,7.1. The χ^2 for this fit is 3267 for 1602 degrees of freedom. The abundances are [Ne/Fe]=2.1, [O/Fe]=1. The right panels show a fit using the ionization balance calculated using the perturbed DR rates shown the right panel of figure (1). With no attempt at iterative improvement this gives χ^2=3610/1602. When this model is iteratively fit to the data χ^2=3522/1602 which is still inferior to the baseline model, and the derived temperatures are: log(T)=6.9,7.2.

4. Photoionized ionization balance

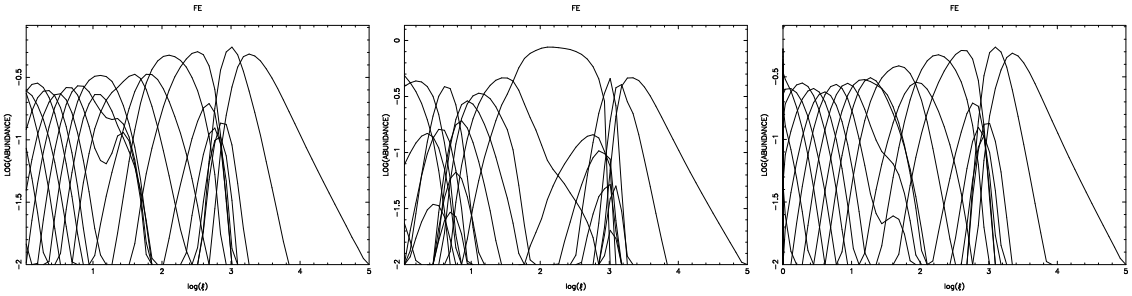

Fig. 3.— Photoionized ionization balance, baseline (left), using perturbed DR (center), and doubled K shell photoionization (right).

Figure (3) shows the ionization balance for gas assuming photoionization equilibrium, assuming a power law ionizing spectrum with energy index 1. The left panel shows the ionization balance of iron calculated using the rates described by Bautista & Kallman (2001) as implemented in the xstar code (Kallman & Bautista 2001). The middle panel shows the ionization balance obtained when the same randomly perturbed dielectronic recombination rates are used as were used in figures 1 and 2. The right panel shows the ionization balance obtained when the K shell photoionization rates are doubled. Since K shell ionization leads to multiple ionization via the Auger mechanism a significant fraction of the time, this is tantamount to a doubling of the Auger ionization rate. The middle panel shows that perturbing the DR rates has a greater effect in the photoionized case, and leads to a change in the ionization parameter where the abundance of a given ion peaks of Δ log(ξ)=0.2 or greater. Increasing the Auger rate in this case has a smaller effect, Δ log(ξ)=0.1.

5. Photoionized Fitting results

Figure (4) shows a small portion of a fit of photoionization model to the 900 ksec Chandra HETG observation of NGC 3783 first reported by Kaspi et al. (2001, 2002). The solid (red) curve shows a fit of 2 component photoionization model, with log(ξ)=2.2, 0.1. The χ^2

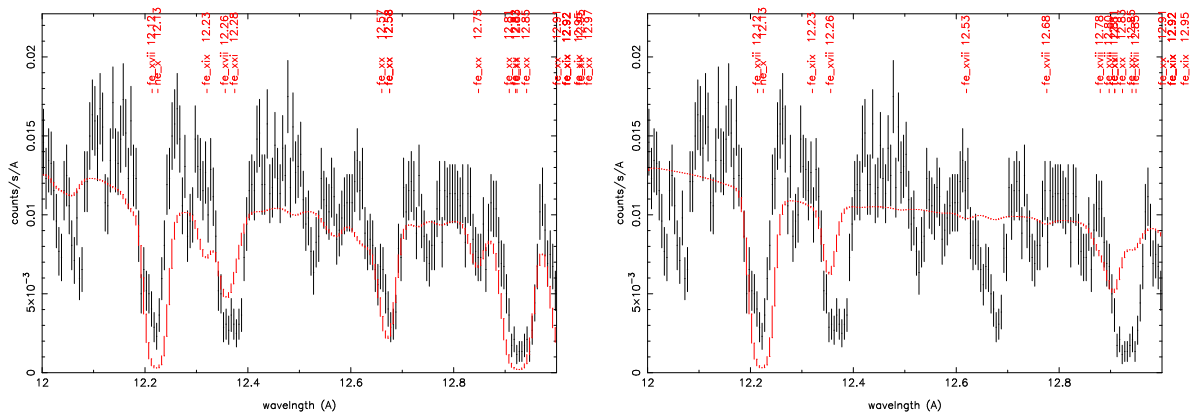

Fig. 4.— Fit of 2 component warm absorber model to the 900 ksec Chandra HETG observation of NGC 3783 in the 12-13 $\AA$ region. Xstar model using baseline (DR) rates (left) and using perturbed DR rates (right).

for this fit (including the entire HETG band) is 11105 for 8192 degrees of freedom. The model is calculated using the xstar code (Kallman & Bautista 2001) including recent compilations of the line energies and oscillator strengths for lines of iron by the Chianti collaboration (Landi et al. 2006). An blueshift of 700 km/s and a turbulent velocity of 300 km/s were assumed The elemental abundances are [Ne/O]=1, [Si/O]=1, [S/O]=2, [Fe/O]=0.4. These parameters are similar to those derived by Krongold et al. (2003).

Comparison between the fit to the NGC 3783 using the baseline ionization balance and that obtained using the perturbed DR rates is shown in figure (4). With no iterative improvement this gives χ^2=17660/8192. The figure shows the fit when this model is iteratively fit to the data. The χ^2 is 13072/8192, which is still inferior to the baseline model, and the derived ionization parameters are log(ξ)=2.9,0.1. This is significantly different from that obtained with the baseline model.

6. Conclusions

We have shown that changes in the DR rates of ∼0.1 in the logarithm of the rate lead to comparable changes in the ionization balance distribution with temperature in the coronal case. The results of fitting to high resolution X-ray data are affected by a comparable amount. In the photoionized case, the ionization balance is more strongly affected by the same changes in DR rates, leading to changes in log(ξ) of 0.2, and comparable changes in the conditions inferred from fitting. Definitive conclusions on the sensitivity of astrophysical results to DR rates, and other rates, require more extensive experimentation, including a large number of such random trials.

REFERENCES

Arnaud, M., & Raymond, J. 1992, ApJ, 398, 39
Bautista, M. A., & Kallman, T. R. 2001, ApJS, 134, 139
Canizares, C. R., et al. 2000, ApJ, 539, L41
Gianetti, D., Landi, E., & Landini, M. 2000, A&A, 360, 1148
Kallman, T., & Bautista, M. 2001, ApJS, 133, 221
Kaspi, S., et al. 2002, ApJ, 574, 643
Kaspi, S., et al. 2001, ApJ, 554, 216
Krongold, Y., Nicastro, F., Brickhouse, N. S., Elvis, M., Liedahl, D. A., & Mathur, S. 2003, ApJ, 597, 832
Landi, E., Del Zanna, G., Young, P. R., Dere, K. P., Mason, H. E., & Landini, M. 2006, ApJS, 162, 261
Netzer, H. 2004, ApJ, 604, 551
Savin, D. W., & Laming, J. M. 2002, ApJ, 566, 1166
Smith, R. K., Brickhouse, N. S., Liedahl, D. A., & Raymond, J. C. 2001, ApJ, 556, L91

NASA LAW, February 14-16, 2006, UNLV, Las Vegas

Recent Excitation, Charge Exchange, and Lifetime Results in Highly Charged Ions Relevant to Stellar, Interstellar, Solar and Comet Phenomena

A. Chutjian[1], S. Hossain[1], R. J. Mawhorter[2] & S. J. Smith[1]

[1]*Jet Propulsion Laboratory/Caltech, Pasadena, CA 91109*

[2]*Dept. Physics and Astronomy, Pomona College, Claremont, CA 91711*

ABSTRACT

Recent JPL absolute excitation and charge exchange cross sections, and measurements of lifetimes of metastable levels in highly-charged ions (HCIs) are reported. These data provide benchmark comparisons to results of theoretical calculations. Theoretical approaches can then be used to calculate the vast array of data which cannot be measured due to experimental constraints. Applications to the X-ray emission from comets are given.

1. Introduction

Fundamental to the understanding of solar heating and radiation mechanisms is the availability of reliable diagnostics of electron density (N_e) and temperature (T_e). This need has provided a challenge to experimentalists and theoreticians to measure or calculate HCI collision strengths, lifetimes, X-ray emission intensities and wavelengths; and charge-exchange, ionization, & recombination (direct and dielectronic) cross sections. The significance of these phenomena is discussed in reviews (ADNDT 1999). For diagnostic emission lines the most important and least-well measured atomic parameter is the collision strength. In equations of statistical equilibrium the collision strength plays a central role in determining the excited-state population. For the case of coronal equilibrium one has the expression (useful in the determination of T_e) for the excited-state population N_i, given by $N_i = N_e\ N_g\ C(g \rightarrow i)/A(i \rightarrow g)$ where g refers to the ground state, and $C(g \rightarrow i)$, $A(i \rightarrow g)$ are the collisional excitation rate coefficient (cm^3/s) and the spontaneous radiative decay rate (sec^{-1}), respectively, for transitions between g and i. Other expressions for N_i exist for emissions involving several excited states, or when coronal equilibrium is not valid. These expressions are sensitive to the collisional rates $C(g \rightarrow i)$, $C\ (g \rightarrow j)$ .... for excited levels i, j.... It has been pointed out that a 20-25% error in the collision rates can lead to order-of-magnitude uncertainties in N_e (Keenan 1993). The motivation of the JPL program is

that: **(a)** *Almost all collision strengths used in astrophysics are calculated, with only isolated experimental data for comparison* [see the *OPACITY* (Badnell and Seaton 2003) and *IRON* (Nahar 2004) projects]. **(b)** Resonance contributions to collision rates can be factors of 2-5 times the direct rate; it is not possible to scale collision strengths, as the contributions do not scale with charge. **(c)** Uncertainties in the target wave function, inclusion of resonances and pseudostates are difficult to assess *a priori*, and are usually derived from a consensus of the various distorted-wave, $R-$Matrix close-coupling, or Flexible Atomic Code calculations. *There are very few cases where experimental data are available for comparison.*

2. Representative Results

The JPL facility has three beam lines dedicated to measurements in HCIs of absolute excitation cross sections using electron energy-loss scattering; X-ray emission spectra using either a germanium detector or a high-resolution grazing incidence X-ray monochromator; absolute single and multiple charge exchange cross sections using a gas cell and retarding-potential analysis of the transmitted ions; and metastable lifetimes using a Kingdon trap [see a facility schematic in Fig. 3 of Chutjian et al. (1999)].

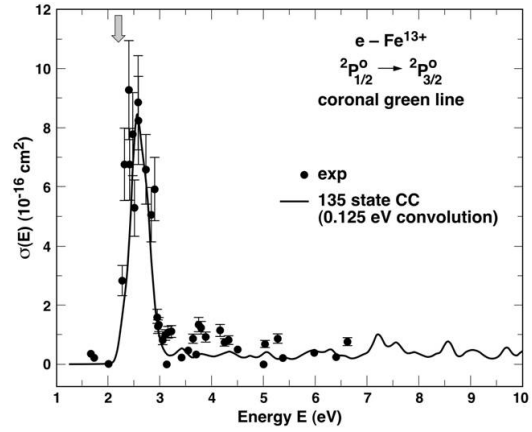

Figure 1. Absolute excitation cross sections for excitation of the forbidden M1 coronal green line in Fe^{13+}, with comparison to a 135 state R-Matrix calculation. Arrow indicates the threshold for this excitation (Hossain et al., unpublished).

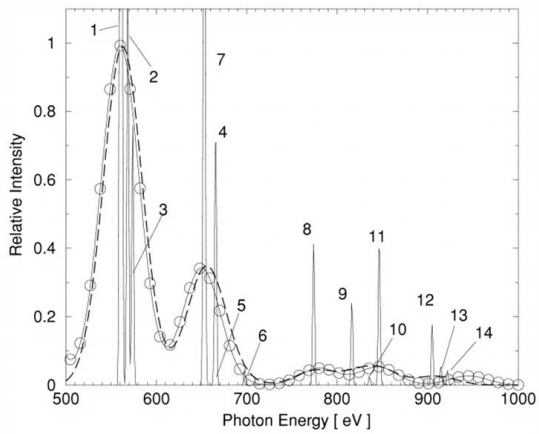

Figure 2. X-ray emission spectra from comet McNaught-Hartley. Solid circles and solid line are best fits to the observational data, and dashed curve is the calculation (Kharchenko et al. 2003).

2.1. *Excitation*

The Fe^{13+} coronal green line (530.3 nm) is the strongest forbidden line in the coronal spectrum, and brightest of all coronal emission lines in the visible spectrum; it is useful as a tracer of *Fe* abundance in galactic emission spectra. Shown in Fig. 1 are the first results of

the absolute electron excitation cross section of the $3s^2 3p\ {}^2P^o_{1/2} \rightarrow {}^2P^o_{3/2}$ transition. There is good agreement with results of a recent accurate 135 state R-matrix calculation.

2.2. *Ion Lifetimes*

JPL Kingdon trap measurements have been recently reported in the ions $Fe^{9,10,13+}$ (Smith et al. 2005). These results include the lifetime of the upper $Fe^{13+}\ {}^2P^o_{3/2}$ level (coronal green line). The result of 17.0±0.2 ms compares well with an EBIT value of 16.74±0.12 ms (Beiersdorfer et al. 2003), and with a less-accurate storage-ring measured lifetime of 18.0±1.2 ms (Träbert et al. 2002). The range of ten calculated lifetimes is 16.51-16.66 ms, which is in very good agreement with measurements in this transition.

2.3. *Charge Exchange and X-Ray Emission*

The detection of X-rays from comets (Lisse et al. 1996) has been successfully interpreted by Cravens (2002) in terms of charge exchange of solar-wind ions with neutrals in the cometary coma, followed by relaxation of the electronically-excited ion by X-ray emission. Shown in Fig. 2 are results of modeling the X-ray emission (Kharchenko et al. 2003) observed by *Chandra* from the comet McNaught-Hartley, in terms of the relative abundances of the ions O^{7+}, O^{8+} and Ne^{9+} in the solar wind, and the total single charge exchange cross sections of Greenwood et al. (2000, 2001). Representative laboratory X-ray spectra are shown in Fig. 3. The excellent agreement between observation and model stems from understanding the underlying solar physics and atomic physics unique to this astrophysical plasma.

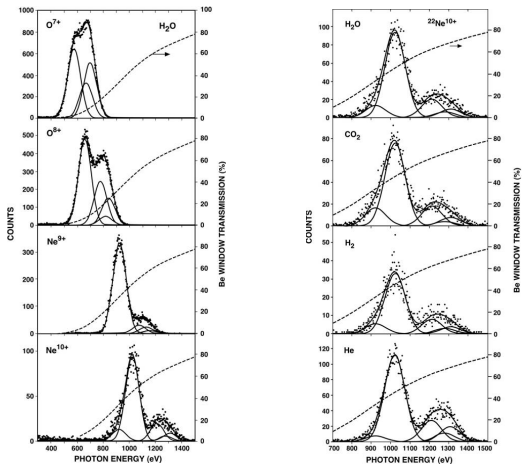

Figure 3. Laboratory X-ray spectra of HCIs colliding with H_2O (left) and $^{22}Ne^{10+}$ colliding with comet gases (right) (Greenwood et al. 2001).

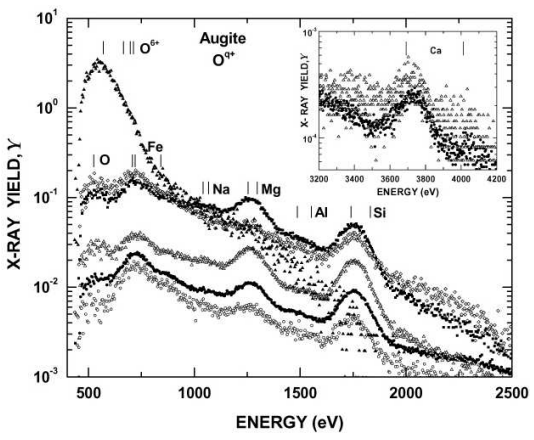

Figure 4. X-Rays emitted from augite [(Ca,Na) (Mg,Fe,Al) $(Al,Si)_2O_6$] bombarded by O^{q+} ions at energies of 7.0q keV. Charge states are given by: ● (q=2), △ (q=3), ○ (q =4), ■ (q=5), ◇ (q =6), and ▲ (q =7) (Djuric et al. 2005).

2.4. *Mineral Prospecting*

Absent in discussions of the interaction of solar wind HCIs with comets and other planetary objects is the role of surfaces. Under what circumstances does a surface contribute to X-ray production, and what wavelengths should be observed? To address these questions studies were carried out on X-rays observed during the collision of O^{q+} ions (q=2-7) [total energies of (2-7) q keV] with augite and olivine, simulants of a comet or planetary surface (Djuric et al. 2005). Spectral X-ray yields for olivine are shown in Fig. 4. Here the K-$L_{2,3}$ and K-$M_{2,3}$ transitions for the olivine components Na, O, Al, Mg, Si, and Ca are seen; as well as the L-M transition in Fe. Good agreement is found in the ratio of X-ray yields for Mg and Si, and the corresponding K-shell ionization cross sections. It appears that X-rays are being produced by electron acceleration into a surface that has been charged to a high positive potential by the HCI beam. One would search for these surface X-rays from a comet located at solar distances where gas evolution is not pronounced – regions with little or no cometopause. In these cases no blockage of the solar wind HCIs occurs, hence HCIs reaching the surface may induce a large surface charge (Lisse et al. 2005; Cravens 2006, private communication). This work was carried out at JPL/Caltech, and was supported through agreement with NASA.

REFERENCES

Atomic Data Nuclear Data Tables 1994, 57, and articles therein.
Badnell, N. R. and Seaton, M. J. 2003, J. Phys. B, 36, 4367
Beiersdorfer, P., E. Träbert, E., and Pinnington, E. H. 2003, Ap. J., 587, 836
Chutjian, A., Greenwood, J. B., and Smith, S. J. 1999, *Applications of Accelerators in Research and Industry* (eds. J. L. Duggan and I. L. Morgan, AIP, New York)
Cravens T. E. 2002, Science, 296, 1042
Djuric, N., Lozano, J. A., Smith, S. J., and Chutjian, A. 2005, Ap. J., 635, 718
Greenwood, J. B., Williams, I. D., Smith, S. J., and Chutjian, A. 2000, Ap. J. Lett., 533, L175; —,2001, Phys. Rev. A, 63, 062707
Keenan, F. P. 1993, in *UV and X-ray Spectroscopy of Laboratory and Astrophysical Plasmas* (ed. E. Silver and S. Kahn, Cambridge, UK)
Kharchenko, V., Rigazio, M., Dalgarno, A., and Krasnopolsky, V. A. 2003, Ap. J., 585, L73
Lisse, C. M. et al. 1996, Science, 274, 205
Lisse, C. M. et al. 2005, Ap. J., 635, 1329
Nahar, S. N. 2004, Astron. & Astrophys., 413, 779, and references therein
Smith, S. J., Chutjian, A., and Lozano, J. A. 2005, Phys. Rev. A, 72, 062504
Träbert, E. et al. 2002, J. Phys. B, 35, 671

INVITED TALK *NASA LAW*, February 14-16, 2006, UNLV, Las Vegas

A brief summary of some of the laboratory astrophysics workshop

William Klemperer

Department of Chemistry, Harvard University, Cambridge, MA 2138

klemperer@chemistry.harvard.edu

Our present knowledge of the molecular universe has come primarily from radio observations [I include here millimeter and submillimeter in this rubric]. There are a number of reasons for this but the primary one is the extremely high spectral resolution. The ease of observing emission from the volume of dense molecular clouds without significant attenuation by scattering from dust has shown this to be the powerful observational tool for molecular astronomy. Finally the relative simplicity of rotational compared to vibrational or electronic spectroscopy allows carrier identification as well as facile evaluation of cloud conditions such as density and temperature.

These virtues become tenuous as the astronomical observations are pushed to higher frequencies for enhanced observational sensitivity. Thus precision rest frequencies are mandatory for the search for new species. We may inquire about which new species require particular attention, and which species may be relatively safely predicted on the basis of lower frequency laboratory measurements. For a **rigid** rotor the three rotational constants are sufficient to completely specify the transition frequencies. The intensities require the three components of the electric dipole moment. For semirigid species, where the centrifugal distortion, may be treated at the quartic level of angular momentum (Bunker et al. 1998), up to five additional constants are required (Watson 1967). There are a number of such species of considerable interest, where laboratory measurements are adequate for astronomical searches. A most interesting species in this class is corannulene (Lovas et al. 2005), $C_{20}H_{10}$, an extremely rigid polar polyaromatic hydrocarbon, with oblate symmetric rotor structure. The important centrifugal distortion constant D_{JK} is vanishingly small, thus the spectrum is essentially that of a linear molecule. The present limits on its abundance may be set as less than . Further the semi-rigid polar heterocyclic aromatic species furan, pyrole, and pyridine have been well studied (Townes & Schawlow 1975). Thus far they have not been observed in the interstellar medium.

The third type of species are those with large amplitude internal motions. These are both interesting since they include molecules that are frequently regarded biologically relevant. Of these glycine is an model example. The adequacy of the semi-rigid rotor discussed above is highly doubtful. Thus low frequency measurements (Kuan et al. 2003) do not allow reliable prediction of higher frequency transitions (Snyder et al. 2005) when the crowded nature of the millimeter spectrum of rich regions such as Sag B2 and OMC1 is considered. While it

is transparently obvious that precision laboratory frequency measurements for each spectral region to be studied will reduce ambiguity in this problem, it is highly desirable to develop accurate higher order theory for species with large amplitude internal motions. This will be interesting in its own right but may provide more reliable methods of extrapolation to higher frequencies. There has been a considerable progress in treating large amplitude motions of weakly bound species (Bunker et al. 1998; Kozin et al. 2004). The ability to execute large numerical calculations in terms of the molecular potential provides a new means to estimate higher energy levels and transitions from fitting of lower ones. The question of how well one can theoretically extrapolate low frequency transitions of non-rigid to the relevant high frequency regions is both interesting and of broad interest.

A second area in which a considerable progress could be achieved is that of plasmas. There is a huge effort, primarily by the Department of Energy in fusion plasmas. This effort is generally a heavily directed large scale engineering one. The scientific content remains low. On the other hand the plasmas play an extremely important role astrophysically. The subject is extremely rich intellectually. There appears to be a wall between these efforts. In this writers opinion the Department of Energy would be wise in investing in basic research of astronomical plasmas.

The power of chemical models for interstellar and circumstellar regions has been well documented. In pushing forward there are many questions in which laboratory astrophysics will be extremely valuable if not essential. First are the rates of ion molecule processes at typical dark cloud temperatures, 10 K. Of primary concern is the direct measurement of radiative association rates well illustrated by the important reaction $CH_3^+ + H_2 \rightarrow CH_5^+ +$ photon (Barlow, Dunn, & Schauer 1984). Since for gas phase reactions determination of reaction cross section allows facile application to interstellar modeling this area is one of high payoff. A further question along these lines is whether there are quantum state selectivity in hydride reactivity. The ubiquitous CH^+ remains of considerable interest especially in translucent clouds, where it is observed in the $J = 0$ level. Can its reactivity in this level be different than in higher rotational levels?

The importance of surface reactions is clear with the recombination of atomic hydrogen occurring on grains. The treatment of this process is important, and apparently not a simple rate equation. The abundance of atomic hydrogen in dark molecular clouds is likely important for a number of reactions. The treatment of the hydrogen recombination avoids the many questions of surface chemistries at 10K such as will reaction products desorb from the cold surface.

REFERENCES

Bunker, P. R., & Jensen, P. 1998, Chap. 13, Molecular Symmetry ans Spectroscopy, 2nd Edition, National Research Council Canada

Watson, J. K. G. 1967, J. Chem. Phys., 46, 1935
Lovas, F. J., McMahon, R. J., Grabow, J.-U., Schnell, M., Mack, J., Scott, L. T., & Kuczkowski, R. L. 2005, J. Am. Chem. Soc., 127, 4345
Townes, C. H., & Schawlow, A. L. 1975, Microwave Spectroscopy (Dover)
Kuan, Y.-J., Charnley, S. B., Huang, H.-C., Tseng, W.-L., & Kisiel, Z. 2003, ApJ, 593, 848
Snyder, L. E., Lovas, F. J., Hollis, J. M., Friedel, D. N., Jewell, P. R., Remijan, A., Ilyushin, V. V., Alekseev, E. A., & Dyubko, S. F. 2005, ApJ, 619, 914
Bunker, P. R., & Jensen, P. 1998, Chap. 16, Molecular Symmetry ans Spectroscopy, 2nd Edition, National Research Council Canada
Kozin, I. N., Law, M. M., Tennyson, J., & Hutson, J. M. 2004, Computer Physics Communications, 163, 117
Barlow, S. E., Dunn, G. H., & Schauer, M. 1984, Phys. Rev. Lett., 52, 902

NASA LAW, February 14-16, 2006, UNLV, Las Vegas

Laboratory Studies of Stabilities of Heterocyclic Aromatic Molecules: Suggested Gas Phase Ion-Molecule Routes to Production in Interstellar Gas Clouds

Nigel G. Adams, L. Dalila Fondren, Jason L. McLain, & Doug M. Jackson

Department of Chemistry, University of Georgia, Athens, GA 30602

ABSTRACT

Several ring compounds have been detected in interstellar gas clouds, ISC, including the aromatic, benzene. Polycyclic aromatic hydrocarbons, PAHs, have been implicated as carriers of diffuse interstellar bands (DIBs) and unidentified infrared (UIR) bands. Heterocyclic aromatic rings of intermediate size containing nitrogen, possibly PreLife molecules, were included in early searches but were not detected and a recent search for Pyrimidine was unsuccessful. Our laboratory investigations of routes to such molecules could establish their existence in ISC and suggest conditions under which their concentrations would be maximized thus aiding the searches. The stability of such ring compounds (C_5H_5N, $C_4H_4N_2$, $C_5H_{11}N$ and $C_4H_8O_2$) has been tested in the laboratory using charge transfer excitation in ion-molecule reactions. The fragmentation paths, including production of $C_4H_4^+$, $C_3H_3N^+$ and HCN, suggest reverse routes to the parent molecules, which are presently under laboratory investigation as production sources.

1. Introduction

A series of small ring molecules (SiC_2, C_3H, SiC_3, C_3H_2, CH_2OCH_2, C_2H_3N, C_2H_5N, C_4H_4NH; Dickins et al. 2001; Kuan et al. 2004) has been detected in interstellar clouds, ISC (Wooten 2002; Kuan et al 2004). In addition, the larger ring, benzene, (C_6H_6) has been detected (Wooten 2002). Benzene has also been tentatively detected in the Titan atmosphere and (although this may be a contaminant; Waite et al. 2005) it has been included in recent models of this atmosphere (Wilson & Atreya 2004). Multiple rings, PAHs, are thought to be responsible for at least some of the DIBs and UIR lines (van der Zwet & Allamandola 1985; Leger & dHendecourt 1985; Salama, & Allamandola 1993), although this is still in contention. Other ring molecules (C_5H_5N Pyridine, $C_4H_4N_2$ Pyrimidine, C_4H_5N Pyrrole, $C_3H_4N_2$ Imidazole) were included in early searches (1973-1981), but were not detected (Simon & Simon 1973; Myers, Thaddeus, & Linke, 1980; Irvine, W., et al. 1981). There has also

been one recent unsuccessful search for $C_4H_4N_2$ (Kuan et al. 2003, 2004). These larger rings are of interest since substituted versions are prebiotic molecules (e.g., the nucleotide bases of DNA (thymine, cytosine, uracil) are substituted pyrimidines). The lack of detections is not surprising since as molecules get larger and more floppy, the emissions are divided amongst more lines and are thus weaker. An example is the disputed detection of glycine (Kuan et al. 2003; Snyder et al. 2005). Here, ion chemical modeling with laboratory data can help by showing where detection is most likely. Indeed, ion chemical modeling may be the only way to establish the presence of some molecules. Thus, based on all this information, it can be concluded that there is little doubt that heterocyclic aromatic rings are present in ISC and in the Titan atmosphere. But what is the stability of such aromatic rings and how long can they survive in these hostile environments? We have investigated this by studying charge transfer reactions with ions having recombination energies from 21.6 to 4.8 eV (the recombination energies of NH_4^+ and H_3O^+ are 4.8 and 6.4 eV respectively to NH_3 + H and H_2O + H).

2. Experimental

Measurements were made using the Selected Ion Flow Tube (SIFT) technique, which has been discussed in detail in the literature (Adams & Smith 1976a, b). Reactant ions were generated in a remote ion source, mass selected and injected into flowing He at ∼0.5 Torr. Reactant gases were added to the flow, and the primary and secondary ions detected by a downstream mass spectrometer with ion counting. All the measurements were made at 300K, although there is the ability to make measurements over the temperature range 80 to 600 K. Rate coefficients are accurate to within 20% (for the sticky gases used in this study) and products to within ± 5 in the percentage.

3. Results

Data were obtained for the reactions of Ne^+, Ar^+, N_2^+, N^+, Kr^+, O^+, O_2^+, NH_3^+, H_3O^+ and NH_4^+ with C_5H_5N, $C_4H_4N_2$, $C_5H_{11}N$ (Piperidine) and $C_4H_8O_2$ (Dioxane). Comparisons were also made with literature data for C_6H_6 (Arnold et al. 1999). All reactions occur with close to unit efficiency when compared with the theoretical collisional rate (Su, & Chesnavich 1982). For ions with recombination energies below ∼12 eV (O_2^+, NH_3^+, H_3O^+ and NH_4^+), there is no fragmentation of C_5H_5N or $C_4H_4N_2$, but the fragmentation increases as the recombination energy gets larger. In particular, initially there is one important type of fragmentation channel, $C_4H_4^+$ + HCN for C_5H_5N and $C_3H_3N^+$ + HCN for $C_4H_4N_2$ charge transfer reactions. Note that these ions have the same masses as $C_3H_2N^+$ and $C_2N_2H^+$, however, so far the identity of the ion as $C_4H_4^+$ has been established by deuterium labeling. Such reactions may be significant since HCN is important in both the Titan atmosphere (the

reactions with N^+ and N_2^+ are particularly important since these are major precursor ions in the Titan chemistry) and dense ISC (Tanguy et al. 1990; Snyder, L. E. & Buhl 1971). Other fragmentation channels become important at the higher exothermicities. For C_6H_6, there is less fragmentation at recombination energies of 12 to 13 eV. This is consistent with the observations of Peeters et al. (2005), which showed benzene to be the more stable against uv radiation than the substituted rings. For the low recombination energy protonated ions (H_3O^+ and NH_4^+), only proton transfer is observed.

4. Conclusion

It has been shown from charge transfer reactions, that although quite stable and able to exist quite well in dense ISC, C_5H_5N and $C_4H_4N_2$ are not as stable as C_6H_6. In particular, at energies at which the ionized species begin to fragment, the fragmentation channels are to $C_4H_4^+$ + HCN and $C_3H_3N^+$ + HCN respectively. This shows connectivity on the potential surfaces from the fragments to the undissociated ions. By microscopic reversibility, association of these product species could, in principle, produce rings. It is intended to study these and analogous reactions as a source of heterocyclic rings.

NSF funding of Grant 0212368 is gratefully acknowledged.

REFERENCES

Adams, N.G. & Smith, D. 1976a, Int. J. Mass Spectrum, Ion Phys., 21, 349
Adams, N.G. & Smith, D. 1976b, J. Phys. B, 9, 1439
Arnold, S.T., Williams, S., Dotan, I., Midey, A.J., Morris, R.A. & Viggiano, A.A. 1999, J. Phys. Chem. A, 103, 8421
Dickins, J.E., Irvine, W.M., Nummekin, A., Mollendal, A., Saito, S., Thorwirth, S., Hjalmarson, A. & Ohishi, M. 2001, Spectrochim. Acta, A57, 643
Ilyushin, V.V., Alekseev, E.A., & Dyubko, S.F. 2005, ApJ, 619, 914
Irvine, W.M. et al. 1981, A&Ap, 97, 192
Kuan, Y.-J., Charnley, S.B., Huang, H.-C., Tseng, W.-L., & Kisiel, Z. 2003a, ApJ, 593, 848
Kuan, Y.-J., Yan, C.-H., Charnley, S.B., Kisiel, Z., Ehrenfreund, P., & Huang, H.-C. 2003b, MNRAS, 345, 650
Kuan, Y.-J., Charnley, S.B., Huang, H.-C.,Kisiel, Z., Ehrenfreund, P., Tseng, W.-L. & Yan, C.-H. 2004, Adv. Space Res., 33, 31
Leger, A. & d'Hendecourt, L. 1985, A&Ap, 146, 81
Myers, P.C., Thaddeus, P., & Linke, R.A. 1980, ApJ, 241, 155
Peeters, Z., Botta, O., Charnley, S.B., Kisiel, Z., Kuan, Y.-J., & Ehrenfreund, P. 2005, A&Ap, 433, 583
Salama, F. & Allamandola, L.J. 1993, J. Chem. Soc. Farad. Trans., 89, 2277

Simon, M.N. & Simon, M. 1973, ApJ, 18, 757
Snyder, L.E. & Buhl, D. 1971, ApJ, 163, L47
Snyder, L.E. et al. 1982, J. Chem. Phys., 76, 5183
Tanguy, L., Bezard, B., Marten, A., Gautier, D., Gerard, E., Paubert, G., & Lecachaux, A. 1990, Icarus, 85, 43
van der Zwet, G.P. & Allamandola, L.J. 1985, A&Ap, 146, 76
Waite, J.H. 2005, Science, 308, 982
Wilson, E.H. & Atreya, S.K. 2004, J. Geophys. Res., 109, E06003
Wooten, H.A. 2002, www.cv.nrao.edu/awooten/allmols.html

NASA LAW, February 14-16, 2006, UNLV, Las Vegas

Visible to Near Infrared Emission Spectra of Electron-Excited H_2

A. Aguilar, G. K. James, & J. M. Ajello

Jet Propulsion Laboratory, California Institute of Technology, Pasadena, CA 91109

H. Abgrall, & E. Roueff

LUTH and UMR 8102 du CNRS, Observatorie de Paris, 92195 Meudon Cedex, France

ABSTRACT

The electron-impact induced fluorescence spectrum of H_2 at 100 eV from 700 nm to 950 nm at a spectral resolution of between 0.2 nm to 0.3 nm has been measured. The laboratory spectrum has been compared with our theoretical simulated spectrum obtained by calculating the lines emission cross sections from the upper states of g symmetry (EF, GK, HH, P, O ; I, R, J, S) towards the states of u symmetry (B, C, B', D) of H_2. The nine above Born-Openheimer g-upper states have been coupled together as well as the four above Born-Openheimer u-lower states. The comparison seems adequate with few minor discrepancies.

1. Introduction

H_2 is the most abundant molecule and is an active component of stellar formation. Collisional excitation by electrons is the source of both UV and Visible-Optical-IR (VOIR) H_2 florescence in circumstellar disks and certain classes of stars (Dalgarno *et al.* 1999). Intense H_2 transitions in the VOIR from various vibrational levels of the ground state have been observed in highly-collimated jets of matter from young stellar objects. These observed lines trace the colder molecular part of the post-shocked gas (Giannini *et al.* 2004).

With the successful missions of HST Space Telescope Imaging Spectrograph (STIS) and FUSE, UV astrophysical spectroscopy has undergone a quantum leap in resolving power (10^5) and precision (1%) demanding higher accuracy of the measured cross sections and oscillator strengths for excitation, ionization and emission processes (Dalgarno *et al.* 1999).

In the last few years we have published analytical models based on laboratory measurements of the two most fundamental sets of electronic cross sections in UV astronomy, the *Lyman* and *Werner* band systems

$$B^1\Sigma_u^+ 1s\sigma 2p\sigma \rightarrow X^1\Sigma_g^+$$
$$C^1\Pi_u^+ 1s\sigma 2p\sigma \rightarrow X^1\Sigma_g^+$$

of H_2 and HD (Ajello *et al.* 2005) (Jonin *et al.* 2000).

These cross sections and models are now the basis for electron transport codes to predict UV emission spectra from secondary electron distributions in weakly ionized plasmas of astrophysical regimes (see (Liu *et al.* 2002), (Abgrall *et al.* 1999)). We have also demonstrated that the *gerade* series (EF $^1\Sigma_g$, GK $^1\Sigma_g$, HH $^1\Sigma_g$, I $^1\Pi_g$, J $^1\Delta_g$ ...) make a significant contribution (about 50% at 20 eV) to the UV spectrum of H_2 (Dziczek *et al.* 2000) via cascading to the n=2$p\sigma$ B and 2$p\pi$ C states.

In this paper we present the optically thin VOIR spectrum of electron-excited H_2 corresponding to the cascading of the EF, GK, HH, ... g-states to the B, C, B' and D u-states.

2. Experimental Apparatus

To measure VOIR spectra of atomic and molecular gas species, the Laboratory at JPL is equipped with an electron impact collision chamber in tandem with a SpectraPro-500i spectrograph. This is a 0.5 meter focal length monochromator with a triple grating turret covering the wavelength range of 195 nm to 1400 nm. The VOIR spectrum of H_2 is measured by crossing a magnetically collimated beam of electrons at 100 eV with a beam of H_2 gas formed by a capillary array. The emitted photons, corresponding to radiative decay of collisionally excited states of H_2, are detected at 90 degrees by the spectrograph equipped with a variable entrance slit and a CCD camera with 20 μm pixels.

3. Theoretical Simulated Spectrum and Comparison

We have calculated the lines emission cross sections from the upper state of g symmetry (EF, GK, HH, P, O ; I, R, J, S) towards the states of u symmetry (B, C, B', D). The excitation cross section of H_2 at 300 K was estimated by using the Franck-Condon approximation as in (Liu *et al.* 2003). We have calculated the transition emission probabilities of each rovibronic state belonging to g in a way similar as in (Abgrall *et al.* 2000) to obtain the rovibronic wavefunction of g symmetry states, we have coupled together the 9 above Born-Openheimer g-states, and to obtain those of u-rovibronic states, we have coupled together the 4 above Born-Openheimer u-states. The excitation rate of the different g-states was calculated as in (Liu *et al.* 2002). Figure 1 shows the comparison between the experimental data and the resulting synthetic spectrum.

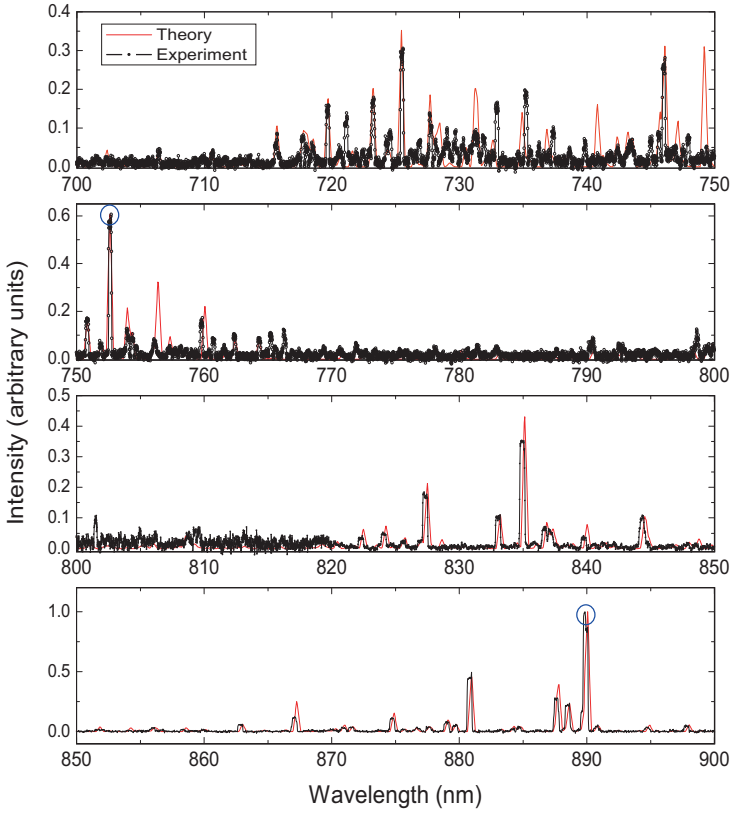

Fig. 1.— The electron-excited H_2 spectrum at 100 eV from 700 nm to 900 nm is composed of two different sets of measurements obtained with different gratings at resolutions of 0.2 nm and 0.3 nm. It is compared to a synthetic spectrum convoluted (red curve) with a 0.3 nm Gaussian FWHM to represent the experimental function. The two open circles at around 752 nm and 890 nm correspond to the identified $EF-B(6-0)P(2)$ transition and to the mixture of $EF-B(3-0)P(2)$ and $EF-B(3-0)P(3)$ transitions, respectively. These transitions were used to normalized the two sets of experimental data to the synthetic spectrum.

4. Summary and Future Work

The laboratory capabilities at JPL are now extended towards the VOIR region, covering the wavelength range from 300 nm to 1200 nm. H_2 electron-impact induced florescence spectrum from 700 nm to 950 nm has been measured at resolutions of between 0.2 nm to 0.3 nm. Recent calculations are compared to the experimental measurements. The calculations include nine coupled *gerade* states and four coupled *ungerade* states. At the present stage only the R and P lines have been included in the simulation and we plan to compute the contributions of Q branches from Σ-Π and Π-Π transitions. The comparison is satisfactory over the whole wavelength region. Minor discrepancies between experiment and theory are still present and are being investigated.

H_2 measurements at wavelengths as low as 300 nm are planned. These measurements will overlap with our previous reported measurements (220 nm to 530 nm) (James *et al.* 1998). We will extend our theoretical and experimental work for HD and D_2 in the VOIR.

This project has been funded in part by the Astronomy and Physics Research and Analysis (APRA) program.

REFERENCES

Abgrall H., Roueff E., Liu X., Shemansky D.E., James G.K., 1999, J. Phys. B, **32**, 3813.
Abgrall H., Roueff E., Drira I. 2000, A&A Suppl. Ser. **141**, 297-300
Ajello J.M., Vatti-Palle, P., Abgrall H., Roueff E., Bhardwaj A., Gustin J., 2005, Ap. J. Supp., **159**, 314-330.
Dalgarno A., Min Yan and Weihong Liu, 1999, Ap. J. Supp., **125**, 237.
Dziczek D., Ajello J.M., James G.K., Hansen D.L., 2000, Phys. Rev. A, **61**, 64702.
Giannini T., McCoey C., Caratti o Garatti A., Nisini B., Lorenzetti D., Flower D.R., 2004 ,A&A, **419**, 999-1014.
James G.K., Ajello J.M., Pryor W.R., 1998, J.Geophys. Res., **103**, 20113.
Jonin C., Liu X., Ajello J.M., James G.K., Abgrall H., 2000, Ap. J. Supp., **129**, 247.
Liu X., Shemansky D.E., Abgrall H., Roueff E., Dziczek D., Hansen D.L., Ajello J.M. 2002, Ap.J. Sup.Ser., **245**, 229-245.
Liu, X., Shemansky, D. E., Abgrall, H., Roueff, E., Ahmed, S. M., Ajello, J. M. 2003, J. Phys. B, **36**, 173.

NASA LAW, February 14-16, 2006, UNLV, Las Vegas

Formation of Silicate Grains in Circumstellar Environments: Experiment, Theory and Observations

A. Castleman, Jr.[1], A. Reber[2], P. Clayborne[2], J. Reveles[2], S. Khanna[2] and A. Ali[3]

[1] *Departments of Chemistry and Physics, The Pennsylvania State University, University Park, PA 16802, USA*

[2] *Department of Physics, Virginia Commonwealth University, Richmond, VA 23284-2000, snkhanna@vcu.edu*

[3] *Solar System Exploration Division, Astrochemistry Laboratory, NASA, Goddard Space Flight Center, Greenbelt, MD 20771, ashraf.ali@ssedmail.gsfc.nasa.gov*

Amongst chemical reactions(1) in the molecular universe(2), condensation reaction is probably the most poorly understood. The condensation of a solid from its components in the gas phase occurs in many parts of our galaxy such as stellar mass outflows, the 'terrestrial' region of protoplanetary disks and in primordial solar nebula(3). But how does the transition occur from molecules to intermediate clusters to macroscopic grains? The major focus of the present work is the identification of chemical condensation reaction pathways that lead to the formation of stoichiometry, composition and crystallinity of cosmic silicates from vapor phase species.

O, Mg, Si, and Fe are the four major cosmically abundant mineral-forming elements(4). Are the initial magnesium-iron silicate condensates formed from the oxygen bearing gas phase species stoichiometric or an ill-defined assemblage of amorphous grains(5)? An answer to this fundamental question is a key step in the identification of chemical condensation pathways of specific molecule-solid transitions and elucidation of subsequent heterogeneous chemistry involving kinetics of gas-solid interactions(6).

It has long been advocated(7) that interstellar silicate grains are amorphous with non-stoichiometric elemental ratios and that circumstellar outflows(8), from evolved stars, are the primary contributors to transitions from molecules to such type of silicates. In contrast to the disordered compositions in silicates, recent infrared space observatory (ISO) observations(9) indicate an important fraction of interstellar silicates appear in crystalline form in the outflows of circumstellar shells of evolved late-type stars at low ambient color temperatures. The latest ISO observations(10) invariably indicate that most crystalline silicates are Mg-rich end members, for e.g. forsterite $(MgO)_2(SiO_2)$, and the Fe/Mg ratio is close to zero. Further, with the Mid-Infrared Interferometric Instrument (MIDI) installed at the Very Large Telescope Interferometer (VLTI), spatially resolved detections and compositional analyses of silicates in the inner-most two astronomical units of three protoplanetary

disks have finally been reported(11). It was observed(11) that silicates within the inner region of protoplanetary disks are highly crystallized, more so than any other dust observed in young stars until now. These observations(11) imply the role of vaporization and subsequent gas-phase condensation processes in the formation of crystalline silicates.

The 'nominal' molecules of observed crystalline silicates such as forsterite $(MgO)_2(SiO_2)$ do not exist in the gas phase(8). The growth of crystalline silicates occurs by heterogeneous chemistry in unique catalytically active pathways through gas-surface interactions at high temperatures. Thus one of the most fundamental questions in grain formation studies is which one among the high-temperature condensable gas-phase species is going to nucleate first at a significant condensation rate to provide a molecular surface (cluster) enabling condensed phase growth of minerals.

SiO is one of the most abundant reacting oxygen bearing condensable gas-phase species in molecular astronomical regions. The current observational data(12) based on UKIRT indicate that SiO_2 is a most plausible solid species contributing to the growth and evolution of various silicates seen in the infrared spectra of oxygen-rich evolved stars. Based on laboratory smoke condensation experiments and analysis of end products, it was conjectured(13) that silicate formation in the circumstellar envelopes surrounding M-type giants begins with the formation of pure SiO_x clusters. There are no direct and almost no experimental studies on the role of molecular processes on formation of silicates in high temperature clouds. In an attempt to resolve this critical question on the formation of SiO_x clusters as initiating condensation of cosmic silicates, we report for the first time, an experimental study of cluster intermediates and their growth during the condensation of a cosmically abundant molecular species silicon monoxide. In addition, first principles gradient corrected density-functional theoretical studies(14) have been carried on the geometry, electronic structure and stability of SiO_x clusters. It is shown that the synergistic approach(14) combining detailed experimental investigations on the clustering of SiO units in molecular beams and first principles electronic structure studies does elucidate the mechanism of condensation processes at the microscopic level that can lead to the formation of silicates on the one hand and silicon nanoparticles on the other.

1. Penn State Astrochemistry Laboratory

The schematic of the experimental set up is shown in Fig. 1. This set-up has been quite successful(15) previously for experiments ranging from intense pump-probe studies to basic photofragmentation processes, and a brief description of the apparatus follows. The surface of a rotating and translating quarter inch diameter silicon/silicon monoxide/silicon dioxide rod is ablated with the second harmonic of a Nd:YAG laser, ∼4mJ/pulse, 8ns (532nm), at an adjustable time delay after which a pulsed valve is actuated. The species formed are quenched in a stream of buffer gas, and are further cooled by subsequent supersonic expansion through

a conical-shaped nozzle. Following expansion into vacuum, the supersonic jet, including both neutral and charged species, is skimmed as it enters the ionization chamber housing the high voltage time-of-flight (TOF) grids. The construction of geometry of this double acceleration region is based on the design of Wiley and McLaren(16). If the ionic species directly form the laser vaporization source are of interest, these species can be pulse extracted into this home built reflectron(17) time-of-flight mass spectrometer using two fast high-voltage transistor switches. This approach is quite straight forward in that the two TOF high voltage repeller and extractor grids (shown in Fig. 1) are initially kept at ground potential and then almost instantaneously ramped up to a higher voltage, resulting in the rapid acceleration of the ions toward the detector, after the ion packet has had the sufficient time to migrate down from the source. The ions of interest travel approximately three meters before reaching a multi-channel plate detector. By choosing appropriate decelerating and reflecting fields in the reflector, the larger initial kinetic energy distribution, compared to neutrals, can be further compensated.

Figure 1. Experimental Apparatus

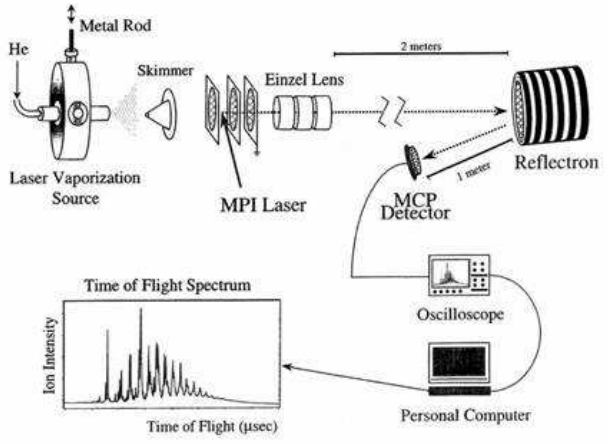

To assess the neutral species distribution coming directly form the condensation source, the experimental set up is only slightly altered in that the TOF grids are now kept at a constant high voltage. Since the charged species are not able to penetrate the area between the acceleration grids, due to charge repulsion, the neutral species in the molecular beam are simply ionized and subsequently accelerated and detected. What makes our experimental setup somewhat unique is our ability to use a femtosecond laser for multiphoton ionization. By utilizing an ultrafast laser, all of the energy is delivered to the system of interest on a time scale that is much shorter than any relaxation pathway(18). In other words, the energy of the ultrafast laser pulse is delivered and absorbed before appreciable internal relaxation occurs. The multiphoton photoionization of neutrals is thus accomplished by focusing the output of a commercial Ti:Sapphire regenerative amplifier system. The 1-2 mJ/pulse, 50 fs, 800 nm laser pulse intersects the cluster beam perpendicularly between the previously mentioned extraction grids and thus provides nearly fragmentation-free ionization and detection of the neutral species in the molecular beam.

2. Results and Discussion

The ratio of oxygen to silicon in SiO is 1 while it is 2 for SiO_2. One of the important astrophysical chemistry questions is whether the transition to SiO_2 occurs through the gradual oxygen enrichment of the agglomerated SiO units. It is also pertinent to ask if the origin of silicon nanoparticles currently believed to be the carrier of extended red emission(19) in diffuse interstellar medium is also rooted in the clustering of SiO units.

The time-of-flight multiphoton ionization mass spectra of neutral clusters formed by vaporizing solid SiO is not shown here, and the results would be published in the literature soon(14). Here we summarize our key findings. In addition to pure $(SiO)_n^+$ clusters, the spectra showed the presence of single oxygen enriched species namely $Si_2O_3^+$, $Si_3O_4^+$, $Si_4O_5^+$, $Si_5O_6^+$, $Si_6O_7^+$ and small amount of $Si_7O_8^+$. There are variations in the intensity across each series. In the pure $(SiO)_n^+$ clusters, there is a precipitous drop in intensity from $(SiO)_5^+$ to $(SiO)_6^+$. A similar decline in intensity is noticeable from $Si_6O_7^+$ to $Si_7O_8^+$. In addition there is a large peak at Si^+. The oxygen rich species $Si_2O_3^+$ and $Si_3O_4^+$ were also observed in the beams where clusters were formed through vaporization of silicon under oxygen or formed through the vaporization of solid SiO_2, indicating that they are particularly stable. The most surprising experimental finding is the conspicuous absence of SiO_2^+ in all the experiments except for very minor intensity of the cations extracted from the silicon vaporized under oxygen. What processes then lead to the formation of observed oxygen enriched Si_xO_y species? Does SiO_2 form in this enrichment cycle? It is important to note that SiO_2 has the highest ionization potential of 12.19 eV of all the species. It would take at least 7 photons to ionize the clusters in our multiphoton ionization scheme. The lack of detection of SiO_2 is then simply related to the inability to ionize the species.

To delineate the molecular surface (cluster) enabling condensed phase growth of minerals, the first principles gradient corrected density-functional theoretical studies(14) have been undertaken. Recently, calculations have been carried out on the geometry, electronic structure and stability of oxygen enriched Si_xO_y clusters. It is found that the structures of the ground states of small Si_xO_x clusters containing up to 4 units are single rings. Si_5O_5 is the smallest cluster where the Si-Si bond appears, and starting at this size, the elementary rings begin to assemble into multiple rings, that eventually lead to cages. It was found that the ground state structures at larger Si_xO_x cluster sizes have a natural tendency to segregate into pure Si cores with oxygen rich and particularly SiO_2 outer shells. To this end, we also investigated the stability of Si_xO_{x-1} and Si_xO_{x+1} species. The density-functional theoretical studies also show that successive collisions of any oxygen enriched Si_xO_{x+1} species with a substrate cluster Si_xO_x (n>5) would lose an SiO unit in each collision and thus providing a microscopic mechanism to the formation of SiO_2 as the terminal member. The observed intensity distribution of Si_6O_7, Si_5O_6, Si_4O_5, Si_3O_4, Si_2O_3 in the mass spectra are completely consistent with the above pathway through reaction cascades. The observed anomalous compositions in Si_xO_y clusters and their formation kinetics must be taken into account, prior to a mechanism is being invoked or an argument is presented against the role of SiO molecules

in chemical models of formation of circumstellar silicates(13; 20).

In our laboratory we intend to make measurements on the vibronic structure of observed compositions of silicon oxide clusters Si_xO_y in the size distribution between two and maximum of twenty atoms. The interpretation of optical spectra would need a close interaction between experiment and ab initio quantum chemical calculations of polyatomic molecules. In the second part of our experimental studies we tend to bring our expertise of real time pump-probe studies(15) of cluster reactions to measure the dissociation ofate (lifetimes(5)) of 'activated complexes' - the reverse process of recombination reactions (and/or disproportionations to products through low-energy exit channel, if any) using femtosecond ultrafast laser pulses. The measured data on lifetimes of collision-complexes coupled with information in energetics of clusters are then incorporated into the rate expression of microcanonical transition state theory(21) to yield cross sections for the reactions between relevant clusters to elucidate the microscopic condensation rates.

REFERENCES

Smith, I.W.M., Chem. Soc. Rev. **31**, 137 (2002).

Fraser, H.J., McCoustra, M.R.S., and Williams, D.A., A&G. **43**, 2.10 (2002).

Ali, A., in Faraday Discuss: Chemistry and Physics of Molecules and Grains in Space, Organising Committee: P.J. Sarre, D. Field, S. Leach, I.W.M. Smith, J. Tennyson, and D.A. Williams, The Royal Society of Chemistry, U.K., No. 109, pp. 372-380 (1998).

Grevesse, N., Noels, A., and Sauval, A.J., in ASP Conf. Ser., Cosmic Abundances, ed. S.S. Holt and G. Sonneborn, **99**, 117 (1996).

Donn, B., Hecht, J., Khanna, R., Nuth, J., Stranz, D., and Anderson, A.B., Surface Science. **106**, 576 (1981).

Marcus, R.A., J. Chem. Phys. **121**, 8201 (2004).

Donn, B., in Experiments on Cosmic Dust Analogues., ed. E. Bussoletti, C. Fusco, and G. Longo, Kluwer Academic Publishers., pp.43-61 (1988).

Patzer, A.B.C., Khler, T.M., and Sedlmayr, E., Planet. Space Sci. **43**, 1233 (1995).

Waters, L.B.F.M., Molster, F.J., de Jong, T., Beintema. D.A., Waelkens, C., Boogert, A.C.A., Boxhoorn, D.R., de Graauw, Th., Drapatz, S., Feuchtgruber, H., Genzel, R., Helmich, F.P., Heras, A.M., Huygen, R., Izumiura, H., Justtanont, K., Kester, D.J.M., Kunze, D., Lahuis, F., Lamers, H.J.G.L.M., Leech, K.J., Loup, C., Lutz, D., Morris, P.W., Price, S.D., Roelfsema, P.R., Salama, A., Schaeidt, S.G., Tielens, A.G.G.M., Trams, N.R., Valentijn, E.A., Vandenbussche, B., van den Ancker, M.E., van Dishoeck, E.F., van Winckel, H., Wesselius, P.R., and Young, E.T., Astron. Astrophys, **315**, L361 (1996).

Waelkens, C., Malfait, K., and Waters, L.B.F.M., in Astrochemistry: From Molecular Clouds to Planetary Systems, IAU Symposium, ed. Y.C. Minh and E.F. van Dishoeck, vol. 197, pp. 435-443 (2000).

van Boekel, R., Min, M., Leinert, Ch., Waters, L.B.F.M., Richichi, A., Chesneau, O., Dominik, C., Jaffe, W., Dutrey, A., Graser, U., Henning, Th., de Jong, J., Khler, R., de Koter, A., Lopez, B., Malbet, F., Morel, S., Paresce, F., Perrin, G., Preibisch, Th., Przygodda, F., Schller, M., and Wittkowski, M., Nature. **432**, 479 (2004).

Speck, A.K., Barlow, M.J., Sylvester, R.J., and Hofmeister, A.M., Astron. Astrophys. Suppl. Ser. **146**, 437 (2000).

Donn, B., and Nuth, J.A., Astrophys. J. **288**, 187 (1985).

Reber, A.C., Clayborne, P.A., Reveles, J.U., Khanna, S.N., Castleman, Jr., A.W., and Ali, A., (To be submitted).

Castleman, Jr., A.W., and Wei, S., Annu. Rev. Phys. Chem. **45**, 685 (1994).

Wiley, W.C., and McLaren, I.H., Rev. Sci. Instru. **26**, 1150 (1955).

Mamyrin, B.A., Karataev, V.I., Shmikk, D.V., and Zagulin, V.A., Sov. Phys. JETP. **37**, 45 (1973).

Zewail, A.H., J. Phys. Chem. **100**, 12701 (1996).

Witt, A.N., in Astrochemistry: From Molecular Clouds to Planetary Systems, IAU Symposium, ed. Y.C. Minh and E.F. van Dishoeck, vol. 197, 317 (2000).

Gail, H.-P., and Sedlmayr, E., in Faraday Discussions: Chemistry and Physics of Molecules and Grains in Space, Organising Committee: P.J. Sarre, D. Field, S. Leach, I.W.M. Smith, J. Tennyson, and D.A. Williams, The Royal Society of Chemistry, U.K., No. 109, pp. 303-319 (1998).

Holbrook, K.A., Pilling, M.J., and Robertson, S.H., Unimolecular Reactions, 2nd edn., Wiley, England (1996).

NASA LAW, February 14-16, 2006, UNLV, Las Vegas

Difficulties in Laboratory Studies and Astronomical Observations of Organic Molecules: Hydroxyacetone and Lactic Acid

A. J. Apponi, M. A. Brewster[1], J. Hoy, & L. M. Ziurys

Life and Planets Astrobiology Center, The University of Arizona, Tucson, AZ, 85721

aapponi@as.arizona.edu

ABSTRACT

For the past 35 years, radio astronomy has revealed a rich organic chemistry in the interstellar gas, which is exceptionally complex towards active star-forming regions. New solar systems condense out of this gas and may influence the evolution of life on newly formed planets. Much of the biologically important functionality is present among the some 130 gas-phase molecules found to date, including alcohols, aldehydes, ketones, acids, amines, amides and even the simplest sugar - glycolaldehyde. Still, many unidentified interstellar radio signals remain, and their identification relies on further laboratory study.

The molecules hydroxyacetone and lactic acid are relatively small organic molecules, but possess rather complex rotational spectra owing to their high asymmetry. Hydroxyacetone is particularly problematic because it possess a very low barrier to internal rotation, and exhibits strong coupling of the free-rotor states with the overall rotation of the molecule. As in the case of acetamide, a full decomposition method was employed to order the resultant eigenstates onto normal asymmetric top eigenvectors.

1. Introduction

Over 130 molecules have now been discovered in the interstellar medium. The prevailing theme of astrochemistry is organic in nature. Most of the molecules found are hydrocarbons and their organic derivatives. There are only two places in which organic molecules are known to exist, (i) in interstellar space and (ii) in living (or once living) organisms on Earth. The question is whether there is a connection between these two regimes. It becomes more and more plausible that organic material delivered to the early Earth via meteorites and

[1]Current address: SFRYI Inc., Seattle, WA, 98109

comets may have provided the necessary building blocks that facilitated the process and evolution of life.

Still, a complete chemical inventory of the interstellar medium is lacking. It is estimated that about 1/2 of the interstellar features in the millimeter and submillimeter wave region 65 to 600 GHz remain unidentified. These unidentified lines are either from highly excited states of already known molecules or from highly asymmetric carriers whose rotational frequencies still remain unknown. Although some lines from excited states of vinyl cyanide and a few other molecules have recently been assigned, many still remain even though most of the relevant excited state spectroscopy is already complete. It is therefore more likely that highly asymmetric molecules whose spectra are unknown account for the bulk of the remaining lines.

2. Rotational Spectrum of Hydroxyacetone

Of all of the stable molecules with the chemical formula $C_3H_6O_2$, hydroxyacetone is the only remaining species requiring further spectroscopy characterization. It has proven very difficult to characterize owing to its methyl rotor, which has a very low barrier to internal rotation of about 65 cm^{-1}. This low barrier allows the free-rotor states to heavily mix with the asymmetric top states to the point where K_a is no longer a good quantum number, except at low-J. We have now been able to solve this system in its ground torsional state with a fit that reproduces the measured frequencies to the measurement uncertainty.

The rotational spectrum of hydroxyacetone was first recorded by Kattija-Ari and Harmony (1980) in the microwave region. They measured a total of 43 lines both in the A and E states, where unfortunately some E-state assignments were incorrect. However, with their work, the A-state was easy to predict at other frequencies and a reasonable structure and barrier height were determined (see Table 2). Braakman et al. 2005 were able to extend the work to include 587 A-state lines at millimeter wavelengths. They also assigned, but could not fit, 288 E-state lines.

At about the same time as Braakman et al. (2005), we started to measure the rotational spectrum of hydroxyacetone using our newly built Fourier transform microwave (FTM) spectrometer and one of the Ziurys group millimeter-wave direct absorption spectrometers in the frequency range of 5 to 20 GHz and 65 to 175 GHz. In all, more than 1000 lines have been assigned to the ground state of hydroxyacetone.

The Rho-axis Hamiltonian was used for the analysis of hydroxyacetone, which couples the internal rotor to the a-axis producing an off-diagonal term in the rotational Hamiltonian

$$\hat{H}_{rot} = \tfrac{1}{2}(B+C)(\hat{P}_b^2 + \hat{P}_c^2) + A\hat{P}_a^2 + \tfrac{1}{2}(B-C)(\hat{P}_b^2 - \hat{P}_c^2) + D_{ab}(\hat{P}_a\hat{P}_b + \hat{P}_b\hat{P}_a), \qquad (1)$$

and results in a torsional coupling of the form

$$\hat{H}_{tors} = F(\hat{P}_\gamma - \rho\hat{P}_a)^2 + \tfrac{1}{2}V_3(1-\cos 3\gamma) + \tfrac{1}{2}V_6(1-\cos 6\gamma), \qquad (2)$$

where $\hat{P}$ are the regular angular momentum operators along the respective axes and A, B, C and F are the associated rotational constants. The terms V_3 and V_6 are potential

terms associated with the internal motion of the methyl rotor. The details of the Rho-axis Hamilitonian and eigenfunction decomposition methods used here can be found in Ilyushin (2004) and the references therein.

Twenty-one rotational constants have been fit to 1045 lines covering $J < 31$ and $K_a < 8$ (see Table 1). Only the leading order terms are included here for conciseness. Both the A and E states were fit simultaneously using the rho-axis method. The E-state is very sensitive to the barrier height of the internal rotor and has been determined to high accuracy. Excited torsional lines have not yet been included in the fit.

Table 1: Leading order parameters for hydroxyacetone

Paramter	Operator	This Work	Kattija-Ari et al.
V_3	$1/2(1-\cos 3\gamma)$	65.377(28) cm^{-1}	68(4) cm^{-1}
F	$\hat{P}^2_\gamma$	159.161(53) GHz	157.931 GHz (fixed)
ρ	$\hat{P}_\gamma \hat{P}_a$	0.058674(77) unitless	ND
A (diagonalized)	$\hat{P}^2_a$	10013.53(61) MHz	10069.410(57) MHz
B (diagonalized)	$\hat{P}^2_b$	3834.36(16) MHZ	3810.412(8) MHz
C (diagonalized)	$\hat{P}^2_c$	2911.04(12) MHz	2864.883(4) MHz
D_{ab}	$(\hat{P}_a, \hat{P}_b)$	1216.18(35) MHz	ND
$\Delta I = I_c - I_a + I_b$		8.7 amuÅ^2	6.4 amuÅ^2
Total Number of Lines		1045	53
Microwave rms		6 kHz	A-state 20 kHz
Millimeter wave rms		70 kHz	E-state 9 MHz

3. Astronomical Searches

We have now been able to search for both hydroxyacetone and lactic acid in the Sgr B2(N) molecular cloud. The millimeter wave spectrum of Lactic acid was recently published by Psczolkowski et al. (2005). The barrier height of methyl rotation is predicted to be around 1100 cm^{-1}; however, the coupling of the internal motion to the rigid frame is not strong enough to produce a resolved E-state for lactic acid. This is unfortunate because it would effectively double the number of possible lines; hence, there would be less chance of confusion by contamination in the space spectrum.

Even though we have found a number of coincidental matches for both of these species, there are too many missing transitions for a definitive identification of either molecule. The frequencies that show 'holes' in the spectra of these molecules lie in very confused regions often times straddled by larger features. These searches yield upper limits to the column densities of $< 5 \times 10^{13}$ cm^{-2} for hydroxyacetone and $< 9 \times 10^{13}$ cm^{-2} for lactic acid. These upper limits can be used in chemical modeling. Some representative spectra are shown in Figure 1.

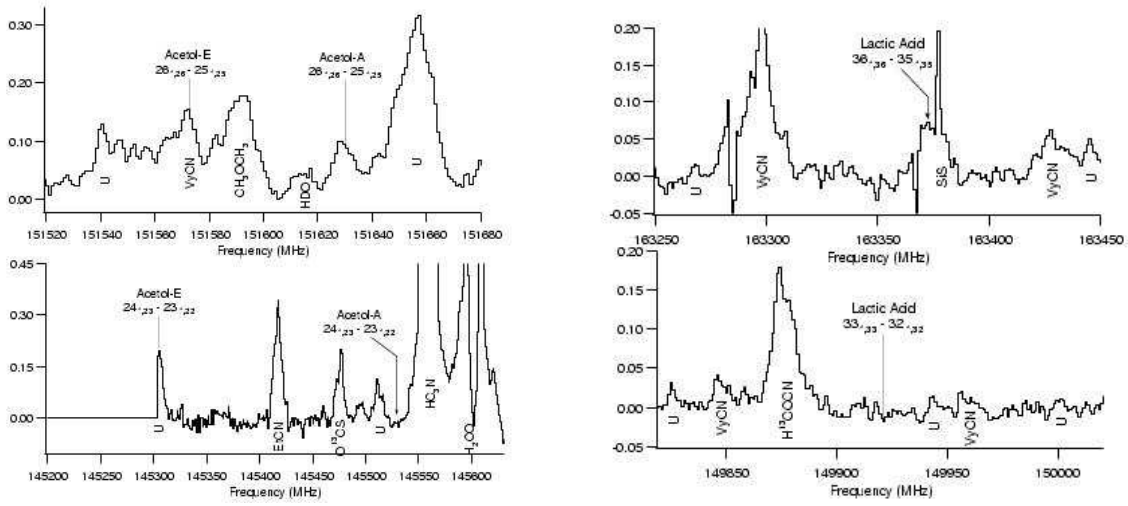

Fig. 1.— Representative astronomical spectra of hydroxyacetone and lactic acid towards Sgr B2(N). These spectra show that even though there are several coincidental matches for these molecules, the absence of features at several favorable transitions indicates that they are not abundant enough for detection.

This material is based upon the work supported by the National Aeronautical and Space Administration through the NASA Astrobiology Institute under cooperative agreement No. CAN-02-OSS-02 issued through the office of Space Science. We would also like to thank Isabella Kleiner for sharing her Hamiltonian computer progam.

REFERENCES

Braakman et al. 2005, 60th Int. Symp. Mol. Spectr., Ohio State University
Halfen et al. 2006, ApJ, 639, 237
Hollis et al. 2000, ApJ, 540, L107
Ilyushin 2004, J. Mol. Spectr., 227, 140
Kattija-Ari and Harmony 1980, Int. J. Quan. Chem., 14, 443
Pszczokowski et al. 2005, J. Mol. Spectr., 234, 106

NASA LAW, February 14-16, 2006, UNLV, Las Vegas

Experimental and Theoretical Studies of Pressure Broadened Alkali-Metal Atom Resonance Lines

F. Shindo, C. Zhu, K. Kirby & J. F. Babb

Harvard-Smithsonian Center for Astrophysics, Cambridge, MA

{fshindo, czhu, kkirby, jbabb}@cfa.harvard.edu

ABSTRACT

We are carrying out a joint theoretical and experimental research program to study the broadening of alkali atom resonance lines due to collisions with helium and molecular hydrogen for applications to spectroscopic studies of brown dwarfs and extrasolar giant planets.

1. Introduction

The broadened resonance lines of sodium and potassium appear prominently in the spectra of certain classes of brown dwarfs, and are expected to be present in the spectra of certain extrasolar planets as well (Burrows et al. 2001; Sudarsky et al. 2003). Accurate line-profiles, as a function of temperature and density, will be invaluable to astrophysicists as diagnostics of the atmospheres of substellar mass objects. Our project currently consists of an experiment to measure pressure broadening of potassium resonance lines by He and by H_2 at about 1000 K combined with theoretical calculations for other temperatures.

2. Description of the experiment

The critical elements in the absorption spectroscopy experiment include a Mach-Zehnder interferometer and a 3 m Czerny-Turner grating spectrograph with CCD camera detector (1024×256 pixels with a size of 26 μm) for dispersing and recording spectra. The spectrometer (McPherson model 2163) covers the wavelength range from 360 to 920 nm through the use of a stepper controller enabling the rotation of a 1200 l/mm plane ruled grating at 116 different angles. As a background light source, we use a tungsten halogen lamp (250 W, 24 V) with the beam collimated through an arrangement of optics before entering the interferometer. A unique feature of the experiment is the accurate determination of the absorber atom number density, which is obtained using the "hook" (or anomalous dispersion) method.

To reproduce the conditions of the environments we want to study, the apparatus was designed to allow measurements at different noble gas pressures, from 10 torr to 700 torr, and at high temperatures (about 900 K). The cell was fabricated according to the design showed in Fig. 1. The cell body is composed of three welded tubes of grade 330 stainless steel,

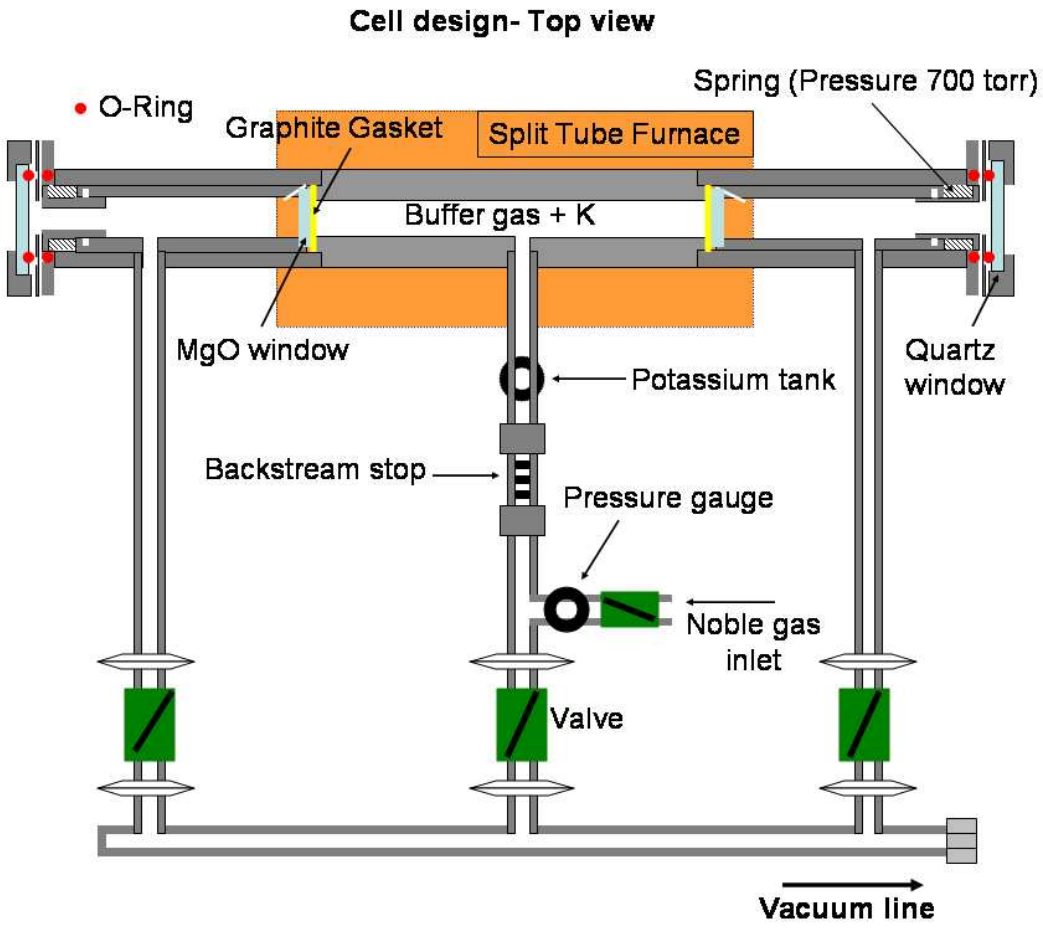

Fig. 1.— Cell design.

chosen for its resistance to the corrosive effects of alkali-metal gases at high temperature. The middle tube (cold path-length $l = 20$ cm) is the gas chamber and it is closed by MgO windows sealed with graphite gaskets. Each of the two tubes on the outside of the gas chamber contains a cylinder and a spring to press the MgO window in, thereby allowing the noble gas pressure in the gas chamber to reach values as high as 700 torr. The cell ends are closed by quartz windows sealed with Viton O-rings. All of the cell body tubes are independently connected to a vacuum line. The potassium sample is placed in a 330 grade stainless steel reservoir attached to the cell by a Swagelok fitting allowing the reservoir to be removed readily for sample replacement.

The reservoir and the tube leading to the gas chamber are heated by homemade heaters regulated through a commercial temperature controller. The gas chamber is inserted in a specially designed split tube furnace that fits within our experimental size constraints. The oven ensures that there is a uniform temperature along the path-length of the gas chamber and facilitates the removal of the cell from the apparatus.

The system oven plus gas cell is situated in one branch of a Mach-Zehnder interferometer whereas a pair of MgO windows and a pair of quartz plates are placed in the other arm to compensate the windows of the gas cell. Then, the interferometer is adjusted at optical zero path difference to produce a set of horizontal interference fringes at each wavelength present in the light source. The fringe pattern is focused by a lens on the entrance slit of the spectrometer. As each arm of the interferometer can be blocked by a shutter, we are able to measure the spectrum arising from the gas cell, a reference spectrum and the fringe pattern.

The association of the interferometer and the spectrometer is essential to apply the so called "hook" method (Rozhdestvenskii 1912), which provides a measurement of the atomic number density of the absorbers vaporized in the gas chamber. This technique uses the change in the refractivity in the vicinity of a resonance line which induces a distortion of the fringe profile. By inserting an additional compensation plate into one of the interferometer arms, the fringes are shifted to higher orders. Consequently, the fringes will appear slanted in line-free spectral regions, whereas close to absorption lines the anomalous dispersion produces maxima and minima in the fringe positions with wavelength, giving the characteristic hook appearance near the lines. As the shape of the fringes is closely related to the number density of absorbers, fitting the fringe distortion near the potassium doublet at 770 nm leads to the determination of the potassium density number.

3. Theoretical work

Accurate calculations of the opacities due to pressure broadening in the wings of resonance lines require accurate potential energy curves and transition dipole moments for the alkali-metal atom and perturber gas atom (or molecule) interactions. Because satisfactory data were not available in the literature for the K-He and K-H_2 systems, the "Molpro" quantum chemistry codes implementing a Multi-Reference Configuration Interaction method were used to compute, at an unprecedented level of accuracy, all of the molecular states involved in the line-broadening of the resonance lines (Santra and Kirby 2005).

The pressure broadening of Li, Na, and K by He in the wings of the resonance lines was investigated using fully quantum-mechanical methods (Zhu et al. 2005, 2006) and the calculated reduced absorption coefficients at several temperatures for Na-He and K-He are presented in Fig. 2. Future experimental and theoretical work will focus on the K-H_2 system.

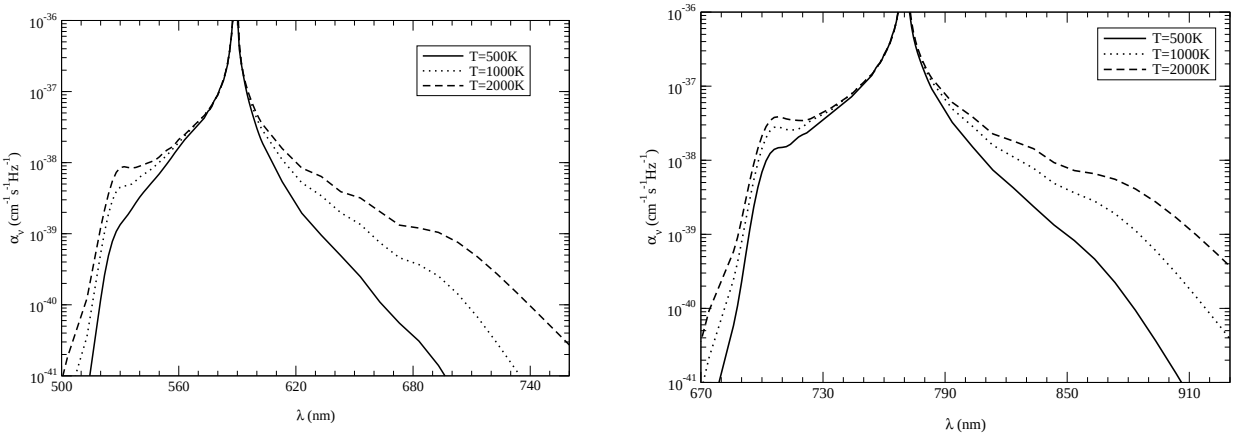

Fig. 2.— Absorption coefficients for a) (left view) Na-He and b) (right view) K-He at temperatures of 500 K, 1000 K, and 2000 K.

This work is supported by NASA Grant NAG5-12751.

REFERENCES

Burrows, A., Hubbard, W. B., Lunine, J. I., and Liebert, J 2001, Rev. Mod. Phys., 73, 719
Rozhdestvenskii, D. S. 1912, Ann. Phys., 39, 307
Santra, R. and Kirby, K. 2005, J. Chem. Phys., 123, 214309
Sudarsky, D., Burrows, A., and Hubeny, I. 2003, ApJ, 588, 1121
Zhu, C., Babb, J. F., and Dalgarno, A. 2005, Phys. Rev. A, 71, 052710
Zhu, C., Babb, J. F., and Dalgarno, A. 2006, Phys. Rev. A, 73, 012506

NASA LAW, February 14-16, 2006, UNLV, Las Vegas

Accurate VUV laboratory measurements of Fe III transitions for astrophysical applications

R. J. Blackwell–Whitehead, J. C. Pickering, & D. Smillie[1]

Blackett Laboratory, Imperial College, London, SW7 2BW, United Kingdom

r.blackwell@imperial.ac.uk

G. Nave & C. I. Szabo

National Institute of Standards and Technology, Gaithersburg, MD 20899, USA

Peter L. Smith

[1]*Harvard–Smithsonian Center for Astrophysics, 60 Garden Street, Cambridge, MA 02138, USA*

K. E. Nielsen[2]

NASA Goddard Space Flight Center, Code 667, Greenbelt, MD 20771, USA

G. Peters

University of Southern California, Los Angeles, CA 90089, USA

ABSTRACT

We report preliminary measurements of Fe III spectra in the 1150 to 2500 Å wavelength interval. Spectra have been recorded with an iron-neon Penning discharge lamp (PDL) between 1600 and 2500Å at Imperial College (IC) using high resolution Fourier (FT) transform spectroscopy. These FT spectrometer measurements were extended beyond 1600Å to 1150Å using high-resolution grating spectroscopy at the National Institute of Standards and Technology (NIST). These recorded spectra represent the first radiometrically calibrated measurements of a doubly-ionized iron–group element spectrum combining the techniques of vacuum ultraviolet FT and grating spectroscopy. The spectral range of the new laboratory measurements corresponds to recent *HST*/STIS observations of sharp-lined B stars and of Eta Carinae. The new improved atomic data can be applied to abundance studies and diagnostics of astrophysical plasmas.

---

[2]Catholic University of America, Washington DC 20064, USA

1. Introduction

The disentangling of complex astrophysical spectra to reveal important information is crucially dependent upon a detailed and precise knowledge of each species present. Atomic spectral data of the iron–group elements (Ti, V, Cr, Mn, Fe, Co, Ni) have a major impact on stellar abundance investigations. Doubly ionized species dominate hot star spectra, however the current laboratory atomic database for those ions is inadequate limiting stellar analyses. In particular, there are no laboratory determined oscillator strengths for any of the doubly ionized iron-group elements (including Fe III) in the vacuum UV (VUV, $\lambda < 2000$Å). The lack of accurate atomic data is the major source of uncertainty in the interpretation of expensively acquired stellar spectra and without new intensity calibrated laboratory measurements future astrophysical analysis will be severely restricted.

Knowledge of elemental abundances in stellar photospheres provides information on the chemical evolution of our galaxy and its neighbors, allowing validity checks of theoretical calculations of stellar nucleosynthesis. Hot stars, such as B type stars, provide insight into the recent enhancements of the moderate–heavy elements as they display the current chemical state of the region of the galaxy in which they reside. Knowledge of the abundance of Fe group elements is especially important, since these species are synthesized late in the life of a star. Sofia, U.J. & Meyer, D.M. (2001) suggest that, in general, B stars are depleted in most elements with respect to the interstellar medium. However the theory may just be an artefact of poor atomic data used in the model atmospheres.

Eta Carinae (η Car) has been of great interest since the nineteenth century when it briefly became the second brightest star in the sky. *HST*/STIS observations of η Car have revealed much information about this variable star including the presence of a number of dense condensations, the "Weigelt blobs". Of particular interest to our current research is the pumping effect of H I Ly α on Fe III.

An intensity anomaly can be observed in the 1914Å vs 1926Å transitions in figure 1a. The upper level involved in the 1914Å transition ($3d^5$ (^{6}S) 4p $^7P_3$) is being preferentially pumped by the H Ly α line, as discussed by Johansson S., et al. (2000). However, there are no currently available experimental oscillator strengths for the UV34 multiplet. Our high resolution FT spectroscopy measurements (Smith, P.L., Pickering, J.C., & Thorne, A.P. 2002) given in figure 1(b) do not exhibit an intensity anomaly and oscillator strengths will be determined for these transitions to experimentally confirm the pumping mechanism.

2. Laboratory Measurements

Recent advances in laboratory techniques, including the use of Image Plates (IP), have allowed, for the first time, accurate intensity calibration of grating spectra below H I Ly α ($\lambda < 1210$Å). Image plates, which were originally developed for soft x–ray medical diagnostics,

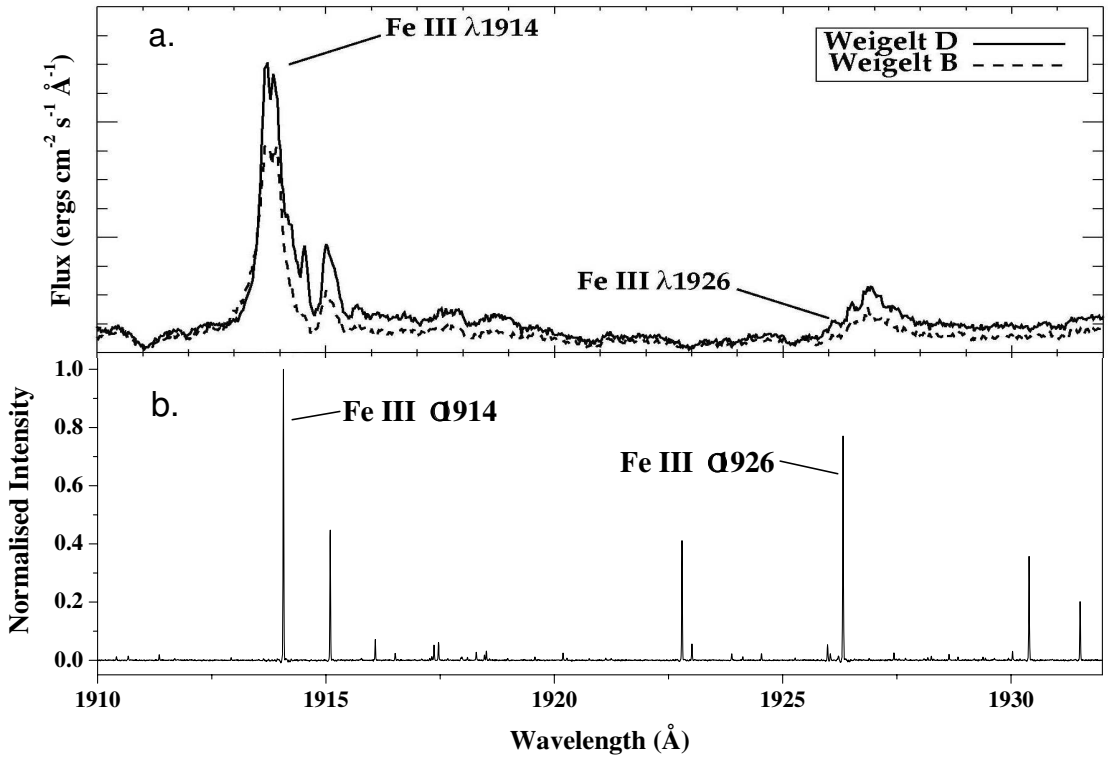

Fig. 1.— (a) *HST*/STIS observations of Weigelt D, see Nielsen et al. and Gull & Nielsen in these proceedings. (b) Fe III spectra recorded by the IC VUV FT spectrometer.

have similar or better sensitivity than other detectors for wavelengths below 2300Å (Reader, J., Sansonetti, C.J., & Deslattes, R.D. 2000). In addition, phosphor image plates have a linear intensity response with a dynamic range of at least 10000. Using a deuterium standard lamp to provided a radiometric calibration of the spectra, branching fractions can be determined to the short wavelength limit of $\lambda > 1150$Å.

Intensity calibrated Fe III spectra have been recorded on the IC VUV FTS over the wavelength range 1600 to 2500Å. In addition, Fe III spectra have been recorded over the wavelength range 1150 to 2500Å on the NIST Normal Incidence Vacuum grating Spectrograph (NIVS). The high resolution FT spectrometer spectra provide an excellent comparison to the NIVS spectra and the intensity calibration of both measurements can be verified over a broad spectral range. The light source used for the Fe III measurements is the Penning discharge lamp (PDL) (Heise, C., et al. 1994). The PDL is the ideal source for the measurements as it combines intensity stability and low to zero field plasma conditions. The Fe III emission spectra are intensity calibrated using two radiometric standard deuterium lamps at

IC and NIST. Taking the ratio of the calibrated line intensities yields branching fractions, which when combined with energy level lifetime values yield oscillator strengths.

3. Conclusion

We have carried out measurements on the IC VUV high resolution FT spectrometer and the NIST NIVS to record spectra of Fe III from 1150 to 2500Å. The source for both NIST and IC measurements was an iron–neon Penning discharge lamp. Using phosphor image plates to record the Fe III spectra on the NIST NIVS and using a deuterium intensity standard lamp we have measured the first ever intensity calibrated Fe III spectra in the wavelength range 1150 to 1600 Å. Preliminary branching ratio measurements for the Fe III transitions from the $3d^5$ (^{6}S) 4p ^7P_j levels have been determined and this work is in progress. Additional lifetime measurements for the $3d^5$ (^{6}S) 4p ^7P_j levels are also underway. Future work will include extending the wavelength range of the intensity calibration to $\lambda < 1150$Å and the measurement of other doubly ionized species of astrophysical interest will be investigated.

This work is supported in part by NASA Grant NAG5-12668, NASA inter-agency agreement W-10,255, PPARC, the Royal Society of the UK and by the Leverhulme Trust.

REFERENCES

Heise, C., Hollandt, J., Kling, R., Kock, M., Kuhne, M. 1994, Appl. Optics, 33, 5111
Johansson, S., Zethson, T., Hartman, H., Ekberg, J.O., Ishibashi, K., Davidson, K., Gull, T. 2000, A& A., 361, 977
Reader, J., Sansonetti, C.J., & Deslattes, R.D. 2000, Appl. Optics, 39, 637
Smith, P.L., Pickering, J.C., & Thorne, A.P. 2002, NASA/CP-2002-21186, 89
Sofia, U.J., & Meyer, D.M. 2001, Ap.J., 554, L22

NASA LAW, February 14-16, 2006, UNLV, Las Vegas

Laboratory measurements of the x-ray line emission from neon-like Fe XVII

G. V. Brown, P. Beiersdorfer, H. Chen, & J. H. Scofield

High Energy Density Physics and Astrophysics Division, Lawrence Livermore National Laboratory, Livermore, CA 94551

K. R. Boyce, R. L. Kelley, C. A. Kilbourne, & F. S. Porter

NASA/Goddard Space Flight Center, Greenbelt, MD 20771

M. F. Gu, & S. M. Kahn

Kavli Institute for Particle Astrophysics and Cosmology and Department of Physics, Stanford University, CA 94305

A. E. Szymkowiak

Department of Physics, Yale University, New Haven, CT 06520

ABSTRACT

We have conducted a systematic study of the dominant x-ray line emission from Fe XVII. These studies include relative line intensities in the optically thin limit, intensities in the presence of radiation from satellite lines from lower charge states of iron, and the absolute excitation cross sections of some of the strongest lines. These measurements were conducted at the Lawrence Livermore National Laboratory electron beam ion trap facility using crystal spectrometers and a NASA-Goddard Space Flight Center microcalorimeter array.

1. Introduction

The x-ray line emission from neon-like Fe XVII has been observed in several astrophysical sources such as the corona of the Sun, other stellar coronae, and elliptical galaxies. Because they create a distinct spectral signature and are present over a large temperature range, Fe XVII x-ray lines are prime diagnostic candidates. To help uncover the diagnostic potential of these lines and understand Fe XVII line emission observed in both celestial and laboratory sources, we have used the LLNL electron beam ion trap facility in conjunction

with crystal spectrometers and a microcalorimeter to conduct a study of the Fe XVII line emission under well-controlled laboratory conditions. Here we give a brief overview of some of the experimental results focussed on measuring the intensities of the resonance and intercombination lines, located at λ=15.01 Å and 15.26 Å, and known as 3C and 3D, respectively.

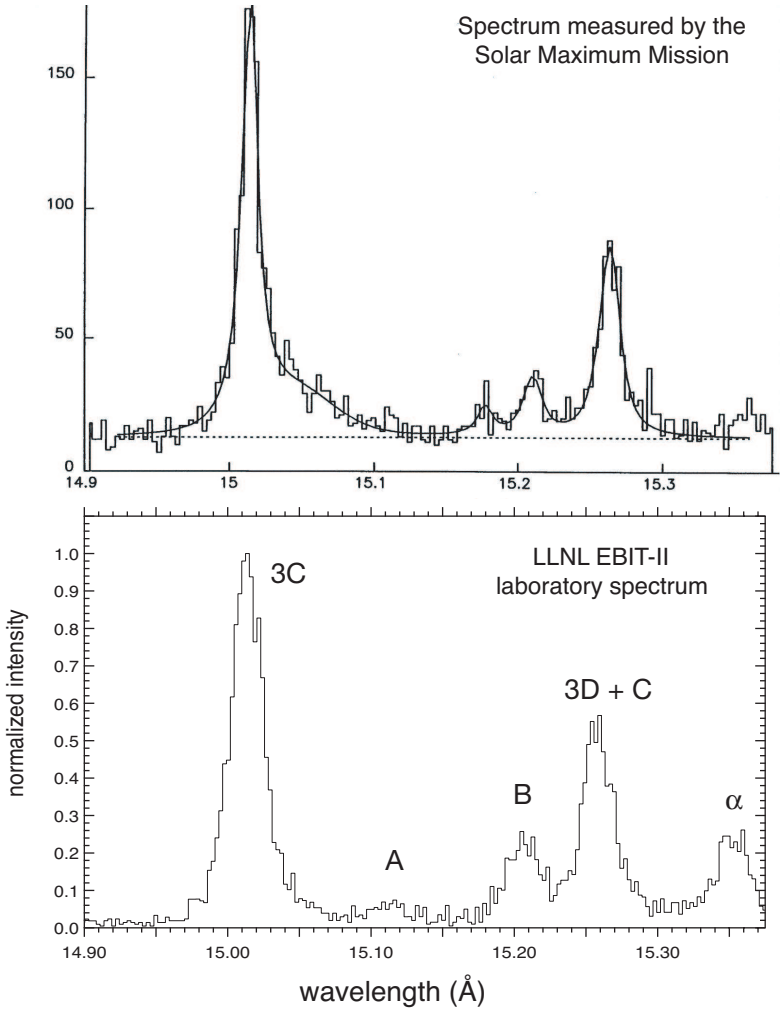

Fig. 1.— (top) Spectrum emitted from a quiescent active region of the Sun and measured by the Solar Maximum Mission (Brickhouse & Schmelz 2006). (bottom) Spectrum measured using a crystal spectrometer and the LLNL EBIT-II (Brown et al. 2001) where the relative abundance of Fe XVI to Fe XVII ions is ∼1. The lines are 3C and 3D from Fe XVII, A, B, and C from Fe XVI, and α from Fe XV.

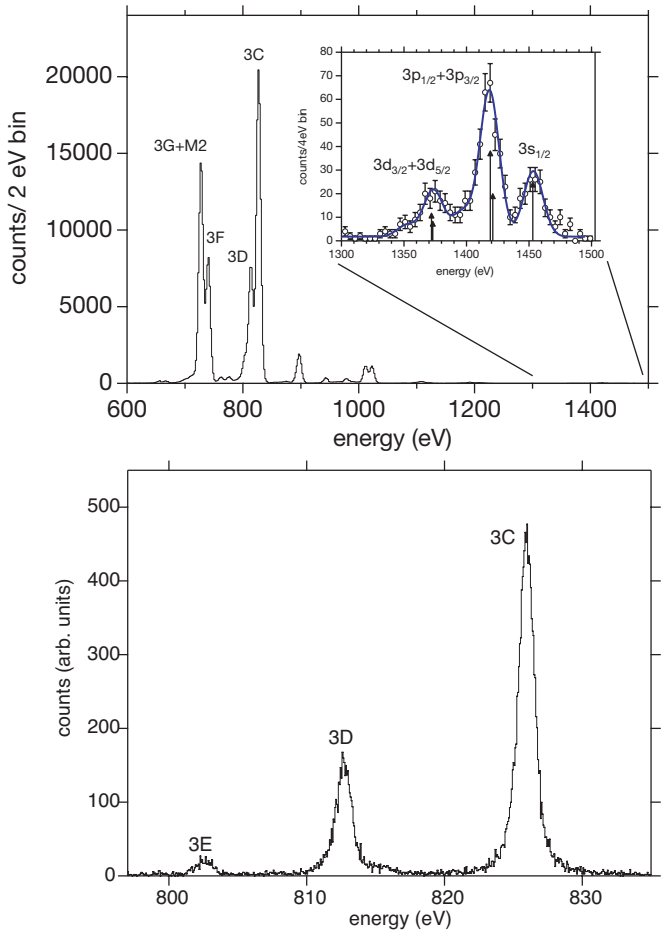

Fig. 2.— (top)Spectrum of Fe XVII measured by the NASA/GSFC 6 × 6 microcalorimeter array. The insert shows a close up of the energy range containing the emission from radiative recombination. (bottom) Fe XVII spectrum measured with a crystal spectrometer in concert with the microcalorimeter spectrum.

2. Measurements

The relative intensity of lines 3C and 3D measured in the Solar corona is significantly less than many predictions. At first, resonant scattering of line 3C was believed to be the source of the discrepancy, and many took advantage of this to infer line 3C's opacity. Measurements by our group (Brown et al., 1998) showed that the relative line intensity in the optically thin limit is less than the theoretical predictions, and in many cases, invoking resonant scattering was not necessary. However, some Solar ratios were still much lower than the laboratory value. Further study by our group found that the lower ratios observed in the Sun could be reproduced in the laboratory when, in addition to the Fe XVII ions, a significant amount of Fe XVI ions are also present (Brown et al. 2001). In this case, an Fe XVI line

produced by inner-shell excitation coincides with the Fe XVII intercombination line 3D. The additional flux added to the 3D feature reduces the apparent ratio, I_{3C}/I_{3D}. A recent study by Brickhouse &Schmelz (2006) revisited spectra measured from the Sun and found distinct line emission from Fe XVI. They concluded that the low values for I_{3C}/I_{3D} were explained by the Fe XVI line coincidence. Invoking resonant scattering was not necessary. A comparison of the laboratory spectrum with the spectrum measured from the Sun is given in figure 1.

To provide a more stringent test of theory, we continued our study of 3C and 3D by measuring each line's absolute excitation cross section, as opposed to relative excitation cross sections. The cross sections are brought to an absolute scale by measuring the photon emission from the direct excitation and radiative recombination simultaneously, and then normalizing to the well-known cross sections for radiative recombination. The spectrum including both the RR and direct excitation was measured using the broad-band NASA/GSFC x-ray microcalorimeter. To verify that no blending occurs we also measure the 3C and 3D line emission with a high resolution crystal spectrometer. Figure 2 shows the measured spectra. When comparing to theory, we find that in the case of the line 3C, the predicted cross section is significantly larger than the measurement (Brown, et al. 2006). The lower cross section for 3C helps resolve the puzzling observations by Xu et al. (2002) and Behar et al. (2001) who in their study of NGC 4656 and Capella, respectively, found that consistent results were obtained only if they normalized their spectrum to 3D not to 3C. We also note that recent theoretical calculations have reproduced some of the relative intensities measured in the laboratory and celestial sources (Loch et al 2006). However, owing to the fact that significant differences have been found when comparing absolute cross sections and that, in some physical regimes the relative intensities also do not agree, further study is required.

Work by the U.C. LLNL was performed under the auspices of the D.o.E. under contract No. W-7405-Eng-48 and supported by NASA APRA grants to LLNL, GSFC, and Stanford University.

REFERENCES

Xu, H., et al., ApJ, 2001, 548, 966.
Brickhouse, N. B. & Schmelz, J. T., 2006, ApJL, 636, L53.
Brown, G. V., et al., 1998, ApJ, 502, 1015.
Brown, G. V., et al., 2001, ApJL, 557, L75.
Brown, G. V., et al., 2006, PRL, submitted.
Loch, S. D., et al., 2006, J. Phys. B., 39, 85.
Xu, H., et al., ApJ, 2002, 579, 600.

NASA LAW, February 14-16, 2006, UNLV, Las Vegas

Collisional Ionization Equilibrium for Optically Thin Plasmas

P. Bryans[1], W. Mitthumsiri[1], D. W. Savin[1], N. R. Badnell[2], T. W. Gorczyca[3], & J. M. Laming[4]

[1]*Columbia Astrophysics Laboratory, Columbia University, New York, NY 10027*
[2]*Department of Physics, University of Strathclyde, Glasgow, G4 0NG, United Kingdom*
[3]*Department of Physics, Western Michigan University, Kalamazoo, MI 49008*
[4]*E. O. Hulburt Center for Space Research, NRL, Code 7674L, Washington, DC 20375*

ABSTRACT

Reliably interpreting spectra from electron-ionized cosmic plasmas requires accurate ionization balance calculations for the plasma in question. However, much of the atomic data needed for these calculations have not been generated using modern theoretical methods and their reliability are often highly suspect. We have utilized state-of-the-art calculations of dielectronic recombination (DR) rate coefficients for the hydrogenic through Na-like ions of all elements from He to Zn. We have also utilized state-of-the-art radiative recombination (RR) rate coefficient calculations for the bare through Na-like ions of all elements from H to Zn. Using our data and the recommended electron impact ionization data of Mazzotta et al. (1998), we have calculated improved collisional ionization equilibrium calculations. We compare our calculated fractional ionic abundances using these data with those presented by Mazzotta et al. (1998) for all elements from H to Ni, and with the fractional abundances derived from the modern DR and RR calculations of Gu (2003a,b, 2004) for Mg, Si, S, Ar, Ca, Fe, and Ni.

1. Introduction

Electron-ionized plasmas (also called collisionally ionized plasmas) are formed in a diverse variety of objects in the universe. These range from stellar coronae and supernova remnants to the interstellar medium and gas in galaxies or in clusters of galaxies. The physical properties of these sources can be determined using spectral observations coupled with theoretical models. This allows one to infer electron and ion temperatures, densities, emission measure distributions, and ion and elemental abundances. Reliably determining these properties requires accurate fractional abundance calculations for the different ionization stages of the various elements in the plasma (i.e., the ionization balance of the gas).

Since many of the observed sources are not in local thermodynamic equilibrium, in order to determine the ionization balance of the plasma one needs to know the rate coefficients for all the relevant ionization and recombination processes. Often the observed systems are optically-thin, low-density, dust-free, and in steady-state or quasi-steady-state. Under these conditions the effects of any radiation field can be ignored, three-body collisions are unimportant, and the ionization balance of the gas is time-independent. This is commonly called collisional ionization equilibrium (CIE) or sometimes coronal equilibrium.

Our work has collected the most recent state-of-the-art theoretical DR and RR rate coefficients and, based on these data, calculated new CIE ionic fractional abundances of all elements from H to Zn.

2. Dielectronic Recombination

Badnell et al. (2003) have calculated the DR rate coefficients using the AUTOSTRUCTURE code for the H- through Na-like isoelectronic sequences of all elements from He through to Zn. We use the convention here of identifying the recombination process by the initial charge state of the ion. These new DR data have been collected together and are available online Badnell (2006a). In addition, some of the original data has been refitted so as to extend the validity of the fits to lower temperatures. Gu (2003a) has calculated DR rate coefficients using the FAC code for the H- through Ne-like isoelectronic sequences of Mg, Si, S, Ar, Ca, Fe and Ni and for the Na-like sequence for Mg through Zn (Gu 2004). For ionization stages not included in the calculations of Badnell (2006a) and Gu (2003a, 2004), we use the DR rate coefficients recommended by Mazzotta et al. (1998) for elements up to and including Ni and Mazzotta (private communication) for Cu and Zn.

3. Radiative Recombination

Gu (2003b) has calculated RR rate coefficients for ions of Mg, Si, S, Ar, Ca, Fe and Ni for bare through F-like ions using FAC. Badnell (2006c) has calculated RR rate coefficients for all elements from H through to Zn for the bare through Na-like isoelectronic sequences using AUTOSTRUCTURE. These are available online (Badnell 2006b). As for DR, we use the RR rate coefficients recommended by Mazzotta et al. (1998) and Mazzotta (private communication) for ions not calculated by Gu (2003b) or Badnell (2006b).

4. Results & Conclusions

The differences in our calculated CIE fractional abundances relative to those of Mazzotta et al. (1998) are, in general, much larger than the differences between our results and the results using the data of Gu (2003a,b, 2004). In the former case, peak abundance differences of nearly 60% are found and the differences can be larger than 1000% at fractional abundances down to 0.01. For the latter case, peak abundance differences are within 10% and differences for fractional abundances down to 0.01 are within 50%. This reflects the fact that the modern DR and RR data are in better agreement with one another than with the older data.

Full results can be found in Bryans et al. (2006) but, for illustrative purposes, we present here our calculated CIE fractional abundances for Fe. Fig. 1 shows how the AUTOSTRUCTURE-based results compare with those of Mazzotta et al. (1998), and Fig. 2 shows the comparison between the AUTOSTRUCTURE-based calculations and the FAC-based calculations.

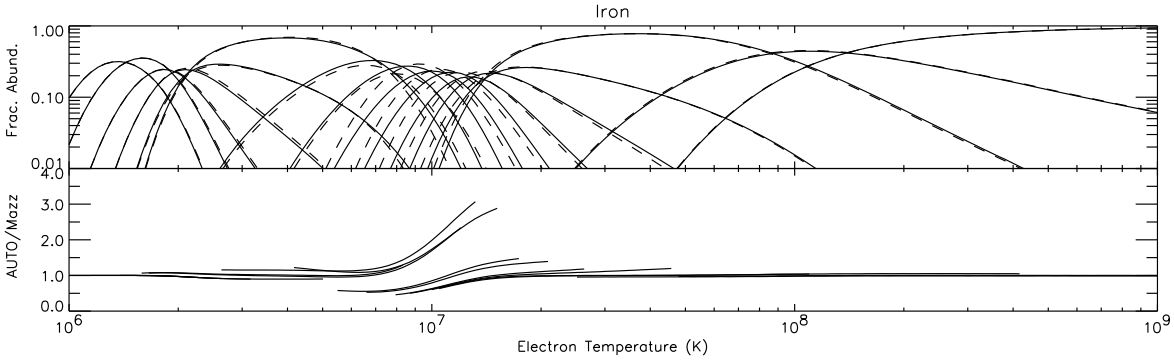

Fig. 1.— Ionization fractional abundance versus electron temperature for Fe. The upper graph shows the AUTOSTRUCTURE-based results (*solid curves*, labeled 'AUTO') and the Mazzotta et al. (1998) results (*dashed curves*, labeled 'Mazz'). The lower graph shows the ratio of the calculated abundances.

Further progress in CIE calculations will require a concerted theoretical and experimental effort to generate the remaining needed atomic data. Modern DR and RR data are urgently needed for ions with 12 or more bound electrons. There is also a need for improved electron impact ionization (EII) and charge transfer (CT) data. There has been no significant revision or laboratory benchmarking of the recommended EII database since around 1990. Additionally, the latest compilation of recommended CT rate coefficients dates back to Kingdon & Ferland (1996). We propose that all future data for DR, RR, CT, and EII should be generated aiming for an accuracy that matches that of the modern electron-ion recombination measurements and calculations. Such an accurate and up-to-date database is crucial for being able to produce reliable CIE calculations for the astrophysics community.

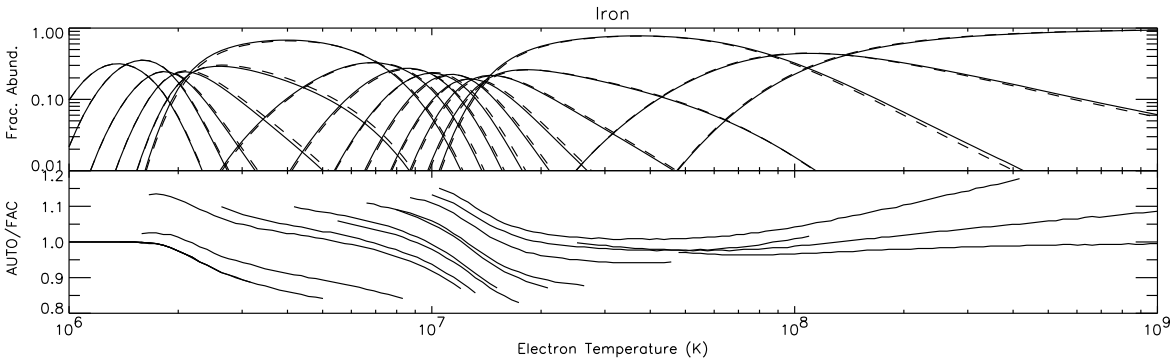

Fig. 2.— Same as Fig. 1 but replacing the Mazzotta et al. (1998) results with the FAC-based results (*dashed curves*, labeled 'FAC').

This work was supported in part by the NASA APRA Program.

REFERENCES

Badnell, N. R., et al. 2003, A&A, 406, 1151
Badnell, N. R. 2006a, `http://amdpp.phys.strath.ac.uk/tamoc/DR/`
Badnell, N. R. 2006b, `http://amdpp.phys.strath.ac.uk/tamoc/RR/`
Badnell, N. R. 2006c, arXiv:astro-ph/0604144
Bryans, P., Badnell, N. R., Gorczyca, T. W., Laming, J. M., Mitthumsiri, W., & Savin, D. W. 2006, arXiv:astro-ph/0604363
Gu, M. F. 2003a, ApJ, 590, 1131
Gu, M. F. 2003b, ApJ, 589, 1085
Gu, M. F. 2004, ApJ, 153, 389
Kingdon, J. B., & Ferland, G. J. 1996, ApJS, 106, 205
Mazzotta, P., Mazzitelli, G., Colafrancesco, S., & Vittorio, N. 1998, A&AS, 133, 403

NASA LAW, February 14-16, 2006, UNLV, Las Vegas

Electron Impact Excitation Cross Section Measurement for n=3 to n=2 Line Emission in Fe^{17+} to Fe^{23+}

H. Chen, P. Beiersdorfer, G.V. Brown and J. H. Scofield

High Temperature and Astrophysics Division, Lawrence Livermore National Laboratory, Livermore, CA 94551

M. F. Gu and S. M. Kahn

Physics Department, Stanford University, CA 94305

K.R. Boyce, R. L. Kelley, C. A. Kilbourne and F. S. Porter

Goddard Space Flight Center, Greenbelt, MD 20771

ABSTRACT

We have measured the electron impact excitation cross sections for the strong iron L-shell $3 \rightarrow 2$ lines of Fe XVIII to Fe XXIV at the EBIT-I electron beam ion trap using a crystal spectrometer and NASA-Goddard Space Flight Centers 6×6 pixel array microcalorimeter. The cross sections were determined by direct normalization to the well established cross section of radiative electron capture through a sophisticated model analysis which results in the excitation cross section for the strong Fe L-shell lines at multible electron energies. This measurement is part of a laboratory X-ray astrophysics program utilizing the Livermore electron beam ion traps EBIT-I and EBIT-II.

Subject headings: molecular data — molecular processes: photodissociation — stars: atmospheres

1. Introduction

The atomic data of iron are very important for interpreting virtually all types of observations since iron is the most abundant high-Z element and radiates profusely in many spectral bands. In specific, the spectral-rich emission from the iron L-shell has been one of the primary diagnostic tools of the high-resolution grating spectrometers on the $XMM-Newton$ and $Chandra$ X-ray observatories. A great deal of theoretical modeling effort has been put forward to interpret these high-resolution X-ray spectra. Despite these efforts in improving

the atomic calculations, the need for laboratory measurements is clear: repeatedly, laboratory data have shown that calculations are inaccurate or incomplete because they miss crucial physics left out as part of necessary approximations (Beiersdorfer 2003). To address the need for validating the calculations using experimental data, our laboratory X-ray astrophysics program, utilizing the electron beam ion traps EBIT-I and EBIT-II at the University of California Lawrence Livermore National Laboratory has measured atomic data including ionization and recombination cross sections for charge balance calculations, emission line lists, excitation cross sections, and dielectronic recombination resonance strengths for interpreting X-ray line formation. On the iron excitation cross measurements, Gu et al. (1999a, 2001) have reported measurements for Fe XXI–Fe XXIV lines that were normalized to calculations in the high energy limit. Although such a normalization can be fairly reliable at high electron-ion collision energies, the accuracy of electron scattering calculations at these energies is estimated to be only to 15 – 30% (Zhang et al. 1989), and may in fact be much worse (factors of two or more, see Section 4 of this paper), if the levels are affected by configuration interactions. A more accurate method is normalizing directly to radiative electron capture, i.e. radiative recombination (RR). Measurements of some Fe L-shell cross sections utilizing RR for normalization has been reported by Chen et al. (2002, 2005) and Brown et al. (2006). These measurements were made possible in part by the availability of a high-resolution, large-area, gain-stabilized microcalorimeter, the engineering spare microcalorimeter from the original $ASTRO-E$ satellite mission. Using this technique, we have recently measured all strong $n = 3 \rightarrow 2$ L-shell Fe lines from Fe^{17+} to Fe^{23+}. The results of these measurements are presented here.

2. Measurement and analysis

Our experiments were carried out on the EBIT-I device (Levine et al. 1988). Similar to the experimental setup described in our previous measurement on EBIT-II (Chen et al. 2005), we used a crystal spectrometer (Beiersdorfer & Wargelin 1994; Brown et al. 1999) together with the XRS/EBIT microcalorimeter detector (Kelley et al. 1999). The microcalorimeter has an energy resolution better than 10 eV and a dynamic range from 0.1 to 10 keV. The crystal spectrometer employed a flat Rubidium hydrogen phthalate (RAP) crystal, which has an energy coverage of about 150 eV per setting. To cover the L-shell Fe lines from different charge states (photon energies between 0.78 to 1.18 keV, equivalent to wavelengths between 10.5 and 15.9 Å), we set the Bragg angles to 30.5, 32, 36 and 40 degrees. The crystal spectrometer had a resolving power of 385 (FWHM of 2.6 eV at a photon energy of 1 keV). Most of the strong Fe 3 →2 L-shell lines observed with the crystal spectrometer were resolved, while only a few of those observed with the microcalorimeter were, illustrating the need to operate both instruments simultaneously. The L-shell lines were previously measured by Brown et al. (2002) and their labels and identifications are used in this paper. Our measurements were made at electron beam energies of 1.35, 1.46, 1.56, 1.7, 1.82, 1.94,

2.05, 2.45, and 2.93 keV, with beam currents ranging between 20 – 30 mA. These energies were slightly above the ionization threshold of individual ion charge states from F-like to Li-like, and they were high enough so that the contributions from dielectronic recombination radiation and resonance excitation to the direct excitation line intensities can be ignored. At these energies, however, cascades from higher levels may contribute to the line intensities. Our method determines the effective cross section that includes all possible cascade processes.

To analyze the complicated Fe L-shell spectra, we developed a new method based on the atomic data calculated with the Flexible Atomic Code (Gu 2003). The model starts with a theoretical data base that includes thousands of lines, most of which were too weak to be measured experimentally but will contribute to the spectrum collectively. When comparing the theoretical model with the experimental data, we adjust the theoretical cross sections for a subset of strong lines in order to achieve acceptable agreement with measurement. This allows us to derive the measured cross sections for this subset of lines, and any possible contamination of weak lines in the determination of intensities of strong lines are accounted for in the analysis with theoretical calculations. More detailed description on the data analysis can be found in (Chen et al. 2006).

Overall the calculations agree to within 20% with the experimental results for all lines. For example, O-like Fe $2p_{1/2}2p_{3/2}^2 3d_{5/2}(J=3) \rightarrow 2p_{3/2}^2(J=2)$ has excitation cross sections of $2.60(\pm 0.34) \times 10^{-20}\mathrm{cm}^2$, $2.49(\pm 0.34) \times 10^{-20}\mathrm{cm}^2$, and $2.39(\pm 0.35) \times 10^{-20}\mathrm{cm}^2$, which compares to the theoretical numbers of $2.73\times10^{-20}\mathrm{cm}^2$, $2.68\times10^{-20}\mathrm{cm}^2$, and $2.60\times10^{-20}\mathrm{cm}^2$, for electron energy of 1.46 keV, 1.56 keV and 1.70 keV, respectively. A few exceptions are a couple of F-like lines (F20a, F20b, F19a, and F17) at electron energies of 1.56 keV and 1.7 keV. The difference between theory and measurements in these few cases are about 30% or greater. The cause of this discrepancy is not clear.

Details of the measurement, results and discussions can be found in (Chen et al. 2006).

This work was performed under the auspices of the U.S. Department of Energy by the University of California Lawrence Livermore National Laboratory under contract No. W-7405-Eng-48 and supported by NASA Astronomy and Physics Research and Analysis grants to LLNL, GSFC, and Stanford University.

REFERENCES

Beiersdorfer, P., & Wargelin, B. J., 1994, Rev. Sci. Instrum. 65, 13
Beiersdorfer, P., 2003, Annu. Rev. Astron. Astrophys., 41, 343
Brown, G. V., Beiersdorfer, P., & Widmann, K., 1999, Rev. Sci. Instrum. 70, 280
Brown, G. V., Beiersdorfer, P., Liedahl, D. A., Widmann, K., Kahn, S. M. & Clothiaux, E. J., 2002, ApJS, 140, 589
Brown, G. V., Beiersdorfer, P., et al., 2006, submitted to Physical Review Letters.

Chen, H., Beiersdorfer, P., Scofield, J. H., Gendreau, K. C., Boyce, K. R., Brown, G. V., Kelley, R. L., Porter, F. S., Stahle, C. K., Szymkowiak, A. E., & Kahn, S. M., 2002, ApJ, 567, L169

Chen, H., Beiersdorfer, P., Scofield, J., K. C., Boyce, K. R., Brown, G. V., Kelley, R. L., Kilbourne, C. K., Porter, F. S., Gu, M. F.,& Kahn, S. M., 2002, ApJ, 618, 1086

Chen, H., Gu, M. F., Beiersdorfer, P. et al., 2006, ApJ, v646

Gu, M. F., Kahn, S. M., Savin, D. W., Beiersdorfer, P., Liedahl, Brown, G. V., Reed, K. J., Bhalla, C. P., & Grabbe, S. R., 1999a, ApJ, 518, 1002

Gu, M. F., Kahn, S. M., Savin, D. W., Bahar, E., Beiersdorfer, P., Brown, G. V., Liedahl & Reed, K., 2001, ApJ, 563, 462

Gu, M. F.,2003, ApJ, 582, 1241

Kelley, R. L., et al, 1999, SPIE, 3765, 114

Levine, M. A., Marrs, R. E., Henderson, J. R., Knapp, D. A., & Schneider, M. B., 1988, Physics Scripta, T22, 157

Zhang, H. L. & Sampson, D. H., 1989, Atomic Data and Nuclear Data Tables, 43, 1

NASA LAW, February 14-16, 2006, UNLV, Las Vegas

Measurements of Polyatomic Molecule Formation on an Icy Grain Analog Using Fast Atoms

A. Chutjian[1] S. Madzunkov[1] B. J. Shortt[2] J. A. MacAskill [1] M. R. Darrach[1]

[1]*Jet Propulsion Laboratory/Caltech, Pasadena, CA 91109*

[2]*Dept. Applied Physics, Cork Institute of Technology, Cork, Ireland*

ABSTRACT

Carbon dioxide has been produced from the impact of a monoenergetic O(^{3}P) beam upon a surface cooled to 4.8 K and covered with a CO ice. Using temperature-programmed desorption and mass spectrometer detection, we have detected increasing amounts of CO_2 formation with O(^{3}P) energies of 2, 5, 10, and 14 eV. This is the first measurement of polyatomic molecule formation on a surface with superthermal atoms. The goal of this work is to detect other polyatomic species, such as CH_3OH, which can be formed under conditions that simulate the grain temperature, surface coverage, and superthermal atoms present in shock-heated circumstellar and interstellar regions.

1. Introduction

Dust, ices, and surfaces of planets, comets, and asteroids play an indispensable role in the chemical evolution of the protostellar regions and the interstellar medium (ISM), from the catalytic production of molecular hydrogen to the formation of organics (CH_3OH, H_2CO, CH_4, NH_3, CN-bonded species, etc.) critical to the origin of life. Laboratory studies of ices and dust grain analogs are crucial to defining and constraining the environmental conditions in dense and dusty clouds. Grain-particle interactions include effects of ion and neutral atomic fluxes, UV radiation intensity, cosmic-ray intensity, and surface temperature. A wide range of laboratory studies has been carried out on effects of ion irradiation; UV photolysis of molecules (including amino acids) on icy grain analogs; thermal-energy atomic irradiation by oxygen atoms, and on thermal desorption characteristics of molecules from analogs of icy dust grains.

Fast neutral species such as H, He, O, OH, CO, and H_2O are present in the circumstellar regions and the ISM by virtue of energetic processes such as stellar outflows, shocks, dissociation and ionization of gas-phase particles by stellar UV photons, and the charge

exchange of outgoing stellar wind ions with circumstellar neutral clouds. Neutral-neutral reactions almost certainly play a major role within cold dark clouds where UV penetration is blocked by dust, and in hot molecular cores where shock heating of neutral atomic species can occur (Ehrenfreund and Charnley 2000). The clearest example of the importance of neutral-neutral reactions is the astrophysical observation that abundant CO_2 is detected in a quiescent dark cloud (Elias 16), where no sources of UV radiation are present, and hence where photochemistry cannot have a role (Whittet et al. 1998).

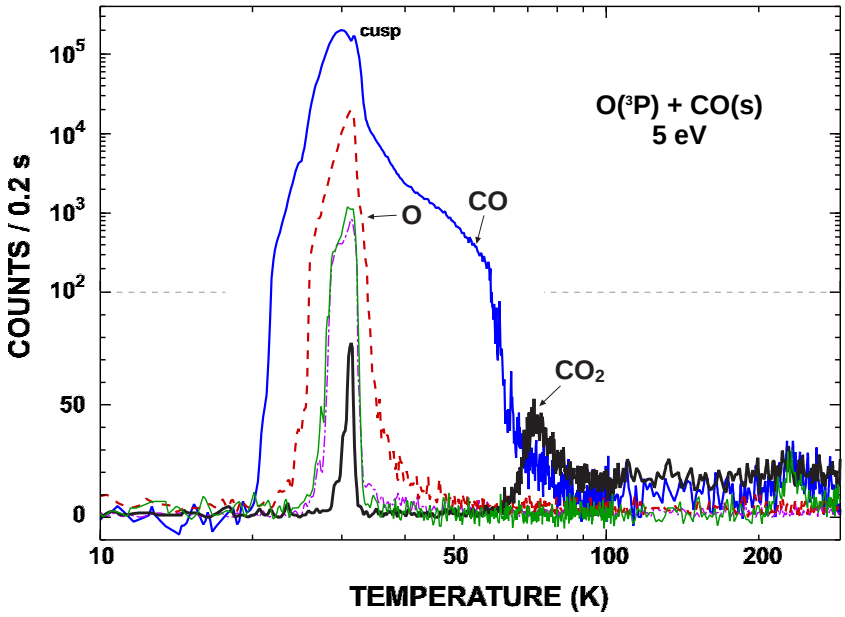

Fig. 1.— TPD spectrum following the exposure to a 5 eV $O(^3P)$ beam of CO frozen on a gold substrate. The TPD consists of a low-temperature physisorbed peak (30 K), and a high temperature (70 K) chemisorbed peak consisting of only CO_2. The mass channels are ^{16}O (broken red line), $^{18}H_2O$ (solid green line), ^{28}CO (solid blue line), $^{32}O_2$ (broken purple line), and $^{44}CO_2$ (thick solid black line). The peak/valley ratio of the cusp is 0.7.

2. Experimental Methods

The fast-atom apparatus is described in detail in (Madzunkov et al. 2006) [see also (Orient et al. 1992; Orient et al. 1993)]. The surface target consists of CO frozen on a gold surface mounted to a linear translation stage. In a typical temperature-programmed desorption (TPD) run a cleaned gold surface is translated into deposition and bombardment position. There, the surface is cooled to 4.8 K by a flow of liquid helium, whereupon CO is introduced into the chamber at a pressure of 10^{-7}Pa (as measured near the target). The CO molecules are deposited onto the cold surface while the surface is simultaneously bombarded by the $O(^3P)$ and ground state beam for one hour. The oxygen beams used in separate

exposures were at energies of 2, 5, 10, and 14 eV, at neutral currents of 10^7atoms/sec. The base pressure in the target region is 5×10^{-10}Pa.

After exposure the O(^{3}P) beam is turned off. The surface is retracted to position where it is then warmed to 350 K at a rate of 1.0 K/min to 100 K, and at a rate of 10 K/min from 100 K to 350 K. The desorbing species are detected as a function of surface temperature with a quadrupole mass spectrometer (MS). An example of the TPD data is shown in Fig. 2 for 5 eV O-atom energy. Comparable results were obtained at 2, 10, and 14 eV. A personal computer is used to monitor and record the electron beam current, target surface temperature, and the mass spectrometer signal for multiple species, while controlling the electron beam energy, electrode potentials, and the surface-target heater. The temperature ramp is sufficiently slow that multiple scans of the MS are performed at each temperature step. The MS is used in a multiple ion monitoring mode to detect the production of up to eight separate masses during the TPD ramp.

3. Experimental Results

Five desorbed species are evident in Fig. 1. The strong, cusped peak at 30 K is interpreted as being due to physisorbed and chemisorbed CO ice layers, in which the bonding is due to relatively weak CO-CO intermolecular (physisorbed) and strong CO-surface (chemisorbed) potentials. Warming the surface up to the 30 K melting point of this ice mlange throws all the reacted and adsorbed species into the vapor phase. The ejected species are $^{18}H_2O$, ^{28}CO, $^{32}O_2$, and $^{44}CO_2$. The ^{12}C and ^{16}O arise from fractionation in the MS ionizer of H_2O, CO, O_2, and CO_2. The contribution of $^{28}N_2$ to the signal at mass 28 was negligible, as evidenced by the fact that no fractionated ^{14}N could be detected in the baseline vacuum prior to and following each TPD measurement. In addition, the detected C^+/CO^+ intensity ratio was consistent with that given by the fraction of CO alone. The source of the H_2O is trace background water in the vacuum chamber. A search was made in a separate measurement for other mass species in the range 5-50 amu. None was found to within the system detection limit.

At 70 K one detects only desorption of CO_2 chemisorbed to the gold substrate, and formed in the reaction $O + CO(s) \rightarrow CO_2(s)$. Finally, one detects at 230 K desorption of the residual H_2O background frozen on the target (Fig. 1). The CO desorption temperature range found here agrees with another study in which CO desorption was found to start at 24 K, and was gone by 33 K [see also (Sandford and Allamandola 1998)]. The behavior of the CO desorption was used to provide an estimate of approximately a 2-3 monolayer CO coverage, in agreement with an estimate based on the CO partial pressure, exposure time, and a unity sticking coefficient.

A TPD normalization procedure was adopted in order to exhibit the clear enhancement of integrated TPD signals, measured for the different ion masses (^{12}C, ^{16}O, $^{18}H_2O$, ^{28}CO,

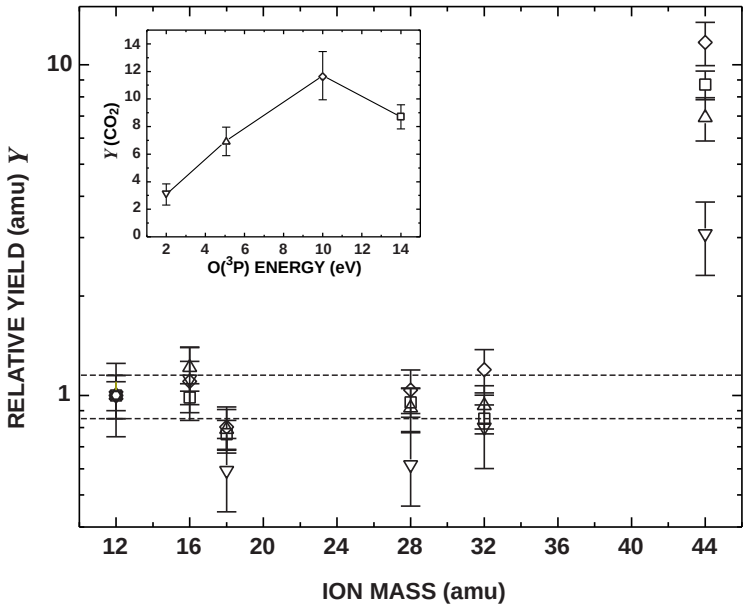

Fig. 2.— Relative production yields $\mathcal{Y}$ of the species ^{12}C, ^{16}O, $^{18}H_2O$, ^{28}CO, $^{32}O_2$, and $^{44}CO_2$ at 2 eV ($\bigtriangledown$), 5 eV ($\bigtriangleup$), 10 eV ($\diamond$), and 14 eV ($\square$). Shown in the insert is the excitation function for production of CO_2 as a function of the $O(^3P)$ energy (Madzunkov et al. 2006).

$^{32}O_2$ and $^{44}CO_2$), due to O-atom exposure (Madzunkov et al. 2006). From this one can then obtain an expression for the relative yield $\mathcal{Y}$ of species production. Plotted in Fig. 2 are measured values of $\mathcal{Y}$ for each ion mass (with the value of $\mathcal{Y}$ for ^{12}C taken as unity). The horizontal band is the average value $\mathcal{Y} = 0.97 \pm 0.1$ (1σ) as measured for the first five masses. Also shown is the error in $\mathcal{Y}$ arising from statistical error, error in measurement of the CO pressure, and error in knowledge of the laser power within the cavity. One sees clear enhancement in CO_2 production (mass 44) at all atomic oxygen energies.

This work was carried out at JPL/Caltech, and was supported by NASA.

REFERENCES

Ehrenfreund, P. and Charnley, S. B. 2000, Ann. Rev. Astron. Astrophys. **38**, 427.
Madzunkov, S., Shortt, B. J., MacAskill, J. A., Darrach, M. R. and Chutjian, A. 2006, Phys. Rev. A **73**, 020901.
Orient, O. J., Martus, K. E., Chutjian, A. and Murad, E. 1992, Phys. Rev. A **45**, 2998.
Orient, O. J., Chutjian, A., Martus, K. E. and Murad, E. 1993, Phys. Rev. A **48**, 427.
Orient O. J. and Chutjian, A. 1999, Phys. Rev. A **59**, 4374.
Sandford, A. S. and Allamandola, L. J. 1988, Icarus 765, 201.
Whittet, D. C. B. et al. 1998, Ap. J. 498, L159.

NASA LAW, February 14-16, 2006, UNLV, Las Vegas

Lifetimes and Oscillator Strengths for Ultraviolet Transitions in P II, Cl II and Cl III

S. Cheng, S. R. Federman, R. M. Schectman, M. Brown, & R. E. Irving

Department of Physics and Astronomy, University of Toledo, Toledo, OH 43606

scheng@physics.utoledo.edu, steven.federman@utoledo.edu, rms@physics.utoledo.edu, mbrown@physics.utoledo.edu, rirving@physics.utoledo.edu

M. C. Fritts

School of Physics and Astronomy, University of Minnesota, Minneapolis, MN 55455

fritts@physics.umn.edu

N. D. Gibson

Department of Physics and Astronomy, Denison University, Granville, OH 43023

gibson@denison.edu

ABSTRACT

Oscillator strengths for transitions in P II, Cl II and Cl III are derived from lifetimes and branching factions measured with beam-foil techniques. The focus is on the multiplets with a prominent interstellar line at 1153 Å in P II which is seen in spectra of hot stars, and the lines at 1071 Å in Cl II and 1011 Å in Cl III whose lines are seen in spectra of diffuse interstellar clouds and the Io torus acquired with the *Far Ultraviolet Spectroscopic Explorer*. These data represent the first complete set of experimental f-values for the lines in the multiplets. Our results for P II λ1153 agree well with Curtis' semi-empirical predictions, as well as the large scale computations by Hibbert and by Tayal. The data for Cl II λ1071 also agree very well with the most recent theoretical effort and with Morton's newest recommendations. For Cl III, however, our f-values are significantly larger than those given by Morton; instead, they are more consistent with recent large-scale theoretical calculations. Extensive tests provide confirmation that *LS* coupling rules apply to the transitions for the multiplets in Cl II and Cl III.

1. Introduction and Experiments

The analysis of atomic abundances in astronomical environments needs accurate oscillator strengths and lifetimes for the species involved. As an example, a prominent interstellar line at 1153 Å seen in spectra of hot stars arises from absorption in P II. Analysis of this line is used to derive phosphorus abundances and the f-value for λ1302 (e.g., Harris and Mas Hesse 1986). Another example for such a need is the precision oscillator strengths and lifetimes for Cl II and Cl III which are needed to infer the total Cl abundance in Io's torus as observed by *FUSE* (Feldman et al. 2001, 2004). We present beam-foil measurements that produce relevant atomic data for those lines in P II, Cl II and Cl III.

The experiments were carried out by the beam-foil technique. Phosphorous or chlorine ions were accelerated to energies of 170 keV or 220 keV, passed through carbon foils with typical thicknesses of $2.2 - 2.5$ μg cm^{-2}, and emerged in a variety of charge states and excited states. The desired transitions were selected by a monochromator with suitable gratings and focused onto a channeltron detector. Various measurements were performed to account for systematic effects such as beam divergence, foil thickening, and nuclear scattering. The stability of the ion beam was monitored by a Faraday cup and by an optical monitor. Decay curves were obtained for each value of j in the upper fine-structure levels associated with the multiplet at 1154 Å in P II, 1071 Å in Cl II, and 1011 Å in Cl III. When an upper level has more than one channel for decay, branching fractions were measured to convert lifetimes into oscillator strengths. A spectrum of the P II multiplet at 1154 Å is shown in Figure 1.

2. Results and Discussion

(a) Lifetimes: The lifetimes for the P II upper states in the multiplet ($3s^2 3p^2\ ^3P - 3s^2 3p4s\ ^3P^o$) are about 0.80 ns. This agrees with previous experimental results (Livingston et al. 1975) and theoretical results (Hibbert 1988). Our lifetimes for the Cl II multiplet λ1071 ($3s^2 3p^4\ ^3P - 3s3p^5\ ^3P^o$) are about 9.0 ns, agreeing with previous experimental results (Lawrence 1969, Bashkin & Martinson 1971) and theoretical calculations (Tayal 2004). The lifetime for the Cl III multiplet λ1011 ($3s^2 3p^3\ ^4S^o - 3s3p^4\ ^4P$) is found to be about 8.0 ns. This result, averaged from those of three decay channels that agree nicely with each other, is about 20% shorter than the result of Bashkin & Martinson (1971), but agrees much better with theoretical lifetimes of Huang (1984).

(b) Branching Fractions: The branching fractions for a given level for allowed transitions can be derived from the multiplet spectrum, such as that shown in Figure 1. Care was taken in extracting the fractions when transitions blend and when there was possible contamination from transitions from higher charge states. The branching fractions for the P II multiplet are given in Table 1, together with comparisons from three theoretical calculations. Our results agree well with Curtis' (2000) semi-empirical predictions, as well as with

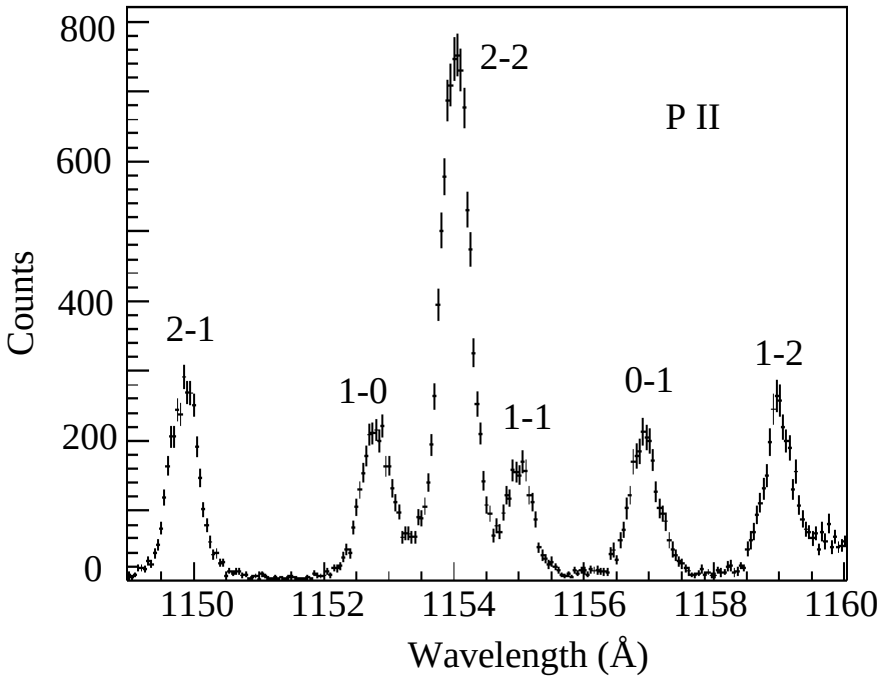

Fig. 1.— Spectrum of P II multiplet at 1154 Å. The j-values involved in the transitions have been labeled accordingly.

the large-scale theoretical computations by Hibbert (1988) and Tayal (2003). A comparison of P II branching fractions with classical LS coupling rules reveals that they are very similar. This implies that the P II multiplet is rather free of configuration interaction.

(c) Oscillator Strengths: From the measured lifetimes and branching fractions, we derived oscillator strengths for Cl II and Cl III, and the tabulated results can be found in Schectman et. al. (2005). Our results for Cl II are in excellent agreement with the extensive Hartree-Fock calculation of Tayal (2004) and with the recommendations of Morton (2003). Thus, there is no need to revise interstellar Cl II abundances obtained previously that are based on these recommendations. Our results for Cl III are consistent with most recent theoretical efforts (e. g., Huang 1984, Ho & Henry 1987). On the other hand, the correspondence with the measurement of Bashkin & Martinson (1971) and the calculations of Aymar (1973) is poor. Since Morton's (2003) recommended f-values are based on the results from Bashkin & Martinson, they are about 30% smaller than those derived from our lifetimes and from most theoretical calculations.

This research was supported by NASA grant NAG5-11440 to the University of Toledo.

Table 1: Branching Fractions for P II ($3s^2 3p^2\ ^3P$- $3s^2 3p 4s\ ^3P^o$).

Transition	Present	*LS*	Hibbert (1988)	Curtis (2000)	Tayal (2003)
λ1153 ($^3P_0 - \ ^3P_1{}^o$)	36.0 ± 2.3	33.3	33.1	33.1	32.8
λ1155 ($^3P_1 - \ ^3P_1{}^o$)	25.3 ± 1.7	25.0	24.6	24.5	24.3
λ1159 ($^3P_2 - \ ^3P_1{}^o$)	38.7 ± 2.8	41.7	41.4	41.0	40.9
λ1150 ($^3P_1 - \ ^3P_2{}^o$)	26.6 ± 1.6	25.0	25.3	25.2	25.3
λ1154 ($^3P_2 - \ ^3P_2{}^o$)	73.4 ± 3.3	75.0	74.7	74.8	74.7

REFERENCES

Aymar, M. 1973, Nucl. Instrum. Methods, 110, 211

Bashkin, S., & Martinson, I. 1971, J. Opt. Soc. Am., 61, 1686

Curtis, L. J. 2000, J. Phys. B, 33, L259

Feldman, P. D., et al. 2001, ApJ, 554, L123

Feldman, P. D., Strobel, D. F., Moos, H. W., & Weaver, H. A. 2004, ApJ, 601, 583

Harris, A. W., & Mas Hesse, J. M. 1986, ApJ, 308, 240

Hibbert, A. 1988, Phys. Scr., 38, 37

Ho, Y. K., & Henry, R. J. W. 1987, Phys. Scr., 35, 831

Huang, K.-N. 1984, At. Data Nucl. Data Tables, 30, 313

Lawrence, G. M. 1969, Phys. Rev., 179, 134

Livingston, A. E., Kernahan, J. A., Irwin, D. J. G., & Pinnington, E. H. 1975, Phys. Scr., 12, 223

Morton, D. C. 2003, ApJS, 149, 205

Ramsbottom, C. A., Bell, K. L., & Keenan, F. P. 2001, At. Data Nucl. Data Tables, 77, 57

Schectman, R. M., et. al. 2005, ApJ, 621, 1160

Tayal, S. S. 2003, ApJS, 146, 459

Tayal, S. S. 2004, A&A, 426, 717

NASA LAW, February 14-16, 2006, UNLV, Las Vegas

Oscillator Strengths and Predissociation Widths for Rydberg Transitions in Carbon Monoxide

S. R. Federman, & Y. Sheffer

Department of Physics and Astronomy, University of Toledo, Toledo, OH 43606

steven.federman@utoledo.edu; ysheffer@physics.utoledo.edu

M. Eidelsberg, J. L. Lemaire[1], J. H. Fillion,[1] & F. Rostas

Observatoire de Paris-Meudon, LERMA UMR8112 du CNRS, France

michele.eidelsberg@obspm.fr; jean-louis.lemaire@obspm.fr; Jean-Hugues.fillion@lamap.u-cergy.fr; francois.rostas@obspm.fr

J. Ruiz

Department of Applied Physics I, Universidad de Málaga, 29071-Málaga, Spain

jruiz@uma.es

ABSTRACT

CO is used as a probe of astronomical environments ranging from planetary atmospheres and comets to interstellar clouds and the envelopes surrounding stars near the end of their lives. One of the processes controlling the CO abundance and the ratio of its isotopomers is photodissociation. Accurate oscillator strengths for Rydberg transitions are needed for modeling this process. We present results of recent analyses on absorption from the $E - X$ (1-0), $B - X$ (6-0), $K - X$ (0-0), $L' - X$ (1-0), $L - X$ (0-0), and $W - X$ (ν'-0, $\nu' = 0$ to 3) bands acquired at the high resolution (R $\approx$ 30,000) SU5 beam line at the Super-ACO Synchrotron (Orsay, France). Spectra were obtained for the $^{12}C^{16}O$, $^{13}C^{16}O$, and $^{13}C^{18}O$ isotopomers. Absorption bands were analyzed by synthesizing the profiles with codes developed independently in Meudon and Toledo. Each synthetic spectrum was adjusted to match the experimental one in a non-linear least-squares fitting procedure with the band oscillator strength, the line width (instrumental and predissociation),

[1]Also at Université de Cergy-Pontoise, LERMA UMR8112 du CNRS, France.

and the wavelength offset as free parameters. In order to perform the synthesis, the CO column density was required. Because a differentially pumped cell was used, the measured CO pressure had to be corrected to determine the CO column density. This was accomplished by fitting absorption obtained at the same pressure from the $E-X$ (0-0) band, whose oscillator strength is well known. For the $K-X$, $L'-X$, and $L-X$ bands, the substantial amount of mixing among the upper states was considered in detail. Predissociation widths determined for the $B-X$ band varied widely among isotopomers. For the $W-X$ bands, when possible, J-dependent widths and widths for both e and f parities were extracted from the data. Our results are compared with earlier determinations.

1. Introduction

The interstellar distribution of CO is determined by the interaction of the molecule and the prevailing radiation field. Both photodissociation and self shielding depend on the strength of Rydberg transitions below 1200 Å. Therefore, precise oscillator strengths (f-values) are required for correct modeling of the molecule's distribution in space. Furthermore, the possibility exists that f-values and predissociation widths for Rydberg bands vary among CO isotopomers. The focus of our recent laboratory measurements are on the three species, $^{12}C^{16}O$, $^{13}C^{16}O$, and $^{13}C^{18}O$; the results are described here.

It has been almost 20 years since the first laboratory measurements were available for theoretical models of interstellar CO (Letzelter et al. 1987; Eidelsberg et al. 1991). Later on it became apparent that many f-values of Rydberg bands were underestimated and required renewed laboratory effort (Federman et al. 2001), as well as input from the astronomical front, such as *FUSE* observations (Sheffer et al. 2003). Here we report on the combined effort by our two teams (Toledo and Meudon) to measure a consistent set of f-values, and predissociation widths when possible, for Rydberg bands that will help to improve theoretical predictions (e.g., van Dishoeck & Black 1988; Warin et al. 1996) of the distribution of CO in astronomical environments, such as diffuse clouds. These data will lead to better agreement between measured CO abundances and predictions (Sheffer et al. 2002).

2. Measurements

All our data were collected at the LURE Super-ACO synchrotron ring in Orsay, France, using the SU5 beam line in its high-resolution spectral mode (R in the range 25,000 to 60,000). This is high enough to resolve individual rotational lines in most bands, as well as to assure successful deblending of superposed bands. Our VUV spectra include a selection of Rydberg bands between 925 Å and 1051 Å: $W(3)$, $W(2)$, $W(1)$, $E(6)$, $L(0)$, $L'(1)$, $K(0)$,

$W(0)$, $B(6)$, and $E(1)$, where we use the upper state solely to designate a transition from the ground state, $X(0)$. Each band was observed multiple times under different CO pressures, together with the primary calibrating band $E(0)$ at 1076 Å, which has a well-determined f-value: 0.068(7) according to Federman et al. (2001).

Two independent fitting routines (one in Toledo and one in Meudon) were used to model the data, yielding consistent results at the level of 1% to 2% agreement. We successfully deblended a cluster of 4 Rydberg bands around 968 to 970 Å from the mutually interacting states $K(0)$, $L'(1)$, $L(0)$, and $E(6)$, and determined new f-values for them (Eidelsberg et al. 2004). The results for the other bands were recently submitted for publication (Eidelsberg et al. 2006). The analysis involves the determination of f-values and predissociation widths. The latter allows us to derive predissociation rates for the upper level. For the W states and the $B(6)$ state, the line width is broad enough to be treated as a free parameter in our simulations of the laboratory spectra.

3. Discussion

Our f-values are usually larger than those determined in the earliest studies for $E(1)$, $K(0)$, $L'(1)$, and $L(0)$, but the agreement improves for the more recent laboratory and astronomical results (Chan et al. 1993; Yoshino et al. 1995; Zhong et al. 1997; Sheffer et al. 2003). We attribute the global trend of higher f-values compared to Eidelsberg et al. (1991) to a better treatment of optical depth effects in our simulations. The same may apply to the results of Stark et al. (1991, 1992, 1993). The improved treatment for mixing among the upper levels involved with the $K(0)$, $L'(1)$, $L(0)$, and $E(6)$ transitions (Eidelsberg et al. 2004) is the reason for the remaining differences with Eidelsberg et al. (1991).

For the other bands, the agreement among results is much better. Since the intrinsic line widths for the W and $B(6)$ bands are much broader (faster predissociation rates), optical depths are always small and do not impact the earlier results. As a result, these bands are likely to play a less important role in selective isotope photodissociation. Our suite of f-values and predissociation widths represent the most complete set currently available. When incorporated into theoretical models for CO in astronomical environments, the larger f-values are expected to yield higher photodissociation rates for all isotopomers, as well as increased levels of self shielding for CO whenever it is sufficiently abundant. The increased number of measured predissociation widths will also lead to improved models.

We thank the LURE Super-ACO facility for time allocation, and the SU5 beam team for their help. This work was funded in part by NASA through grant NAG5-11440 and the CNRS-PCMI program.

REFERENCES

Chan, W. F., Cooper, G., & Brion, C. E. 1993, Chem. Phys., 170, 123
Eidelsberg, M., Benayoun, J. J., Viala, Y. P., & Rostas, F. 1991, A&AS, 90, 231
Eidelsberg, M., et al. 2004, A&A, 424, 355
Eidelsberg, M., et al. 2006, submitted to ApJ
Federman, S. R., et al. 2001, ApJS, 134, 133
Letzelter, C., Eidelsberg, M., Rostas, F., Breton, J., & Thieblemont, B. 1987, Chem. Phys., 114, 273
Sheffer, Y., Federman, S. R., & Andersson, B.-G. 2003, ApJ, 597, L29
Sheffer, Y., Federman, S. R., & Lambert, D.L. 2002, ApJ, 572, L95
Stark, G., Smith, P. L., Ito, K., & Yoshino, K. 1992, ApJ, 395, 705
Stark, G., et al. 1993, ApJ, 410, 837
Stark, G., Yoshino, K., Smith, P. L., Ito, K., & Parkinson, W. H. 1991, ApJ, 369, 574
van Dishoeck, E. F., & Black, J. H. 1988, ApJ, 334, 771
Warin, S., Benayoun, J. J., & Viala, Y. P. 1996, A&A, 308, 535
Yoshino, K., et al. 1995, ApJ, 438, 1013
Zhong, Z. P., et al. 1997, Phys. Rev. A, 55, 1799

NASA LAW, February 14-16, 2006, UNLV, Las Vegas

Measurements of Electron Impact Excitation Cross Sections at the Harvard-Smithsonian Center for Astrophysics

L. D. Gardner & J. L. Kohl

Harvard-Smithsonian Center for Astrophysics, Cambridge, MA 02138

lgardner@cfa.harvard.edu, jkohl@cfa.harvard.edu

ABSTRACT

The analysis of absolute spectral line intensities and intensity ratios with spectroscopic diagnostic techniques provides empirical determinations of chemical abundances, electron densities and temperatures in astrophysical objects. Since spectral line intensities and their ratios are controlled by the excitation rate coefficients for the electron temperature of the observed astrophysical structure, it is imperative that one have accurate values for the relevant rate coefficients. Here at the Harvard-Smithsonian Center for Astrophysics, we have been carrying out measurements of electron impact excitation (EIE) for more than 25 years. We will illustrate our experimental approach and apparatus by discussing a measurement of EIE in C^{2+} ($2s2p\ ^3P^o \rightarrow 2p^2\ ^3P$).

1. Introduction

Electron impact excitation (EIE) is the dominant mechanism for the formation of emission lines in many astrophysical and laboratory plasmas. Intensities of spectral lines arising from EIE can provide diagnostics of the temperature and density of an emitting plasma, and of the abundance of elements in the plasma. In the cases where the decay photon comes from a state excited from a metastable state of a particular ion, the ratio of the intensity of this emission to other emission lines from the same ion can provide a valuable density diagnostic for solar plasmas (Keenan & Warren 1993, Orrall & Schmahl 1976), for cool stars (Guinan *et al.* 2003, Jordan *et al.* 2001), and for cataclysmic variable binary systems (Prinja *et al.* 2003). The C^{2+} ($2s2p\ ^3P^o \rightarrow 2p^2\ ^3P$) multiplet at λ 117.6 nm compared to the C^{2+} ($2s^2\ ^1S^o \rightarrow 2s2p^2\ ^1P_1^o$) line at λ 97.7 nm is just such an example. Although density diagnostics require accurate knowledge of the cross section for EIE out of metastable levels, few measurements of such cross sections have been performed (Janzen *et al.* 2003, Bannister *et al.* 1999). Using the unique capabilities of the synchronous photon detection with modulated inclined beams technique, we have carried out the first measurement of the EIE cross section for C^{2+}

($2s2p\ ^3P^o \rightarrow 2p^2\ ^3P$) that covers the energy range required to determine rate coefficients for density diagnostics (Daw *et al.* 2006). We are currently working on measuring the EIE cross section and rate coefficient for C^{2+} ($2s^2\ ^1S^o \rightarrow 2s2p^2\ ^1P^o_1$).

2. Apparatus and Technique

The method used entails the measurement of the absolute intensity of the light emitted from ions excited by electron impact. A carefully prepared beam of C^{2+}, generated in a 5 GHz electron cylotron resonance (ECR) ion source and extracted at 5 kV, is charge/mass and energy/charge analyzed to remove other ions and charge states and then is crossed with an electron beam at 45° (see Figures 2 and 3 in Daw *et al.* 2006). A magnetic field is applied co-axially with the electron beam to constrain it and increase its density. The distributions of current of both beams are measured. Beams are chopped and photons are detected synchronously to enable background subtraction. A mirror below the collision volume subtending slightly over π steradians concentrates photons onto a microchannel plate detector (MCP). The mirror has a broad-band reflectance coating that optimizes the reflectance at the wavelength of the decay photon under study. Calibrations of optical elements are performed separately and, together with a three-dimensional ray-tracing of the complete system, are used to determine the overall absolute photon detection efficiency.

The fraction of C^{2+} ions in the metastable $2s2p\ ^3P^o$ state is determined with the beam attenutation method, which involves measuring the transmitted ion beam current as a function of pressure for a gas admitted to a section of the beamline. Because the electron capture cross section for C^{2+} in He is known to be significantly larger for the metastable state than for the ground state (Lennon *et al.* 1983), we can identify the fraction with the higher attenuation rate as the metastable fraction.

The cross section is determined from experimentally measured quantities via the equation:

$$< \sigma >= \frac{\mathrm{R_{sig}}}{\xi \bar{v}_r} \frac{1}{\int N_I(x,y,z) n_e(x,y,z) \eta(x,y,z,\tau) dx dy dz} \qquad (1)$$

where $\mathrm{R_{sig}}$ is the signal rate, ξ is the fraction of metastable C^{2+} ions, N_I is the ion beam spatial density, n_e is the electron beam spatial density, $\bar{v}_r$ is the average relative velocity, η is the detection efficiency for photons, and τ is the lifetime of the excited state.

3. Electron Impact Excitation Results

Measured energy-averaged EIE cross section for the C^{2+} ($2s2p\ ^3P^\circ \rightarrow 2p^2\ ^3P$) transition are shown in Figure 2. The heavy error bars represent the statistical uncertainty at a 90% confidence level (1.65 σ), and the thin error bars at 12.3 and 18.1 eV represent the total

experimental uncertainty at a 90% confidence level (1.65 σ). Above 16 eV the measured cross section includes small contributions from other states. The dashed blue curve shows the 6-term close-coupling R-matrix calculation of Berrington, *et al.* (1977), and the solid curve shows the 90-term R-matrix with psuedostates calculation of Mitnik, *et al.* (2003) for only the ($2s2p\ ^3P^\circ \rightarrow 2p^2\ ^3P$) transition. Each has been convolved with the experimental energy spread of 0.9 eV (FWHM). The solid red curve shows the sum of the theoretical contributions of all transitions to the weighted cross section, incorporating the calculations of Mitnik *et al.*, and the measured detection efficiencies and metastable fraction. Theory and experiment agree to within the experimental uncertainties. Empirical rate coefficients and effective collision strengths, calculated using the measured EIE cross sections, for temperatures of interest in astrophysics are presented in Daw *et al.* 2006).

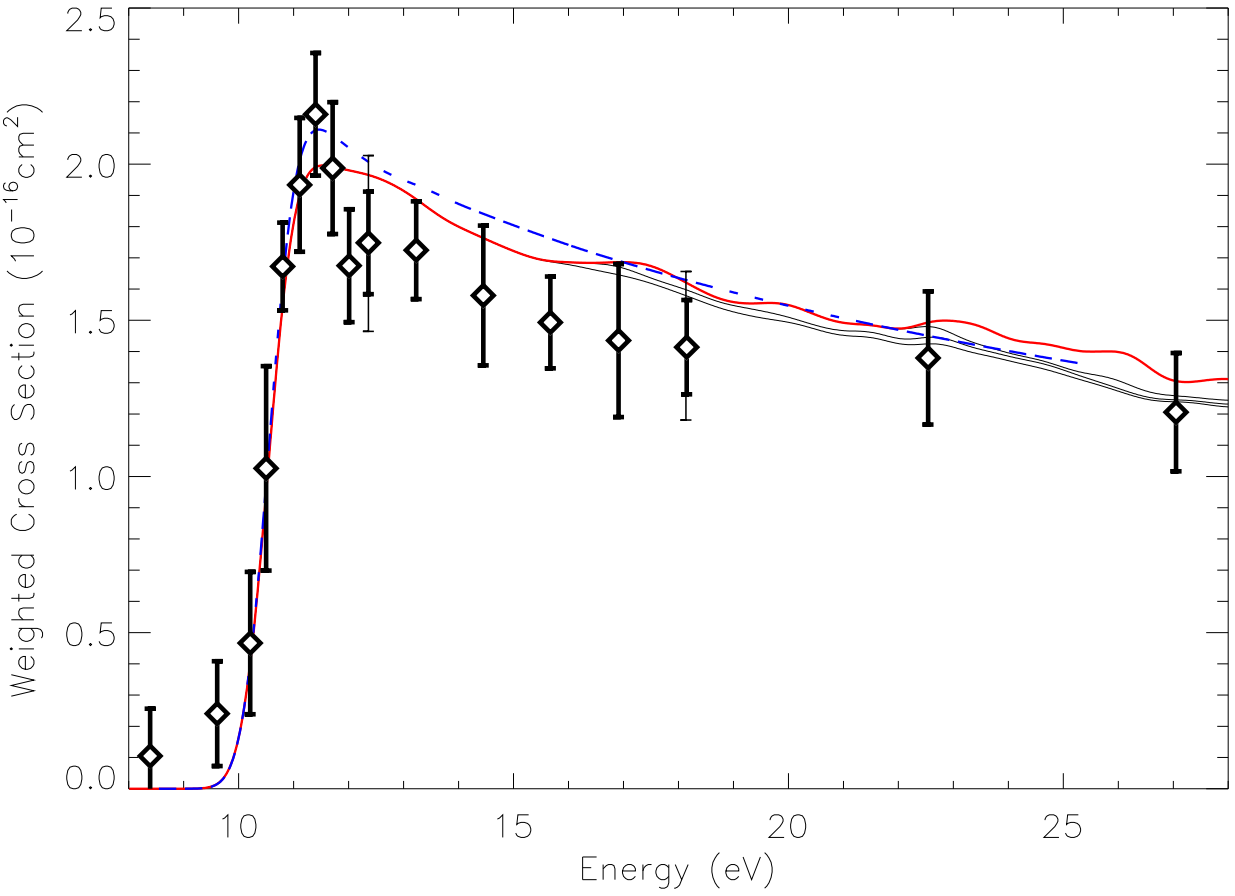

Fig. 1.— Measured energy-averaged EIE cross section for the C^{2+} ($2s2p\ ^3P^\circ \rightarrow 2p^2\ ^3P$) transition. See the text for explanatory information.

4. Summary

We have measured the EIE cross section for the C^{2+} ($2s2p\ ^3P^o \rightarrow 2p^2\ ^3P$) transition from threshold to more than 15 eV above. The photon detection method used in this work uniquely covers the energy range required to provide empirical rate coefficients for solar and stellar UV spectroscopy. We provide measurements of rate coefficients with an absolute uncertainty of typically $\pm$ 8.5 % (1 σ).

This work is supported by NASA Supporting Research and Technology grants NAG5-9516 and NAG5-12863 in Solar and Heliospheric Physics and by the Smithsonian Astrophysical Observatory.

REFERENCES

Bannister, M.E., Djuric, N., Woitke, O., Dunn, G.H., Chung, Y.S., Smith, A.C.H., Wallbank, B., and Berrington, K.A., *Int. J. Mass Spectrom.* **192**, 39 (1999).

Berrington, K.A., Burke, P.G., Dufton, P.L., and Kingston, A. E., *J. Phys. B* **10**, 1465 (1977).

Daw, A., Gardner, L.D., Janzen, P.H., and Kohl, J.L., *Phys. Rev. A* **73**, 032709 (2006).

Guinan, E. F., Ribas, I., and Harper, G. M., *Ap. J.* **594**, 561 (2003).

Janzen, P. H., Gardner, L. D., Reisenfeld, D. B., and Kohl, J. L., *Phys. Rev. A*, **67**, 052702 (2003).

Jordan, C., Sim, S.A., McMurry, A.D., and Aruvel, M. *MNRAS* **326**, 303 (2001).

Keenan, F.P., and Warren, G.A., *Sol. Phys.* **146**, 19 (1993).

Lennon, M., McCullough, R.W., and Gilbody, H.B., *J Phys B*, **16**, 2191 (1983).

Mitnik, D. M., Griffin, D. C., Ballance, C. P., Badnell, N. R., *J Phys B* **36**, 717 (2003).

Orrall, F.Q., and Schmahl, E.J., *Sol. Phys.* **50**, 365 (1976).

Prinja, R.K., Long, K.S.; Froning, C.S., Knigge, C., Witherick, D.K., Clark, J.S., and Ringwald, F.A., *MNRAS* **340**, 551 (2003).

NASA LAW, February 14-16, 2006, UNLV, Las Vegas

Calculation of Atomic Data for NASA Missions

T. W. Gorczyca,[1] K. T. Korista,[1] J. Fu,[1*] D. Nikolić,[1*] M. F. Hasoglu,[1†] I. Dumitriu,[1†]
N. R. Badnell,[2] D. W. Savin,[3] and S. T. Manson[4]

[1]*Department of Physics, Western Michigan University, Kalamazoo, MI 49008-5252*
[2]*Department of Physics, University of Strathclyde, Glasgow, G4 0NG, UK*
[3]*Columbia Astrophysics Laboratory, Columbia University, New York, NY 10027*
[4]*Department of Physics and Astronomy, Georgia State University, Atlanta, GA 30303*
[*]*Postdoctoral Research Associates supported by NASA*
[†]*Graduate Students supported by NASA*

ABSTRACT

The interpretation of cosmic spectra relies on a vast sea of atomic data which are not readily obtainable from analytic expressions or simple calculations. Rather, their evaluation typically requires state-of-the-art atomic physics calculations, with the inclusion of weaker effects (spin-orbit and configuration interactions, relaxation, Auger broadening, etc.), to achieve the level of accuracy needed for use by astrophysicists. Our NASA-supported research program is focused on calculating data for three important atomic processes, 1) dielectronic recombination (DR), 2) inner-shell photoabsorption, and 3) fluorescence and Auger decay of inner-shell vacancy states. Some additional details and examples of our recent findings are given below.

1. Dielectronic Recombination

We have completed the computation of DR rate coefficients, including fitting formula, for all H-like through Na-like ions up to nuclear charge $Z = 30$. For the Fe ions, we are able to benchmark R-matrix and AUTOSTRUCTURE results using storage ring experiments. These data are available electronically at `http://homepages.wmich.edu/~gorczyca/atomicdata` and `http://amdpp.phys.strath.ac.uk/tamoc/DATA/`. Our latest challenging work is for 3^{rd} and 4^{th} row elements where partially filled $n = 3$ and $n = 4$ shells lead to more complicated calculations (relaxation, larger configuration-interaction, etc.)

An example of our latest difficulties when addressing occupation of the $n = 3$ shell is DR of Ne-like Mg III. Figure 1 shows how the computed DR rate coefficients are extremely sensitive to the choice of atomic orbitals, and thus more sophisticated approaches for determining

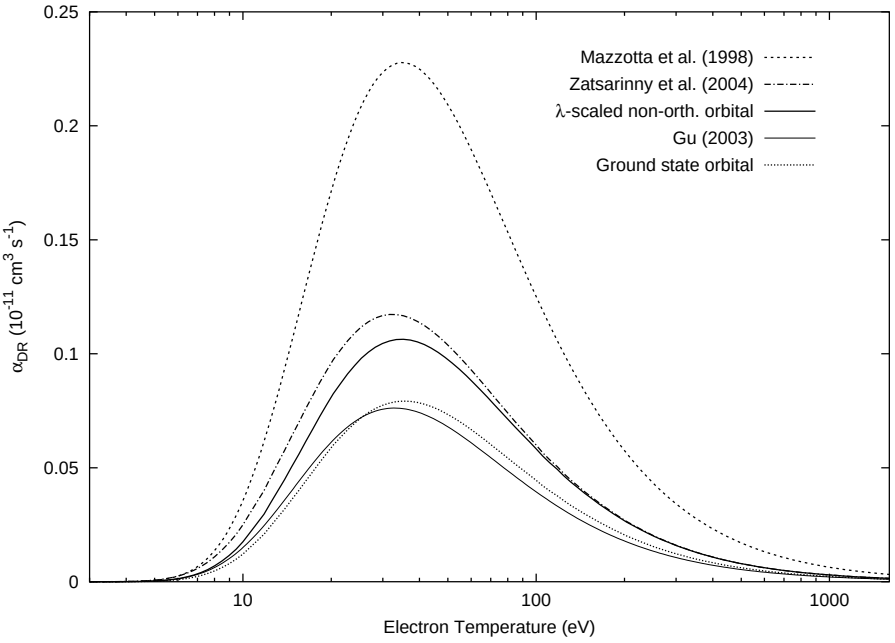

Fig. 1.— Sensitivity of Maxwellian DR rate coefficients to the choice of target orbitals used.

atomic structure is necessary. Our latest calculations utilizing λ-scaled non-orthogonal orbitals resolve a factor of ≈ 2 difference between our earlier results (Zatsarinny et al. 2004) and the results of Gu (2003), and are less than half the recommended data of Mazzotta et al. (1998).

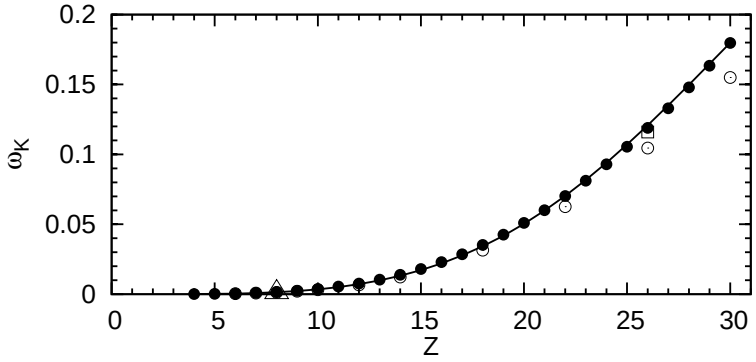

Fig. 2.— Calculated fluorescence yields ω_K^{CI} (solid circles) and fitted formula $\omega_K^{fit} = [1 + (aZ^4 - bZ^7)^{-1}]^{-1}$ (solid line) for K-shell vacancy Li-like $1s2s^2$ ions.

2. K-Shell Fluorescence Yields

We have also calculated new fluorescence yields for all second-row K-shell-vacancy isoelectronic sequences, where the inclusion of higher-order effects (fine structure, configuration interaction, term dependence, etc.) frequently give results (Gorczyca et al. 2003) that differ considerably from the currently recommended data of Kaastra & Mewe (1993). For instance, recent work on the Li-like sequence (Gorczyca et al. 2006) demonstrated the importance of $1s2s^2 + 1s2p^2$ CI: this state cannot radiate in a single-configuration model description. Further, we were able to develop a two-parameter fitting formula for all Z: $\omega_K^{fit} = [1 + (aZ^4 - bZ^7)^{-1}]^{-1}$. These results are shown in Figure 2.

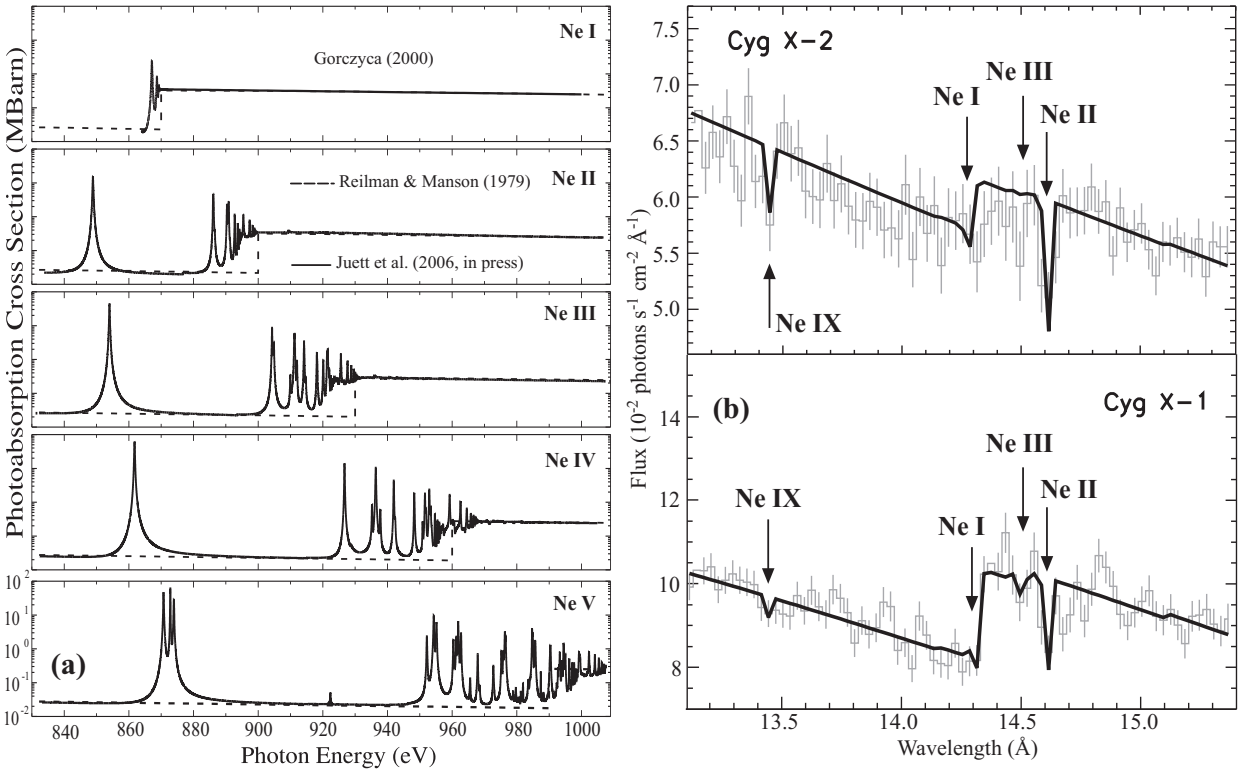

Fig. 3.— (a) Theoretical R-matrix photoabsorption cross sections for neutral neon (Gorczyca 2000) and ionized neon (Juett et al. 2006) compared to independent particle results (Reilman & Manson 1979) which do not include resonances. (b) Using our atomic cross sections $\sigma(\lambda)$, X-ray absorption spectra of the Cygnus black hole X-ray binary were fitted using intensities $I = I_0 e^{-\sigma(\lambda)N}$ to determine elemental abundances (column densities N) by Juett et al. (2006).

3. K-Shell Photoabsorption

We have recently calculated K-shell photoabsorption cross sections for all oxygen and neon ions (see Fig. 3a for neon ions). While results for the neutral O I and Ne I species compare favorably to experimental measurements (Gorczyca & McLaughlin 2000; Gorczyca 2000), our results for ionized oxygen (Garcia et al. 2005) and neon (Juett et al. 2006) are the only complete data available to our knowledge. These newly computed data have already been used to infer elemental abundances in the ISM by Juett et al. (2004, 2006) (see Fig. 3b for neon ion abundances).

This work was supported in part by the NASA APRA program.

REFERENCES

Garcia, J., Mendoza, C., Bautista, M. A., Gorczyca, T. W., Kallman, T. R., & Palmeri, P. 2005, Astrophys. J. Suppl. Ser., 158, 68

Gorczyca, T. W. 2000, Phys. Rev. A, 61, 024702

Gorczyca, T. W., & McLaughlin, B. M. 2000, J. Phys. B, 33, L859

Gorczyca, T. W., Kodituwakku, C. N., Korista, K. T., Zatsarinny, O., Badnell, N. R., Behar, E., Chen, M. H., & Savin, D. W. 2003, Astrophys. J., 592, 636

Gorczyca, T. W., Dumitriu, I., Hasoglu, M. F., Korista, K. T., Badnell, N. R., Savin, D. W., & Manson, S. T. 2006, Astrophys. J., 638, L121

Gu, M. F. 2003, ApJ, 590, 1131

Juett, A. M., Schulz, N. S., & Chakrabarty, D. 2004, Astrophys. J., 612, 308

Juett, A. M., Schulz, N. S., Chakrabarty, D., & Gorczyca, T. W. 2006, Astrophys. J., in press

Kaastra, J. S., & Mewe, R. 1993, Astron. Astrophys. Suppl. Ser., 97, 443

Mazzotta, P., Mazzitelli, G., Colafrancesco, S. & Vittorio, N. 1998, Astron. Astrophys. Suppl. Ser., 133, 403

Reilman, R. F., & Manson, S. T. 1979, Astron. Astrophys. Suppl. Ser., 40, 815

Zatsarinny, O., Gorczyca, T. W., Korista, K., Badnell, N. R., & Savin, D. W. 2004, Astron. Astrophys., 426, 699

NASA LAW, February 14-16, 2006, UNLV, Las Vegas

The Homunculus: a Unique Astrophysical Laboratory

T. R. Gull & K. E. Nielsen[1]

NASA Goddard Space Flight Center, Code 667, Greenbelt, MD 20771

gull@milkyway.gsfc.nasa.gov, nielsen@milkyway.gsfc.nasa.gov

ABSTRACT

η Car is surrounded by bipolar shells, the Homunculus and the internal Little Homunculus, that are observed in both emission and absorption. Thin disks, located between the bipolar lobes, include the very bright Weigelt blobs and the neutral emission structure called the Strontium filament. All are affected by changes in UV and X-Ray flux of the binary system. For example, the normally ionized Little Homunculus recombines during the few month long spectroscopic minimum and then reionizes. Spectral data, obtained with *Hubble Space Telescope*/ Space Telescope Imaging Spectrograph (*HST*/STIS) and with *Very Large Telescope*/ UltraViolet Echelle Spectrograph (*VLT*/UVES), provide a wealth of information on spectroscopic properties of neutral and singly-ionized metals and on chemistry of nitrogen rich, carbon, oxygen poor, dense, warm gas. This information is important to understand gamma ray bursters (GRB) that reveal red-shifted near-UV metallic absorptions from pre-GRB stellar ejecta.

1. Introduction

The high spatial resolution of *HST*, combined with appropriate spectral resolutions of the STIS, has been utilized to: 1) Pull out the geometry of the expanding bi-lobed structures. Based upon the infrared emission from the Homunculus and a 100:1 gas-to-dust ratio, the Homunculus, a neutral, dusty hourglass-shaped shell ejected in the 1840s, has at least 10 $M_\odot$ of material (Smith et al. 2003). 2) Discover the Little Homunculus, an internal ionized, bipolar shell associated with an event in the 1890s. 3) Separate of the stellar spectrum from the very bright narrow-lined emission Weigelt blobs located 0.″1–0.″3 from the star. 4) Discover the Strontium Filament, an unusual neutral emission nebulosity, photoexcited by radiation filtered by Fe II (<7.9eV). 5) Characterize temporal variations of these structures

[1]Catholic University of America, Washington, DC 20064

imposed by the binary interaction of massive stars and their winds.

The 5.54-year periodicity of η Car was first noted by Damineli (1996) through the time variability of [Ne III], [Ar III], He I narrow nebular emission lines. This led to monitoring of the object with the *Rossi X-Ray Timing Explorer* (Corcoran 2005) and coordinated observations with, for example, *HST*/STIS and *VLT*/UVES . The evidence abounds that η Car is a massive binary system composed of a 15,000 K/100 $M_\odot$ primary stars and a 35,000K secondary star. The hot companion is in a highly elliptical orbit, penetrating the extended primary star's atmosphere during periastron. For several months, the Lyman radiation from the binary system is trapped. Ejecta will during this short period of time recombine and cool. This period is defined as η Car's spectroscopic minimum.

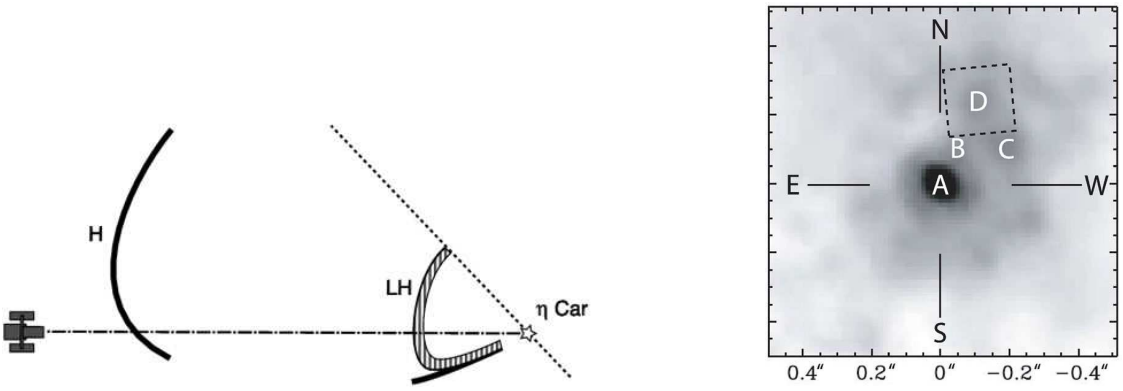

Fig. 1.— Left: We see η Car through two major expanding shells, the Homunculus (H) and the Little Homunculus (LH), that change in ionization and temperature as the UV radiation is modulated by the massive central binary system. Right: The central 1″ region, imaged by *HST*, shows beads on a necklace surrounding the central source. Three beads to the upper right, labeled B, C, and D, are the bright emission line Weigelt blobs.

2. Abundances

International Ultraviolet Explorer and ground based observations in the 1980s (Davidson et al. 1986) demonstrated an overabundance of nitrogen and helium. More recently, Meynet & Maeder (2003) suggested that massive stars late in their CNO-cycle, due to mixing, tend to have an overabundance in nitrogen, while carbon and oxygen are nearly 100-fold depleted. Analysis of the Weigelt blob spectra (Verner, Bruhweiler & Gull 2005) confirmed this abundance pattern. Recently, Bautista et al. (2006) found that Ti/Ni is 80×solar for the Strontium Filament.

Near and Far UV STIS echelle observations have revealed thousands of narrow absorption lines originating in the expanding bipolar shells. Spectra of molecules, neutral and singly ionized iron-group elements at velocity −513 km s^{-1} are associated with the Homunculus. Its level populations correspond to thermal temperatures of 760 K and a density $>10^6$ cm^{-3}.

Spectral lines in mainly singly ionized iron-group elements at -146 km s^{-1} are associated with the Little Homunculus and characterize a 6400 K gas with a density of 10^{6-8} cm^{-3}.

3. The Astrophysical Laboratory

The nitrogen rich, carbon, oxygen poor ejecta are unique. We know their origin, their source of excitation, and have a means of measuring temperatures and modeling densities. Observations with the *Far Ultraviolet Spectroscopic Explorer* (*FUSE*) (Iping et al. 2005) and *HST*/STIS (Hillier et al. 2006), leading up to the 2003.5 spectroscopic minimum, confirmed the disappearance of FUV radiation. The -146 km s^{-1} (Little Homunculus) Fe II level populations dropped from 6400 K to 5000 K, then nine months later returned to 6400 K. Strong Ti II absorptions (IP 13.58eV) appeared and disappeared confirming Lyman continuum interruption (Gull et al. 2006). The -513 km s^{-1} (Homunculus) Ti II, and other species, level populations did not change indicating the atomic temperature remained at 760 K. However, the nearly 1000 H2 absorptions extending up to 1600 Å (Nielsen et al. 2006) abruptly disappeared, the much weaker CH and OH absorptions weakened. CH and OH level populations are consistent with 60K (Verner et al. 2005), and H_2 temperatures appear to be about 150 K (N.Smith, priv comm). Recent high-dispersion visible and IR GRB spectra (Chen et al. 2005; Prochaska et al. 2006) revealed multiple lines of Fe II originating from warm circum-protoGRB gas. Temperatures similar to those measured in the Homunculus were derived. While very different abundances and chemistry, the analog of η Car ejecta will provide much insight to protoGRB environments.

Oxygen and carbon are grossly deficient leading to many metals being trapped in gaseous phase as they cannot form oxides. Further evidence indicates that the ejecta dust is composed of silicates and alumina. Given the metals trapped in gas phase, we suggest that the gas-to-dust ratio is significantly greater than 100, which leads to an even greater mass loss estimate. Metal abundances in the ejecta and models of environments with chemical composition observed in the η Car ejecta, are needed.

4. Conclusion

Much is to be learned about ejecta of massive stars, especially in the late stages of the CNO-cycle. The major changes in excitation by the UV fluxes of η Car provide insight to the physics of this circumstellar gas. Testing the models provides feedback to atomic spectroscopy, especially wavelengths, relative transition probabilites and metastable level lifetimes measurable in this astrophysical laboratory: η Car's ejecta.

This work was supported by STIS GTO and Space Telescope Science Institute (STScI) grants 9420 and 9973. Observations were done with the *HST* through STScI and with the

VLT/UVES through European Southern Observatory.

REFERENCES

Bautista, M. et al. 2006 MNRAS submitted
Chen et al. 2005 ApJ 634, L25
Corcoran, M. 2005 AJ 129, 2018
Damineli, A. 1996 ApJ 460, L49
Davidson, K. et al. 1986 ApJ 305, 867
Gull, T., Kober, G. & Nielsen, K. 2006 March ApJS
Hillier, D.J. et al. 2006 March ApJ
Iping, R. et al. 2005 ApJ 633, L37
Nielsen, K. E., Gull, T. R. & Kober, G. V. 2006, ApJS 157, 138
Meynet, & Maeder 2003 A&A 404, 975
Prochaska et al. 2006 Astroph 060157
Smith, N. et al. 2003 AJ 125, 1458
Verner, E., Bruhweiler, F. & Gull, T. 2005 ApJ 624, 973
Verner, E. et al. 2005, ApJ 629, 1034

NASA LAW, February 14-16, 2006, UNLV, Las Vegas

Laboratory astrophysics on ASDEX Upgrade: Measurements and analysis of K-shell O, F, and Ne spectra in the $9 - 20$ Å region

S. B. Hansen & K. B. Fournier

Lawrence Livermore National Laboratory, Livermore, CA, 94550

M. J. Finkenthal & R. Smith[1]

Plasma Spectroscopy Group, The Johns Hopkins University, Baltimore, MD 21218

T. Pütterich, R. Neu, & ASDEX Upgrade Team

Max-Planck-Institut für Plasmaphysik, EURATOM Association, D-85748 Garching, Germany

ABSTRACT

High-resolution measurements of K-shell emission from O, F, and Ne have been performed at the ASDEX Upgrade tokamak in Garching, Germany. Independently measured temperature and density profiles of the plasma provide a unique test bed for model validation. We present comparisons of measured spectra with calculations based on transport and collisional-radiative models and discuss the reliability of commonly used diagnostic line ratios.

1. Introduction

Ratios of K-shell emission lines are commonly used to diagnose temperatures (T_e) and densities (n_e) of astrophysical plasmas. While simple line ratios can give quick estimates of uniform plasma conditions, they may have limited utility for diagnosing integrated spectral measurements from plasmas with gradients or non-equilibrium ion distributions. With modern simulation capabilities and independent laboratory diagnostics, tokamaks can help validate sophisticated models for complex, astrophysically relevant plasma environments. We have modeled K-shell emission spectra from an H-mode discharge of the ASDEX Upgrade tokamak using the transport code STRAHL, which predicts ion distributions accounting for

[1]NASA/GSFC

transport processes, and the collisional-radiative code SCRAM, which uses these ion distributions to create synthetic spectra. The agreement of synthetic and experimental spectra is quite good, demonstrating the value of tokamak data as a benchmark for laboratory astrophysics. Comparisons of simple line ratios from two independent atomic models, SCRAM and ATOMDB, are also presented and their utility as diagnostics for complex plasmas is discussed.

2. ASDEX Upgrade data and models: benchmark comparison

The ASDEX Upgrade device at the Max-Planck Institute für Plasmaphysik is a midsized tokamak divertor tokamak with a major radius of $R = 1.65$ m and a poloidal radius of $a = 0.5$ m [Herrmann and Gruber (2003)]. The plasma can reach temperatures up to 4 keV and densities near 10^{14}cm^{-3} at its center. Radial profiles of n_e and T_e are obtained by interferometers, analysis of the excitation profiles of a radial lithium beam, Thomson scattering (VTA), and measurements of electron cyclotron emissions (ECE) – see Fig. 1. Spectral emission in the $9 - 20$ Å region is collected using a Bragg crystal spectrometer [Bolshukhin et al. (2001)].

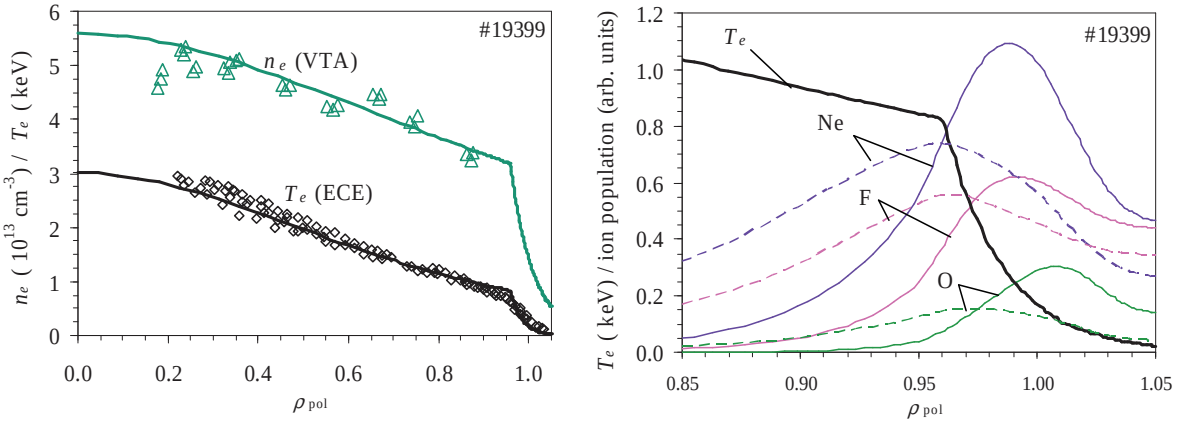

Fig. 1.— Left: measured n_e and T_e along the poloidal axis. Right: He-like (solid) and H-like (dashed) ion populations from STRAHL in the radiating region $\rho_{pol} = 0.85 - 1.05$.

Since in the hot center of the plasma, O, F, and Ne atoms are fully stripped, the measured emission from H- and He-like O, F, and Ne ions originates from the edge region of the plasma. The local distributions of these impurity ions in the edge region are strongly influenced by plasma transport, which shifts emitting ions to regions of higher T_e than they would be found in a transportless equilibrium. The STRAHL program quantifies this deviation from equilibrium. Following previous investigations on the transport parameters of ASDEX Upgrade plasmas [Dux (2003)], and using typical diffusion coefficient profiles (0.5 to

2.0 m^2/s) and drift velocity profiles (time averaged values with a maximum inward drift velocity of 8 m/s at a narrow radial region) along with the measured T_e and n_e profiles, STRAHL combines plasma transport with the rate equations for ionization and recombination of impurity ions to predict the non-equilibrium charge state distribution. The steady-state of the impurity distribution was found by taking a constant impurity source for constant plasma conditions. Figure 1 shows the measured T_e and n_e profiles and the resultant relative populations of H- and He-like ions for the three impurity elements. We note that predictions for the radial position of abundance maxima involve considerable uncertainties at the edge of a tokamak plasma, where gradients of plasma and transport parameters change dramatically within a few cm. However, because the line of sight is performing a radial integral, variations in these parameters within the uncertainties do not change the basic results of the modeling.

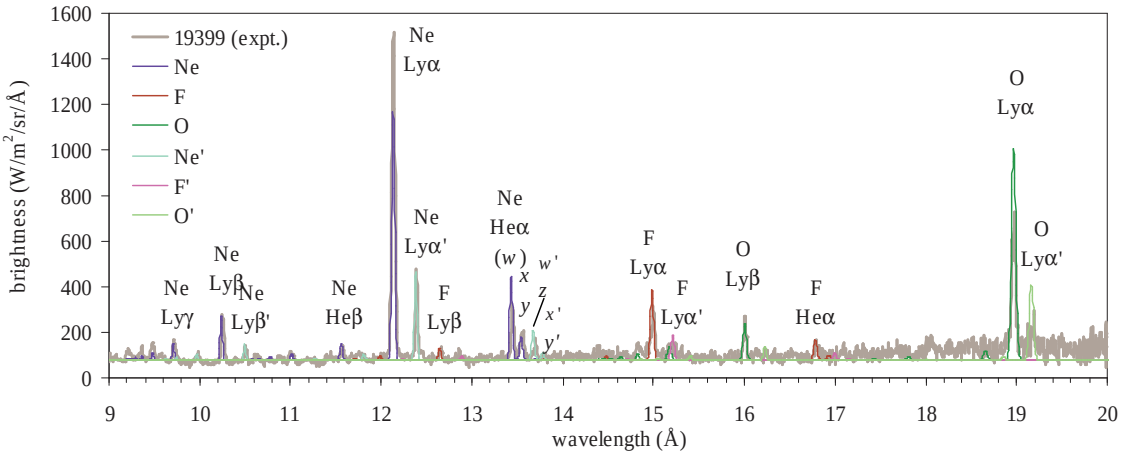

Fig. 2.— Comparison of modeled and experimental spectra for the H-mode shot 19399. Lines marked with ′ are spectrometer artefacts. High-intensity lines may be saturated.

Once STRAHL has determined ion distributions, we generate synthetic spectra using the collisional-radiative kinetics model SCRAM [Hansen (2003)]. SCRAM is based on data from the Flexible Atomic Code FAC [Gu (2003)] and includes all collisional and spontaneous processes among and between ions. The models for Ne, F, and O include singly excited states up to $n = 10$ in H- and He-like ions and $n = 6$ in Li- and Be-like ions, and doubly excited states up to $n = 4$ in He-, Li- and Be-like ions. Collisional ionization rates were modified to enforce the transport-influenced ion distributions given by STRAHL while retaining the accuracy of a full collisional-radiative treatment. The final spectrum, generated by integrating emission along the spectrometer line of sight, agrees quite well with the experimental data, as shown in Fig. 2.

3. Equilibrium line ratios and model comparison

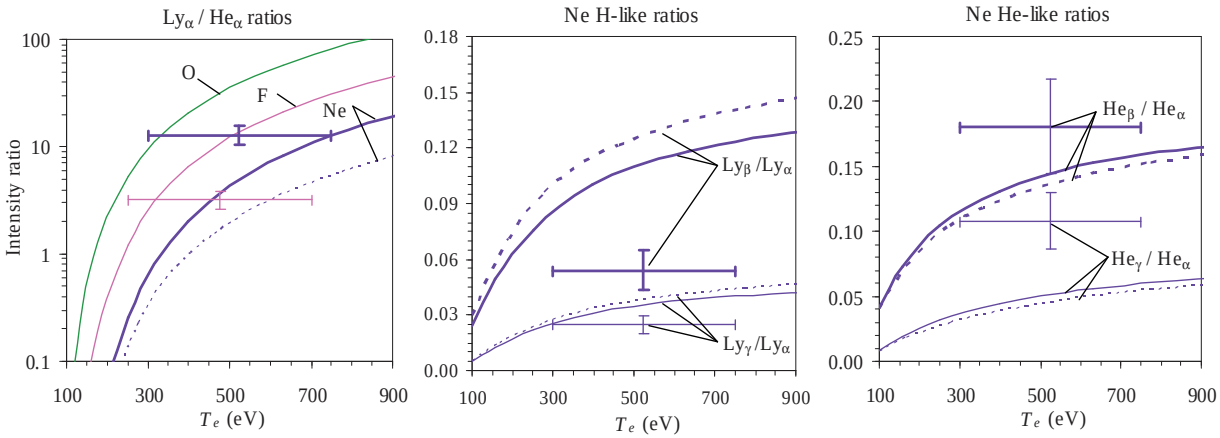

Fig. 3.— T_e-dependent $\mathrm{Ly}_\alpha/\mathrm{He}_\alpha$ ratios for O, F, and Ne ions with equilibrium ion distributions from SCRAM (solid) and ATOMDB (dashed). Error bars on the experimental points indicate the T_e range separating STRAHL predictions for H- and He-like abundance maxima.

Figure 3 shows equilibrium T_e-dependent diagnostic line ratios from independent collisional-radiative models SCRAM and ATOMDB [Smith (2001)]. While the T_e values diagnosed using experimental $\mathrm{Ly}_\alpha/\mathrm{He}_\alpha$ ratios would at least fall within the measured T_e range, the intra-ion ratios are of little diagnostic utility due to the strong temperature gradient. The collisional excitation rates of the two models agree to within 15% in the given temperature range; this agreement is reflected in the given intra-ion ratios. The disagreement between SCRAM and ATOMDB for the $\mathrm{Ly}_\alpha/\mathrm{He}_\alpha$ ratio is mostly due to differences in the model predictions for the ionization distribution.

REFERENCES

Bolshukhin, D. et al. 2001, Rev. Scientific Instruments, 72, 4115
Dux, R., 2003 Fusion Science and Technology 44, 708
Gu, M. F. Gu, 2003 Ap. J. 590, 1131; *ibid* 582, 1241
Hansen, S. B. 2003, PhD Dissertation, University of Nevada, Reno
Herrmann, A. and Gruber, O., 2003 Fusion Science and Technology 44, 569
Smith, R. K. et al. 2001, Ap. J. L., 556, 91

NASA LAW, February 14-16, 2006, UNLV, Las Vegas

Critical Evaluation of Chemical Reaction Rates and Collision Cross Sections of Importance in the Earth's Upper Atmosphere and the Atmospheres of Other Planets, Moons, and Comets

D. L. Huestis

Molecular Physics Laboratory, SRI International, Menlo Park, CA 94025

david.huestis@sri.com

ABSTRACT

We propose to establish a long-term program of critical evaluation by domain experts of the rates and cross sections for atomic and molecular processes that are needed for understanding and modeling the atmospheres in the solar system. We envision data products resembling those of the JPL/NASA Panel for Data Evaluation and the similar efforts of the international combustion modeling community funded by US DoE and its European counterpart.

1. The Need for Critical Evaluation

Modelers in all disciplines prefer that the underlying physical and chemical parameter values in their models, the "material properties," would be accurately known in advance and accessible from a computer-readable on-line database of "trusted" values. What is needed is not just a list of processes and numbers (i.e. a "database"), but also documentation of serious critical evaluation of the available information and specific statements from independent expert laboratory/theory data providers about what should be believed, what uncertainty to assign, and what is most in need of redetermination.

2. Topic Areas

1. Chemical reactions of neutral atoms and molecules in their ground electronic states
2. Ion-molecule reactions
3. Chemistry, relaxation, and radiation of electronically excited atoms and molecules
4. Vibrational and rotational relaxation and radiation

5. Photoabsorption, photodissociation, and photoionization

6. Electron-impact excitation, dissociation, ionization, and recombination

7. Energetic heavy particle excitation and charge exchange

We envision a gradual progression through the most important microscopic processes in each of the Topic Areas, making maximum use of existing and forthcoming evaluations, reviews, tabulations, and databases. The process should be ongoing, to keep up with developments in the laboratory and to tackle newly discovered needs.

3. Evaluation Example in Topic 2: Ion-Molecule Reactions $H^+ + H_2$ Ion-Molecule Reactions in the Ionospheres of the Outer Planets

For the past 30 years, models of outer planet ionospheres have used estimated rate coefficients for charge transfer Reaction (1), which is a critical step in controlling the electron density. No confirmation has been available from the laboratory or theory.

$$H^+ + H_2(v \geq 4) \quad \rightarrow \quad H + H_2^+ \tag{1}$$

By analysis and extrapolation of the results from recent theoretical work from the plasma fusion community we suggest that Reaction (1) has a rate coefficient of approximately 1.3×10^{-9} cm^3/s, consistent with numbers in current models. In addition we suggest that vibrational relaxation Reaction (2) will also be fast, with rate coefficients of approximately 1.5×10^{-9} cm^3/s for v = 4–8 and 2.8×10^{-9} cm^3/s for v = 1–3. Inclusion of Reaction (2) will significantly reduce calculated vibrational temperatures in ionospheric models. New quantum dynamics calculations are needed.

$$H^+ + H_2(v_i) \quad \rightarrow \quad H^+ + H_2(v_f < v_i) \tag{2}$$

4. Evaluation Example in Topic 3: Kinetics of Excited Electronic States Rates and Products of Collisional Relaxation of $O_2(a\,^1\Delta_g)$ and $O_2(b\,^1\Sigma_g^+)$

The low-lying excited states of molecular oxygen, $O_2(a\,^1\Delta_g)$ and $O_2(b\,^1\Sigma_g^+)$, are produced directly or indirectly after absorption of ultraviolet solar radiation in the atmospheres of Venus, Earth, and Mars. At high altitudes, both are weakly quenched and produce strong airglow emission at 1270 nm (Venus, Earth, and Mars) and 762 nm (Earth), respectively. At

lower altitudes collisional relaxation produces vibrationally excited oxygen molecules in the ground electronic state, which can result in observable infrared emission after vibrational energy transfer to H_2O or CO_2.

Analysis of published kinetics experiments in gaseous and liquid, normal and isotopic oxygen, with or without added nitrogen, allows us to construct functional forms for the temperature dependence of the relaxation rates. In addition, the reactions below illustrate the conclusion relaxation of $O_2(a\,^1\Delta_g)$ and $O_2(b\,^1\Sigma_g^+)$ eventually produces 5 and 8 vibrational quanta, respectively.

$$O_2(b\,^1\Sigma_g^+, v = 0) + O_2(X\,^3\Sigma_g^-, v = 0) \rightarrow O_2(a\,^1\Delta_g, v') + O_2(X\,^3\Sigma_g^-, 3 - v') \quad (3)$$

$$O_2(b\,^1\Sigma_g^+, v = 0) + N_2(v = 0) \rightarrow O_2(a\,^1\Delta_g, v = 2) + N_2(v = 1) \quad (4)$$

$$O_2(a\,^1\Delta_g, v = 0) + O_2(X\,^3\Sigma_g^-, v = 0) \rightarrow O_2(X\,^3\Sigma_g^-, v') + O_2(X\,^3\Sigma_g^-, 5 - v') \quad (5)$$

5. Evaluation Example in Topic 4: Vibrational and Rotational Relaxation and Radiation Vibrational Energy Transfer and Relaxation in O_2 and H_2O

Vibrational energy transfer from oxygen molecules to water molecules helps control the local temperature in the mesosphere through radiative cooling. The reactions in question are

$$O_2(1) + O_2(0) \rightarrow O_2(0) + O_2(0) \quad (6)$$

$$O_2(1) + H_2O(000) \rightarrow O_2(0) + H_2O(000) \quad (7)$$

$$O_2(1) + H_2O(000) \leftrightarrow O_2(0) + H_2O(010) \quad (8)$$

$$H_2O(010) + H_2O(000) \rightarrow H_2O(000) + H_2O(000) \quad (9)$$

$$H_2O(010) + O_2(0) \rightarrow H_2O(000) + O_2(0) \quad (10)$$

The chemical kinetics literature provides reliable values for the rates of Reactions (6) and (9) and strong evidence that Reactions (7) and (10) are slow in comparison with Reaction (8). Our analytical solution to the chemical reaction system above shows that the rate of Reaction

(8) can only be measured with water mole fractions higher than 1%. The only measurement that satisfies this requirement is reported in a Ph.D. thesis and a conference presentation from the combustion community. Reanalysis of that data yields our recommended value of $(5.5 \pm 0.4) \times 10^{-13}$ cm^3/s, between the values favored by the atmospheric and laser modeling communities.

6. Evaluation Example in Topic 5: Photoabsorption, Photodissociation, and Photoionization Cross Sections and Yields of O(^{1}S) and O(^{1}D) in Photodissociation of H_2O and CO_2

A number of observers have used the relative strengths of the oxygen O(^{1}S $\rightarrow$ ^{1}D) *green* and O(^{1}D $\rightarrow$ ^{3}P) *red* lines make inferences about cometary composition. The key questions are the yields of O(^{1}S) and O(^{1}D) in photodissociation of H_2O and CO_2 by solar radiation. We find that the secondary references used by the cometary community are not mutually consistent and not sufficiently detailed about how the yields were derived from convolution of the solar spectrum with photodissociation yield spectra. After a careful review of the laboratory literature we have concluded that

1. Production of O(^{1}S) by photodissociation of H_2O has never been reported in the laboratory literature. In fact, no experiment has been attempted that could have detected production of O(^{1}S). Thus there is no experimental basis for an estimate of its yield.

2. The situation is almost reversed for photodissociation of CO_2. The yield of O(^{1}S) has been measured in a number of studies to approach unity in a narrow wavelength window around 112.5 nm. The yield of O(^{1}D) has never been measured (very difficult because of rapid quenching). However, all photochemists believe that it is the primary product over much of the absorption spectrum.

3. Additional experimental yield determinations are needed with high spectral resolution.

NASA LAW, February 14-16, 2006, UNLV, Las Vegas

Mestastable State Population in Laser Induced Plasmas

V. H. S. Kwong, C. Kyriakides, & W. K. Ward

Department of Physics, University of Nevada Las Vegas, Las Vegas, NV 89154

vhs@physics.unlv.edu, athos@physics.unlv.edu, wward@physics.unlv.edu

ABSTRACT

Laser induced plasma has been used as a source of neutrals and ions in the study of astrophysical plasmas. The purity of state of this source is essential in the determination of collision parameters such as the charge transfer rate coefficients between ions and neutrals. We will show that the temperature of the laser induced plasma is a rapidly decreasing function of time. The temperature is initially high but cools off rapidly through collisions with the expanding plasma electrons as the plasma recombines and streams into the vacuum. This rapid expansion of the plasma, similar to a supersonic jet, drastically lowers the internal energy of the neutrals and ions.

1. Introduction

Laser induced plasma has been used as a source of neutrals and ions. The purity of state of this source is essential to the measurement of collision parameters such as the charge transfer rate coefficients between ions and neutrals that are used in the modeling of astrophysical plasmas. We will address the purity of state by reviewing theoretical and experimental evidence on the expansion dynamics of laser induced plasmas. Furthermore, we will also examine several pieces of experimental evidence available to us that can review the metastable fractions in both the neutrals and ions in the laser ablation source.

2. Charge transfer of O^{2+}, C^{2+} and H_2

Laser induced plasma was used as an ion source for O^{2+} in the measurement of the charge transfer rate coefficient for O^{2+} ions and H_2 in an ion trap (Fang and Kwong 1995). O^{2+}, however, has several low lying metastable states. The $2p^2\ ^1D$ metastable state, for example, is 2.5 eV above the $2p^2\ ^3P$ ground state. The mean lifetime of this state is 37s, which is much longer than the storage time during the measurement. Significant amounts of

the metastable ion, if they are present in the laser induced plasma, can also be stored in the trap and react with the H_2 target gas. The measured rate coefficient can therefore reflect the convolution of two independent charge transfer processes involving the ground state and the metastable state O^{2+} ions. The contribution of the metastable state ions can be assessed by comparing our measurement with the known charge transfer rate coefficients of the ground state and the metastable state.

The ground state and the metastable state rate coefficients have been measured by Church and Holzscheiter (1989). Their rate coefficients are 1.71 ± 0.15 x 10^{-9} and 9.6 ± 0.6 x 10^{-9} for the $2p^2\ ^3P$ ground state and the $2p^2\ ^1D$ metastable state respectively. Our measured charge transfer rate coefficient of 2.36 ± 0.22 x 10^{-9} is within 30% of the measured value for the $2p^2\ ^3P$ ground state. This suggests that the ions produced by laser ablation and stored in the trap are mainly in the ground state.

In the charge transfer cross section measurement of C^{2+} and H_2 with a reflection time of flight mass spectrometer, we examined the metastable content of the laser ablation ion source 20μs after the ions were produced. Metastable state ions with lifetimes greater than 20μs can be present in significant amounts since the electron temperature of the laser induced plasma is expected to be very high during laser ablation.

C^{2+} has low lying $2s2p\ ^3P_{0,1,2}$ metastable states with energy $\leq$ 6.5 eV above the ground state. These low lying metastable states have a charge transfer cross section about 6 times larger than that of the ground state (Unterreiter et al. 1991). The $2s2p\ ^3P_1$ metastable state lifetime was measured to be 8.26ms (Kwong et al. 1993) and the $2s2p\ ^3P_{0,2}$ metastable states lifetimes are 10^4 times longer. If these metastable state ions are present, changing the population ratio between the metastable state and the ground state will alter the measured cross section significantly. The mean electron temperature of the laser induced plasma is raised from 9 eV to 12 eV by increasing the energy of the ablation laser from 10 mJ to 20 mJ. The estimated population ratio of the metastable state to the ground state should increase from 0.5% to 1.9% (Wang 1997). Because of that change in ratio, one would expect to see the observed charge transf er cross section increase by as much as 60%. Our measured cross section, however, remains unchanged (6.90 ± 0.78 x 10^{-16} cm^{-2}) within the experimental uncertainty (see Fig.1). This suggests that the internal temperature of the laser ablation ions must be cold and the metastable ion fractions in the beam are negligibly small (Wang and Kwong 1997).

3. Expansion dynamics of metastable fractions in laser induced plasmas

This unique characteristic of low metastable fractions in both neutrals and ions in the laser induced plasma can be explained by the cooling of plasma electrons in the rapidly expanding plasma (Rumsby and Paul 1974). During laser ablation, a hot and high density plasma is formed and expands rapidly into the vacuum. The estimated initial density is

$\approx 10^{21}$ cm^{-3}. At such a high density, the collision time between ions and electrons is orders of magnitude shorter than the laser pulse. Local thermodynamic equilibrium is established within the time duration of the laser pulse. The temperature of the plasma has been estimated to be in excess of 10^5 K (Kwong 1979). At such a high temperature, we can safely assume complete dissociation and ionization of the material inside the ablation plume.

The internal temperature of the atomic and ionic species, however, is closely coupled to the temperature of the plasma electrons through rapid collision. Three body and radiative recombination occur with the formation of neutral atoms from plasma ions. As the temperature of the plasma electrons drops, their initial energy is converted into directed energy of expansion. The internal temperature of the atomic and ionic species follows and decreases as well. The time dependence of the electron density, n_e , and electron temperature, T_e , is proportional to t^{-3} and t^{-1} respectively (Rumsby and Paul 1974). Therefore the internal temperature of the atomic and ionic species freezes out when n_e drops below the threshold density to maintain collision equilibrium.

This rapid decrease of electron temperature in a laser induced plasma has been demonstrated by Drewell (1979) in plasma diagnostic experiments seeded with neutral Cr. In Drewell's experiment, Cr plasma was produced through laser ablation of a pure Cr target. The population ratio between the a^5S_2 metastable state and the a^7S_3 ground state of neutral Cr was measured by the intensity ratio of the laser induced fluorescence linked to these states. The a^5S_2 metastable state and the a^7S_3 ground state have an energy difference of 0.94 eV. The time dependence of the population ratio is shown in Figure 2 (Drewell, 1979). The population ratio freezes out 4μs after laser ablation. This ratio is $\approx 10^{-3}$, which gives a freeze-out temperature of $\approx$1000K.

4. Conclusion

Since the power density of the ablation laser used in our measurement is similar to that used by Drewell (1979), we expect that the internal temperature of the ions and neutrals in our laser ablation ion source to be similar. At this low temperature, it is highly unlikely that the metastable state atoms with energy greater than 1 eV above the ground state will be present in a measurable quantity in the pulsed atom or ion beam. This is consistent with all our measured rate coefficients and cross sections which correspond to the ground state. On the other hand, the freeze-out temperature of the plasma electron ($\approx$1000 K) limits the purity of state of stored ions and neutrals with low lying metastable states $\leq$ 0.4eV above the ground state.

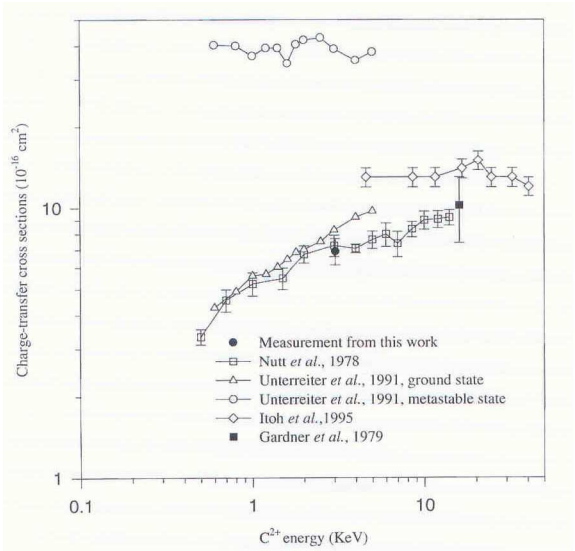

FIG. 1. Single electron charge-transfer cross sections for $C^{2+} + H_2$ at low energies reported by several research groups.

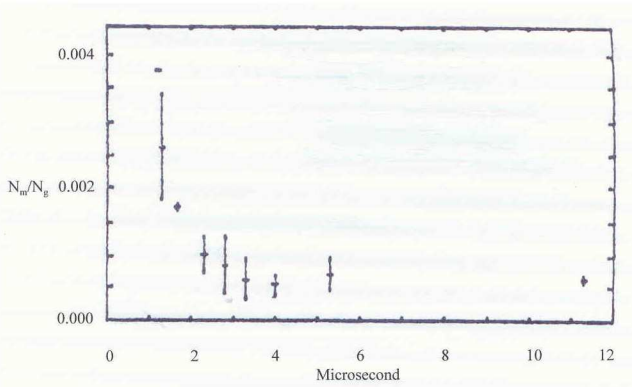

Fig. 2. Population ratio between the a^5S_2 metastable state and the a^7S_3 ground state of neutral chromium in laser produced plasma after laser ablation.

REFERENCES

Church, D. A., & Holzscheiter, H. M.. 1989, Phys Rev., A40, 54
Drewell, N. 1979, Ph.D. Thesis, University of Toronto, Toronto, Ont. Canada, 48-53
Fang, Z., & Kwong, V.H.S. 1995, Phys. Rev., A51, 1321
Kwong, V.H.S. 1979, Ph.D. Thesis, University of Toronto, Toronto, Ontario, Canada
Kwong, V.H.S., Fang, Z., Gibbons, T.T., Parkinson, W.H., Smith, P.L. 1993, ApJ, 411, 431
Rumsby, P.T., & Paul, J.W.M. 1974, Plasma Phys., 16, 247
Unterreiter, E., Schweinzer, J., Winter, H. 1991, J. Phys., B24, 1003
Wang, J., & Kwong, V.H.S. 1997, Rev. Sci. Instrum., 68, 3712

NASA LAW, February 14-16, 2006, UNLV, Las Vegas

Astrochemistry in the Early Universe: Collisional Rates for H on H_2

S. H. Lepp & D. Archer

Physics Dept., University of Nevada, Las Vegas, NV 89154

N. Balakrishnan

Chemistry Dept., University of Nevada, Las Vegas, NV 89154

ABSTRACT

We present preliminary results of a full quantum calculation of state to state cross sections for H on H_2. These cross sections are calculated for v=0,4 j=0,15 for energies up to 3.0 eV. The cross sections are calculated on the BKMP2 potential surface (Boothroyd et al. 1996) with the ABC scattering code (Skouteris et al. 2000).

1. Introduction

The chemistry of the early universe is dominated by hydrogen. The standard big bang model produces only hydrogen, helium and trace amounts of lithium. These elements must makeup the gas that forms the first compact objects and cooling from these allows these first objects to form. A comprehensive model of the chemistry has been developed in Stancil, Lepp and Dalgarno (1996, 1998, 2002).

As part of that project we started calculations to get improved cooling curves for H_2, we found a large difference in H on H_2 collision rates. There was good agreement within the ground vibrational state, but excited state transitions could differ by orders of magnitude. See figures below.

Our calculations were done using the ABC program by Skoteris, Castillo, and Manolopoulos(2000). We have modified it to use the potential surface of Boothroyd, Keogh, Martin,and Peterson (1996). The ABC program uses the coupled-channel hyperspherical coordinate method to solve the Schrodinger equationfor three nuclei on a single Born-Oppenheimer potential energy surface. The program was run for a grid of energies up to 3.5 eV, so that we can calculate state to state rates for v=0-5, j=0-15.

2. Results

To compare with Sun and Dalgarno (1994) we ran some calculations on the DMBE potential surface (Varandas 1987). The results from the ABC code agree well with the earlier Sun and Dalgarno (1987) results as can be seen in Figure 1.

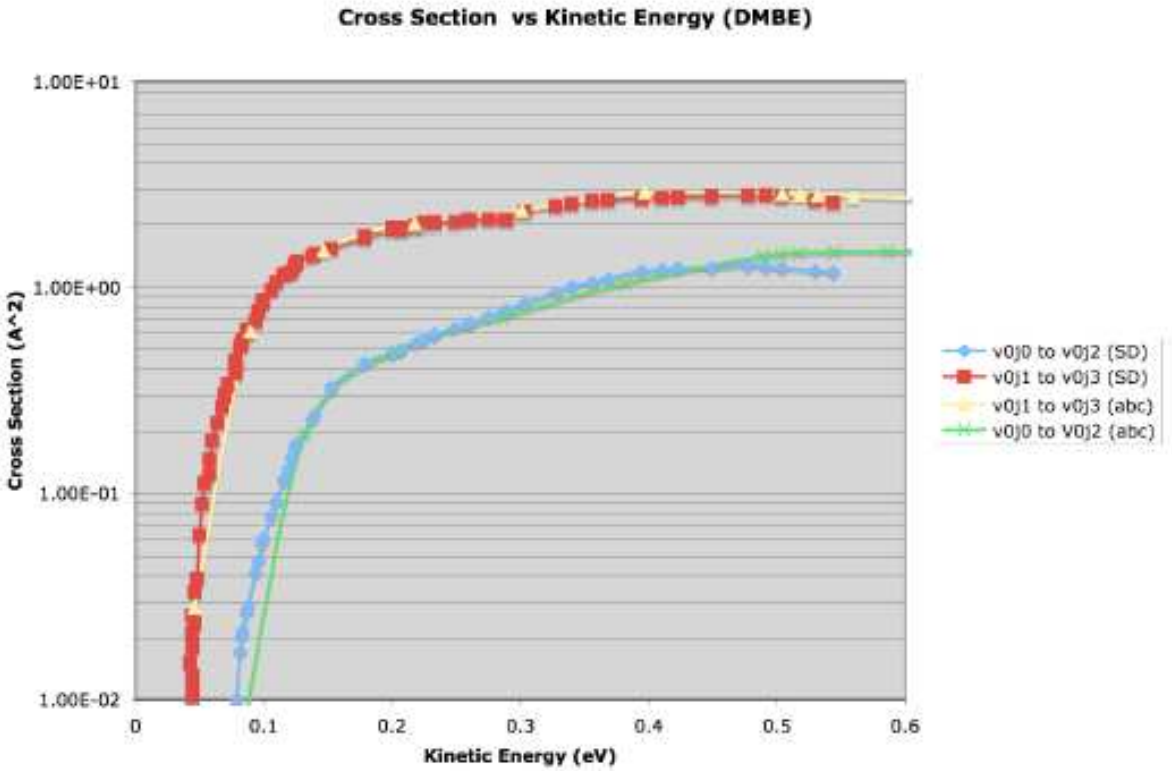

Fig. 1.— The cross section for the lowest two transitions for SD (Sun and Dalgarno 1987) and ABC (this calculation).

We have completed the calculations for the state-state cross sections on the BKMP surface (Boothroyd et al 1996) and will soon publish them (Archer 2006). These will be the first complete study of the state-state rates for H on H_2 for lower levels.

This work is based upon work supported by the Department of Energy under Award Number DE-FG36-05G085028.

REFERENCES

Archer, David, 2006 Ph.D Thesis.

A.I. Boothroyd, W.J. Keogh, P.G. Martin and M.R. Peterson, 1996 J. Chem. Phys., 104, 7139.

Stancil, P. C., Lepp, S., & Dalgarno, A. 1996, ApJ, 458, 401

Stancil, P. C., Lepp, S., & Dalgarno, A. 1998, ApJ, 458, 401.

Lepp, S., Stancil, P.C. and Dalgarno, A. 2002 J. Phys. B, 35, R57.

Skouteris, D., Castillo, J. F. and Manolopoulos, D. E. 2000, Comput. Phys. Commun. 133, 128.

Sun, Y. and Dalganro A. 1994 ApJ, 427, 1053.

Varandas, A.J.C., Brown, F.B., Mead, C.A., Truhlar, D.G. and Blaise, N.G. 1987, J Chem. Phys. 90,300.

Laboratory Measurements of the Line Emission from Mid-Z L-Shell Ions in the EUV

J. K. Lepson

Space Sciences Laboratory, University of California, Berkeley, CA 94720-7450

P. Beiersdorfer & H. Chen

High Temperature and Astrophysics Division, Lawrence Livermore National Laboratory, Livermore, CA 94550

M. F. Gu & S. M. Kahn

Physics Department, Stanford University, Palo Alto, CA 94305

ABSTRACT

We are continuing EBIT measurements of line lists in the EUV region for use as astrophysical diagnostics and have recently measured the same transitions in much denser plasma of the NSTX tokamak. This allows us to calibrate density-sensitive line ratios at their upper limits. We compare our observations at low and high density with calculations from the Flexible Atomic Code.

1. Introduction

Satellite observations in the soft x-ray and EUV provide valuable diagnostic opportunities for astronomers and astrophysicists. This region contains a wealth of emission lines that can be used to determine plasma properties and elemental abundances over a temperature range from 10^5 to 10^7 K. Because this region had been poorly studied, even in the laboratory, the relevent data sets were nearly empty, hampering efforts to develop EUV diagnostics.

In order to address this deficiency, we are continuing measurements of line lists in the EUV region for use in astrophysical diagnostics. We have published line lists for M-shell iron (Fe VII - Fe X; Lepson et al 2002), L-shell argon (Ar IX - Ar XVI; Lepson et al. 2003), and L-shell sulfur (S VII - S XIV; Lepson et al 2005a). We are close to completing the analysis of L-shell silicon (Si V - Si XII; Lepson & Beiersdorfer 2005, Lepson et al. 2005b), and have measured magnesium and aluminum. These measurements, which included wavelengths and intensities, were carried out at the Lawrence Livermore National Laboratory's electron beam ion traps, which use a monoenergetic electron beam.

We have recently taken additional measurements for the same transitions in collisional plasmas produced in the Princeton Plasma Physics Laboratory's NSTX tokamak. Because

the NSTX plasmas are two orders of magnitude denser than the EBIT plasmas, they provide an opportunity to calibrate these diagnostic ratios at their upper limits.

2. Spectroscopic measurements

Spectra were measured with two grazing-incidence spectrometers with variable line spacing flat-field gratings (Harada & Kita 1980, Nakano et al. 1984). The first has an average line spacing of 1,200 ℓ/mm with a 3° angle of incidence and an instrumental resolution of $\sim$ 300 at 100 Å. The second has an average line spacing of 2,400 ℓ/mm with a 1.3° angle of incidence and an instrumental resolution of $\sim$ 150 at 15 Å to $\sim$ 500 at 50–60 Å. Readouts were taken with a 1,024 x 1,024 pixel, liquid nitrogen cooled CCD.

Wavelength calibrations were performed periodically throughout the experimental runs using the well known hydrogenic and helium-like K-shell emission lines (commonly refered to as Lyman-α and w, respectively) of carbon, oxygen, and nitrogen and their higher orders, providing a calibration for 19–173 Å.

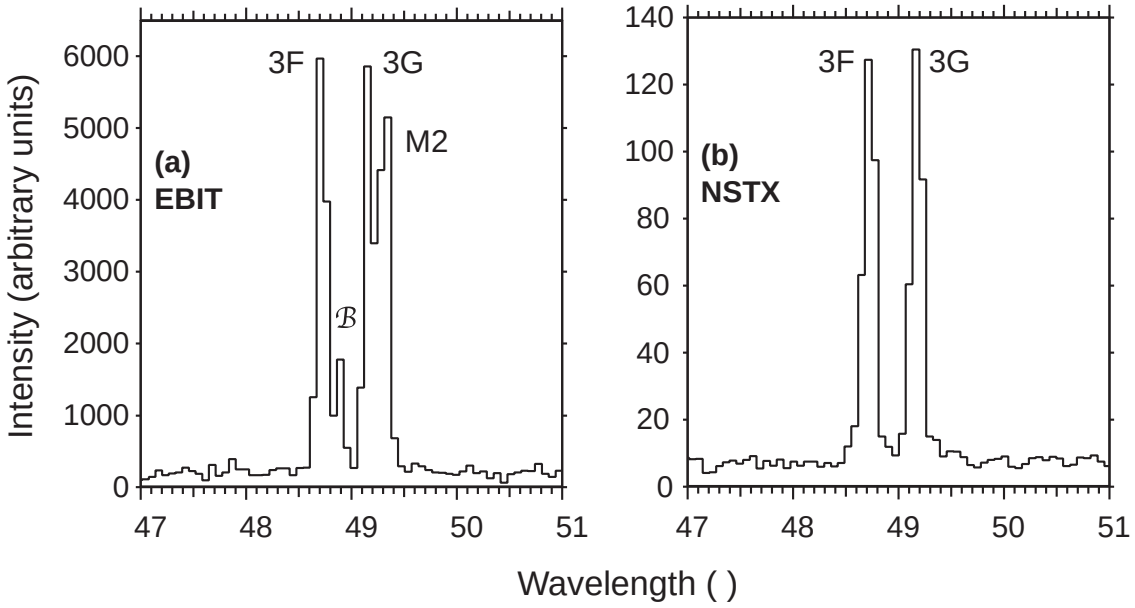

Fig. 1.— Comparison of $3s \rightarrow 2p$ transitions of Ar IX in (a) low density plasma from EBIT and (b) high density plasma from NSTX. The B V line at 48 Å was removed for clarity.

Spectra on NSTX were taken with a grazing-incidence spectrometer utilizing the 2,400 line/mm flat-field grating as described above. Wavelength calibrations were performed using the well known hydrogenic and helium-like K-shell emission lines of oxygen, carbon, and boron (from boronization of the tokamak), which provided a calibration for 19-60 Å. Nitrogen was typically not visible in NSTX spectra.

We used the program IPLab to remove cosmic rays using the "bad pixel" filter and manually subtracted the background by fitting a smoothed curve to the shots we examined. We fitted Gaussian curves to the lines using the program Igor. After identification, we measured the relative fluxes of the emission lines for each charge state, and corrected for differing sensitivity of the spectrometer (grating detector) at different wavelengths (Lepson et al. 2003, May et al. 2003).

We used the density differences between the EBIT and NSTX plasmas to investigate the density-sensitive lines of Ar IX and Ar XIV. Electron density in the electron beam ion traps, as determined using the ratios of the helium-like nitrogen lines commonly known as z and y (Chen et al. 2004), was approximately $10^{11}\mathrm{cm}^{-3}$. Electron density in the tokamak, as determined by Thompson scattering using in situ probes, was approximately $10^{13}\mathrm{cm}^{-3}$.

In Fig. 1 we focus on the $3s \rightarrow 2p$ transitions of neon-like Ar IX. Fig. 1a shows a low-density spectrum from EBIT-II. The 3F, 3G, and density- sensitive M2 lines are easily seen and nearly equal in strength. In adddition, we note the presence of a line, labelled $\mathcal{B}$, which is a newly described magnetic field diagnostic (Beiersdorfer et al. 2003). Fig. 1b shows a high-density spectrum from NSTX. Note that at this density the M2 line has essentially disappeared. The magnetically sensitive line $\mathcal{B}$ is also gone.

Figure 2 shows curves of the M2/3F and M2/3G line ratios as calculated by the Flexible Atomic Code (Gu 2003) for a range of electron densities from 10^5 to $10^{16} cm^{-3}$. We used these ratios to infer the density of the EBIT plasma (dashed lines). As both line ratios are present at the same time, they should yield the same result. In fact, the inferred densities differ by factor of 5, indicating that theory still needs some work.

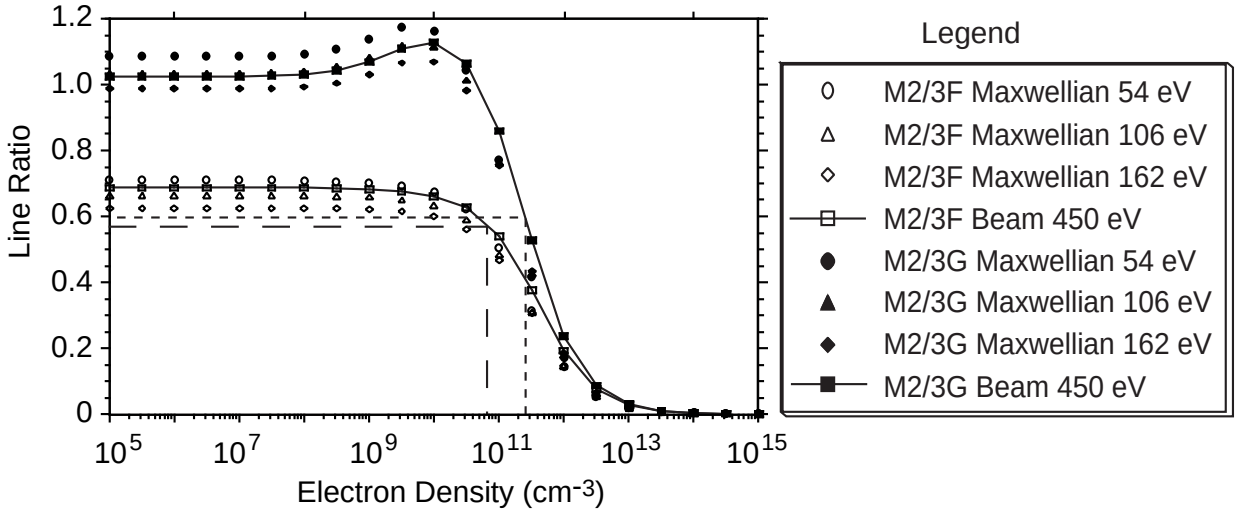

Fig. 2.— Comparison of density-sensitive line ratios using the Flexible Atomic Code. Points are shown for Maxwellian plasmas of three densities and for a monoenergetic plasma.

3. Conclusions

We have made considerable progress using the LLNL EBITs to compile a comprehensive catalogue of extreme ultraviolet and soft x-ray emission lines from highly charged ions of astrophysically relevent mid-Z elements. We have published line lists of iron, argon, and sulfur, with silicon nearly ready and other elements in progress. By comparing these data to modeling calculations and measurements in higher density tokamak plasmas we have identified a variety of density-sensitive lines, allowing us to better calibrate theoretical models.

This work supported by NASA Astronomy and Physics Research and Analysis program work order NNH04AA751 and performed under the auspices of DOE by the Univ. of California Lawrence Livermore National Laboratory under contract W-7405-ENG-48.

REFERENCES

Beiersdorfer, P., Scofield, J. H., & Osterheld, A. L. 2003, Phys. Rev. Lett. 90, 235003.

Chen, H., Beiersdorfer, P., Heeter, L. A., Liedahl, D. A., Naranjo-Rivera, K. L., Trbert, E., Gu, M. F., & Lepson, J. K. 2004, ApJ, 611, 598.

Gu, M.F. 2003, ApJ, 582, 1241.

Harada, T., & Kita, T. 1980, Appl. Opt., 19, 3987.

Lepson, J. K., & Beiersdorfer, P. 2005, Phys. Scripta T120, 62.

Lepson, J. K., Beiersdorfer, P., Brown, G. V., Liedahl, D. A., Utter, S. B., Brickhouse, N. S., Dupree, A.K., Kaastra, J.S., Mewe, R., & Kahn, S.M. 2002, ApJ, 578, 648.

Lepson, J. K., Beiersdorfer, P., Behar, E., & Kahn, S.M. 2003, ApJ,590, 604.

Lepson, J. K., Beiersdorfer, P., Behar, E., & Kahn, S.M. 2005, ApJ,625, 1045.

Lepson, J. K., Beiersdorfer, P., Behar, E., & Kahn, S.M. 2005, NIMB, 235, 131.

May, M., Lepson, J., Beiersdorfer, P., Thorn, D., Chen, H., Hey, D., & Smith, A. 2003, Rev. Sci. Instrum., 74, 2011.

Nakano, N., Kuroda, H., Kita, T., & Harada, T. 1984, Appl. Opt., 23, 2386.

NASA LAW, February 14-16, 2006, UNLV, Las Vegas

Quenching of excited Na due to He collisions

C. Y. Lin, P. C. Stancil

Department of Physics and Astronomy and Center for Simulational Physics, University of Georgia, Athens, GA 30602

cylin@hal.physast.uga.edu, stancil@physast.uga.edu

H. P. Liebermann, P. Funke, & R. J. Buenker

Fachbereich C-Mathematik und Naturwissenschaften, Bergische Universität Wuppertal, D-42097 Wuppertal, Germany

ABSTRACT

The quenching and elastic scattering of excited Sodium by collisions with Helium have been investigated for energies between 10^{-13} eV and 10 eV. With the *ab initio* adiabatic potentials and nonadiabatic radial and rotational couplings obtained from multireference single- and double-excitation configuration interaction approach, we carried out scattering calculations by the quantum-mechanical molecular-orbital close-coupling method. Cross sections for quenching reactions and elastic collisions are presented. Quenching and elastic collisional rate coefficients as a function of temperature between 1 μK and 10,000 K are also obtained. The results are relevant to modeling non-LTE effects on Na D absorption lines in extrasolar planets and brown dwarfs.

1. Introduction

In cool stellar and planetary atmospheres, the electron abundance is extremely low so that thermalization is only possible through collisions of the dominant neutral species, H_2, He, and H. Typically, neutral cross sections are much smaller than those due to electrons, so that the level populations of the atmospheric constituents may display departures from equilibrium. Unfortunately, these cross sections are generally not available for collision energies typical of stellar/planetary environments. In this work, we investigate collisions of Na with He through the elastic scattering channels, $\mathrm{Na}(3s\ ^2S) + \mathrm{He} \rightarrow \mathrm{Na}(3s\ ^2S) + \mathrm{He}$ and $\mathrm{Na}(3p\ ^2P^o) + \mathrm{He} \rightarrow \mathrm{Na}(3p\ ^2P^o) + \mathrm{He}$, and the inelastic scattering channel, $\mathrm{Na}(3p\ ^2P^o) + \mathrm{He} \leftrightarrow \mathrm{Na}(3s\ ^2S) + \mathrm{He}$.

2. Theoretical Methods and Results

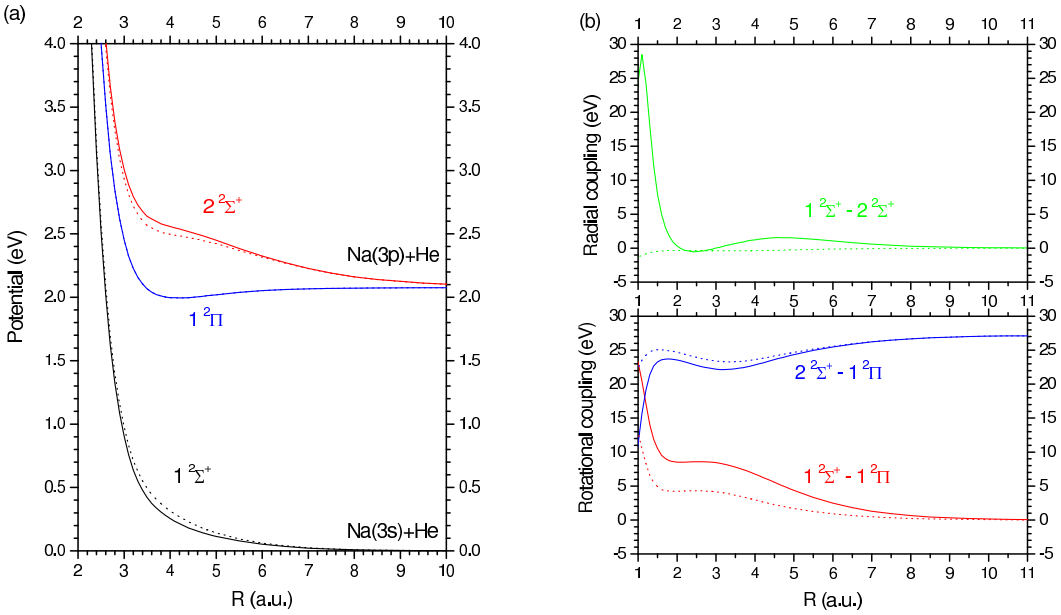

Fig. 1.— Adiabatic (Solid curves) and diabatic (dotted curves) potentials (a) and couplings (b) for Na-He.

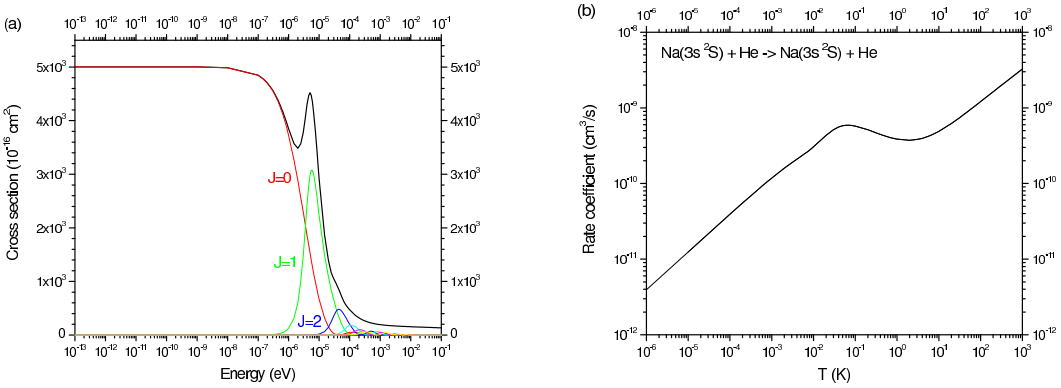

Fig. 2.— Elastic total and partial cross sections (a) and rate coefficients (b) for $1\,^2\Sigma^+$ state.

The adiabatic potential energy curves and nonadiabatic radial and rotational couplings were obtained using the multireference single- and double-excitation configuration interaction (MRD-CI) method (Krebs & Buenker 1995). The quantum-mechanical MOCC approach (Zygelman 1992) is used in the present scattering calculations. An unitary transformation is applied to convert adiabatic potentials and nonadiabatic couplings into diabatic representation. A coupled set of second-order differential scattering equations can then be solved using the log-derivative method of Johnson (Johnson 1973) to obtain scattering cross sections.

In Fig. 1, we display the comparison of adiabatic and nonadiabatic results to diabatic results. Elastic total cross sections with low partial-wave analysis and rate coefficients are presented in Fig. 2-4. In Fig. 5 and 6, the state-to-state cross sections, total cross sections and rate coefficients for quenching and excitation processes are illustrated.

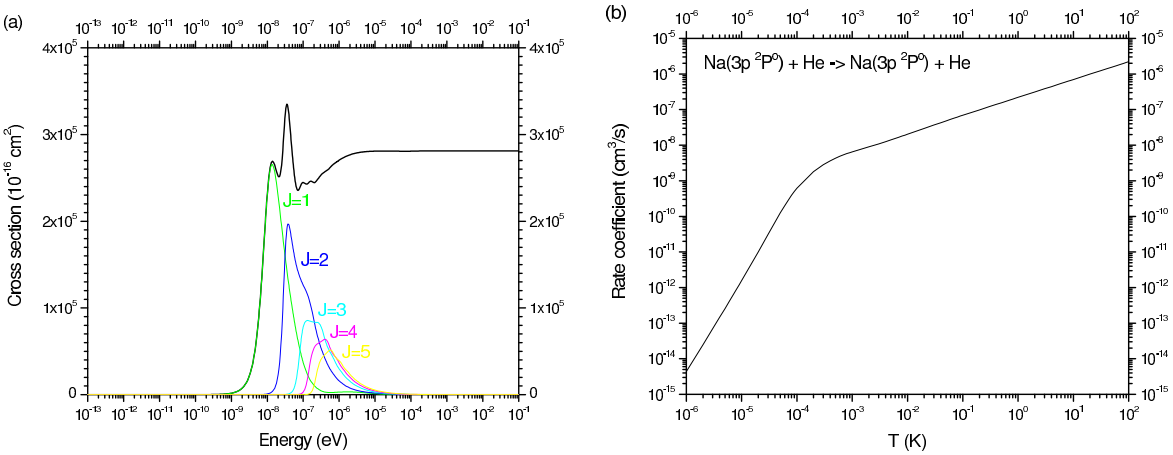

Fig. 3.— Elastic total and partial cross sections (a) and rate coefficients (b) for 1 $^2\Pi$ state.

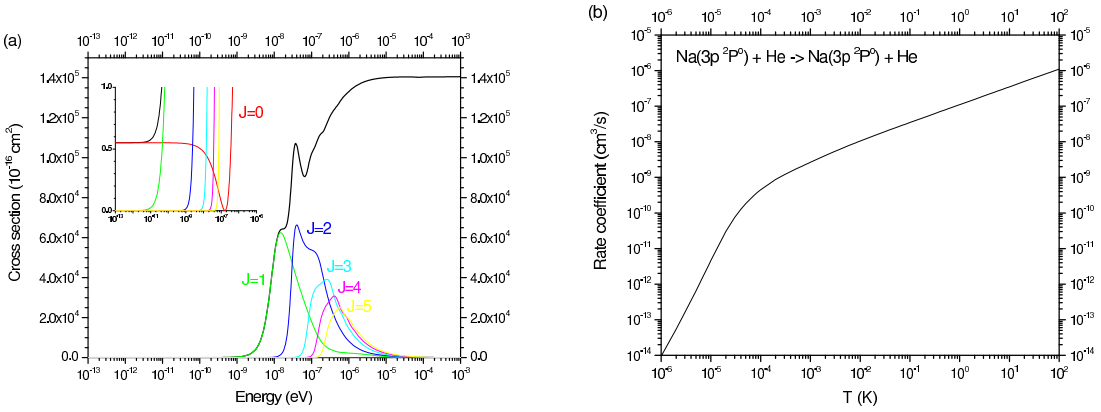

Fig. 4.— Elastic total and partial cross sections (a) and rate coefficients (b) for 2 $^2\Sigma^+$ state.

3. Summary

We have investigated elastic and inelastic collisions of Na with low-energy He. Elastic cross sections for each of three molecular states are analyzed by their partial cross sections to explain wiggles and peaks of cross sections. Several distinct orbiting resonances occuring on quenching and excitation cross sections are due to quasi-bound states of the quasimolecule. The threshold of Na(3p)+He results in the rapid drop of excitation cross sections.

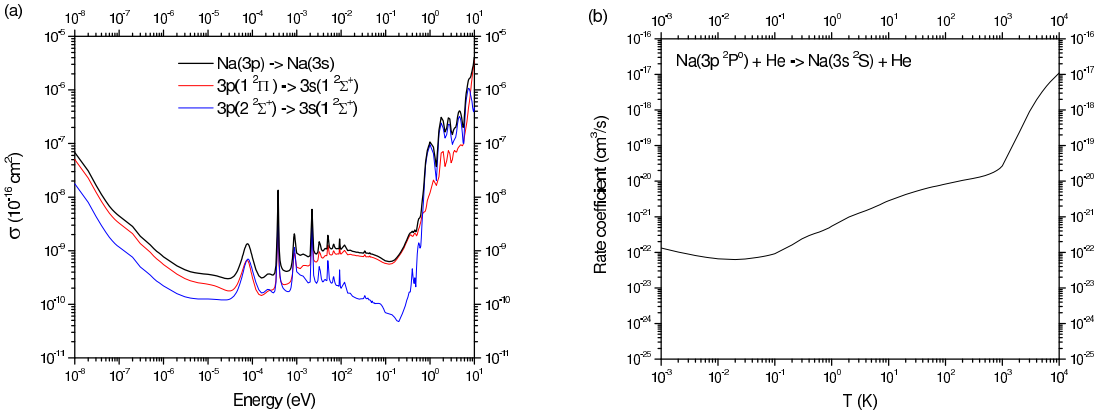

Fig. 5.— Quenching cross sections (a) and rate coefficients (b) for Na($3p\ ^2P^o$) + He → Na($3s\ ^2S$) + He.

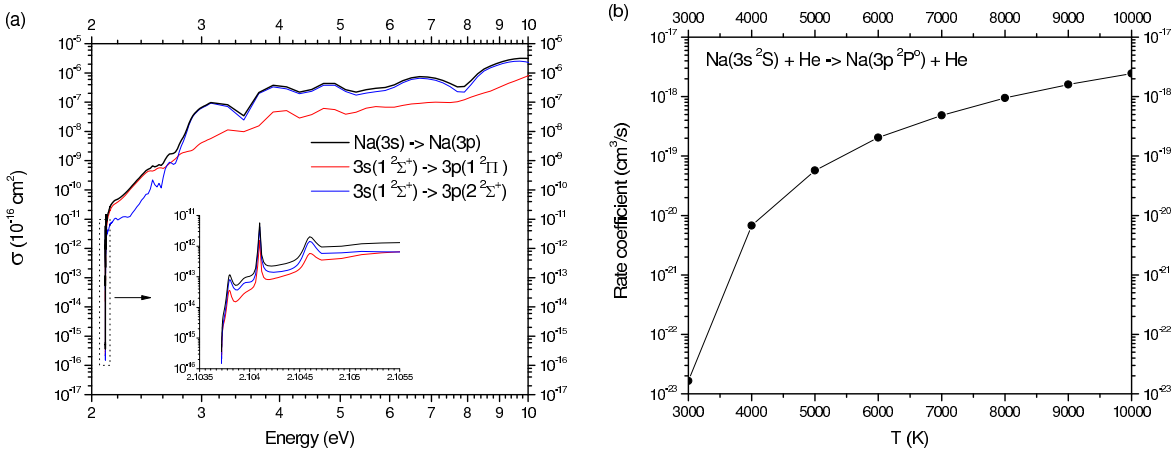

Fig. 6.— Excitation cross sections (a) and rate coefficients (b) for Na($3s\ ^2S$) + He → Na($3p\ ^2P^o$) + He.

CYL and PCS acknowledge support from NASA grant NNG04GM59G.

REFERENCES

Krebs, S. & Buenker, R. J. 1995, J. Chem. Phys., 103, 5613
Zygelman, B. *et al* 1992, Phys. Rev. A, 46, 3846
Johnson, B. R. 1973, J. Comput. Phys., 13, 445

NASA LAW, February 14-16, 2006, UNLV, Las Vegas

Dielectronic Recombination In Active Galactic Nuclei

D. V. Lukic[1], M. Schnell, and D. W. Savin

Columbia Astrophysics Laboratory, Columbia University, New York, NY 10027, USA

Z. Altun

Department of Physics, Marmara University, Istanbul 81040, Turkey

N. Badnell

Department of Physics, University of Strathclyde, Glasgow, G4 0NG Scotland, UK

C. Brandau[2], E. W. Schmidt, A. Müller, and S. Schippers

Institut für Atom- und Molekülphysik, Justus-Liebig-Universität, D-35392 Giessen, Germany

F. Sprenger, M. Lestinsky, and A. Wolf

Max-Planck-Institut für Kernphysik, D-69117 Heidelberg, Germany

ABSTRACT

XMM-Newton and Chandra observations of active galactic nuclei (AGN) show rich spectra of X-ray absorption lines. These observations have detected a broad unresolved transition array (UTA) between $\sim$ 15-17 Å. This is attributed to inner-shell photoexcitation of M-shell iron ions. Modeling these UTA features is currently limited by uncertainties in the low-temperature dielectronic recombination (DR) data for M-shell iron. In order to resolve this issue, and to provide reliable iron M-shell DR data for plasma modeling, we are carrying out a series of laboratory measurements using the heavy-ion Test Storage Ring (TSR) at the Max-Plank-Institute for Nuclear Physics in Heidelberg, Germany. Currently, laboratory measurements of low temperature DR can only be performed at storage rings. We use the DR data obtained at TSR, to calculate rate coefficients for plasma modeling and to benchmark theoretical DR calculations. Here we report our recent experimental results for DR of Fe XIV forming Fe XIII.

---

[1]On a leave from Institute of Physics, 10001 Belgrade, Serbia and Montenegro

[2]Present address: Gesellschaft für Schwerionenforschung (GSI), D-64291 Darmstadt, Germany

1. Introduction

A new absorption feature between 15-17 Å has been detected in recent Chandra and XMM Newton X-ray observations of active galactic nuclei (AGNs). This has been identified as an unresolved transition array (UTA) due mainly to 2p → 3d inner shell absorption in M-shell iron ions (Fe III - XVI). AGN photoionization models generally match spectral features from abundant second and third row elements but over-predict the average iron ionization stage derived from these UTAs. This is believed to be due to an underestimation of the relevant low temperature dielectronic recombination (DR) rate coefficients for M-shell iron (Netzer 2004; Kraemer et al. 2004). To address this issue we have initiated a series of laboratory DR measurements for iron M-shell ions. Here we report our recent progress.

DR begins when a free electron collides with an ion, excites a bound electron in the target, and is simultaneously captured. The resulting doubly-excited state lies in the continuum of the recombined system. This intermediate state can either autoionize (the time reverse of the capture process) or decay by emitting a photon. DR is complete when the intermediate state emits a photon, thereby reducing the total energy of the system to below the ionization threshold of the recombined system. Energy conservation requires that the kinetic energy of the incident electron E_k and the binding energy released E_b sum up to the excitation energy of the core electron ΔE in the presence of the captured electron, i.e., $\Delta E = E_k + E_b$. Because E_b and ΔE are quantized, the kinetic energies at which DR can go forward is also quantized. Thus DR is a resonant process, as can be seen in Fig. 1a.

2. Heavy Ion Storage Ring Experiments

At the Test Storage Ring (TSR) of the Max-Plank-Institute for Nuclear Physics in Heidelberg, Germany, electron-ion collision experiments are performed using the merged electron-ion beams technique. Measurements can be carried out for most ions of the cosmically abundant elements H, He, C, N, O, Ne, Na, Mg, Al, Si, S, Ar, Ca, Fe, and Ni. Ions are injected into the ring, stored, and their initial energy spread is reduced using electron cooling. The electrons and ions are merged over a distance of 1.5 m. After cooling, electrons and ions possess the same relative velocity. For the DR measurements, the electron beam is detuned from cooling conditions and the number of recombined ions is recorded as a function of the corresponding relative energy. The recombination products are separated from the primary beam using the first bending magnet in the ring after the electrons and ions are demerged. The recombined ions are stopped and counted using a particle detector. The measured recombination signal, normalized to the primary electron and ion beam intensities, represents the DR cross section times the relative velocity averaged over the relative velocity spread between the electrons and ions (i.e., a merged-beams rate coefficient). Further details can be found in Schmidt et al. (2006) and references therein.

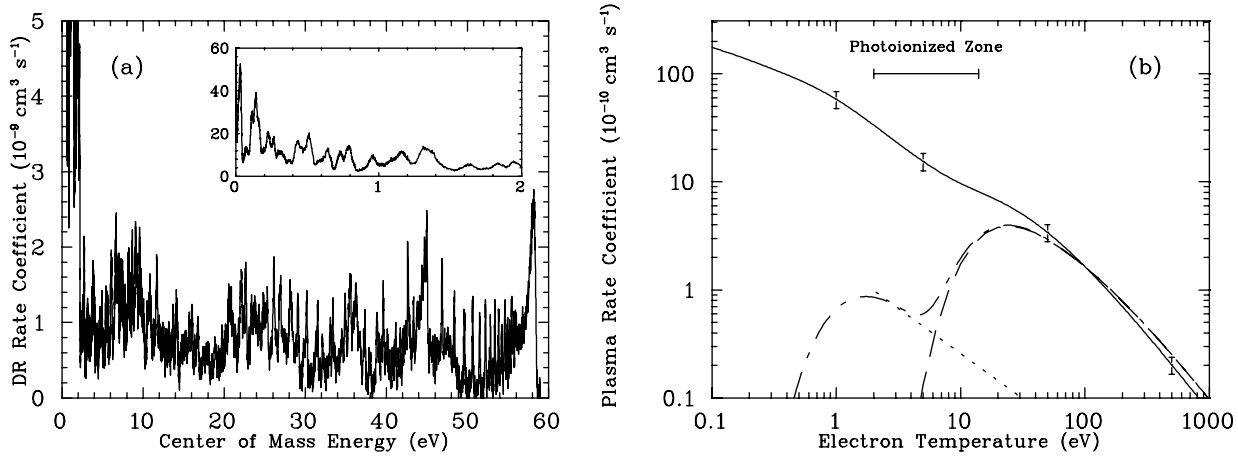

Fig. 1.— (a) Measured TSR DR resonance spectrum for Fe XIV forming Fe XIII via $\Delta n = 0$ core electron excitations. (b) DR plasma rate coefficient for Fe XIV forming Fe XIII via $\Delta n = 0$ core electron excitations. The solid curve is our experimentally-derived plasma rate coefficient. The experimental uncertainty is estimated to be ±18%. Also shown are the recommended DR data of Arnaud & Raymond (1992; dashed curve), the deliberate modification of the DR data by Netzer (2004; dash-dotted curve), and the recommended RR data of Woods et al. (1981; dotted curve). The temperature range where Fe XIV is predicted to form in a photoionized plasma (Kallman & Bautista 2001) is shown by the horizontal line which shows where the Fe XIV fractional abundance exceeds 10% of its peak value.

3. Recent Laboratory Results

As an example of our recent results, we show in Fig. 1a the measured DR resonance spectrum for Fe XIV forming Fe XIII via $\Delta n = 0$ core electron excitations (Schmidt et al. 2006). The energy range spans from zero relative energy up to the $3s^2 3d(^2D)$ DR series limit at $\sim$ 58.9 eV. This exceedingly rich resonance structure shows the importance of DR laboratory measurements and has triggered new theoretical studies. We have convolved our merged-beams DR data with a Maxwellian energy distribution to produce a plasma rate coeficient. In Fig. 1b we compare our experimentally-derived plasma recombination rate coefficient with the DR rate coefficient of Arnaud & Raymond (1992). In the temperature range where Fe XIV is expected to form in a photoionized plasma (Kallman & Bautista 2001), the experimentally-derived plasma rate coefficient is several orders of magnitude larger than the presently available theoretical DR data of Arnaud & Raymond (1992). Netzer (2004) in order to improve agreement between AGN models and observations arbitrarily increased the low temperature DR rate coefficient for all the M-shell iron ions. Our experimentally-derived rate for Fe XIV is still about an order of magnitude larger than his deliberate modification of the theoretical DR data. Also shown in Fig. 1b is the the recommended radiative recombination (RR) rate coefficient of Woods et al. (1981). The RR contribution is insignificant relative to DR at all temperatures considered here.

4. Conclusion

We are in the process of carrying out DR measurements for other M-shell iron ions. As they become available, we recommend that these experimentally-derived plasma rate coefficients be incorporated into future models of AGN spectra in order to arrive at more reliable results.

This work has been supported in part by NASA, the German Federal Ministry for Education and Research, and the German Research Council under contract no. Schi 378/5.

REFERENCES

Arnaud, M., & Raymond, J. 1992, ApJ, 398, 394
Kallman, T. R., & Bautista M. 2001, ApJS, 133, 221
Kraemer, S. B., et al. 2004, ApJ, 604, 556
Netzer, H., 2004, ApJ, 604, 551
Schmidt, E. W., et al. 2006, ApJL, 641, L157
Woods, D. T., Shull, J. M., & Sarazin, C. L. 1981, ApJ, 249, 399

NASA LAW, February 14-16, 2006, UNLV, Las Vegas

The Effect of Non-equilibrium Kinetics on Oxygen Chemistry in the Interstellar Medium

Balakrishnan Naduvalath

Department of Chemistry, University of Nevada Las Vegas, Las Vegas, NV 89154

naduvala@unlv.nevada.edu

ABSTRACT

It has been suggested that in photon-dominated regions, oxygen chemistry is initiated by the O+H_2 →OH+H reaction. The reaction has an energy barrier of about 0.4 eV with ground state reactants and it is slow at low temperatures. There is strong experimental evidence that vibrational excitation of the H_2 molecule increases the reactivity significantly. We present extensive quantum calculations of cross sections and rate coefficients for the O+$H_2(v)$ reaction for $v = 0 - 3$ of the H_2 molecule and show that the vibrational excitation of the molecule has a significant effect on reactivity, especially at low temperatures.

1. Introduction

The study of photodissociation regions or photon-dominated regions (PDRs) has attracted considerable attention in recent years. Its importance is derived from the fact that far-ultraviolet (FUV) photons penetrate the clouds, heat the gas, and influence the chemical and energy balance of the neutral interstellar medium. They also play significant role in star forming processes in galaxies (Hollenbach & Tielens 1997). Theoretical models (Tielens & Hollenbach 1985; van Dishoeck & Black 1988; Sternberg et al. 1989; Le Bourlot et al. 1993; Sternberg et al. 1997) of this phenomenon have been developed and used for the interpretation of different events occurring in the neutral interstellar medium. Detailed analysis of the relevant chemical reactions in dense molecular clouds exposed to intense far-ultraviolet radiation has been given by Sternberg and Dalgarno (1995).

Chemistry of PDR differs significantly from usual ion-molecular chemical reactions. Because of the FUV flux, nonthermal processes are very important and vibrationally excited H_2 (denoted as H_2^*) can play significant role in PDR chemistry. When the gas is hot ($T > 500$ K), the activation energy for reactions of atoms and radicals with H_2 and H_2^* can be overcome and these reactions are dominated. Recombination and charge transfer reactions can also significantly contribute to the ionization balance.

In this work, we give an overview of quantum calculations of the O+$H_2(v)$ reaction for vibrational levels $v = 0-3$ to explore the effect of vibrational excitation of H_2 on the reaction rates.

2. Results and discussion

The quantum scattering calculations were performed using the ABC reactive scattering program (Scouteris, Castillo & Manolopoulos 2000). We have extensively adapted this program for a number of atom-diatom reactions over the last few years, including the O+H_2 reaction (Balakrishnan 2004; Sultanov & Balakrishnan 2005; Weck & Balakrishnan 2005). While the O+H_2 reaction is amenable to numerically exact quantum calculations without any decoupling approximations, such calculations become computer intensive for excited vibrational levels. In our previous studies (Balakrishnan 2004; Sultanov & Balakrishnan 2005) we have demonstrated that the simpler J-shifting approximation (Bowman 1991) can be used to compute cross sections and rate coefficients for the O+H_2 reaction without losing much accuracy. Therefore, most of the results for vibrationally excited H_2 shown here are computed using the J-shifting approximation. The J-shifting method works well for systems which involve an energy barrier as in the case of the present system. We will explicitly show the validity of the J-shifting approximation by comparing with results from numerically exact calculations. More details of the calculations are given in our recent article (Sultanov & Balakrishnan 2005).

The O+H_2 reaction involves two lowest adiabatic potentials, $^3A'$ and $^3A''$. While an explicit quantum calculation must include non-adiabatic coupling between the two surfaces, such effects have been shown to be negligible for the present system using both the trajectory surface hopping method as well as coupled wave packet calculations. Thus, the results shown here are computed separately on the $^3A'$ and $^3A''$ potential surfaces of Rogers et al. (2000) and scaled by a multiple surface coefficient of 1/3. That is, the total cross sections and rate coefficients are given by $1/3(^3A' + ^3A'')$.

In Fig.1 we compare results for O+$H_2(v = 0)$ reaction from the full quantum calculations and the J-shifting method (Balakrishnan 2004) with the experimental and theoretical results of Garton et al. (2003). The theoretical results of Garton et al. are obtained using the time-dependent quantum mechanical approach in which the coupled-states approximation was used to reduce the computer time. It is seen that all three theoretical results agree well with each other and also with the experimental results. Fig. 1 also illustrates that the error introduced by the J-shifitng method is within 10-15% which is within the uncertainty of astrophysical models predictions.

In Fig. 2 we show integral cross sections for the O+p-$H_2(v = 0 - 3)$ (left panel) and O+o-$H_2(v = 0 - 3)$ (right panel) reactions as functions of the incident kinetic energy. It

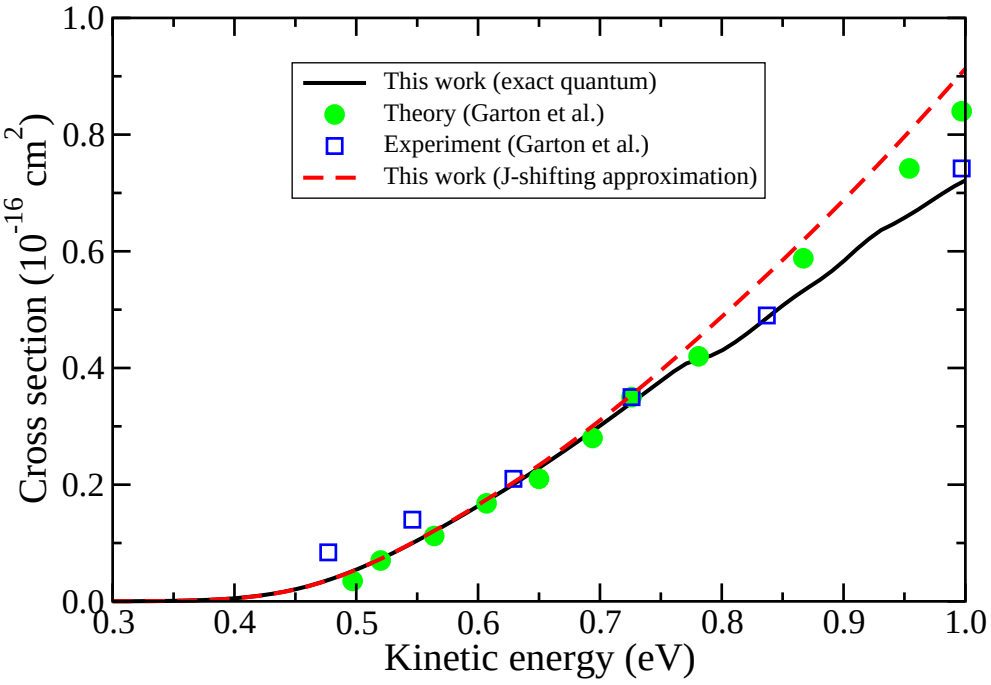

Fig. 1.— Comparison of reaction cross sections for the $O(^3P)+H_2(v = 0, j = 0)$ from the present calculations (Balakrishnan 2004) and Garton et al. (2003) as functions of the incident kinetic energy.

is seen that vibrational excitation has a dramatic effect on reactivity. The effect is much larger at low kinetic energy than at high kinetic energies. This is because at low energies the reaction is dominated by tunneling. Since the energy barrier for the reaction is substantial, tunneling probability is much smaller. Vibrational excitation lowers the adiabatic barrier for the reaction and tunneling occurs much more favorably at low energies.

As seen in the right panel of Fig. 2, vibrational excitation has an even more dramatic effect on ortho-H_2 results at low energies. We believe that this is due to the slightly higher internal energy of o-H_2 which effectively leads to lower barrier height for the reaction. Rate coefficients are obtained by Boltzmann averaging the cross sections at a given temperatures. Tabulated values of the rate coefficients in the temperature range 100-4000 K are reported in our recent publication (Sultanov & Balakrishnan 2005). It has been found that vibrational excitation has a dramatic effect on reactivity at low temperatures with rate coefficient increasing by a about 11 orders magnitude between $v = 0 - 3$ of H_2. The effect is less significant at high temperatures. For example, at 4000 K, the rate coefficients for $v = 0$

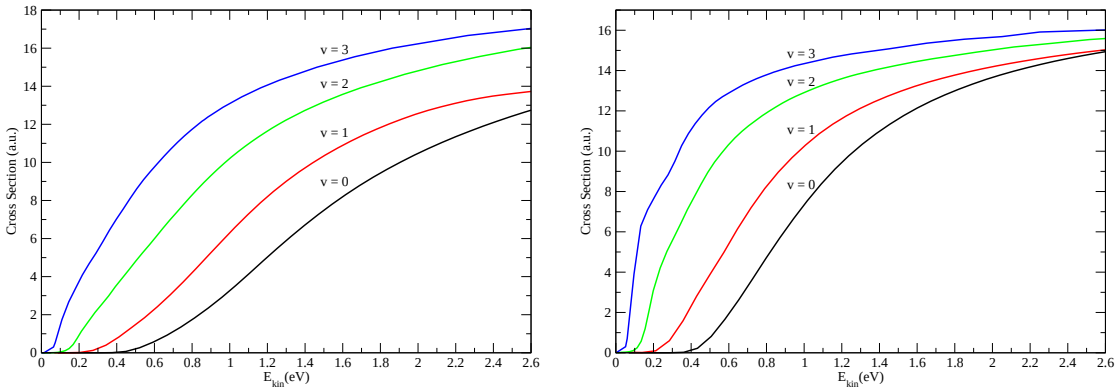

Fig. 2.— Reaction cross section vs. energy for the $O(^3P)+H_2(v)$ reaction for $v = 0-3$. Left panel: results for p-H_2 reaction; right panel: results for o-H_2 reaction.

and $v = 3$ differ only by an order of magnitude. Thus, non-equilibrium effect become more important at lower temperatures than at higher temperatures.

This work was supported by in part by NSF grant ATM-0205199 and DOE grant DE-FG36-05GO85028.

REFERENCES

Hollenbach, D. J., Tielens A. G. G. M. 1997, Annu. Rev. Astron. Astrophys., 35, 179
Tielens, A. G. G. M., & Hollenbach, D. 1985, ApJ, 291, 722
van Dishoeck, & E. F., Black, J. H. 1988, ApJ, 334, 771
Sternberg, A., Dalgarno, A. & Lepp, S. 1989, ApJ, 320, 676
Le Bourlot, J., Pineau des Forêts, G., Roueff, E., & Flower, D. R. 1993, A&A, 267, 233
Sternberg, A., Yan, M. & Dalgarno, A. 1997, Molecules in Astrophysics: Probes and Processes, E. F. van Dishoeck, Dordrecht: Kluwer, 1997, 141
Sternberg, A., & Dalgarno, A. 1995, ApJS, 99, 565
Scouteris, D., Castillo, J. F., & Manolopoulos, D. E. 2000, Comput. Phys. Commun., 133, 128
Balakrishnan, N., 2004, J. Chem. Phys. 121, 6346
Sultanov, R. A., & Balakrishnan, N., 2005, Astrophysical Journal 629, 305
Weck, P. F., & Balakrishnan, N., 2005, J. Chem. Phys. 123, 144308
Bowman, J. M. 1991, J. Phys. Chem., 95, 4960
Rogers, S., Wang, D., Kupperman, A., & Walch, S. 2000, J. Phys. Chem. A, 104, 2308
Garton, D. J., Minton, T. K., Maiti, B., Troya, D., & Schatz, G. C., 2003, J. Chem. Phys., 118, 1585

NASA LAW, February 14-16, 2006, UNLV, Las Vegas

Atomic Oscillator Strengths in the Vacuum Ultraviolet

Gillian Nave, Craig J. Sansonetti, Csilla I. Szabo

National Institute of Standards and Technology, Gaithersburg, MD 20899

gillian.nave@nist.gov, craig.sansonetti@nist.gov, csilla.szabo@nist.gov

ABSTRACT

We have developed techniques to measure branching fractions in the vacuum ultraviolet using diffraction grating spectroscopy and phosphor image plates as detectors. These techniques have been used to measure branching fractions in Fe II that give prominent emission lines in astrophysical objects.

1. Introduction

Transitions in singly-ionized and doubly-ionized iron-group elements give rise to prominent emission lines from a wide variety of astrophysical objects. Some of the most important lines are formed when the upper energy level is excited by radiation from hydrogen at 1216 Å(Ly-α), giving strong fluorescence lines from the vacuum ultraviolet to the infrared. Although these emission lines are important diagnostics of astrophysical plasmas, laboratory oscillator strengths are often unavailable.

The established way to measure accurate oscillator strengths for atomic lines combines the measurement of a lifetime of an upper energy level with a separate measurement of the branching fractions of all the lines emitted from that level. This technique relies on being able to observe *all* the spectral lines emitted by the upper level, which range down to Ly-α or below for many fluorescence lines. Methods of measuring branching fractions using Fourier transform (FT) spectroscopy have high accuracy, but are limited to wavelengths above about 1400 Å. However, to obtain complete sets of branching fractions for singly- and doubly-ionized elements, it is necessary to observe spectral lines with wavelengths as short as 900 Å or less. In recent work we have investigated the feasibility of using phosphor storage image plates to make radiometrically calibrated observations in this short wavelength region.

Phosphor image plates can be used as a direct replacement for glass photographic plates in high-resolution spectrographs. They are coated with a phosphor layer that can be excited into a very long-lived metastable state by an ultraviolet photon. Exposure of the plate produces a latent image in the phosphor that can be recovered by scanning the plate with

a red laser. Red light de-excites the phosphor which emits blue fluorescence that can be detected with a photomultipler tube. The laser, scanning mechanism, and photomultipler are housed in a compact reader. Previous experiments in our group have shown that image plates have good sensitivity at wavelengths below 500 Å (Reader et al. 1999). We have found that their sensitivity is similar to or better than photographic plates for wavelengths between 900 Å and 2300 Å, with some sensitivity to wavelengths as long as 3000 Å. Observations of a deuterium radiometric standard lamp with varying exposure times show that the plates have a linear intensity response over at least four orders of magnitude (Nave et al. 2005).

We have demonstrated a capability for making radiometrically calibrated observations in the spectral region short of 1400 Å. We have used it to measure branching fractions for transitions in Fe II that give prominent emission lines in astrophysical spectra. Our new technique combines the high resolution and broad spectral coverage of our 10.7 m normal incidence vacuum spectrograph (NIVS) with the linear intensity response of phosphor storage image plate detectors to produce results that approach the accuracy of FT methods in longer wavelength regions.

2. Experimental Technique

Fig. 1.— The 10.7-m normal-incidence vacuum spectrograph with foreoptics system.

Two different sources were used to generate the spectra of Fe II. The first is a high-current hollow cathode lamp (Danzmann et al. 1988), which we have used in our previous investigations of iron group and rare earth spectra. Although this source generates both neutral and singly-ionized spectra, high-excitation lines of singly-ionized spectra are weakly excited. For these lines we use a Penning discharge lamp (Heise et al. 1994), which generates singly- and doubly-ionized spectra, depending on the current and gas pressure. All spectra were radiometrically calibrated using a deuterium standard lamp.

In order to measure accurate branching fractions, it is necessary to ensure that all sources illuminate the spectrograph in the same way. We thus constructed a fore-optics system for our NIVS to image the spectral source onto the slit of the spectrograph and fully illuminate the grating. This system is shown in figure 1. The vacuum chamber **A** is evacuated with a turbomolecular pump. It contains two remotely adjustable mirrors which focus the light from the hollow cathode source **B** onto the slit of the spectrograph. These mirrors are of sufficient size to fully illuminate the grating, ensuring that small differences in the positioning of the sources do not affect the radiometric calibration. The mirrors are specially coated to have good reflectivity in the 1200 Å region.

3. Results

Transitions from the $3d^5(^6S)4s4p\,x^6P^\circ$ levels in Fe II give prominent emission features in astrophysical spectra. The $x^6P^\circ_{3/2}$ and $3d^6(^1D)4p\,w^2P^\circ_{3/2}$ levels interact strongly, giving unexpected doublet-sextet transitions for each transition between two sextet levels. These 'parasite' transitions have been studied in detail (Johansson et al. 1995) and oscillator strengths have been calculated for many lines throughout the ultraviolet. There are no laboratory oscillator strengths for any of these lines, but a number of these have been studied in HST/GHRS spectra, and astrophysical oscillator strengths have been derived for three pairs of lines at 1870.6 Å, 2325.3 Å and 2436.5 Å. We have measured spectra of Penning lamps from 1150 Å to 2300 Å, which we will combine with these astrophysical gf values to obtain experimental oscillator strengths for the multiplet UV 9 of Fe II around 1270 Å (see figure 2). Comparison of our experimental branching ratios with the calculated values of (Johansson et al. 1995) agree well in the region around 1270 Å, but the calculated branching ratios differ from our experimental values by over an order of magnitude at longer wavelengths.

In addition to these measurements in Fe II, we have used this technique to measure spectra of Fe III and Co III. These measurements are described in two other papers in these proceedings (Blackwell-Whitehead et al. 2006; Smillie et al. 2006)

This work was partially funded by NASA under inter - agency agreement W-10,255.

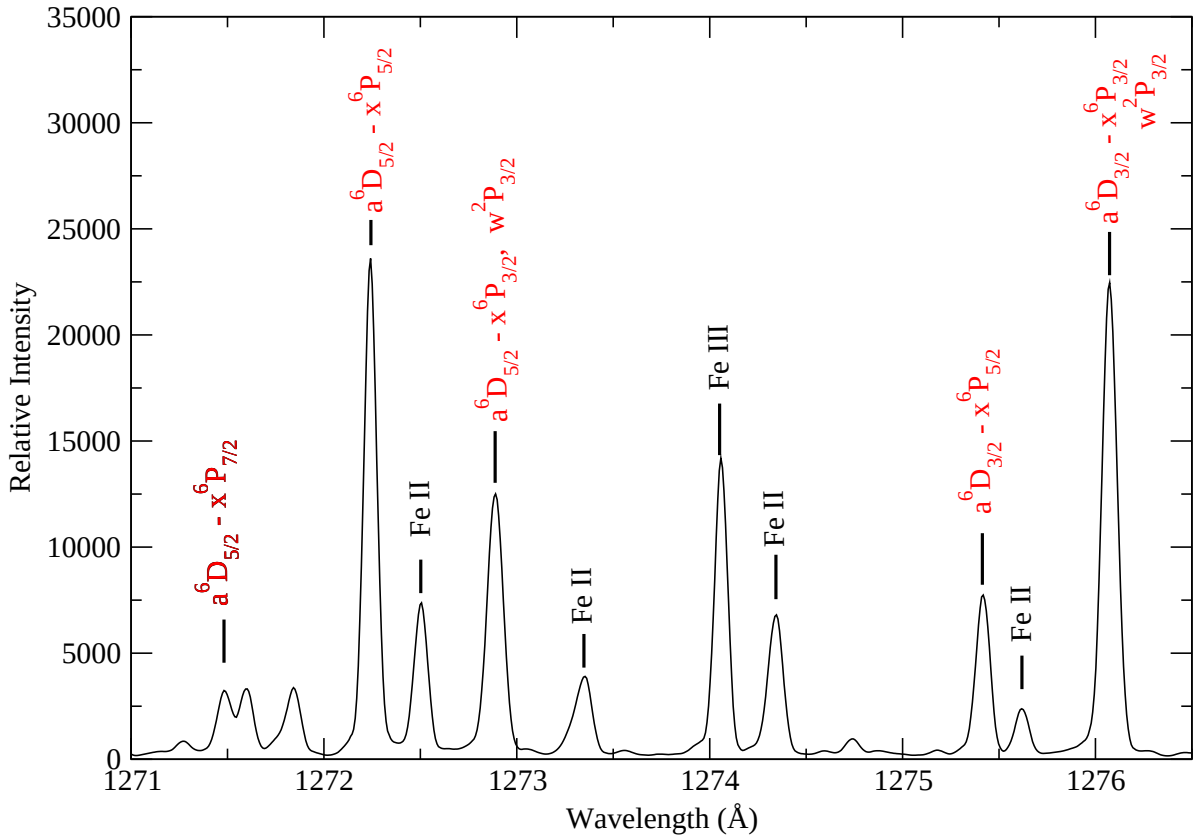

Fig. 2.— The region of the $a^6D - x^6P^\circ$ transitions in Fe II in the spectrum of a Penning discharge observed with phosphor image plates in the NIVS (UV 9).

REFERENCES

Danzmann, K., Günther, M. Fischer, J., Kock, M., & Kühne, M. 1988, Appl. Opt., 27, 4947

Heise, C., Hollandt, J., Kling, R. & Kühne, M. 1994, Appl. Opt. 33, 5111

Nave, G., Li, Z., Sansonetti, C. J., Griesmann, U., Fried, A. D. 2005, Physica Scripta T119, 35

Reader, J., Sansonetti, C. J. & Deslattes, R. D. 1999, Appl. Opt. 39, 637

Johansson, S., Brage, T., Leckrone, D. S., Nave, G., Wahlgren, G. M. 1995, Ap. J. 446, 361

Smillie, D. G., Pickering, J. C., Blackwell-Whitehead, R. J., Smith P. L., Nave, G. 2006, These proceedings.

Blackwell-Whitehead, R. J., Pickering, J. C., Smillie, D., Nave, G., Szabo C. I., Nielsen K. E., Peters, G. 2006, These proceedings.

NASA LAW, February 14-16, 2006, UNLV, Las Vegas

THz Spectroscopy and Spectroscopic Database for Astrophysics

J. C. Pearson & B. J. Drouin

Jet Propulsion Laboratory, California Institute of Technology, Mail Stop 301-429, Pasadena, CA 91109

John.C.Pearson@jpl.nasa.gov, Brian.J.Drouin@jpl.nasa.gov

ABSTRACT

Molecule specific astronomical observations rely on precisely determined laboratory molecular data for interpretation. The Herschel Heterodyne Instrument for Far Infrared, a suite of SOFIA instruments, and ALMA are each well placed to expose the limitations of available molecular physics data and spectral line catalogs. Herschel and SOFIA will observe in high spectral resolution over the entire far infrared range. Accurate data to previously unimagined frequencies including infrared ro-vibrational and ro-torsional bands will be required for interpretation of the observations. Planned ALMA observations with a very small beam will reveal weaker emission features requiring accurate knowledge of higher quantum numbers and additional vibrational states. Historically, laboratory spectroscopy has been at the front of submillimeter technology development, but now astronomical receivers have an enormous capability advantage. Additionally, rotational spectroscopy is a relatively mature field attracting little interest from students and funding agencies. Molecular data base maintenance is tedious and difficult to justify as research. This severely limits funding opportunities even though data bases require the same level of expertise as research. We report the application of some relatively new receiver technology into a simple solid state THz spectrometer that has the performance required to collect the laboratory data required by astronomical observations. Further detail on the lack of preparation for upcoming missions by the JPL spectral line catalog is given.

1. Introduction

The first step in the interpretation of any spectroscopic astronomical observation is to identify the carriers of the emission or absorption features present. Identification has proven to be a challenge in all wavelengths. Atomic and Molecular Line catalogs provide the astronomical community with a tool to assist in the identification of spectral lines or bands. Any

further interpretation of the identified lines for chemical, physical and energetic conditions requires more laboratory data including line strengths, energy levels and collision excitation cross sections. The energy levels, line strengths and cross sections are all input parameters for radiative transfer and collisional excitation models. The models and underlying molecular data enable the molecular abundances and physical conditions of the astrophysical object to be derived. Once this is done, the chemical evolution can be extracted by modeling the observed abundances. The existence of more than 130 different molecules and numerous isotopically substituted variants makes ready access to molecular data mandatory whenever there is astronomical spectroscopy.

The more than 130 different known astrophysical molecules have provided a unique picture of the current state-of-the-art in molecular physics. For diatomic molecules, there are neutrals, radicals and ions with fine structure, hyperfine structure and spin-orbit effects. Many of these molecules provide examples of interacting electronic bands. In addition to displaying all the effects seen in diatomics, the astrophysical triatomic molecules feature case studies in non-rigidity and interactions between vibrational states (e.g. H_2D^+, D_2H^+, H_2O^+, CH_2, NH_2, H_2O). The symmetric top molecules with three hydrogen atoms in the top (e.g. NH_3, H_3O^+, CH_3CCH, CH_3CN and CH_3NC) all eventually suffer from breakdown of separation of rotation and vibration higher K quantum numbers. Internal rotation theory, as it is known today, was developed to analyze the spectra of CH_3OH, CH_3CHO and CH_3COOH. What is known about two top internal rotors (e.g. CH_3OCH_3, CH_3COCH_3) was largely developed to support astronomy. Additionally, there are a number of known astrophysical molecules that are still at the cutting edge of molecular physics. These include extreme cases of non-rigidity (e.g. NH_2, CH_2, H_2O and H_2O^+), vibration-torsion interactions in three fold internal rotors (e.g CH_3OH and CH_3CH_2CN), Asymmetric-top asymmetric-frame internal rotation (e.g. CH_2DOH and CH_3CH_2OH) and coupling of multiple large amplitude motions (e.g. CH_3NH_2, CH_3CH_2OH, and CH_2DOCH_3).

Rotational spectroscopy, unlike infrared or optical spectroscopy, has historically only measured a few transitions with high accuracy due to technical limitations. The rest of the spectrum is determined by fitting a molecular model to the data. This process can have a number of serious limitations that depend strongly on the quality and range of quantum numbers and energy levels in the data set. As a result of the complexity of the molecular physics and the limitations of most molecular data sets, significant expertise is required to calculate and understand the spectra for most of the known astronomical species. Catalogs are necessary since accumulation of all the existing data represents a lifetime of work. The JPL Microwave, Millimeter and Submillimeter Spectral line Catalog (Pickett et al. (1998)) was created to be a repository of rotational molecular data for atmospheric chemistry and astrophysics. For the last 6 years only the atmospheric chemistry portion has been funded and regularly updated. The Cologne Database for Molecular Spectroscopy CDMS (Müller et al. (2005)) was created using the same approach and programs for molecular analysis. CDMS has filled in many missing species and updated a number of older entries with newer data, but even when combined, these database fall well short of what is ultimately need to support the astrophysical need of Herschel, SOFIA and ALMA.

2. Instrument Capability And Data Limitations

The Herschel Space Observatory, SOFIA and ALMA represent several billion dollars of investments by ESA, NASA and the NSF in far-infrared astronomy. A suite of extremely powerful spectroscopic instruments is planned for these missions primarily to study gas phase molecular emission and absorption in unprecedented detail. The bottom line is high resolution spectroscopy $R > 10^6$ will now be possible to 5 THz and $R = 5\text{x}10^5$ will be possible over the 5-28 μm region as well. ALMA will not suffer from the beam dilution that limits most single dish instruments, allowing it to observe and even image the most dense and highly excited astronomical regions to 950 GHz. Additionally, the instruments on Herschel, SOFIA and ALMA have wider instantaneous bandwidths allowing much more spectral coverage to be collected per observation. The improved technical capability of these instruments will result in spectra with thousands of molecular features. This results in an unprecedented need for larger quantum numbers, additional vibrational states and precise vibrational and torsional band spectra. Analyzing large line-confused observational data sets will require the underlying laboratory data to be accurate to 1/10 of observational resolution as well as available electronically for computer aided tools to assist in line identification.

The existing databases generally fill the needs for on line access, but a slightly closer examination of their contents relative to the rapidly approaching need results in some rather disturbing discoveries:

i Isotopic data is generally very limited if available at all.
ii There are few excited vibrational states (rotational hot bands).
iii Torsional or vibrational band data is nearly non-existent.
iv Many existing data sets end below 400 GHz and at small quantum numbers.

The implication of item $i - iii$ is there will be forest of U-lines with predictable intensity. Item *iv* emphasizes that the spectrum of many molecules with high abundance is unknown at the frequencies available to Herschel and SOFIA. The problem is already apparent at in 1-3mm spectral surveys where 1/3 of the lines are unassigned even though these are in the range of the existing data. The problem will be significantly worse for ALMA, Herschel and SOFIA where the consensus estimate above 800 GHz is that 80% of the lines will be initially unassigned at the line confusion limit.

A deeper investigation into the databases and available data results in a serious cause for alarm. The following has been noted:

i Many low J data sets are older and have systematic predictive errors.
ii There is little infrared data in the region below 400 cm^{-1} (12 THz).
iii Theoretical challenging species are in the worst shape.
iv There is no database of infrared or electronic transitions for astrophysical molecules.
v Very few of the potential discovery molecules are in catalogs (or have data).
vi Uncertainties generated in extrapolation are overly optimistic.

i) results in molecular data that is often too poor for careful velocity studies. This causes confusing and erroneous results on cloud collapse and dynamics studies. Item *ii* amplifies the fact that little is known about the long wavelength bands of large molecules. Current constraints of theory are recognized in item *iii*. A complete lack of a catalog for infrared

and electronic transitions of known astrophysical molecules is pointed out in item *iv*. This is absolutely crazy since the electronic bands will be seen in absorption if the dust is not optically thick. The implication of item *v* is Herschel, SOFIA and ALMA all sold discovery science as a fundamental reason for their existence, but discoveries cannot be made without laboratory data to identify the carriers of lines. Lastly, item *vi* results in any extrapolated line position being much worse than expected. Additionally, many astronomical molecules have pathologies, like internal motions and non-rigidity, which make extrapolation a non-linear problem compounding the estimated errors in ways that are not obvious.

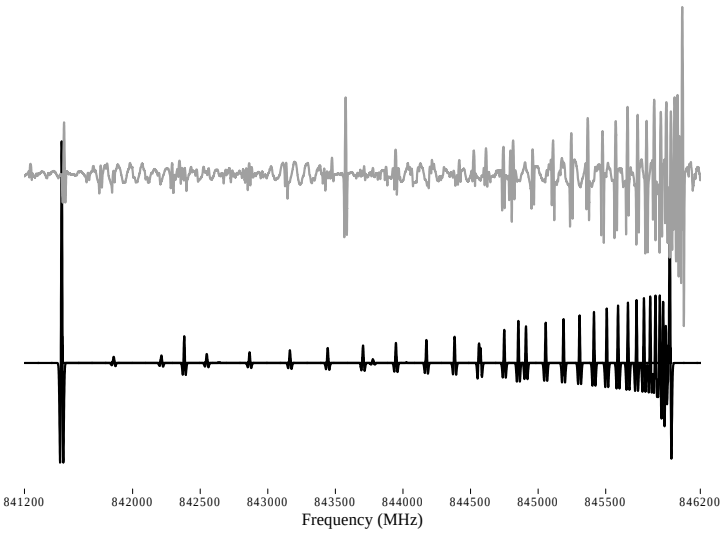

Fig. 1.— The second derivative laboratory absorption spectrum (grey) of dimethyl either (CH_3OCH_3) near 845 GHz compared to the JPL catalog prediction (black).

Figure 1 compares the best available calculation of CH_3OCH_3 (in the JPL catalog) to a laboratory spectrum at 845 GHz. The strong Q-branch origin is off by about 100 MHz and deviates from the predicted shape at higher J. As a result, it would be difficult to assign this in an astronomical spectrum and the band could easily be attributed to a PAH. The HCO^+ molecule, which has been called "the most stable molecule in the Universe", provides a second example. The ground state has been studied with microwave spectroscopy (Woods et al. (1975); Bogey et al. (1981); Sastry et al. (1981)) and laser sideband (van den Heuvel & Dymanus (1982)) to 1 THz and the three fundamental vibrational modes have been studied with infrared spectroscopy (Davies & Rothwell (1984); Kawaguchi et al. (1985); Davies et al. (1984,?); Foster et al. (1984); Gudeman et al. (1983); Amano (1983); Liu et al. (1988)). However, the available data failed to reproduce the observed transitions at 800 GHz within their error bars or 5 times the measurement uncertainty (Pearson & Drouin (2006)). Lastly there is no data on the electronic transitions. Given that HCO^+ is abundant in the diffuse ISM (Liszt & Lucas (1994)) and the only two recent diffuse interstellar band assignments were to the not very complex CH molecule (Watson (2001)), it is astonishing

that the fundamental laboratory work remains to be done and that the lack of data is not glaringly apparent to those working in the field. A comprehensive database would address both issues.

3. Current Status

The status of molecular databases for NASA astronomy is sad at best. In the optical there is no data base, in the infrared there is no database and in the far-infrared there has been no funding to support databases for the last 6 years. In Europe the situation is not much better with ESA recently retracting their commitment to support CDMS for the next three years, even though the Herschel observational planning tool uses the JPL and CDMS databases. Virtual Observatories, Herschel, ALMA and SOFIA have all sought to address the problem, but so far there is no progress other than software to read what is already available into another data format. The recent Laboratory Astrophysics NRA calls explicitly solicit new research rather than data management efforts, so there has been no place to even apply for support. Unfortunately, database preparation requires an enormous amount of experience and expertise. As a result, the only real solution is to pay for the database work to be done or to expect each astronomer to spend a significant amount of time maintaining their own data. From the point of molecular physics, it makes the most sense to collect all the available information together since vibrational and electronic spectra ultimately determine or use the rotational and low lying hot-bands. The combined approach requires more expertise and effort but it does allow for the known state of knowledge to be tracked.

It will require 20-30 work years of effort to catalog what is known about astrophysical molecules. In just the rotational band the data on known molecules could be catalogued in a 2-5 work years of effort. However, the existing data is not complete and a significant amount of new data will have to be generated to support observations. Additionally there are a wide range of molecules that are highly desirable to search for, which should be cataloged as well. Cataloging all these results will require significantly more effort.

4. Conclusions

NASA, ESA and the NSF are spending billions of dollars building wonderfully powerful instruments with unprecedented exploration capability. Additionally, similar sums of money are planned to support observations and data analysis, but there has been little thought or planning of the laboratory work and databases that will be required to support these observatories. Currently, database efforts are not funded and there is no mechanism to get funding within the current NASA NRA structure. NASA missions, Herschel and SOFIA, have explicitly been instructed not to get into the laboratory astrophysics business and are

not doing so. As a result, individual instrument users have one of three choices 1) propose only simple observations where the molecular physics is known e.g. CO, 2) Learn the molecular physics themselves and keep their own catalogs, or 3) not fully exploit the data, ignore the discovery potential, and forget about potentially biogenic molecules.

NASA will pay a price for not funding a catalog effort. Spectroscopic observations will be incompletely and erroneously analyzed and fewer observers will able to perform the spectroscopy necessary to fully understand astronomical objects. Ultimately, this will translate into non-optimal designs for future missions. Requests of individual missions to catalog 100 years of spectroscopy for internal purposes is equally nearsighted, since molecular spectra cover multiple wavelengths. Cataloging the rotational, vibrational and electronic bands simultaneously allows all wavelengths to benefit from investigations at other wavelengths and facilitates rapid updates when better laboratory data become available. Since this cuts across wavelengths and missions it only makes sense for this data to be provided as a service like catalogs of astronomical objects.

The work described in this paper was performed at the Jet Propulsion Laboratory, California Institute of Technology under contract with the National Aeronautics and Space Administration

REFERENCES

Pickett, H.M., Poynter, R.L., Cohen, E.A., Delitsky, M., Pearson, J.C., & Müller, H.S.P., 1998, J. Quant. Spectrosc. Radiative Transfer 60, 883.
Müller, H.S.P., Schlöder, F., Stutzki, J., & Winnewisser, G., 2005, J. Mol. Struct., 742, 215
Woods, R.C., Dixon, T.A., Saykally, R.J.,& Szanto, P.G., 1999, Phys. Rev. Lett., 35, 1269
Bogey, M., Demuynck, C., & Destombes, J.L., 1981, Mol. Phys., 43, 1043
Sastry, K.V.L.N., Herbst, E., & De Lucia, F.C., 1981, J. Chem. Phys. 75, 4169
van den Heuvel, F.C., & Dymanus, A., 1982, Chem. Phys. Lett., 92, 21
Davies, P.B., & Rothwell, 1984, J. Chem. Phys., 81, 5239
Kawaguchi, K., Uamada, C., Saito, S., & Hirota, E., 1985, J. Chem. Phys., 82, 1750
Davies, P.B., Hamilton, P.A., & Rothwell, 1984, J. Chem. Phys., 81, 1598
Foster, S.C., McKeller, A.R.W., & Sears, T.J., 1984, J. Chem. Phys., 81, 578
Gudeman, C.S., Begemann, M.H., Pfaff, J., & Saykally, R.J., 1983, Phys. Ref. Lett., 50, 727
Amano, T., 1983, J. Chem. Phys., 79, 3595
Liu, D.-J., Lee, S.-T., & Oka, T., 1988, J. Mol. Spectrosc., 128, 236
Pearson, J.C., & Drouin, B.J., 2006, This volume
Liszt, H.S.,& Lucas, R., 1994, ApJ, 431, L131
Watson, J.K.G., 2001, ApJ, 555, 472

NASA LAW, February 14-16, 2006, UNLV, Las Vegas

Atomic Spectroscopic Databases at NIST

J. Reader, A. E. Kramida, & Yu. Ralchenko

National Institute of Standards and Technology, Gaithersburg, MD 20899-8422

jreader@nist.gov, akramida@nist.gov, yuri.ralchenko@nist.gov

ABSTRACT

We describe recent work at NIST to develop and maintain databases for spectra, transition probabilities, and energy levels of atoms that are astrophysically important. Our programs to critically compile these data as well as to develop a new database to compare plasma calculations for atoms that are not in local thermodynamic equilibrium are also summarized.

The NIST Physics Laboratory provides a number of atomic spectroscopic databases on the World-Wide-Web that are widely used in astrophysics. The data consist mainly of wavelengths, energy levels, and oscillator strengths that have been critically evaluated in the NIST Atomic Spectroscopy Data Center. These data play an important role in line identification, spectra modeling, and other astrophysical research. All databases can be accessed from the NIST Physics Laboratory home page http://www.physics.nist.gov, select Physical Reference Data.

Since the last Workshop, some of the existing databases were significantly expanded, and a number of new databases became available on the Web. The NIST **Atomic Spectra Database** (ASD) has been upgraded from version 2.0 to 3.0. It now contains detailed information on more than 75,000 energy levels and almost 130,000 spectral lines for ions of 99 elements. New large sets of data were recently added for the spectrum lines and energy levels of Ne I, Hg I and II, Be II, Xe and Rb in all ionization stages, highly-charged ions of the iron period of elements, Cu, Mo, and Kr (taken from Mon. 8 of J. Phys. Chem. Ref. Data), Zr III and IV, Ba I and II, and W I and II. Data for the transition probabilities of Ba I and II were also added.

Our program to carry out critical compilations of the spectra, transition probabilities, and energy levels of atoms of astrophysical interest also continues actively. A major reassessment of transition probabilities for Fe I and II (W. Wiese and J. Fuhr) has been completed

and is in press at the Journal of Physical and Chemical Reference Data (JPCRD). Recent work on transition probabilities for neutral and singly ionized C, N, and O is described in an accompanying paper by W. Wiese and J. Fuhr in these proceedings. Work on Na and Mg in all stages (D. Kelleher and L. Podobedova) is now in press at JPCRD and new compilations for Si and Al (D. Kelleher and L. Podobedova) will be submitted shortly.

For wavelengths and energy levels, a compilation of Kr in all stages of ionization (E. Saloman) is now in press at JPCRD as are compilations for Hg I (E. Saloman), and Rb in all stages (J. Sansonetti). The data for Hg I and Rb have already been added to ASD, and the addition of the data for Kr is now in progress. A compilation of Cs spectra in all stages (J. Sansonetti) is nearing completion. Similar compilations for Na, K, and Fr are in progress (J. Sansonetti). The compilations for alkali metals include transition probabilities, where available. An extensive compilation for Ne I (E. B. Saloman and C. Sansonetti) was recently published in JPCRD. Works on Ne II (A. Kramida and G. Nave) and Ne VIII (A. Kramida and M.-C. Buchet-Poulizac) are in press at the European Journal of Physics. Compilations for Ne III (A. Kramida and G. Nave) and Ne VII (A. Kramida and M.-C. Buchet-Poulizac) have already appeared in that journal. A compilation for W I and W II (A. Kramida and T. Shirai) was recently published in JPCRD, and work on the higher stages of W (A. Kramida and T. Shirai) will be submitted to JPCRD shortly. Also in press at JPCRD is work on Ga in all stages (T. Shirai, J. Reader, A. Kramida, and J. Sugar). A compilation for Be II (A. Kramida) was published recently in Physica Scripta. Work on B II and B III (A. Ryabtsev, I. Martinson, and A. Kramida) is in progress. A compilation of Ar in all stages (E. Saloman) is also in progress.

We have recently implemented a new relational database management system that allows a high level of data integration and consistency. Its innovative user interface provides convenient access to various parameters. Several new additions to the ASD interface should be of special value to astrophysicists. Among those is the online Saha-LTE spectrum generation tool, which allows calculation of plasma emission spectra under Saha-LTE equilibrium for user-defined values of electron density and temperature. The calculated spectrum can also be Doppler-broadened for arbitrary values of ion temperature. This also may be used for simulation of instrumental broadening. Fig. 1 shows a synthetic spectrum for ions of Fe with wavelengths calculated from the known energy levels and intensities as calculated for an electron temperature of 8 eV, an ion temperature of 1000 eV, and an electron density of 1×10^{22} cm^{-3}. As can be seen, under these conditions the spectrum is dominated by lines of Fe II.

Another feature of the new graphical interface is the availability of Grotrian diagrams. These diagrams provide an intuitive visualization of the atomic energy level structure and transitions, as well as direct access to the fundamental atomic data (energy levels, wavelengths, transition probabilities). Fig. 2 shows a Grotrian diagram for Na I constructed in real time from data in the database.

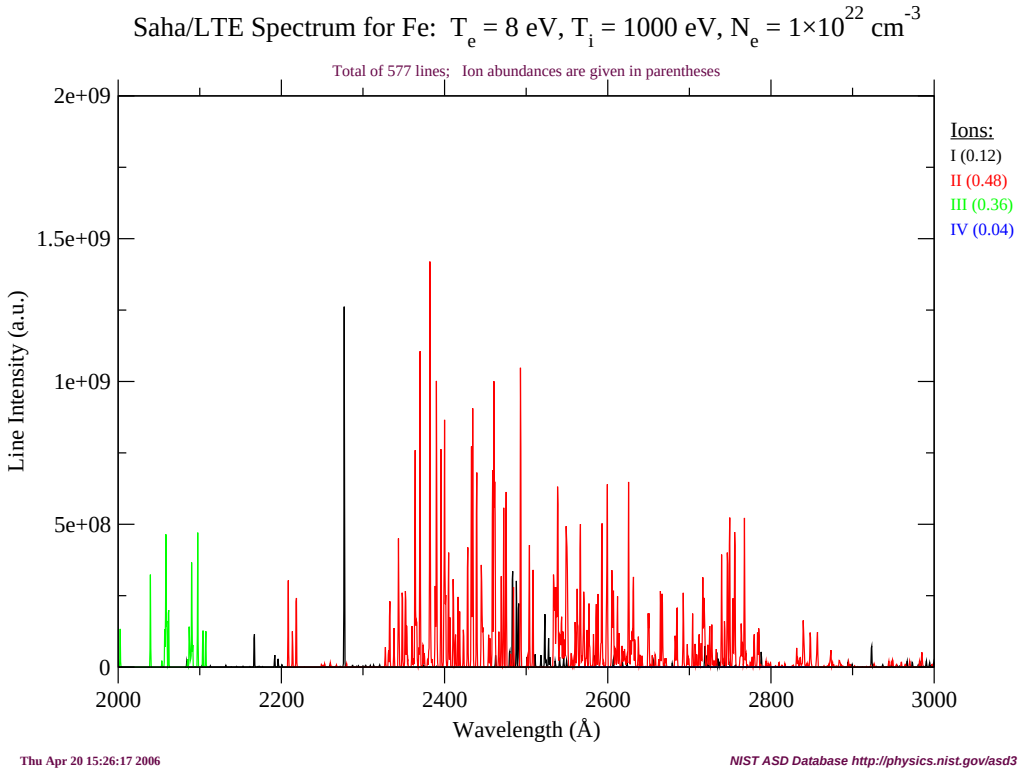

Fig. 1.— NIST ASD Database: Saha/LTE spectrum for Fe I-IV at electron density 10^{22} cm^{-3} and electron temperature 8 eV.

In recent years, three new databases became available. The first, **Handbook of Basic Atomic Spectroscopic Data**, now upgraded to v.1.1, provides the most frequently used atomic spectroscopic data in an easily accessible format. It includes data for the neutral and singly-ionized atoms of all elements hydrogen through einsteinium (Z = 1-99). Wavelengths, intensities, line classifications, and transition probabilities are given in a separate table for each element. The data for 12,000 lines of all elements are also collected into a finding list sorted by wavelength. This has now appeared as a journal paper in the JPCRD.

The second, **Spectral Data for the Chandra X-ray Observatory**, contains critically compiled wavelengths, energy levels, line classifications, and transition probabilities for ionized spectra of neon (Ne V to Ne VIII), magnesium (Mg V to Mg X), silicon (Si VI to Si XII), and sulfur (S VIII to S XIV) in the 20 Å to 170 Å region. These tables provide data of interest for the Emission Line Project in support of analyses of astronomical data from the Chandra X-Ray Observatory. The transition probabilities were obtained mainly from recent sophisticated calculations carried out with complex computer codes. These data have also appeared as journal papers in JPCRD.

The third is our **SAHA Plasma Population Kinetics Database**. This database

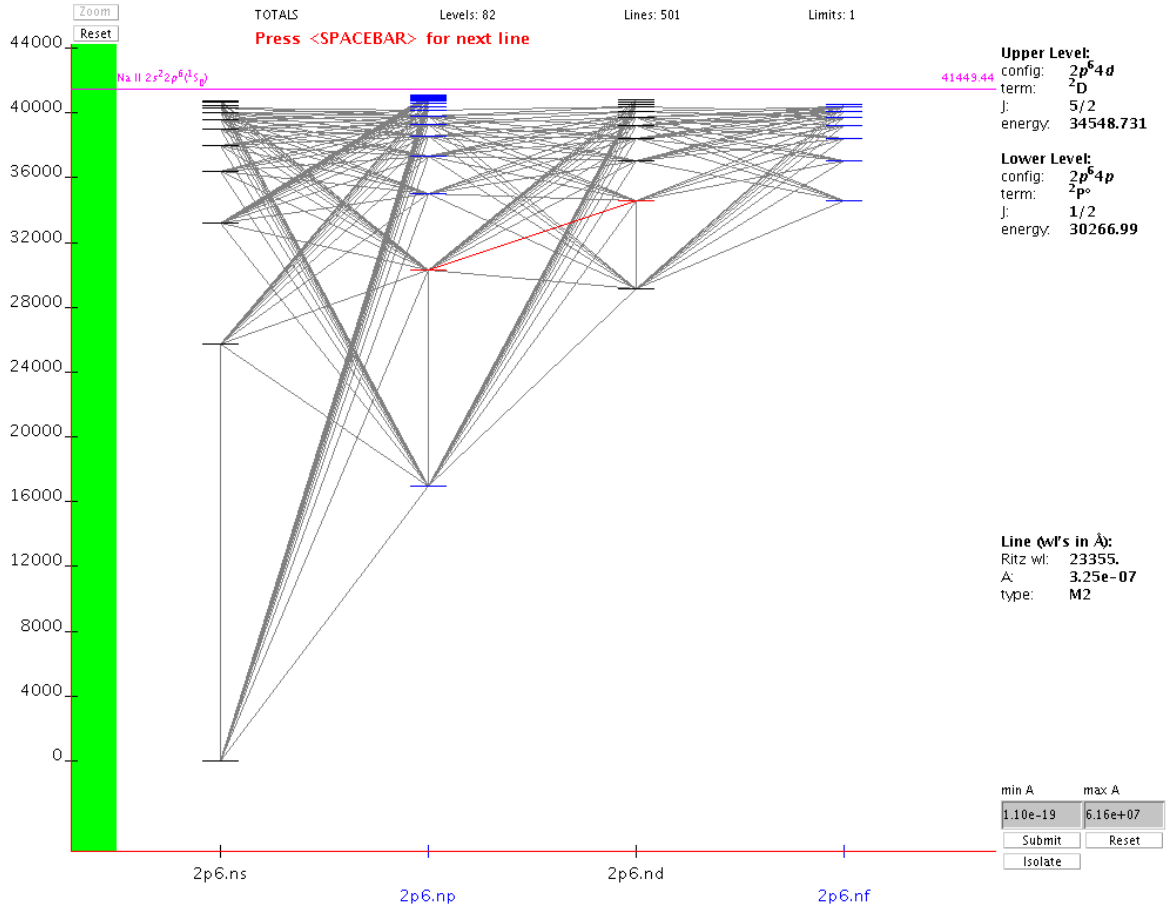

Fig. 2.— NIST ASD Grotrian diagram for radiative transitions in Na I.

provides benchmark theoretical results for population kinetics of various plasmas under non-local-thermodynamic-equilibrium conditions. Results of the 3rd Non-LTE Code Comparison Workshop held at NIST in December 2003 are given there. Parameters available for comparisons include mean ion charge, ion populations, synthetic spectra, and rates of collisional and radiative processes. The database will be complemented by a collisional-radiative code to allow online calculations in real time.

Work continues on our bibliographic databases for atomic transition probabilities and spectral line broadening, as well as our database on electron impact ionization cross sections. We expect our bibliographic database on energy levels and spectral lines to be available in the near future.

Work on these databases and critical compilations is supported in part by the National Aeronautics and Space Administration and by the Office of Fusion Energy Sciences of the U. S. Department of Energy.

NASA LAW, February 14-16, 2006, UNLV, Las Vegas

Laboratory Spectroscopy of Large Carbon Molecules and Ions in Support of Space Missions

F. Salama, X. Tan, L. Biennier[1], J. Cami & J. Remy[2]

NASA Ames Research Center, Space Science Division, Moffett Field, CA, 94035

Farid.Salama@nasa.gov, xtan@mail.arc.nasa.gov,
ludovic.biennier@univ-rennes1.fr, jcami@mail.arc.nasa.gov, jremy@epo.org

ABSTRACT

One of the major objectives of Laboratory Astrophysics is the optimization of data return from space missions by measuring spectra of atomic and molecular species in laboratory environments that mimic interstellar conditions (WhitePaper (2002, 2006)). Among interstellar species, PAHs are an important and ubiquitous component of carbon-bearing materials that represents a particularly difficult challenge for gas-phase laboratory studies. We present the absorption spectra of jet-cooled neutral and ionized PAHs and discuss the implications for astrophysics. The harsh physical conditions of the interstellar medium have been simulated in the laboratory. We are now, for *the first time*, in the position to *directly* compare laboratory spectra of PAHs and carbon nanoparticles with astronomical observations. This new phase offers tremendous opportunities for the data analysis of current and upcoming space missions geared toward the detection of large aromatic systems (HST/COS, FUSE, JWST, Spitzer).

1. Introduction, Laboratory Approach & Results

Polycyclic aromatic hydrocarbons (PAHs) constitute the building blocks of interstellar dust grains and play an important role in mediating the energetic and chemical processes in the interstellar medium (ISM). Their specific contribution to the interstellar extinction, and in particular to the diffuse interstellar bands (DIBs) remains, however, unclear. The DIBs are ubiquitous spectral absorption features observed in the line of sight of stars that

[1]current address: PALMS, UMR 6627, Rennes 1 University, Campus de Beaulieu, 35042 Rennes, France.

[2]current address: EPO, European Patent Office, 2280 HV, Rijswijk, The Netherlands - EU

are obscured by diffuse interstellar clouds. More than 300 bands have been reported to date spanning from the near UV to the near IR with bandwidths ranging from 0.4 to 40 Å(Tielens & Snow (1995)). The present consensus is that the DIBs arise from gas-phase organic molecules and ions that are abundant under the typical conditions reigning in the diffuse ISM. The PAH hypothesis is consistent with the cosmic abundance of Carbon and Hydrogen and with the required photostability of the DIB carriers against the strong VUV radiation field in the diffuse interstellar clouds.

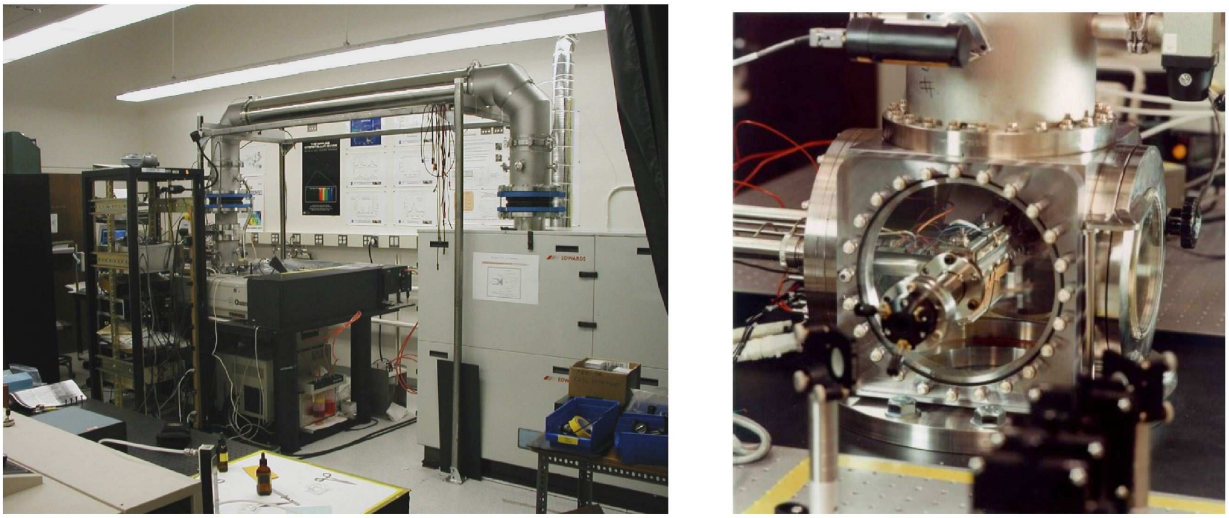

Fig. 1.— *Left side:* Current configuration of the Laboratory Facility. *Right side:* close-up view of the Chamber consisting of a Pulsed Discharge Nozzle coupled to a Cavity Ringdown Spectrometer apparatus and Reflectron time-of-flight mass spectrometer.

To properly address the issue of the identification of the DIBs, astronomical observations must be compared to laboratory spectra that are measured in an astrophysically relevant environment i.e. with the molecules/ions isolated, cold and in the *gas phase*. This task represents a serious experimental challenge because PAHs are large, non-volatile molecules. Furthermore, due to the ultra-fast non-radiative processes of internal electronic conversion that take place in these large molecular systems, detection by laser-induced fluorescence or by multiphoton excitation cannot be employed. Because of all these technical limitations, it was only recently that direct measurements of the absorption spectra of cold neutral and ionized PAHs in the gas-phase were achieved (Romanini et al. (1999); Biennier et al. (2003, 2004); Tan & Salama (2005a,b, 2006); Huisken (2006)). Our approach, relies on the association of a cold plasma source (pulsed discharge nozzle) with high sensitivity direct absorption techniques (cavity ring down spectroscopy, CRDS, multiplex integrated cavity output spectroscopy (MICOS) and time-of-flight mass spectrometry and is independent of inter- and intra- molecular processes (Salama et al. (2006)). The experimental approach has been described previously (Biennier et al. (2003, 2004); Tan & Salama (2005a)). Briefly, the pulsed discharge nozzle combines a supersonic slit jet that cools down the carrier gas

seeded with aromatics ($\sim 1\%$), with two electrodes that produce a discharge in the stream of the planar expansion to ionize the mixture when needed. The PAH vapor pressure is increased by heating a pick-up cell that contains the sample upstream the Argon flow. A cavity ringdown spectrometer probes the expansion several mm downstream with a sub-ppm absorption sensitivity. A reflectron time-of-flight (RETOF) mass spectrometer is coupled to the chamber to detect the radicals and particles that are formed in the discharge (Figure 1). We report the experimental results regarding the electronic spectroscopy of several cold neutral and ionized PAH in the gas phase that have been obtained with this new approach (Biennier et al. (2003, 2004); Tan & Salama (2005a,b, 2006)).

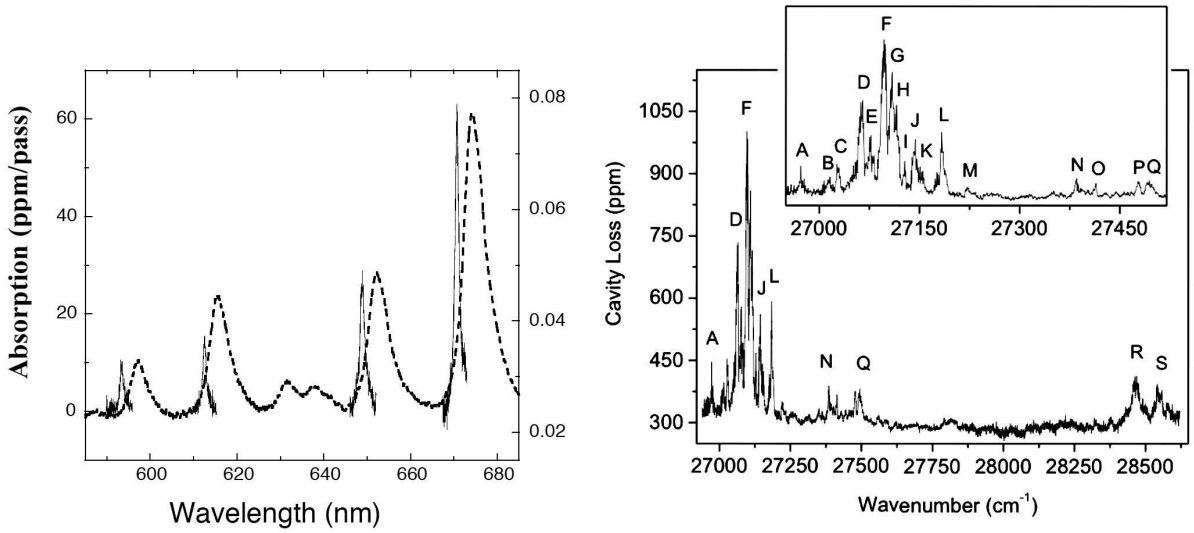

Fig. 2.— *Left:* Comparison of CRDS (Biennier et al. (2003)) and MIS/Ne (Salama & Allamandola (1991)) spectra. The interactions of the trapped Np^+ with the atoms of the solid neon matrix induce a frequency shift and a spectral broadening of the electronic spectrum. This figure illustrates dramatically the need for gas-phase experiments for a decisive, unambiguous, identification of the DIBs. MIS remains however critical for the pre-selection of potential candidates. *Right:* Cavity ringdown spectrum of the neutral PAH benzoperylene ($C_{22}H_{12}$), the largest PAH molecule measured to date in the gas phase (Tan & Salama (2005b)).

PAH ions: The electronic spectra of the cold naphthalene ($C_{10}H_8^+$), acenaphthene ($C_{12}H_{10}^+$), pyrene ions ($C_{16}H_{10}^+$) and some derivatives, methyl pyrene ($C_{17}H_{12}^+$) and carboxaldehyde pyrene ($C_{17}H_{10}O^+$) were measured in order to derive their *intrinsic* characteristics for comparison with interstellar spectra. A typical spectrum is shown in Figure 2 where the gas-phase CRD spectrum is compared to the solid matrix spectrum illustrating the strongly perturbing effect induced by the phonons of the solid lattice on band profiles and bandwidths. The vibronic bands are typically broad and without substructure, a characteristic of non-radiative intramolecular relaxation processes that explains the UV photon pumping mechanism that occurs in the ISM and the observations of the UIR emission by radiative

cascade. Detailed analysis of the band profile leads to the determination of FWHM of of the order of 25 cm^{-1}. This value corresponds to a 220 fs ultra fast relaxation time and is very close to the value derived for the strong 4428 ÅDIB (Snow et al. (2002)). We have also demonstrated that the discharge does not affect the vibrational temperature of the aromatic ions formed in the cold plasma expansion (Remy et al. (2005); Biennier et al. (2006)).

Neutral PAHs: The electronic spectra of the cold neutral Methyl Naphthalene ($C_{11}H_{10}$), Acenaphthene ($C_{12}H_{10}$), Phenanthrene ($C_{14}H_{10}$), Pyrene ($C_{16}H_{10}$), Perylene ($C_{20}H_{12}$), Pentacene ($C_{22}H_{14}$) and Benzoperylene ($C_{22}H_{12}$) were also measured in order to compare directly with astronomical spectra of DIBs. A typical spectrum is shown in Figure 2. By comparison with astronomical observations we were able to derive upper limits to the abundances of individual PAHs in the observed lines of sight. Values of the order of 10^{-4} to 10^{-6} are derived for the fraction of cosmic carbon locked up in these PAHs.

2. Perspectives and Conclusions

These preliminary results strongly validate our original experimental approach associating a cold plasma source with a cavity ringdown spectrometer and a time-of-flight mass spectrometer. These experiments provide first hand data on the spectroscopy and on the molecular dynamics of *free, cold* large carbon-containing molecules and ions in the gas phase. We are now, for the first time, in the position to directly search for *individual* PAH molecules and ions in in astronomical observations in the UV-NIR range. This new phase offers tremendous opportunities for the data analysis of current and upcoming space missions.

This work is supported by the NASA Astronomy and Physics Research and Analysis (APRA) Program of the Science Mission Directorate. This research was performed while X. Tan, J. Cami and L. Biennier held NRC awards at NASA-Ames Research Center and J. Remy a NASA/NWO internship at NASA-Ames. The authors wish to acknowledge the outstanding technical support of R. Walker.

REFERENCES

Salama, F., Leckrone, D., Mathis, J., McGrath, M., Miller, R., Phillips, T., Sanders, W., Smith, P., Snow, T., Tielens, A. 2002, Laboratory Astrophysics White Paper, Proceed. NASA Laboratory Astrophysics Workshop, Salama (ed.), NASA/CP 211863, 3

Federman, S., Brickhouse, N., Kwong, V., Salama, F., Savin, D., Stancil, P., Weingartner, J., Ziurys, L. 2006, Laboratory Astrophysics White Paper, Proceed. NASA Laboratory Astrophysics Workshop, Salama (ed.), NASA/CP in press

Salama, F. et al. 2006, Astrochemistry: From Laboratory Studies to Astronomical Observations, R. Kaiser et al. Eds, AIP, in press

Salama, F. & Allamandola, L. J. 1991, J. Chem. Phys., 94, 6964
Tielens, A. G. G. M. & Snow, T. P., eds. 1995, The Diffuse Interstellar Bands (Dordrecht, the Netherlands: Kluwer Academic Publishers)
Romanini, D., Biennier, L., Salama, F., Allamandola, L. J., & Stoeckel, F. 1999, Chem. Phys. Lett., 303, 165
Snow T., Zukowski, D., Massey, P. 2002, Astrophys. J. 578, 877
Huisken F. 2006, this volume, Proceed. NASA Laboratory Astrophysics Workshop, NASA/CP, in press
Tan, X. & Salama, F. 2005a, J. Chem. Phys. 122, 084318
Tan, X. & Salama, F. 2005b, J. Chem. Phys. 123, 014312
Tan, X. & Salama, F. 2006, Chem. Phys. Lett. in press
Biennier, L., Salama, F., Allamandola, L., Scherer, J. 2003, J. Chem. Phys. 118, 7863
Biennier, L., Salama, F., Gupta, M., O'Keefe, A. 2004, Chem. Phys. Lett. 387, 287
Biennier, L., Benidar, A., Salama, F. 2006, Chem. Phys. in press
Remy J., Biennier L., Salama F. 2005, IEEE Transactions on Plasma Science 33, 554.
Cami, J., Tan, X., Biennier, L., Salama, F. 2005, In Astrochemistry Throughout the Universe, IAU Symposium 231, Lis, Blake & Herbst eds. Cambridge University Press.

NASA LAW, February 14-16, 2006, UNLV, Las Vegas

Cosmological Implications of the Uncertainty in Astrochemical Rate Coefficients

S. C. O. Glover[1,2], D. W. Savin[3], and A.-K. Jappsen[2]

[1] *American Museum of Natural History, New York, NY, USA*
[2] *Astrophysikalisches Institut Potsdam, Germany*
[3] *Columbia Astrophysics Laboratory, New York, NY, USA*

ABSTRACT

The cooling of neutral gas of primordial composition, or with very low levels of metal enrichment, depends crucially on the formation of molecular coolants, such as H_2 and HD within the gas. Although the chemical reactions involved in the formation and destruction of these molecules are well known, the same cannot be said for the rate coefficients of these reactions, some of which are uncertain by an order of magnitude. Here we discuss two reactions for which large uncertainties exist – the formation of H_2 by associative detachment of H^- with H and the destruction of H^- by mutual neutralization with protons. We show that these uncertainties can have a dramatic impact on the effectiveness of cooling during protogalactic collapse.

1. Primordial H_2 Chemistry

In the early universe, during the epoch of first star formation H_2 forms primarily via the radiative association process

$$H + e^- \rightarrow H^- + h\nu \tag{1}$$

followed by the associative detachment reaction

$$H^- + H \rightarrow H_2 + e^-. \tag{2}$$

For gas with a high fractional ionization, H^- is also destroyed rapidly by

$$H^- + H^+ \rightarrow H + H \tag{3}$$

However, the rate coefficients for reactions 2 and reaction 3 are both highly uncertain, as shown respectively in figure 1 below. Here we report on some of the cosmological implications of these uncertainties. A more detailed discussion is given in Glover et al. (2006).

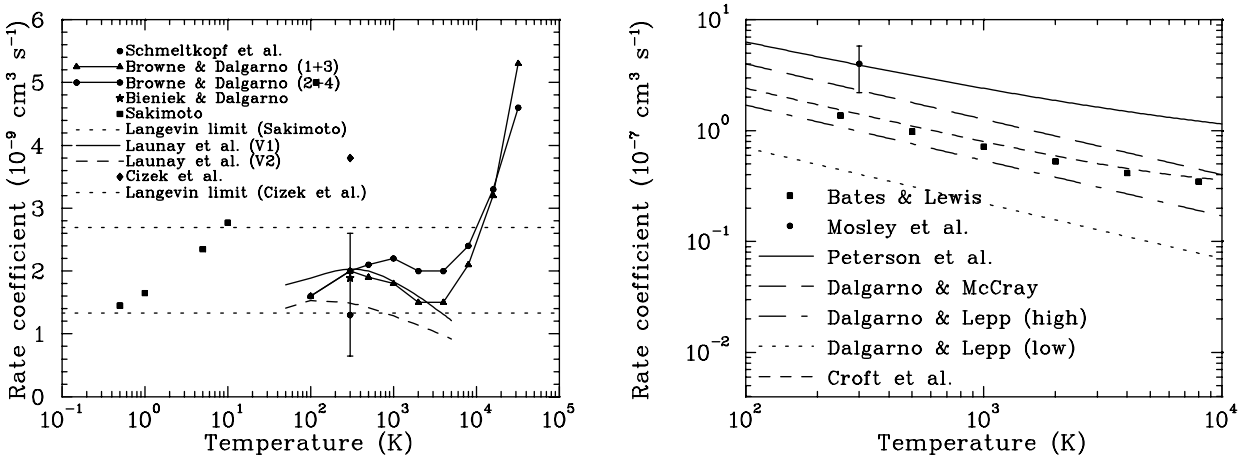

Fig. 1.— A summary of the various values found in the literature for the associative detachment rate coefficient for reaction 2 (left) and the mutual neutralization rate coefficient for reaction 3 (right). See Glover et al. (2006) for a fuller discussion.

2. Simulations

To study the impact of these astrochemical rate coefficient uncertainties, we have simulated the chemistry, cooling, and collapse of initially ionized gas into small protogalactic halos. Our simulations use a modified version of the GADGET smoothed particle hydrodynamics (SPH) code (Springer et al. 2001), to which we have added a treatment of primordial cooling and chemistry. For full details of the code see Glover et al. (2006). We simulate collapse at $z = 20$ into 10^7 $M_\odot$ dark matter halos, with various levels of background radiation. For each set of parameters, we perform 9 runs, with different combinations of values for the associative detachment and mutual neutralization rate coefficients. Between them, these combinations span the full range of plausible values.

We initialized each of our simulations at a redshift z = 20 and allowed them to run for 220 Myr; given our adopted cosmological parameters, this interval corresponds to approximately 1.25 Hubble times, with the simulations terminating at a redshift $z = 11.2$. Protogalaxies that fail to cool and collapse during this interval are unlikely to get the chance to do so thereafter, as the typical interval between major mergers of dark matter halos is of the order of a Hubble time (Lacey & Cole 1993).

3. Results

Simulations were carried out for a wide range of initial conditions. A full discussion and presentation of our results is given in Glover et al. (2006). Representative results are shown in figure 2 for the model predicted central H_2 fractional abundance of the primordial gas

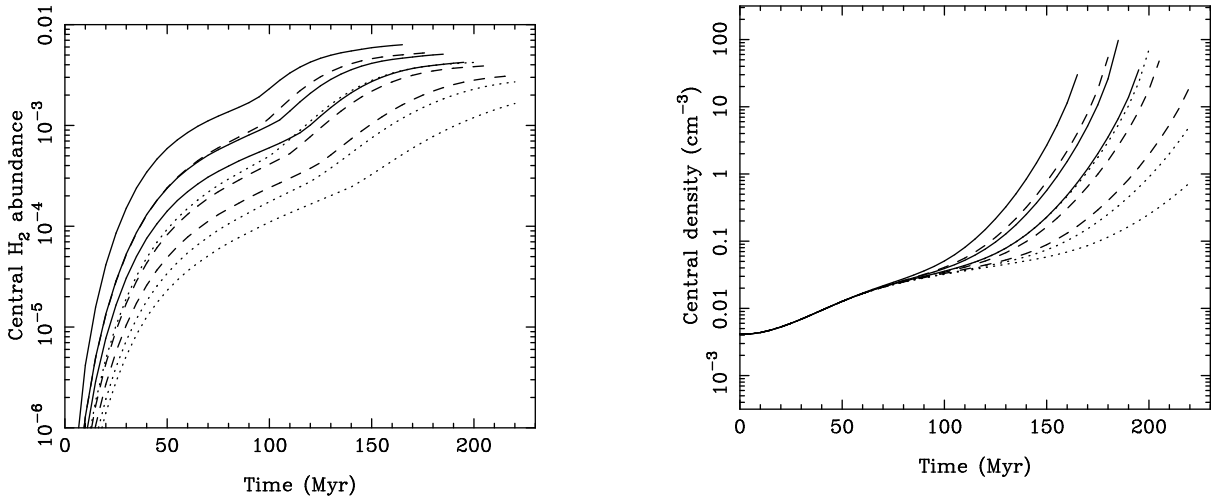

Fig. 2.— The evolution of the central H_2 abundance (left) and density (right) of a primordial gas cloud in a set of runs performed without an ultraviolet background. Mutual neutralization rates for these runs were taken from: Dalgarno & Lepp (1987) - solid lines; Croft et al. (1999) - dashed lines; and Peterson et al. (1971) - dotted lines. For each choice of mutual neutralization rate, three different associative detachment rates were used – the measured value of Schmeltekopf et al. (1967), which has a factor of at least two uncertainty, along with values 3.85 times larger and 2 times smaller to represent the range of published values for this reaction.

cloud and for the central density of the gas.

4. Summary

We have found that uncertainties in the associative detachment and mutual neutralization rate coefficients lead to uncertainties in the H_2 formation rate and the final H_2 fraction. These uncertainties have a measurable impact on the thermal and dynamical evolution of the collapsing gas. Though not shown here, the effect is particularly large when a UV field is present. In those cases, the final H_2 abundance may be uncertain by as much as a factor of 100. In summary, the predicted ability of the gas to cool in a given model protogalaxy depends in part on the choice of chemical rate coefficients used.

SCOG was supported in partly by a NASA Education grant and an NSF AST grant. DWS was supported in part by a NASA APRA grant. AKJ was supported in part by the Emmy Noether Program of the Deutsche Forschungsgemeinschaft.

REFERENCES

Bates, D. R., & Lewis, J. T. 1955, Proc. Phys. Soc. A, 68, 173
Bieniek, R. J., & Dalgarno, A. 1979, ApJ, 228, 635
Browne, A., & Dalgarno, A. 1969, J. Phys. B, 2, 885
Čížek, M., Horáček, J., & Domcke, W. 1998, J. Phys. B, 31, 2571
Croft, H., Dickinson, A. S., & Gadea, F. X. 1999, MNRAS, 304, 327
Dalgarno, A., & McCray, R. A. 1973, ApJ, 181, 95
Dalgarno, A., & Lepp, S. 1987, in Astrochemistry, ed. M. S. Vardya & S. P. Tarafdar, Dordrecht: Reidel, 109
Glover, S. C. O., Savin, D. W., & Jappsen, A.-K. 2006, ApJ, 640, 553
Lacey, C., & Cole, S. 1993, MNRAS, 262, 627
Launay, J. M., Le Dourneuf, M., & Zeippen, C. J. 1991, A&A, 252, 842
Moseley, J., Aberth, W., & Peterson, J. R. 1970, Phys. Rev. Lett. 24, 435
Peterson, J. R., Aberth, W. H., Moseley, J. T., & Sheridan, J. R. 1971, Phys. Rev. A, 3, 1651
Sakimoto, K. 1989, Chem. Phys. Lett., 164, 294
Schmeltekopf, A. L., Fehsenfeld, F. C., & Ferguson, E. E. 1967, ApJ, 118, L155
Springel, V., Yoshida, N., & White, S. D. M. 2001, NewA, 6, 79

NASA LAW, February 14-16, 2006, UNLV, Las Vegas

Studying Atomic Physics Using the Nighttime Atmosphere as a Laboratory

B. D. Sharpee, T. G. Slanger, D. L. Huestis, & P. C. Cosby

Molecular Physics Laboratory, SRI International, Menlo Park, CA 94025

brian.sharpee@sri.com

ABSTRACT

A summary of our recent work using terrestrial nightglow spectra, obtained from astronomical instrumentation, to directly measure, or evaluate theoretical values for fundamental parameters of astrophysically important atomic lines.

1. Introduction

While the terrestrial nightglow is dominated both in total emission intensity and numbers of emission lines by molecular emitters such as OH and O_2, emission lines corresponding to atomic transitions are also prevalent. The optically forbidden [O I] $2p^4\ {}^1D_2$-$^1S_0$ λ5577 "green line" and [O I] $2p^3\ {}^3P_{2,1}$-$^1D_2$ $\lambda\lambda$6300,6364 "red" lines are strong and well-known components of the nightglow. The high sensitivity of astronomical instrumentation also reveals much weaker features such as [N I] $2p^4\ {}^4S^o_{3/2}$-$^2D^o_{3/2,5/2}$ $\lambda\lambda$5198,5200, the [O II] $2p^3\ {}^2D^o_{3/2,5/2}$–$^2P^o_{1/2,3/2}$ $\lambda\lambda$7320,7330 doublets, and permitted transitions of neutral O arising from electron radiative recombination of O^+.

Many of these lines are present in low-ionization astrophysical plasmas such as those found in planetary nebulae and H II regions, and are used as diagnostics of their kinetics, physical conditions, and abundances. The use of these lines as diagnostics assumes accurate knowledge of their fundamental atomic parameters, namely wavelengths, spontaneous emission coefficients, and electron recombination cross-sections. Given that many of the emitting levels are metastable and therefore difficult to observe in the laboratory, a great reliance has been placed on theoretical calculations of these parameters. However, due to the rarefied nature of the atmosphere and the abundance of emitters in the nightglow layers, the nighttime sky acts as a laboratory where these parameters can either be directly measured or inferred, and compared to theoretical values.

Table 1: HIRES Measurements of Atomic Nightglow Line Wavelengths versus NIST

Atomic Line	HIRES λ (Å)	NIST λ (Å)	HIRES-NIST λ (Å)
Slanger et al., *J. Chem. Phys.*, 2000			
[O I] $2p^4\ ^1D_2$–$2p^4\ ^1S_0$	5577.335	5577.339	-0.004
[O I] $2p^4\ ^3P_2$–$2p^4\ ^1D_2$	6300.302	6300.304	-0.002
[O I] $2p^4\ ^3P_1$–$2p^4\ ^1D_2$	6363.780	6363.776	0.004
[N I] $2p^3\ ^4S^o_{3/2}$–$2p^3\ ^2D^o_{3/2}$	5197.922	5197.902	**0.020**
[N I] $2p^3\ ^4S^o_{3/2}$–$2p^3\ ^2D^o_{5/2}$	5200.281	5200.257	**0.024**
Sharpee et al., *Astrophys J.*, 2004			
[O II] $2p^3\ ^2D^o_{5/2}$–$2p^3\ ^2P^o_{1/2}$	7319.044±0.004	7318.92	**0.124**
[O II] $2p^3\ ^2D^o_{3/2}$–$2p^3\ ^2P^o_{1/2}$	7320.121	7319.99	**0.131**
[O II] $2p^3\ ^2D^o_{5/2}$–$2p^3\ ^2P^o_{3/2}$	7329.675	7329.67	0.005
[O II] $2p^3\ ^2D^o_{3/2}$–$2p^3\ ^2P^o_{3/2}$	7330.755	7330.73	**0.020**

2. Forbidden Line Wavelengths

The High Resolution Echelle Spectrometer (HIRES) on the Keck I telescope, W.M. Keck Observatory, has provided a wealth of individual nightglow spectra, which have been co-added together (∼100 hours) to provide a very high signal-to-noise spectrum that has been proven useful for transition wavelength measurements (Slanger et al. 2000). Wavelength calibration by ThAr lamp and comparison with numerous OH Meinel band system nightglow line wavelengths provide a level of accuracy of about 0.004Å. Comparisons with National Institute of Standards and Technology (NIST) wavelengths for various atomic lines, listed in Table 1, show good agreement for some lines, but poorer agreement for others.

Other HIRES nightglow spectra, supplemented by selected planetary nebula and H II region spectra, have been used to establish new energy levels for the $2p^3$ ground electron configuration of O II, and for inferring new wavelengths for the [O II] $\lambda\lambda$7320,7330 doublet lines (Sharpee et al. 2004). As can be seen in Table 1, the difference between NIST and observed values is quite substantial (upwards of 5.4 km s^{-1}) adversely affecting, for example, the use of these lines as a Orion Nebula outflow velocity indicator (Baldwin et al. 2000).

3. Diagnostic Line Intensity Ratios

Nightglow spectra from HIRES and the Echellette Spectrograph and Imager (ESI) on Keck II, have been used to measure the optically forbidden line intensity ratios [O I] λ6300/λ6364 and [N I] λ5198/5200. While not providing a direct determination of these lines' spontaneous emission coefficients, these measurements allow discrimination between competing and sometimes widely varying theoretical values.

For [N I] λ5198/λ5200, the observed value, 1.759±0.014, departs significantly from that

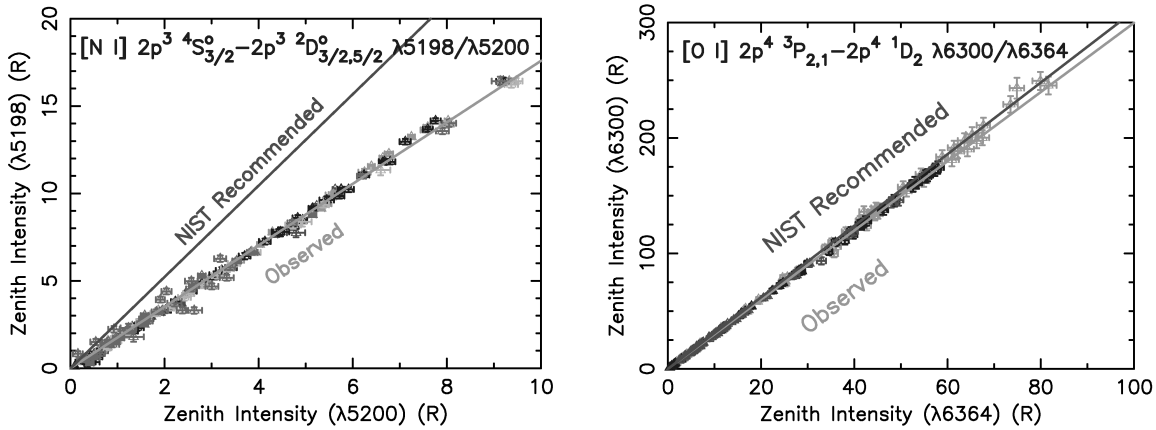

Fig. 1.— LEFT: [N I] λ5198/λ5200 intensity ratio from 190 HIRES and ESI nightglow spectra, best fit (1.759), and ratio determined from NIST spontaneous emission coefficients (2.61). RIGHT: Observed [O I] λ6300/λ6364, best fit (2.997), and NIST (3.10).

calculated with the spontaneous emission coefficients recommended by NIST (2.61), as is seen in Figure 1 (Sharpee et al. 2005). The ratio is used as an electronic density diagnostic, and the difference in densities determined using the NIST coefficients and those yielding the best agreement with observation can reach an order of magnitude for an observed ratio at typical nebular temperatures. By contrast, the observed [O I] λ6300/λ6364 ratio of 2.997$\pm$0.016 shows better agreement with the consensus theory value of $\sim$3.1 including NIST, as is seen in Figure 1 (Sharpee & Slanger 2006), but is slight lower reflecting the subtle effects of the inclusion of relativistic corrections to the magnetic dipole operator made during the recent coefficient calculation of Storey & Zeippen (2000).

4. Weak Permitted Lines From Electron Radiative Recombination of O^+

HIRES and ESI spectra have revealed numerous weak permitted lines of neutral oxygen that are produced by electron radiative recombination of O^+ to excited levels, and subsequent radiative cascade (Slanger et al. 2004). Recombination lines, while generally much weaker than their forbidden counterparts in planetary nebulae and H II regions, are the lines of choice for abundance determinations due to their insensitivity to variations in electron temperature and density along a line of sight through a nebula.

The effective recombination coefficients that directly link the intensities of these lines with parental abundances combine several fundamental parameters, including electron recapture cross-sections and cascade branching ratios. Line intensities from both the triplet and quintet sequences measured in HIRES and ESI spectra are found to be proportional to their effective recombination coefficients (Escalante & Victor 1992) by the same constant, the

product of electron and O^+ densities, which in turn yields a sensible O^+ abundance for conditions likely to prevail in the ionosphere at the time of the observation. This validates their coefficient calculation methods, providing greater confidence in similar calculations made for other astrophysically important ions.

This work was supported by NSF grant ATM-0221700, NSF CEDAR program grant ATM-0123136 and the NASA Office of Space Science.

REFERENCES

Baldwin, J.A. et al. 2000, ApJS, 129, 229

Escalante, V. & Victor G. A. 1992, Planet. Space Sci., 40, 1705

Sharpee, B. D., Slanger, T. G., Huestis, D. L., & Cosby, P. C. 2004, ApJ, 606, 605

Sharpee, B. D., Slanger, T. G., Cosby, P. C.,& Huestis, D. L. 2005, Geophys. Res. Lett., doi:10.1029/2005GLO23044, L12106

Sharpee, B. D. & Slanger T. G. 2006, J. Phys. Chem. A, in press

Slanger, T. G., Huestis, D. L., Cosby, P. C., & Osterbrock, D. E. 2000, J. Chem. Phys., 113, 8514

Slanger, T. G., Cosby, P. C., & Huestis, D. L. 2004, J. Geophys. Res., doi:10.1029/2004JA010556, A10309

Storey, P. J. & Zeippen, C. J. 2000, MNRAS, 312, 813

NASA LAW, February 14-16, 2006, UNLV, Las Vegas

New Measurements of Doubly Ionized Iron Group Spectra by High Resolution Fourier Transform and Grating Spectroscopy

D. G. Smillie[1], J. C. Pickering, & R. J. Blackwell-Whitehead

Blackett Laboratory, Imperial College, London SW7 2BW, United Kingdom

darren.smillie@imperial.ac.uk, j.pickering@imperial.ac.uk, r.blackwell@imperial.ac.uk

Peter L. Smith

Harvard-Smithsonian Center for Astrophysics, 60 Garden Street, Cambridge, MA 02138, USA

plsmith@cfa.harvard.edu

G. Nave

National Institute of Standards and Technology (NIST), Gaithersburg, MD 20899, USA

gnave@nist.gov

ABSTRACT

We report new measurements of doubly ionized iron group element spectra, important in the analysis of B-type (hot) stars whose spectra they dominate. These measurements include Co III and Cr III taken with the Imperial College VUV Fourier transform (FT) spectrometer and measurements of Co III taken with the normal incidence vacuum spectrograph at NIST, below 135 nm. We report new Fe III grating spectra measurements to complement our FT spectra. Work towards transition wavelengths, energy levels and branching ratios (which, combined with lifetimes, produce oscillator strengths) for these ions is underway.

1. Astrophysical Applications

Huge improvements in the quality of astrophysical spectra in recent years have not, in many cases, been matched by corresponding improvements in the laboratory measurements necessary to fully interpret them. Space-based spectrographs such as those onboard the

[1]Also affiliated to: Smithsonian Astrophysical Observatory, 60 Garden Street, Cambridge, MA 02138, USA

Hubble Space Telescope (HST) — the Goddard High Resolution Spectrograph (GHRS) and its successor, the Space Telescope Imaging Spectrograph (STIS) — have pushed observations far into the vacuum UV (VUV) and, together with ground-based spectrographs such as HIRES at the Keck 1 telescope, are responsible for spectra of unprecedented resolution. Current laboratory measurements however are, in many cases, of too low an accuracy or lacking entirely in spectral regions required to interpret these astrophysical spectra accurately. Transition wavelengths with an uncertainty of a few parts in 10^7 and oscillator strengths accurate to within 10% are urgently needed by astronomers to interpret observations at high resolution.

Due to their relatively high abundance and line rich spectra, the Fe (3d) group elements dominate observed stellar opacity. Our measurements have included many neutral and singly ionized elements (for example, Cr I, Fe I, V I and II, Co I and II, Mn I and II and Ti II) in response to the above data needs. We have also undertaken a program of extensive measurements of doubly ionized Fe group elements, including Fe III, Co III and Cr III. The doubly ionized transition elements are important because they dominate the VUV region of hot (B-type) star spectra and the existing laboratory measurements are extremely poor.

2. Laboratory Measurements

A Fourier transform (FT) spectrometer (FTS) is based on a Michelson interferometer and offers the combination of a large free spectral range and high resolution. The unique high resolution Imperial College (IC) VUV FTS see (Pickering (2002)) uses a MgF_2 beamsplitter allowing measurements down to a world-record short wavelength of 135 nm in the VUV wavelength region. Transition wavelengths with an uncertainty of a few parts in 10^8 are achievable. The IC VUV FTS has a resolving power of 2,000,000 at 200 nm, corresponding to a resolution limit of 0.0001 nm. A hollow cathode lamp is used to excite neutral and singly ionized spectra, but this is unable to excite the doubly ionized species. For these, we use a Penning discharge lamp (PDL) (Heise *et al* (1994)) which provides the stable intensity output necessary for measurements by FTS.

With an FTS, the contribution to the noise in each line is distributed throughout the spectrum, thus producing a uniform noise level that can sometimes mask weaker lines. When this is the case, and also for measurements below the FTS wavelength cut-off (135 nm), we use the Normal Incidence Vacuum Spectrograph (NIVS) located at the National Institute of Standards and Technology (NIST), Maryland, USA. We recorded the NIVS spectra using phosphor image plates (see Reader *et al* (2000)) instead of photographic plates. These have the advantages over photographic media of greater availability, comparative sensitivity, and crucially, a linear intensity response that allows branching ratios to be calculated from measured intensities. Another advantage of the image plates is that they can be scanned

several times which allows stronger lines to be resolved, avoiding saturation effects observed with photographic plates.

3. Results

Co III & Cr III: 4p-4s Co III spectra, intensity calibrated with a D_2 lamp in the range 150 to 300 nm, have been recorded using the IC VUV FTS and the PDL. Image plate spectra have also been recorded for Co III in the range from about 250 nm down to below the ionization limit (approximately 37 nm). Analysis is underway. An example of a scanned image plate using the PDL with Co cathodes is shown in Fig. 1, and a spectrum extracted from one of the image plate tracks in shown in Fig. 2. Additional intensity calibrated, measurements of Co III spectra are planned to allow branching ratios, which can be combined with level lifetimes to yield oscillator strengths, to be calculated. Approximately 60 to 70 Cr III 4p-4s transition lines, several with a signal-to-noise ratio in the hundreds have also been recorded with the IC VUV FTS and the PDL. Again, analysis is underway.

Fe III: Fe III spectra have already been measured in the VUV with the IC VUV FTS (Pickering (2002)) covering several hundred 4p-4s transitions, the strongest of which have an uncertainty of 0.5 Å, an order of magnitude improvement in accuracy on previous measurements. These new measurements were supplemented by spectra measured in the infra-red (IR) by FT spectroscopy at NIST, and now by measurements recorded on image plates using the NIVS, which observed 4d-4p and 5s-4p transitions in the VUV that had been masked by noise from strong Fe II lines in the FT spectroscopy measurements at Imperial College.

Analysis planned and underway includes producing intensity and wavelength / wavenumber calibrated linelists and completing term analysis, i.e. classifying the transition lines and establishing the energy level structure by firstly using known energy levels to classify as many lines as possible, and then using the unidentified lines, combined with the known energy levels, to calculate possible new energy levels that can be verified by theoretical predictions.

Fig. 1.— A NIVS image plate scan. The top & bottom images are for a D_2 lamp, and the others are for Co in the PDL for different angles of incidence and running conditions.

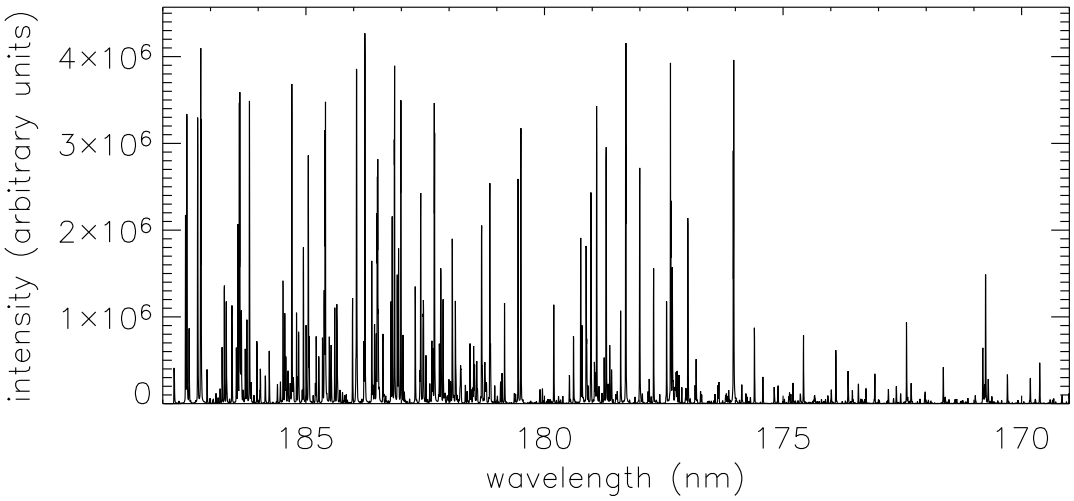

Fig. 2.— A spectrum of Co cathodes in the PDL, extracted from the image plate scan shown in Fig. 1 (second track from the top).

This work is supported in part by NASA Grant NAG5-12668, NASA Interagency Agreement W-10,255, PPARC (Particle Physics and Astronomy Research Council), the Royal Society of the UK and by the Leverhulme Trust.

REFERENCES

Pickering, J. C. 2002, Vib. Spec., 29, 27
Heise, C., Hollandt, J., Kling, R., Kock, M., & Kühne, M. 1994, Appl. Optics, 33, 5111
Reader, J., Sansonetti, C. J., & Deslattes, R. D. 2000, Appl. Optics, 39, 637

NASA LAW, February 14-16, 2006, UNLV, Las Vegas

Cross Sections for Electron Impact Excitation of Astrophysically Abundant Atoms and Ions

S. S. Tayal

Department of Physics, Clark Atlanta University, Atlanta, GA 30314

stayal@cau.edu

ABSTRACT

Electron collisional excitation rates and transition probabilities are important for computing electron temperatures and densities, ionization equilibria, and for deriving elemental abundances from emission lines formed in the collisional and photoionized astrophysical plasmas. Accurate representation of target wave functions that properly account for the important correlation and relaxation effects and inclusion of coupling effects including coupling to the continuum are essential components of a reliable collision calculation. Non-orthogonal orbitals technique in multiconfiguration Hartree-Fock approach is used to calculate oscillator strengths and transition probabilities. The effect of coupling to the continuum spectrum is included through the use of pseudostates which are chosen to account for most of the dipole polarizabilities of target states. The B-spline basis is used in the R-matrix approach to calculate electron excitation collision strengths and rates. Results for oscillator strengths and electron excitation collision strengths for transitions in N I, O I, O II, O IV, S X and Fe XIV have been produced.

1. INTRODUCTION

Collisions of electrons with atoms and ions are major excitation mechanism in a wide range of astrophysical objects such as planetary nebulae, H II regions, stellar and planetary atmospheres, active galactic nuclei, novae and supernovae. The astrophysical plasma diagnostic techniques based on spectroscopic line intensities, profiles and wavelengths have been used to determine temperatures, densities, emission measures, mass motions and elemental abundances. The high quality of spectroscopic data made available by the recent flight instruments has highlighted the need for improvements in the number and accuracy of atomic data. In many cases the accuracy of the astrophysical analysis is limited by the inadequacy of atomic data. Spectral synthesis codes have been developed to generate synthetic spectrum by converting a database of atomic quantities into a model spectrum that can be compared

with the observed spectrum. The relative ion abundances can be determined by generating isothermal models for each ion.

Electron collisional excitation rates and transition probabilities are important for computing plasma electron temperatures and densities, ionization equilibria and to derive abundances from emission lines formed in the collisional and photoionized plasmas. The photoionization cross sections are needed for the radiative transfer calculations. Oscillator strengths of abundant and trace elements are needed to study absorption by gases in the interstellar medium. Hot plasmas can be diagnosed using both emission and absorption lines. The computation of true opacity of stellar matter requires both continuum and line opacities.

2. THEORETICAL DETAILS

Recently our research program has been focused to produce accurate and extensive data for transition probabilities and oscillator strengths, photoionization cross sections and electron excitation rates for a large number of lines of O I, N I, O II, O IV, S II, S X and Fe XIV. Being open-shell systems, these atoms and ions pose a serious theoretical challenge because of the difficulty in the determinations of accurate target wave functions and slow convergence of the close-coupling expansion. An accurate description of target wave functions is essential for a reliable scattering calculation. The short-range correlation and long-range polarization effects are expected to be very important for an open-shell system. Consequently, accurate representations of the target wave functions require extensive configuration expansions, with additional complications arising from a strong term dependence of the valence orbitals. The effect of coupling to the continuum is included through the use of pseudostates which are chosen to account for most of the dipole polarizabilities of target states. The non-orthogonal orbitals technique in the multiconfiguration Hartree-Fock approach has been successfully used to describe term dependence of target wave functions and to represent correlation corrections and interactions between the Rydberg states and the perturber states.

The wave function describing the (N+1)-electron system in an internal region surrounding the atom with radius r is expanded in terms of energy-independent functions (Zatsarinny & Tayal 2001; Zatsarinny 2006)

$$\Psi_k \;=\; A \sum_{ij} a_{ijk} \overline{\Phi_i} u_j(r), \tag{1}$$

where $\overline{\Phi_i}$ are channel functions formed from the multi-configurational functions of the target states and the operator A antisymmetrizes the wave function. The radial functions u_j are expanded in the B-spline basis. Use of the B-spline basis leads to a generalized eigenvalue problem of the form

$$\mathbf{H}c = E\mathbf{S}c \tag{2}$$

where **S** is the overlap matrix, which in the case of the usual orthogonal conditions on scattering orbitals reduces to the banded matrix, consisting of overlaps between individual B-splines, but in the more general case of non-orthogonal orbitals has more complicated structure.

3. A BRIEF SUMMARY OF NEW RESULTS

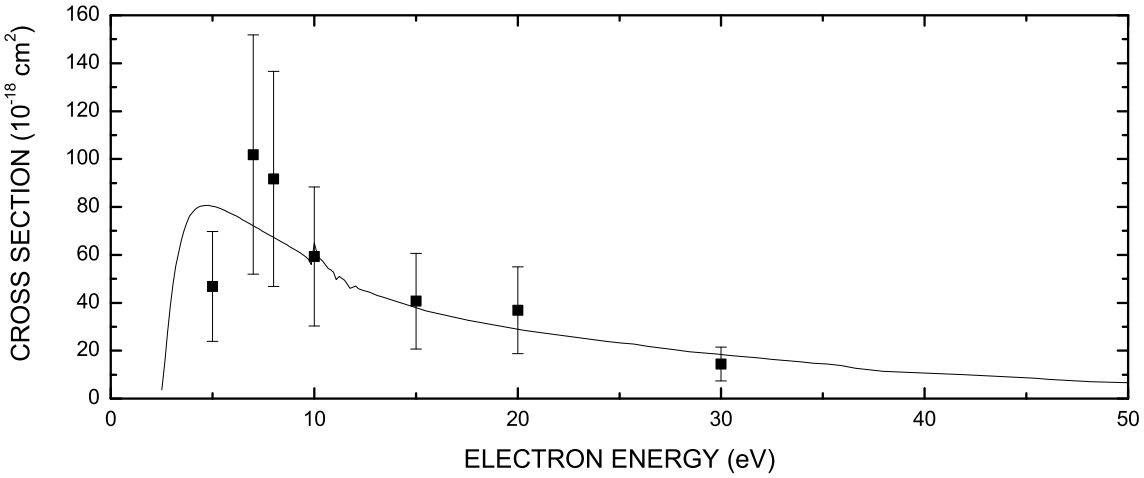

Fig. 1.— Excitation cross section for the N I 5200 $\mathring{A}$ line as a function of electron energy. Solid curve: 39-state theory; soild rectangles: measured cross sections (Yang & Doering 1996).

The O I ultraviolet features at 1304 and 1356 $\mathring{A}$ due to excitation of the 3s $^3S^o$ and $^5S^o$ levels are among the dominant features in the spectra of atmospheres of Io, Mars and Venus. In recent years we have carried a collaborative effort with experimental group at the Jet Propulsion Laboratory and our 52-state R-matrix with pseudostates calculation shows excellent agreement with experiment for the 1304 $\mathring{A}$ resonance line (Johnson et al. 2005). The cross sections for this prominent transition are now considered very well established. We also reviewed O I data and made recommendations regarding the existing theoretical and experimental data sets (Johnson et al. 2005). Collisions of electrons with N I are responsible for many of the strong emission lines observed in the atmospheres of Titan, Sun and in a variety of other astrophysical objects. The 39-state B-spline R-matrix with pseudostates approach has been used to calculate excitation rates (Tayal & Zatsarinny 2005; Tayal 2006). The measured cross sections are available only at a limited number of energies for lines at 5200, 1200 and 1135 $\mathring{A}$. A good agreement with measured cross sections can be seen in Fig. 1 except at 5 eV for the forbidden line at 5200 $\mathring{A}$. We also recently completed a 47-state

B-spline Breit-Pauli R-matrix calculation for electron impact excitation of O II. Several O II lines are temperature and density sensitive and can provide useful astrophysical plasma diagnostics.

Electron collisional excitation rates for ultraviolet and X-ray lines arising from transitions in S X have been calculated using the Breit-Pauli R-matrix method (Tayal 2005). The 25-state R-matrix theory was used for O IV and the rich resonance structure for the $2s^2 2p\ ^2P^o$ - $2s2p^4\ ^4P$ transition showed excellent agreement with experiment (Smith et al. 2003). The electron impact excitation calculation for O IV is now extended to 54-state Breit-Pauli R-matrix calculation to cover a large number of transitions in a wide range of temperature. We have investigated electron impact excitation of Fe XIV in collaboration with the experimental group at the Jet Propulsion Laboratory where cross sections have been measured for the $3s^2 3p\ ^2P^o$ - $3s3p^2\ ^4P$ transition in the low-energy region close to threshold using merged-beams electron-energy-loss method. There is excellent agreement between theory and experiment.

This work was supported in part by NASA grant NNG06GD39G from the Astronomy and Physics Research and Analysis Program.

REFERENCES

Zatsarinny, O., & Tayal, S. S. 2001, J. Phys. B, 34, 1299
Zatsarinny, O. 2006, Comput. Phys. Commun., 174, 273
Johnson, P. V., McConckey, J. W., Tayal, S. S., & Kanik, I. 2005, Can. J. Phys., 83, 589
Tayal, S. S. & Zatsarinny, O. 2005, J. Phys. B, 38, 3631
Tayal, S. S. 2006, ApJS, 163, 207
Tayal, S. S. 2005, ApJS, 159, 167
Yang, J., & Doering, J. P. 1996, J. Geophys. Res., 101, 765
Smith, S. J., Lozano, J. A., Tayal, S. S., & Chutjian, A. 2003, Phys. Rev. A, 68, 062708

NASA LAW, February 14-16, 2006, UNLV, Las Vegas

Fluorescence Spectroscopy of Gas-phase Polycyclic Aromatic Hydrocarbons

J. D. Thomas & A. N. Witt

Department of Physics and Astronomy, The University of Toledo, Toledo, OH 43606

jthomas@physics.utoledo.edu, awitt@dusty.astro.utoledo.edu

ABSTRACT

The purpose of this investigation was to produce fluorescence spectra of polycyclic aromatic hydrocarbon (PAH) molecules in the gas-phase for comparison with blue luminescence (BL) emission observed in astrophysical sources Vijh et al. (2004, 2005a,b). The BL occurs roughly from 350 to 450 nm, with a sharp peak near 380 nm. PAHs with three to four rings, e.g. anthracene and pyrene, were found to produce luminescence in the appropriate spectral region, based on existing studies. Relatively few studies of the gas-phase fluorescence of PAHs exist; those that do exist have dealt primarily with the same samples commonly available for purchase such as pyrene and anthracene. In an attempt to understand the chemistry of the nebular environment we also obtained several nitrogen substituted PAHs from our colleagues at NASA Ames. In order to simulate the astrophysical environment we also took spectra by heating the PAHs in a flame. The flame environment counteracts the formation of eximers and permits the spectroscopy of free-flying neutral molecules. Experiments with coal tar demonstrate that fluorescence spectroscopy reveals primarily the presence of the smallest molecules, which are most abundant and which possess the highest fluorescence efficiencies. One gas-phase PAH that seems to fit the BL spectrum most closely is phenanthridine. In view of the results from the spectroscopy of coal tar, a compound containing a mixture of PAHs ranging from small to very large PAH molecules, we can not preclude the presence of larger PAHs in interstellar sources exhibiting BL.

1. Introduction

Dust is a ubiquitous catch-all term used when referring to the multitude of known and unknown particles larger than molecules in the universe; it has been studied a great deal,

yet the true nature and composition has eluded astronomers for some time. One component of dust known to exist is polycyclic aromatic hydrocarbon (PAH) molecules.

This study was undertaken in response to a recently discovered blue emission feature Vijh et al. (2004) in nebulae, known to contain PAHs from infrared observations of the aromatic emission features. The blue luminescence (BL) can be seen in Figure 1; the spectrum was measured at the wavelengths of the hydrogen Balmer lines, denoted with the triangles. The BL spans the spectral region from 350 to 500 nm with peaks near 375 and 390 nm. The luminescence has been interpreted as arising from photo-induced fluorescence by small, neutral PAH molecules Vijh et al. (2004).

Only a small handful of readily available PAHs have been studied in the gas phase. With the few existing gas-phase spectra, it was found that PAH with three to four rings best fit the BL. It is important to study these molecules in the gas phase because of the matrix shift. A matrix shift is the shifting of the spectral features to different wavelengths, which depends upon the phase and environment of the sample. For example, molecules in a solution will have the same spectral features as the same molecules in the gas phase; however, the wavelengths of the features and their relative strengths will be different: this makes identification of molecules in astrophysical environments nearly impossible based on data taken in solution. To that end we have studied a number of PAHs in the gas phase. Many of the spectra were acquired for the commonly studied PAHs, and our spectra agreed well with those in the literature. In addition to the commonly studied PAHs we also studied several nitrogen heterocyclic PAHs, these samples were provided by Lou Allamandola.

2. Experiment

The laser induced fluorescence of gas-phase PAHs was studied with a helium-cadmium laser operated at 326 nm. In some cases a flame was utilized to provide a high temperature environment for both high temperature spectra and to dissociate PAH eximers (a cluster of two or more molecules). The fluorescence was observed with a CCD spectrometer.

3. Discussion

Figure 2 is a concise presentation of the relevant data collected through the course of this research. PAHs that exhibit gas-phase fluorescence in the peak region of the BL, from 375-390 nm, have masses between 178 and 252 g mole^{-1}.

Small molecules tend to be more efficient at fluorescing, which implies that in a mixed environment small PAHs will be preferentially detected over large PAHs with relatively lower fluorescence efficiencies. Coal tar provides a crude mixture of large and small PAHs. Through our experiments with coal tar we showed that there is indeed a preference for small PAHs

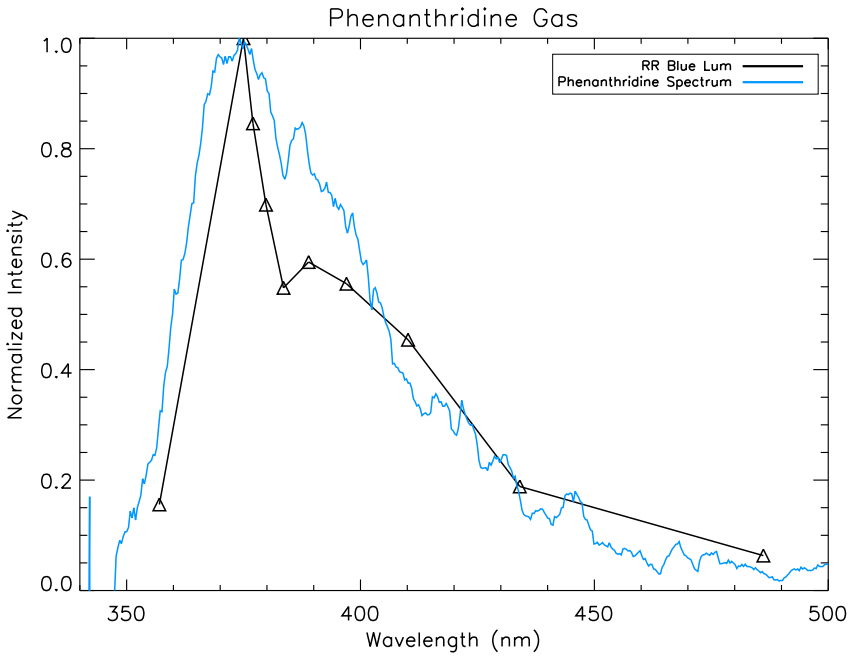

Fig. 1.— Phenanthridine gas phase fluorescence spectrum fit to the blue luminescence (BL). The BL spectrum is from the Red Rectangle (Vijh et al. 2005a), denoted by black triangles. The phenanthridine shown as the solid blue curve is from this study. This sample came from Lou Allamandola at NASA Ames.

to be detected through the observation of their fluorescence. This implies that large PAHs would be hard to observe in a mixture containing both small and large PAHs.

In both pure samples and mixtures we observed the formation of eximers. Eximer fluorescence occurs at longer wavelengths than the monomer (or single molecule) fluorescence. In our study of coal tar we found that the relative fluorescence efficiencies of these clusters was lower than the fluorescence efficiencies of smaller monomer PAHs. Comparing the spectral region in which the eximer fluorescence commonly occurs to that of the BL one can see that fluorescence by eximers is unlikely to be the source of the BL. Eximers are also unlikely to be responsible for the extended red emission.

Figure 1 shows a spectrum of phenanthridine (a three ringed PAH with a single nitrogen substitution); it can be seen that its peak falls on the first BL peak, demonstrating the ability of PAHs to fluoresce over the entire spectral region covered by the BL. It should be pointed out that this is not a spectral identification, because the fluorescence efficiency of phenanthridine is low when compared to other PAHs similar in size. Therefore, it is most likely a mixture of small neutral monomer PAHs that are responsible for the BL.

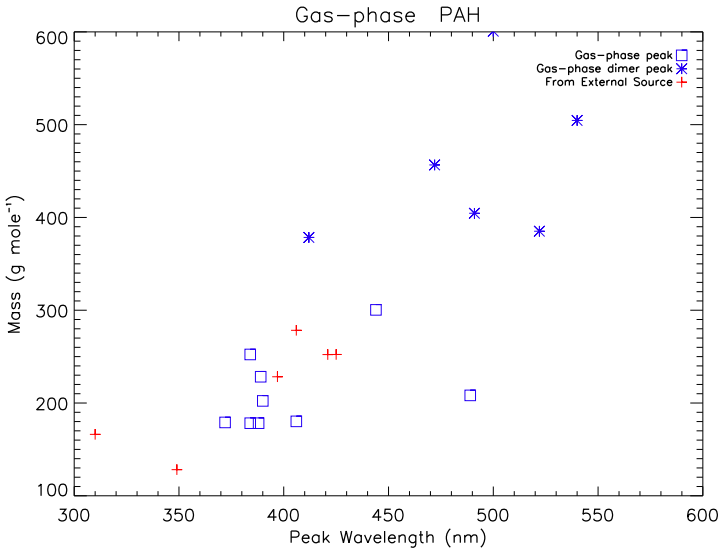

Fig. 2.— This plot shows the trend of the peak wavelength of fluorescence increasing with mass. The open blue squares were measured in this study with our setup. The blue stars represent the peak fluorescence for those molecules that formed eximers were assumed to be dimers (two molecules). To make the graph the molecular weight was doubled. The red crosses are values from Mastral et al. (2004), also done in the gas phase.

4. Conclusions

We have demonstrated that small PAHs could be responsible for the BL. If correct, the BL is most likely due to a mixture of small neutral monomer PAH (3-4 rings), and not a single PAH. We can also conclude that small PAH may not be the most prevalent PAH in nebulae, but their luminescence is easier to detect due to their higher fluorescence efficiencies.

We would like to thank Lou Allamandola and his team at NASA Ames for providing the some of samples used in this study. This research was made possible by Laboratory Astrophysics Grants from NASA to the University of Toledo.

REFERENCES

Mastral, A. M., García, T., López, M., Murillo, R., Callén, M. S., & Navarro, M. V. 2004, Polycyclic Aromatic Compounds, 24, 325
Vijh, U. P., Witt, A. N., & Gordon, K. D. 2004, ApJ, 606, L65
Vijh, U. P., Witt, A. N., & Gordon, K. D. 2005a, ApJ, 619, 368
Vijh, U. P., Witt, A. N., & Gordon, K. D. 2005b, ApJ, 633, 262

NASA LAW, February 14-16, 2006, UNLV, Las Vegas

The effect of bonding on the fragmentation of small systems

R. D. Thomas, A. Ehlerding, W. Geppert, F. Hellberg, M. Larsson, V. Zhaunerchyk

Department of Physics, Albanova, Stockholm University, S106 91 Stockholm, Sweden.

E. Bahati, M. E. Bannister, M. R. Fogle, C. R. Vane

Physics Division, Oak Ridge National Laboratory, Oak Ridge, TN 37831-6377 USA.

A. Petrignani

FOM Instituut for Atomic and Molecular Physics, Kruislaan 407, 1098 SJ Amsterdam, The Netherlands.

W. J. van der Zande

Molecule and Laser Physics, IMM, Radboud University Nijmegen, 6525 ED Nijmegen, The Netherlands.

P. Andersson, J. B. C. Pettersson

Department of Chemistry, Göteborg University, SE-412 96 Göteborg, Sweden.

rdt@physto.se

ABSTRACT

Recent dissociative recombination (DR) experiments have reported that the observed reaction products depend on the structure, bonding, and charge centre of the molecular ion. For examples, the dominant product channel observed in the DR of D_5^+ (2), $N_2O_2^+$ (1), and $D_5O_2^+$ (3) suggests that the former two ions have the form $D_3^+ \cdot D_2$, and $NO^+ \cdot NO$ (1), respectively, whilst the latter is known to have the form $D_2O \cdot D^+ \cdot D_2O$ (3). Here we compare and contrast these observations by investigating the DR of one of the simplest such systems, $Li^+ \cdot H_2$. This system, a weakly bound cluster with the charge centre located on the lithium atom, will provide us with an excellent opportunity for investigating the role played by the type of bonds and charge centre in the DR process.

1. Introduction

Dissociative recombination (DR) is a process in which a molecular ion recombines with a low-energy free electron and subsequently dissociates into neutral fragments. For low temperature plasmas containing molecular ions, DR is the most important neutralising process and is therefore of great importance to the chemistry occurring in such diverse regions as interstellar clouds, planetary atmospheres and in semi-conductor etching.

Recent DR studies have focussed on polyatomic ions, driven mostly by the fact that given the apparent simplicity of the DR process, developing a general theory to predict product branching ratios for even the simplest polyatomic ions, e.g. XH_2^+, has proven to be difficult. The earliest models suggested that the reaction would predominantly proceed via the least amount of internal rearrangement, i.e. fracture of the weakest X-H bond, producing H + XH. However, the majority of storage ring studies on the DR of such ions show a propensity for three-body break-up, i.e. X + H + H (see (4) for a comprehensive list). It is worth noting that a recent theoretical models developed in the group of Greene for H_3^+ shows great agreement with experimental data (5; 6; 7). High quality experimental data on basic systems is needed to both illuminate the fundamental processes underlying DR and to provide much needed and valuable input to theoretical models.

To understand the dynamics occurring in such simple systems, the effect of the structure, bonding, and charge centre of the molecular ion needs to be investigated. Small molecular cluster ions represent good toy models and several systems have recently been investigated, for examples $N_2O_2^+$, D_5^+, and $D_5O_2^+$. These systems are small enough to allow complete detection of the product fragments and represent systems for which there are several different bond types, i.e. dative, covalent, hydrogen, and dipole, and either localised or delocalised charge centres, and the combination of these will influence how the neutral molecular system dissociates. Based on the experimental data obtained on the DR of these systems, the simplest model system which combines all of the features just discussed was chosen for investigation, i.e. LiH_2^+.

2. Dissociative Recombination in Storage Rings

All the experiments discussed in this paper were carried out at the heavy ion storage ring CRYRING, located at the Manne Siegbahn Laboratory, Stockholm University, Sweden. Such a facility has several experimentally desirable aspects for studies into DR. The ion-beam energies used are typically a few MeV. At such energies the electron capture cross section in collisions between the stored ion beam and residual gas molecules is small, which significantly reduces the contribution of background signals to the true data. For zero eV relative collisions between the electrons and the ions, it is much easier to create and control a stable and dense electron beam if the beam velocity is high, and this also requires MeV

ion beams. The good vacuum $< 10^{-11}$ Torr in the ring indicates that the number of residual gas molecules is extremely low, further decreasing the background contributions as well as enabling a long storage lifetime of the ion beam. This time, which can be tens of seconds, allows metastable and vibrationally excited components in the ion beam to decay to the ground state. A recent review on the use of merged-beams in atomic and molecular physics can be found in the literature(8).

3. Experimental Results and Discussion

In the collisions of D_5^+, $D_5O_2^+$, and $N_2O_2^+$ with 0 eV electrons, the following reaction channels, with their associated kinetic energy release (KERn), are observed to be the most dominant:

$$\begin{aligned} D_5^+ + e^- &\rightarrow 3D + D_2 + KER_1 && (1)\\ &\rightarrow 2D_2 + D + KER_2 && (2)\\ D_5O_2^+ + e^- &\rightarrow D + 2(D_2O) + KER_3 && (3)\\ (NO)_2^+ + e^- &\rightarrow NO + N + O + KER_4 && (4)\\ &\rightarrow NO + NO + KER_5 && (5) \end{aligned}$$

It is noted that the available KER is a maximum for ground state fragments and the production of internally excited products reduces this. These results were obtained with the standard detection techniques used for obtaining chemical branching from DR and these techniques are discussed in Ref. (3).

The ionic structure, charge centre, and bonding of these ions is of relevance when analysing the dominant fragmentation channels. The weakly bound NO dimer ion has the form $NO^+ \cdot NO$ (1) while D_5^+ has the form $D_3^+ \cdot D_2$, i.e. it is a weakly hydrogen-bonded cluster, while $D_5O_2^+$ has a proton-bridge structure, and has an almost linear geometry given by $D_2O \cdot D^+ \cdot D_2O$(3). In each case, the dominant product channels observed in the DR reaction are similar to those which would be expected if the "solvent" neutrals played little or no role in the reaction, i.e. the dominant channels in the DR of $D_3^+ \cdot D_2$ is similar to that from the DR of $D(H)_3^+$ (9), and the completely dominant production ($> 90\%$ (3)) of $2D_2O + D$ from the DR of $D_2O \cdot D^+ \cdot D_2O$ would also be expected. For $NO^+ \cdot NO$ the only other significantly populated channel is NO + NO.

The question that arises from these results is how much of the available reaction energy has been used in excitation of the molecular fragments. This is an important aspect in the case of both $NO^+ \cdot NO$ and $D_3^+ \cdot D_2$ as this would illuminate the role played in the DR reaction by the solvent molecule(s). A technique is needed which can measure the kinetic energy given to the reaction fragments, and such a technique has been developed and used with great success in studying the DR of both diatomic and triatromic molecular ions. Using a

position-sensitive detector (briefly, a stack of multi-channel plates (MCPs), a phosphor screen and a photo-multiplier tube (PMT) (10; 11)) monitoring the position of the fragments from the DR reaction allows the kinetic energy given to the fragments to be determined.

An example of the power of this technique is given in the following example, where the kinetic energy given to the D and D_2O fragments from the DR of $D_5O_2^+$ has been determined. The preliminary results are shown in Fig.1, together with a simulation of the experimental data. The simulation, described in detail in Ref.(10), indicates that up to 3 eV is used in exciting the molecular D_2O products, i.e. the fragments share kinetic energy of 2.1 eV. It is obvious that the D_2O molecules solvating the D^+ play a significant role in the reaction after the initial electron attachment. The data obtained from the DR of the $NO^+ \cdot NO$ dimer ion has also been reported, as well as a discussion on the reaction dynamics (1). The data for $D_3^+ \cdot D_2$ are under analysis.

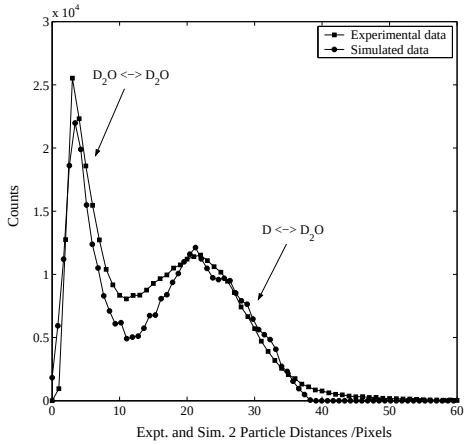

Fig. 1.— Distance distributions obtained from the DR of $D_5O_2^+$.

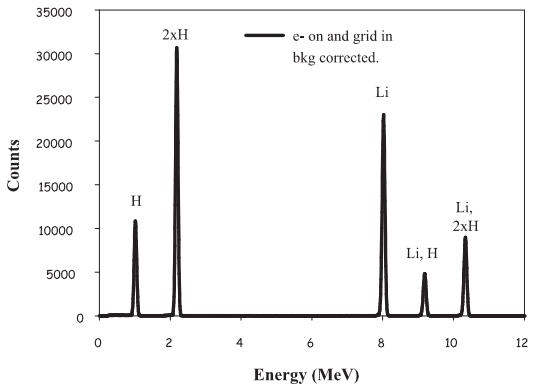

Fig. 2.— Multi-channel analyser data of the fragments produced from the DR of $Li^+ \cdot H_2$.

Even from such preliminary analysis, the dynamics occurring in the dissociation step immediately following the attachment of the electron are very important for an understanding of the DR process. To help further understand the dynamics, a much simpler system was selected: the cluster ion $Li^+ \cdot H_2$. This represents a nice model system. The charge centre is extremely localised on the lithium atom, the bonding between the Li^+ and the H_2 molecule is controlled by the charge on the Li atom, i.e. is ion-induced, and the dative bond in the H_2 molecule is extremely strong in comparison. The neutral system, i.e. $Li \cdot H_2$, is even more weakly bound than the ionic system, being Van der Waal's in nature.

An initial prediction for the DR reaction would be that only the channel producing Li + H_2 would be populated and any deviation from this would be illustrative of the post attachment interactions happening in a very weakly bound system. In 0 eV collisions the

following reaction channels, with their associated kinetic energy release (KERn), are possible:

$$\begin{aligned} Li^+.H_2 + e^- &\rightarrow Li + H_2 + KER_6 \quad (6) \\ &\rightarrow LiH + H + KER_7 \quad (7) \\ &\rightarrow Li + 2H + KER_8 \quad (8) \end{aligned}$$

Preliminary data are shown in Fig. 2 where the peaks in the spectrum correspond to the various combinations of products possible in the reaction. Details on the data analysis techniques are discussed in Ref. (3). The results from this analysis shows that although the dominant channel populated in the DR reaction is that producing Li + H_2, i.e. channel (6), it is not the only channel. Just over a fifth of the reactions lead to the production of both LiH + H, and Li + 2H. These observations indicate that the post-attachment interaction is sufficiently strong, leading both to the fracture of the strongest bond in the system, the molecular hydrogen bond, and the formation of a much weaker-bonded molecular system, LiH.

4. Conclusions

In the light of recent experimental observations the development of a simple model to describe the DR process for even a small polyatomic ion does not seem to be a trivial matter. The preliminary results discussed here for the DR of some model systems show that the products depend on the structure, bonding, and charge centre of the molecular ion. The transition of the molecular system in moving from a single ionic state to an ensemble of highly-excited neutral states induces a dynamical interaction between the molecular and atomic constituents of the system. More work is needed to understand which types of interactions are the most dominant, and this could lead to the development of at least semi-empirical models.

We would like to thank the CRYRING staff at the Manne Siegbahn Laboratory for their tireless work and excellent support. This work was supported by the Swedish Research Council, the Swedish Foundation for International Cooperation in Research and Higher Education. RT is funded under the IHP Programme of the EC under contract HPRN-CT-2000-00142. The work of WJvdZ is part of the research of the 'Stichting voor Fundamenteel Onderzoek der Materie', made possible by financial support by the Stichting voor Wetenschappelijk Onderzoek. The Oak Ridge collaboration is sponsored by the U.S. Department of Energy, Office of Basic Energy Sciences, Division of Chemical Sciences under Contract No. DE-AC05-00OR22725 with UT-Battelle, LLC.

REFERENCES

A. Petrignani *et al.*, J. Chem. Phys. **123**, 194306 (2005).
P. Andersson *et al.* in *Proceedings of the XXIII ICPEAC, Stockholm, 2003. Abstracts*, edited by J. Anton *et al.* (ICPEAC CDROM) Contribution Mo109.
M. Någård *et al.*, *J. Chem. Phys.* **117**, 5264 (2002).
M. Larsson, and R. Thomas, *Phys. Chem. Chem. Phys.*, **3**, 4471 2001.
V. Kokoouline, and C. H. Greene, Phys. Rev. Lett. **90**, 133201 (2003).
V. Kokoouline, and C. H. Greene, Phys. Rev. A **68**, 012703 (2003).
H. Kreckel *et al.*, Phys. Rev. Lett. **95**, 263201 (2005).
R. A. Phaneuf *et al.*, *Rep. Progr. Phys.* **62**, 1143 (1999).
S. Datz *et al.*, *Phys. Rev. Lett.* **74** 896 (1995).
R. Thomas *et al.*, *Phys. Rev. A*, **66**, 032715 (2002).
Z. Amitay, and D. Zajfman, *Rev. Sci. Instrum.*, **68** 1387 (1997).

NASA LAW, February 14-16, 2006, UNLV, Las Vegas

Metal Hydride and Alkali Halide Opacities in Extrasolar Giant Planets and Cool Stellar Atmospheres

Philippe F. Weck

Department of Chemistry, University of Nevada-Las Vegas, Las Vegas, NV 89154

weckp@unlv.nevada.edu

Phillip C. Stancil

Dept. of Physics & Astronomy and Center for Simulational Physics, The University of Georgia, Athens, GA 30602

stancil@physast.uga.edu

Kate Kirby

ITAMP, Harvard-Smithsonian Center for Astrophysics, 60 Garden Street, Cambridge, MA 02138

kirby@cfa.harvard.edu

Andreas Schweitzer & Peter H. Hauschildt

Hamburger Sternwarte, Universitaet Hamburg, Gojenbergsweg 112, D-21029 Hamburg, Germany

Andreas.Schweitzer@hs.uni-hamburg.de,phauschildt@hs.uni-hamburg.de

ABSTRACT

The lack of accurate and complete molecular line and continuum opacity data has been a serious limitation to developing atmospheric models of cool stars and Extrasolar Giant Planets (EGPs). We report our recent calculations of molecular opacities resulting from the presence of metal hydrides and alkali halides. The resulting data have been included in the PHOENIX stellar atmosphere code (Hauschildt & Baron 1999). The new models, calculated using spherical geometry for all gravities considered, also incorporate our latest database of nearly 670 million molecular lines, and updated equations of state.

The study of the spectra of cool stars requires detailed knowledge of molecular opacities. This includes important absorbers such as TiO, CO, and water vapor, which have bands that cover large wavelength ranges and are very important for the structure of the atmosphere due to their overall cooling or heating effects. In addition, there are a number of molecules that have bands covering comparatively small wavelength ranges (e.g., 10-100 Å). Many of them are trace molecules that have only small effects on the overall physical conditions inside the atmosphere but that are important for spectral classification and for the determination of stellar parameters such as effective temperatures, gravities and abundances. We have therefore started a project to update or provide for the first time molecular data of astrophysical interest for important trace molecules. These data are computed using state-of-the-art molecular physics codes and should improve our ability to model and analyze cool stellar atmospheres considerably (Weck *et al.* 2003a,b,c, 2004a,b; Homeier *et al.* 2005).

Ab initio potential energy curves and dipole moment functions have been calculated for the $X\ ^1\Sigma^+$ and $B\ ^1\Sigma^+$ electronic states of $^7Li^{35}Cl$ (Weck *et al.* 2004a). The line oscillator strengths were computed for all allowed transitions between the 29,370 rovibrational levels calculated neglecting spin-splitting for the $X\ ^1\Sigma^+$ state, thus giving a total of 3,357,811 lines (Weck *et al.* 2004b).

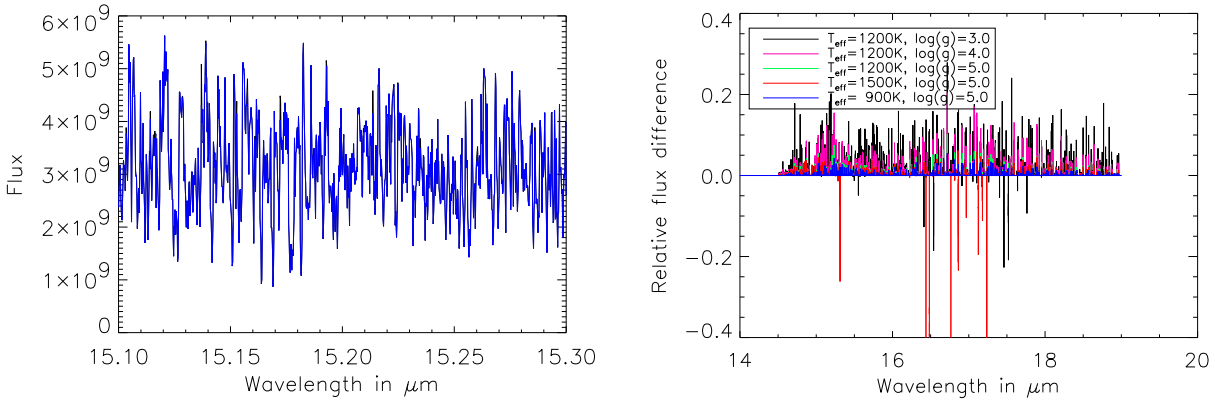

Fig. 1.— Left: LTE synthetic spectra computed with (blue) and without (black) LiCl line absorption as a function of the wavelength for $T_{\rm eff} = 1200\,{\rm K}$, $\log(g) = 4.0$ and solar abundances; 2 Å resolution, i.e. $R = 76,000$. Right: Relative flux difference for brown dwarf models with $T_{\rm eff} = 900 - 1500\,{\rm K}$, $\log(g) = 3.0 - 5.0$ and solar abundances

To assess LiCl line absorption in the spectra of brown dwarfs, we have calculated LTE synthetic spectra with and without the new LiCl data. Several brown dwarf models somewhat in the L/T-dwarf regime with $T_{\rm eff} = 900 - 1500\,{\rm K}$, $\log(g) = 3.0 - 5.0$ and solar abundances were considered using the `PHOENIX` code. The small differences shown in the left panel of Figure 1 suggest that the line opacity due to LiCl in cool brown dwarf atmospheres is relatively insignificant. The opacity in the far infrared is apparently dominated by H_2O.

As depicted in the right panel of Figure 1, relative flux differences are typically less than 20% for young ($\log(g) = 3.0, \simeq 100$ Myrs) to old ($\log(g) = 5.0, > 1$Gyr) brown dwarfs for $T_{\rm eff} = 900 - 1200$ K

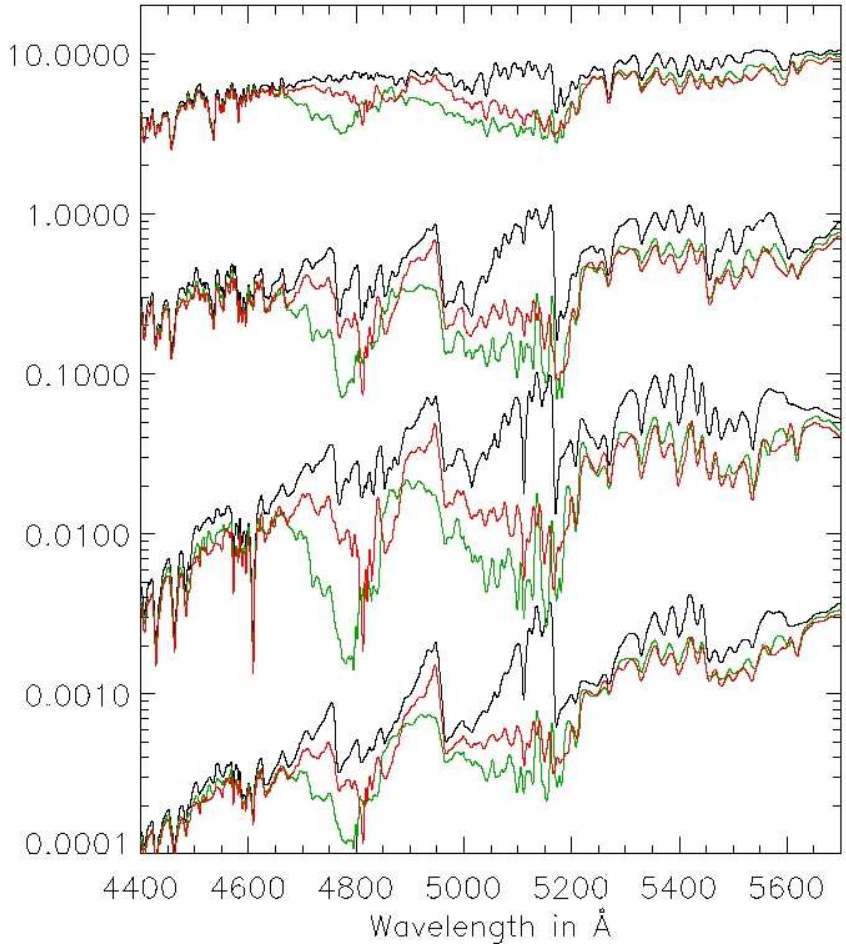

Fig. 2.— Spectra of the strongest MgH bands (log scale for flux in 1013 erg/cm2/s/cm) for models with $T_{\rm eff} = 4000, 3000, 2000$ K (AMES-Cond model) and $T_{\rm eff} = 2000$ K (AMES-Dusty model) (from top to bottom). The 2000 K AMES-Cond models have an artificial offset of +1.0 dex for better legibility. All models have log(g)=5.0 and are AMES-Cond unless noted otherwise. Black: no MgH data; red: new MgH data; green: MgH data calculated with a model Hamiltonian.

In Figure 2 we show comparisons between spectra, in the spectral region where the MgH bands are most prominent, from models using: a) no MgH data, b) our new MgH line list (Weck *et al.* 2003b), and c) the Kurucz (1993) MgH line list. The comparisons have been done at $T_{\rm eff} = 2000$ K, 3000 K, and 4000 K to sample the temperature range in which MgH is visible in the spectrum. As can be seen, the line list calculated with a model Hamiltonian

overestimates the opacity obtained with our new MgH line list. The differences between the spectra with the new and model Hamiltonian MgH line lists are very similar for the AMES-Cond and AMES-Dusty models although the overall flux level and the overall flux shape are different for AMES-Cond and AMES-Dusty in the optical. As can be seen, there are significant differences spreading among both the $A - X$ and the $B' - X$ transitions.

Conclusion

We have calculated theoretical spectra for different stellar models of brown dwarfs including our latest metal hydride and alkali halide molecular data obtained from *ab initio* calculations. The present synthetic spectra generated for stellar models somewhat in the M/L/T-dwarf regime clearly illustrate the current needs for accurate molecular data to improve our ability to identify, characterize and classify the increasing number of cool stellar objects as well as extrasolar giant planets found in recent observational surveys.

This work was supported by NASA grants NAG5-12751, NAG5-8425, NAG5-9222, and NAG5-10551 as well as NASA/JPL grant 961582, and in part by NSF grants AST-9720704 and AST-0086246 (and a grant to the Institute for Theoretical Atomic, Molecular & Optical Physics, Harvard-Smithsonian CfA). Some of the calculations were performed on the IBM SP2 of the UGA EITS, on the IBM SP "Blue Horizon" of the San Diego Supercomputer Center, with support from the NSF, and on the IBM SP of the NERSC with support from the DoE.

REFERENCES

Hauschildt, P. H., & Baron, E. 1999, J. Comput. App. Math., 102, 41

Homeier, D., Allard, N. F., Allard, F., Hauschildt, P. H., Schweitzer, A., Stancil, P. C., & Weck, P. F. 2005, ASP Conf. Series, 334, 209

Kurucz, R. L. 1993, CD-ROM No.15 Diatomic molecular data for opacity calculations (Harvard-Smithsonian Center for Astrophysics)

Weck, P. F., Stancil, P. C. & Kirby, K. 2003a, J. Chem. Phys., 118, 9997

Weck, P. F., Schweitzer, A., Stancil, P. C., Hauschildt, P. H., & Kirby, K. 2003b, ApJ, 584, 459

Weck, P. F., Schweitzer, A., Stancil, P. C., Hauschildt, P. H. & Kirby, K. 2003c, ApJ, 582, 1263

Weck, P. F., Kirby, K. ,& Stancil, P. C. 2004a, J. Chem. Phys., 120, 4216

Weck, P. F., Schweitzer, A., Kirby, K., Hauschildt, P. H., & Stancil, P. C. 2004b, ApJ, 613, 567

NASA LAW, February 14-16, 2006, UNLV, Las Vegas

New Critical Compilations of Atomic Transition Probabilities for Neutral and Singly Ionized Carbon, Nitrogen, and Iron

W. L. Wiese & J. R. Fuhr

National Institute of Standards and Technology, Gaithersburg, MD 20899

wolfgang.wiese@nist.gov

ABSTRACT

We have undertaken new critical assessments and tabulations of the transition probabilities of important lines of these spectra. For Fe I and Fe II, we have carried out a complete re-assessment and update, and we have relied almost exclusively on the literature of the last 15 years. Our updates for C I, C II and N I, N II primarily address the persistent lower transitions as well as a greatly expanded number of forbidden lines (M1, M2, and E2). For these transitions, sophisticated multiconfiguration Hartree-Fock (MCHF) calculations have been recently carried out, which have yielded data considerably improved and often appreciably different from our 1996 NIST compilation.

1. Introduction

Our new compilations of the atomic transition probabilities for neutral and singly ionized carbon, nitrogen, and iron have been mainly done in response to strong continuing interests and needs of the astrophysical community.

Those needs have also been responsible for significant experimental and theoretical activity on these spectra during the last ten-to-fifteen years that produced a large amount of new material after the publication of our earlier 1988 and 1996 tables [Fuhr (1988); Wiese (1996)]. Thus our earlier compilations are superseded by this new, enlarged edition which is produced in the same format.

2. Fe I and Fe II

For the allowed or electric dipole (E1) lines of Fe I, we have compiled data for 2425 transitions, an expansion of about 25%. All material originates from experimental sources.

For Fe II, the great majority of the data again comes from recent experiments, but this material is supplemented by some results of a new semi-empirical calculation. We compiled a total of 926 transitions, which is an increase of 42% from our earlier tables.

For the forbidden lines, specifically magnetic dipole (M1) and electric quadrupole (E2) transitions, the data situation is greatly improved for Fe II due to new comprehensive calculations as well as a few experimental checks. However, for Fe I, no activity has taken place in recent years, and consequently our earlier data tables remain unchanged.

Most of the new data are of significantly better quality than those listed in our earlier compilation. For example, 1050 allowed (E1) lines of Fe I are now estimated to have uncertainties less than ±10%, while only 199 lines were estimated to be this accurate in our 1988 compilation. Figure 1 shows the overall improvement graphically for the allowed lines of Fe I and Fe II.

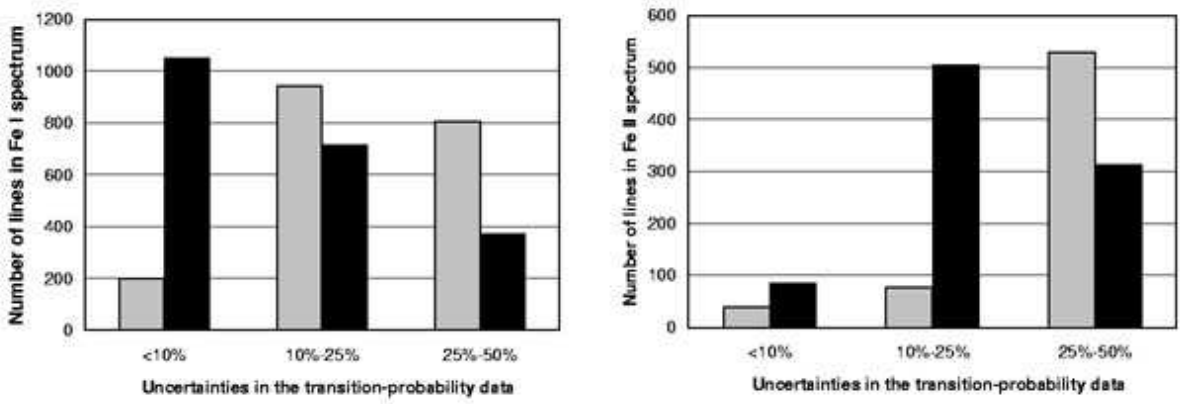

Fig. 1.— Improvement of the data quality for Fe I (left) and Fe II (right). The columns in gray show the number of lines for the three indicated uncertainty ranges compiled in 1988, the black columns show them for the new tables.

We provided detailed explanations of our data evaluation method and our error assessment in earlier transition probability compilations [Wiese (1996)] and will not discuss this here, in view of the very limited space. Our estimated uncertainties are again indicated by letter symbols from A to E as in our earlier data volumes [Fuhr (1988); Wiese (1996)].

3. C I and II, and N I and II

This compilation is a partial update of the NIST transition probability tables for these spectra. Data were previously compiled by us as part of a comprehensive tabulation for the three elements C, N, and O, that was published in 1996 [Wiese (1996)]. We have carried out this new compilation not only because of continuing strong user interest in these four spectra,

especially from astronomers, but also because data of significantly better quality have become available for the persistent transitions in these spectra. For numerous transitions, the new results have produced many significant changes in our tables. Also, data available for the electric-dipole-forbidden lines of the types M1, M2, and E2 were very limited at the time of the publication of our previous tables in 1996, but have now greatly increased. Thus, an update of the principal transition probability data for the four above-cited spectra appears to be timely.

Our 1996 data volume [Wiese (1996)] for C, N, and O was primarily based on the very extensive calculational results of the OPACITY Project [Opacity (1995)], a coordinated undertaking by an international group of about 20 atomic structure theoreticians. But we found from new, very detailed multiconfiguration-Hartree-Fock (MCHF) calculations and from recent lifetime and emission experiments that the OPACITY data are often not as accurate as we had estimated on the basis of limited available comparison data at the time of our previous compilation, that is, pre-1996. This statement applies especially to neutral and singly-ionized carbon and nitrogen.

We have thus carried out a partial update for the transition probabilities of C I, C II, N I and N II, especially utilizing the results of sophisticated MCHF calculations that were performed by Froese Fischer and coworkers in the last six years [Froese Fischer (2004); Zasarinny (2002); Frose Fischer (web site)]. Their multiconfiguration treatment has been very extensive, with wavefunction expansions containing up to 20 000 configuration state functions (CSFs). Also, they included relativistic effects of the Breit-Pauli type, i.e., spin-orbit, spin-spin and spin-other-orbit interactions as well as mass correction and Darwin terms. Thus, they obtained transition probabilities for individual lines including many intersystem and forbidden lines (E2, M1, and M2). The latter were completely missing in the OPACITY results for C and N.

Froese Fischer and coworkers presented their results in the "dipole length" form of the line strength, but they also calculated the "dipole velocity" form. Ideally, these two different formulations of the same quantity should of course agree, so that the differences remaining between the two are good indicators of the achieved accuracy. For each transition, they have listed the difference between the length and velocity results in percent. Indeed, in the best cases, the differences are quite small, of the order of 1–2%.

These new MCHF calculations [Froese Fischer (2004); Zasarinny (2002); Frose Fischer (web site)] are significantly more sophisticated and have been done in a more detailed manner than earlier calculations that were similar in spirit. Froese Fischer et al. also made use of the strong increase in computer power that is now available. Only a few high-accuracy experimental and theoretical results are available to closely test these calculations, especially the results for weaker transitions. Nevertheless, several meaningful comparisons are possible, and we have selected here a comparison with the recent calculations of Corrégé and Hibbert for C II [Corrégé (2002)]. They used the CIV3 code, which is also a sophisticated

multiconfiguration atomic structure code, and they applied it in a similarly detailed manner, with up to 6000 configuration state functions (CSFs). They calculated the line strengths in both the dipole-length as well as the dipole-velocity form, too, as in the work of Froese Fischer and coworkers. The agreement they achieved between these two formulations is nearly as good as Tachiev and Froese Fischer's results. It is thus useful to compare these two sophisticated calculations, which is done in Fig. 2. It is seen that over a wide range of oscillator strengths (gf-values), the agreement between the two calculations is excellent, with the differences never larger than 6%, even for the very weak transitions. To put this into perspective, graphical comparisons of earlier atomic structure calculations, including the Opacity Project calculations [Yan (1987)] always showed large scatter, of factors of two or more, for the weaker transitions.

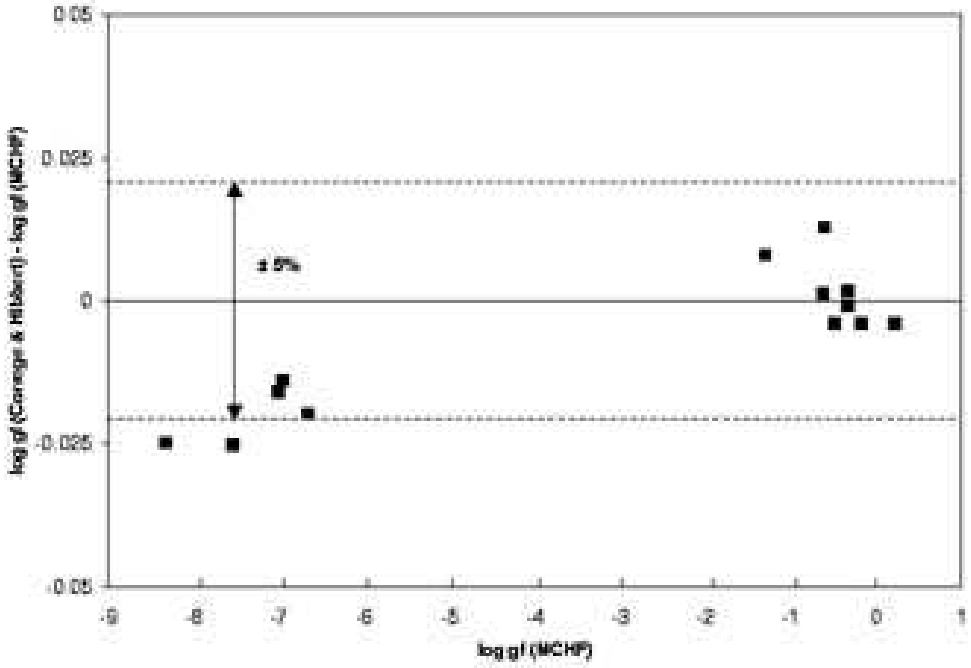

Fig. 2.— Comparison of results from the MCHF and CIV3 calculations, on a logarithmic scale, for C II.

4. Conclusion

We intend to enter all this new material into our comprehensive NIST Atomic Spectra Database (ASD) and publish it in the Journal of Physical and Chemical Reference Data.

This work was supported in part by the NASA Office of Space Science.

REFERENCES

Corrégé, G. and Hibbert, A., 2002, J. Phys. B, 35, 1211

Froese Fischer, C., The MCHF/MCDHF Collection, http://www.vuse.vanderbilt.edu/~cff/mchf_collection/

Froese Fischer, C. and Tachiev, G. 2004, At. Data Nucl. Data Tables, 87, 1

Fuhr, J. R., Martin, G. A., and Wiese, W. L. 1988, *Atomic Transition Probabilities-Iron through Nickel*, J. Phys. Chem. Ref. Data, 17, Suppl. 4

The Opacity Project Team, The Opacity Project-Vol. I (Institute of Physics, Bristol, England, 1995)

Wiese, W. L. Fuhr, J. R. and Deters, T. M. 1996, *Atomic Transition Probabilities of Carbon, Nitrogen, and Oxygen, A Critical Data Compilation*, J. Phys. Chem. Ref. Data, Monograph No. 7

Yan, Yu, Taylor, K. T. and Seaton, M. J. 1987, J. Phys. B, 20, 6399

Zatsarinny, O. and Froese Fischer, C. 2002, J. Phys. B, 35, 4669

NASA LAW, February 14-16, 2006, UNLV, Las Vegas

EUV-VUV Photolysis of Molecular Ice Systems of Astronomical Interest

C. Y. Robert Wu[1] & D. L. Judge[1].

Space Sciences Center and Department of Physics and Astronomy, University of Southern California, Los Angels, California, 90089-1341

robertwu@usc.edu, Judge@usc.edu,

B. -M. Cheng[2]

National Synchrotron Radiation Research Center, Hsinchu, Taiwan, R.O.C.

ABSTRACT

We wish to report laboratory simulation results obtained from extreme ultraviolet (EUV) and vacuum ultraviolet (VUV) photolysis of molecular ices relevant to the cometary-type ices and icy satellites of planetary systems. Specifically, we identify the type of molecules that form in the ices and/or those that come off the ice surfaces, quantify their production yields and destruction yields, understand their production mechanisms, and ascertain their significance in astronomical environments.

1. Introduction

Recently, much progress has been made in the area of laboratory simulations of chemical processes present in astronomical environments and in planetary systems. The body of this work includes the study of photon irradiation and charged particle impact of ice grains and ices. Such studies are fundamental to the understanding of the evolution of the interstellar medium, and the chemical composition of primitive material in our solar system. Laboratory simulation has now become a major tool in deciphering these complex phenomena which could have many other important implications in astrophysics and astrobiology. We have

[1]Space Sciences Center, USC

carried out laboratory simulation studies of several ice systems. A brief summary of this research work is presented here. The experimental set up and experimental procedures have been previously described (Wu et al. 2002).

2. Results and Discussion

Using the FTIR spectrometry we have studied (a) pure ices such as pure CH_4, CO, N_2, and NH_3 ices, (b) mixtures of two molecules such as $H_2O + CH_4, H_2O + C_2H_2, H_2O + CO, H_2O + CO_2, CH_4 + NH_3, CO + NH_3$, and $N_2 + CH_4$, and (c) mixtures of three or more molecules such as $H_2O + CH_4 + NH_3, CO + CH_4 + NH_3, H_2O + NH_3 + CH_4$, and $H_2O + CO + CH_4 + NH_3$. Examples of the data obtained are shown in the following. The difference of absorbances of the $CH_4 + H_2O$ (100:1) ice mixtures at 10 K produced by photolysis at the 58.4 nm (upper panel) and 30.4 nm (bottom panel) are shown in Fig. 1. The IR absorption features due to reaction products of $CH_2, CH_3, C_2H_6, C_3H_8$, CO

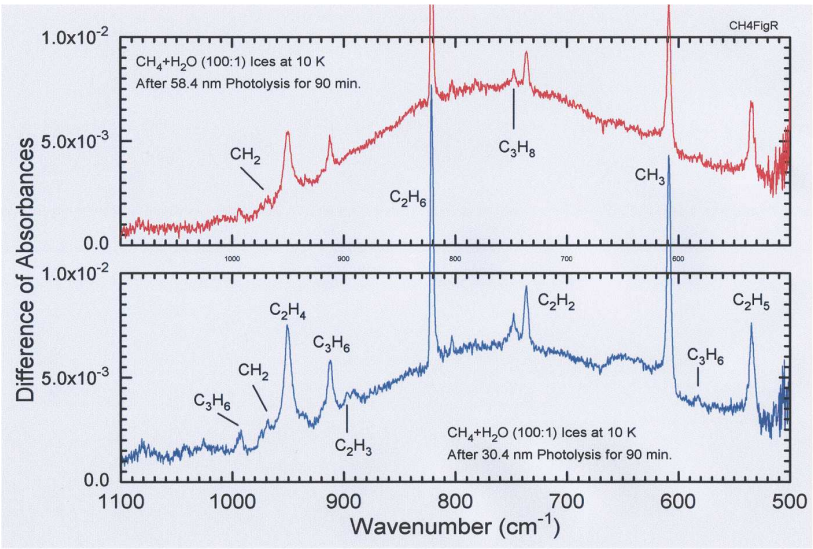

Fig. 1.— It displays the difference of absorbances of the $CH_4 + H_2O$ (100:1) ice mixture at 10 K taken after irradiation by the 58.4 nm (upper panel) and 30.4 nm (bottom panel) photolysis

.

and CO_2 are identified and indicated in the figure. We have also investigated $CH_4 + H_2O$ (1:7) and $CH_4 + H_2O$ (3:7) mixed ices. However, the products observed are mainly the CO, CO_2, and H_2CO. Evidently the radicals such as CH_2, CH_3, and C_2H_5 are converted into CO, CO_2, and H_2CO for the low CH_4 to H_2O ratios. In photolysis of pure CO ices at

10 K, the chemical species produced were found to be primarily C_3O_2, C_2O, CO_3, and CO_2 (Gerakines & Moore 2001). We have also studied the $H_2O + CO$ mixed ice systems with two different compositions, i.e., 1:1 and 4:1, at 10 K in the photolysis at 40.78, 21.23, and 10.196 eV. The major products are $HCO, H_2CO, HCOOH$, and CH_3OH. That is to say, in the presence of H_2O, the suboxides are converted to aldehydes, acides, and alcohols. In the EUV photolysis studies of $H_2O + C_2H_2$ (4:1) ices new molecules identified were mainly C_2H_6, CO_2, CO, CH_3OH, and H_2CO. In addition, we have tentatively assigned several unidentified absorption features to HCO, C_3H_8 and C_2H_5OH (Wu et al. 2002). Several production yields produced through VUV and EUV photolysis of the above molecular ice systems are summarized in Table 1.

Table 1: Summary of the production yields produced through EUV photolysis of ice systems at 10 K

ICY SYSTEMS AT 10K	PRODUCT	$Y(PHOTON^{-1})$		
		30.4 nm	58.4 nm	121.6 nm [a]
$C_2H_2 + H_2O(1:4)$	CO	$2.8(\pm0.2) \times 10^{-2}$	$4.6(\pm0.2) \times 10^{-2}$	
	CO_2	$9.1(\pm0.4) \times 10^{-3}$	$3.3(\pm0.4) \times 10^{-3}$	
$CO_2 + H_2O(1:4)$	CO	$9.4(\pm0.4) \times 10^{-3}$	$4.0(\pm0.4) \times 10^{-3}$	$3.3(\pm1.5) \times 10^{-2}$
	H_2CO_3	$5.7(\pm0.4) \times 10^{-3}$	$2.3(\pm0.2) \times 10^{-3}$	$3.1(\pm1.6) \times 10^{-3}$
$PureCO$	CO_2	$6.1(\pm0.3) \times 10^{-3}$	$5.8(\pm0.4) \times 10^{-3}$	
	C_3O_2	$5.1(\pm0.4) \times 10^{-3}$	$4.4(\pm0.4) \times 10^{-3}$	
	CO_3	$2.3(\pm0.3) \times 10^{-3}$	$2.8(\pm0.4) \times 10^{-3}$	
$PureCH_4$	CH_3	$1.2(\pm0.2) \times 10^{-3}$	$9.0(\pm0.2) \times 10^{-4}$	
	C_2H_2	$6.4(\pm0.5) \times 10^{-4}$	$4.6(\pm0.5) \times 10^{-4}$	
	C_2H_4	$1.9(\pm0.5) \times 10^{-3}$	$1.8(\pm0.5) \times 10^{-3}$	
	C_2H_6	$2.9(\pm0.2) \times 10^{-2}$	$2.2(\pm0.2) \times 10^{-3}$	

[a] The mixed icy system has a composition of $CO_2 + H_2O(1:1)$ at 18 K (Gerakines et al. 2000)

The EUV photolysis of the $N_2 + CH_4$ (1:1) and the $N_2 + CH_4$ (1:4) ice mixtures show IR absorption features belong to CH_3, C_2H_4, C_2H_6, and C_3H_8. The sharp HCN feature at 2096 cm^{-1} (Hudson & Moore 2000; Gerakines & Moore 2001) is clearly identified in the photolyzed $N_2 + CH_4$ (1:1) ice sample although the peak size is relatively weak. A peak at 2524 cm^{-1} appears to be an unknown feature. Its identity is unknown at the present time.

One of the clear differences between the two different compositions is that the HCN peak at 2096 cm^{-1} becomes too weak to be positively identifiable in the $N_2 + CH_4$ (1:4) ice sample.

A comparison of the FTIR spectra of the differences of absorbances in the spectral region between 1800 and 2200 cm^{-1} of the $N_2 + CH_4$ (1:1), $H_2O + CH_4 + NH_3$ (1:1:1), and $CO + CH_4 + NH_3$ (1:1:1) ices at 10 K produced through photolysis at 30.4 nm is displayed in Fig. 2. The salient features are briefly mentioned here. First, HCN has been clearly

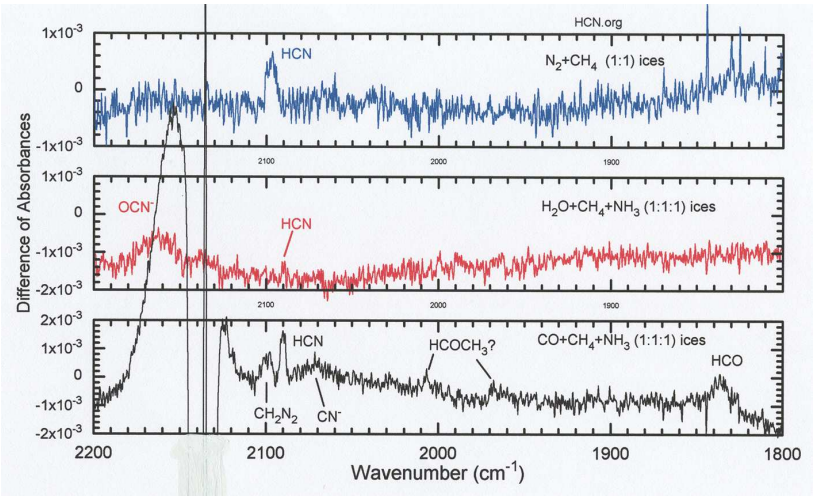

Fig. 2.— It displays a comparison of the FTIR spectra of the differences of absorbances in the 1800 2200 cm^{-1} region of the $N_2 + CH_4$ (1:1), $H_2O + CH_4 + NH_3$ (1:1:1), and $CO + CH_4 + NH_3$ (1:1:1) ices at 10 K produced through photolysis at 30.4 nm

.

produced in the $N_2 + CH_4$ (1:1) and the $CO + CH_4 + NH_3$ (1:1:1) mixed ice systems at 10 K, but it appears to be barely discernible in the $H_2O + CH_4 + NH_3$ (1:1:1) solid ice sample under the present experimental conditions. The HCN spectral position in the $N_2 + CH_4$ ice is about 10 cm^{-1} higher than those of the other two ice samples because of different host-site conditions. Secondly, the feature of OCN^- is clearly observed from EUV photolysis of the $H_2O + CH_4 + NH_3$ (1:1:1) mixed ice systems, see the middle panel. However, it is not clear whether the OCN^- is produced or not in the photolysis of $CO + CH_4 + NH_3$ (1:1:1) ices. This is because its absorbance can possibly be buried by the strong peak of the parent CO molecules at 2140 cm^{-1} (see the bottom panel). Thirdly, the CH_2N_2 and the CN^- anions are uniquely observed in the photolysis of the $CO + CH_4 + NH_3$ (1:1:1) mixed ice systems, the bottom panel. Further, we have tentatively identified the $HCOCH_3$ from photolysis of the $CO + CH_4 + NH_3$ (1:1:1) mixed ice systems. Therefore, by comparing the EUV photolyzed results of the ice samples of $CO + CH_4 + NH_3$ (1:1:1) and $H_2O + CH_4 + NH_3$ (1:1:1), we can conclude that the oxidizing power of H_2O in the icy environments is stronger than that

of CO. This is supported by the absence of $CH_2N_2, HCOCH_3$, and HCO products in the spectra of the photolyzed $CO + CH_4 + NH_3$ (1:1:1) ice samples at 10 K.

To determine the quantitative dependence of the production yield as a function of photon dose we first measure the product column density which is obtained by dividing the integrated peak of the change of absorbances with the band strengths. The photon dose in units of photons/cm^2 is obtained by dividing the integrated numbers of photons impinging on the ices by the photon beam size at the ice sample. The product yield per photon is determined from a plot of the product column density (cm^{-2}) as a function of photon dose. In Table 1 we summarize the product yields of several ice systems that we have recently studied (Wu et al. 2003, 2002) and that of (Gerakines et al. 2000).

3. Conclusion

By comparing the EUV photolyzed results of the EUV photolysis of (a) $CH_4 + H_2O$ (100:1), $CH_4 + H_2O$ (1:7) and $CH_4 + H_2O$ (3:7) ice systems; (b) $CO, H_2O + CO$ (1:1) and $H_2O + CO$ (4:1) ices and (c) $CO + CH_4 + NH_3$ (1:1:1) and $H_2O + CH_4 + NH_3$ (1:1:1) ices, we conclude that the oxidizing power of H_2O in the icy environments is stronger than that of CO. Similar results are observed from photolysis at other EUV photon energies but with different production yields. The present results suggest that XCN can be readily produced in mixed ices containing H, C, and N atoms. The intriguing photochemistry of ices deserves further investigations in order to improve our understanding of chemical evolution in cosmic environments.

This research is based on work supported by the NASA Planetary Atmospheres Program under Grant NAG5-11960 and the Astrophysics and Astrochemistry Program of the NSRRC.

REFERENCES

Gerakines, P. A., & Moore, M.H. 2001, Icarus, 154, 372

Gerakines, P. A., Moore, M.H.& Hudson, R.L. 2000, Astron. Astrophys, 357, 793

Hudson, R. L., & Moore, M.H. 2000, Astron. Astrophys, 357, 793

Wu, C.Y.R., Judge, D.L., Cheng, B. -M., Lee, C.S., Yih, T.S., & Ip, W. H. 2003, J. Geophys. Res, 108(E4), 5032

Wu, C.Y.R., Judge, D.L., Cheng, B. -M., Chih, Yih, T.S., & Ip, W. H. 2002, Icarus, 156, 456

NASA LAW, February 14-16, 2006, UNLV, Las Vegas

Vibrational and rotational quenching of CO by collisions with H, He, and H_2

Benhui Yang[1,2], P. C. Stancil[1,2], N. Balakrishnan[3] and R. C. Forrey[4]

[1]*Department of Physics & Astronomy and* [2]*Center for Simulational Physics, The University of Georgia, Athens, GA 30602-2451*

[3]*Department of Chemistry, University of Nevada Las Vegas, Las Vegas, NV 89154*

[4]*Department of Physics, Penn State University, Berks-Lehigh Valley College, Reading, PA 19610-6009*

ABSTRACT

Collisional quenching of molecular species is an important process in a variety of astrophysical environments including interstellar clouds, photodissociation regions, and cool stellar/planetary atmospheres. In this work, quantum mechanical scattering calculations are presented for the rotational and vibrational relaxation of rotationally-excited CO due to collisions with H, He and H_2 for collision energies between 10^{-6} and $\sim$15000 cm^{-1}. The calculations were performed using the close-coupling approach and the l-labeled form of the coupled-states approximation. Cross sections and rate coefficients for the quenching of the v=0-2, j=0-6 levels of CO are presented and comparisons with previous calculations and measurements, where available, are provided.

1. Introduction

Due to their astrophysical importance as these species are the most common ones in a wide range of astronomical sources, collisions of CO with H, He, and H_2 have been the subject of numerous experimental (1-6) and theoretical studies (7-13) Accurate data for state-to-state cross sections and rate coefficients for these systems are crucial to quantitative models of astrophysical environments. Accurate potential surfaces are needed for reliable theoretical simulations of energy transfer in collisions of CO by H, He, and H_2. To date, impressive progress has been made in the construction of potential energy surfaces (PESs) for neutral H-CO. In our calculations, we adopted the WKS PES (13; 14) for H-CO, Heijiman *et al.*'s PES (15) for He-CO, and the PES by Jankowski and Szalewicz (16) for H_2-CO scattering. Theoretical calculations for rovibrational excitation have been used to obtain rate coefficients needed to interpret astrophysical data, and the present work is part of a project aimed at calculating the required rate coefficients for CO excited by H, He and H_2.

2. Results

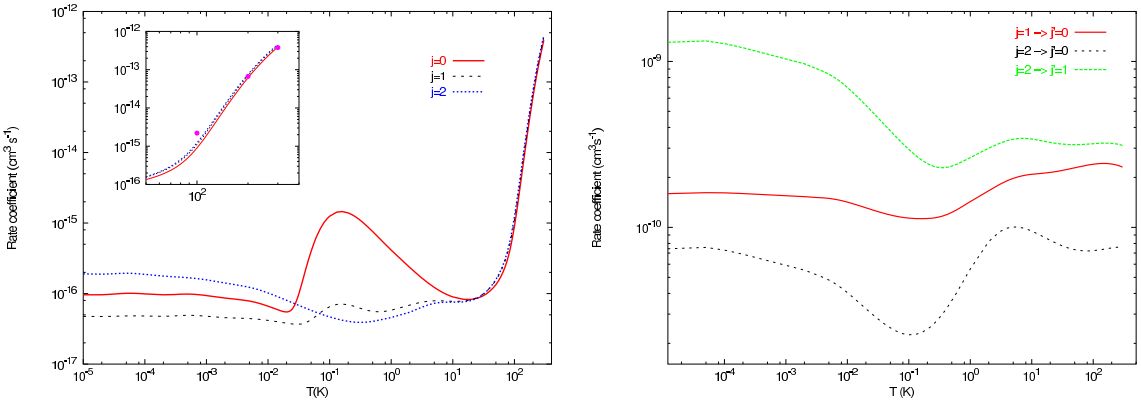

Fig. 1.— Left panel: Rate coefficients for the quenching of v=1, j=0, 1, and 2 for CO scattering by H. Symbols are IOS results (8). Right panel: Rate coefficients for the rotational quenching of v=1 for CO scattering with H.

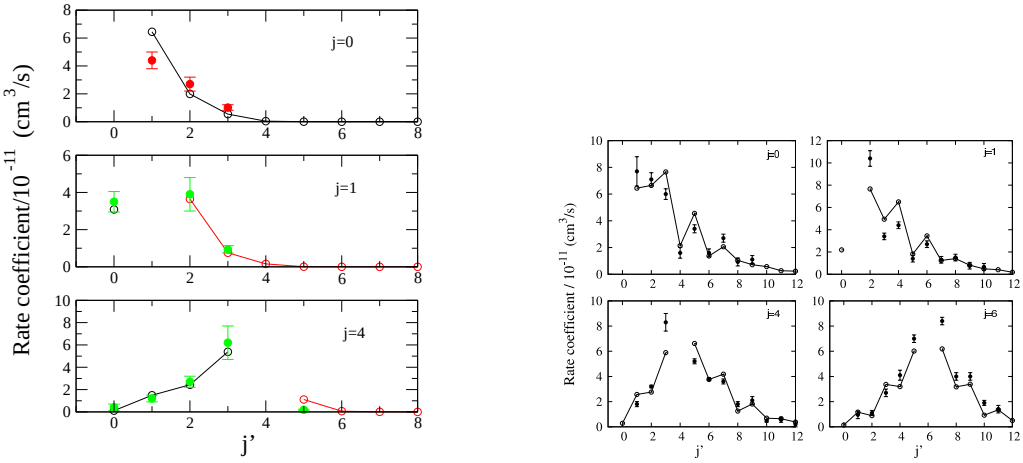

Fig. 2.— State-to-state rate coefficients for rotationally inelastic collisions of CO(v=2) with He atom. Left panel: at 15 K, (a) $j = 0$, (b) $j = 1$, (c) $j = 4$. Right panel: at 294 K, (a) $j = 0$, (b) $j = 1$, (c) $j = 4$, (d) $j = 6$. Lines with open circles: current CC calculations; solid circles with error bar: measurements (4).

Calculations were done with the molecular scattering progam MOLSCAT (17) to generate integral state-to-state cross sections. The coupled-channel equations were integrated using the modified log-derivative Airy propagator of Alexander and Manolopoulos (18). Calculations were performed for collision energies between 10^{-6} cm^{-1} and 15000 cm^{-1} in order to present accurate thermally averaged rate constants from 10^{-5} to 3000 K. At each energy a sufficient number of total angular momentum partial waves has been included to secure convergence of the cross sections. Examples of our results are shown in Figs. 1, 2 and 3 for CO scattering with H, He and H_2.

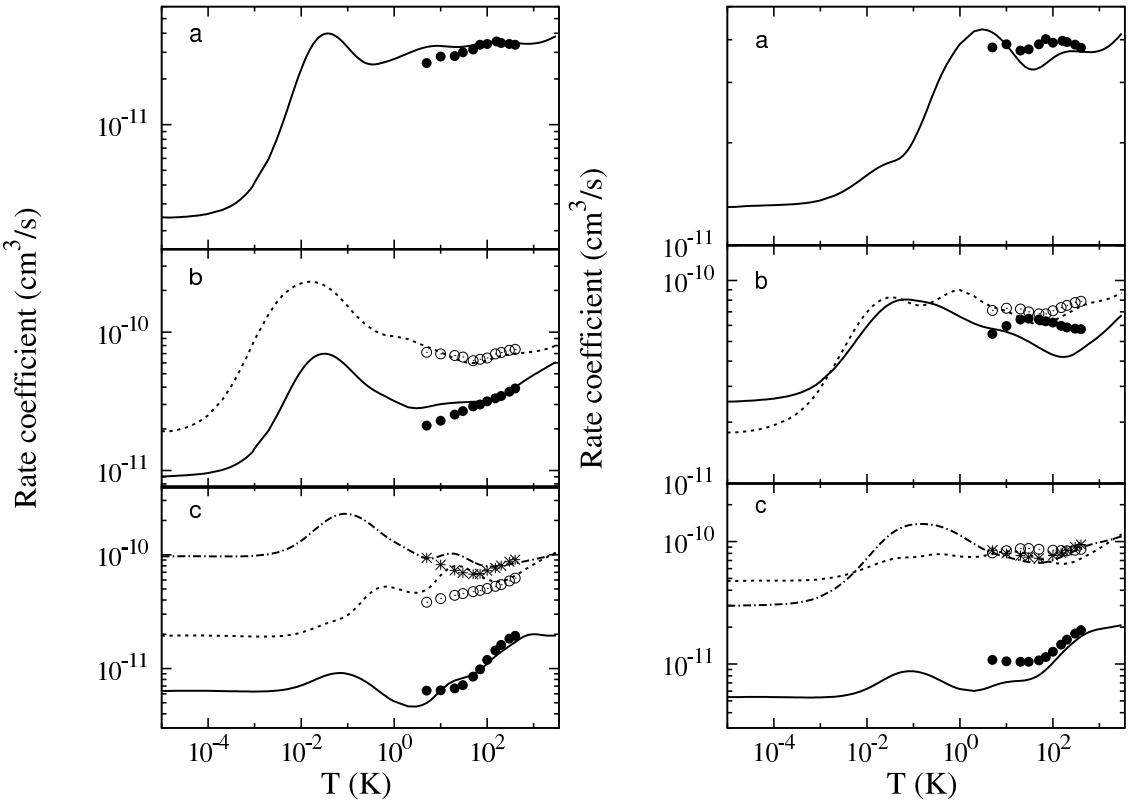

Fig. 3.— Rate coefficients for the quenching of CO by collisions with para-H_2 (Left panel) and orth-H_2 (Right panel) as functions of the temperature. Lines indicate current calculations. Symbols denote Flower's results (11). (a) $j_2 = 1 \rightarrow j_2' = 0$. (b) solid line: $j_2 = 2 \rightarrow j_2' = 0$, dashed line: $j_2 = 2 \rightarrow j_2' = 1$, solid circles: $j_2 = 2 \rightarrow j_2' = 0$, open circles: $j_2 = 2 \rightarrow j_2' = 1$; (c) solid line: $j_2 = 3 \rightarrow j_2' = 0$, dashed line: $j_2 = 3 \rightarrow j_2' = 1$, dash dotted line: $j_2 = 3 \rightarrow j_2' = 2$, solid circles: $j_2 = 3 \rightarrow j_2' = 0$, open circles: $j_2 = 3 \rightarrow j_2' = 1$, stars: $j_2 = 3 \rightarrow j_2' = 2$.

3. Summary

Rotational and vibrational quenching cross sections have been presented for a range of initial rotational states j and initial vibrational levels $v = 0$, 1, and 2. Good agreement was found with most other calculations where overlap exists and available experimental data. Future calculations will be performed to attempt to extend the range of v and j.

BY and PCS acknowledge support from NASA grant NNG04GM59G. NB acknowledges support from NSF through grant PHY-0245019 and the Research Corporation. RCF acknowledges support from the NSF through grant PHY-0244066 and a grant to ITAMP at Harvard University and Smithsonian Astrophysical Observatory.

REFERENCES

1. G. C. McBane, S. H. Kable, P. L. Houston, and G. C. Schatz, J. Chem. Phys., 94, 1141 (1991).
2. J. D. Tobiason, J. R. Dunlop, and E. A. Rohlfing, J. Chem. Phys. **103**, 1448 (1995).
3. T. C. Smith, D. A. Hostufler, G. D. Hager, M. C. Heaven, and G. C. McBane, J. Chem. Phys. **120**, 2285 (2004).
4. D. Carty, A. Goddard, I. R, Sims, and I. W. M. Smith, J. Chem. Phys. **121**, 4671 (2004).
5. A. R. W. McKellar, J. Chem. Phys. **108**, 1811 (1998).
6. S. Antonova, A. P. Tsakotellis, A. Lin, and G. C. McBane, J. Chem. Phys. **112**, 554 (2000).
7. J. M. Bowman, J. S. Bittman, and L. B. Harding, J. Chem. Phys. **85**, 911 (1986).
8. N. Balakrishnan, M. Yan, and A. Dalgarno, Astrophy. J **568**, 443 (2002).
9. J. P. Reid, C. J. S. M. Simpson, and H. M. Quiney, J. Chem. Phys. **107**,
10. E. Bodo, F. A. Gianturco, and A Dalgarno, Chem. Phys. Lett. **353**, 127 (2002).
11. D. R. Flower, J. Phys. B **34**, 2731 (2001).
12. M. Mengel, F. C. DeLucia, and E. Herbst, Can. J. Phys. **79**, 589 (2001).
13. H.-J. Werner, C. Bauer, P. Rosmus, H.-M. Keller, M. Stumpf, and R. Schinke, J. Chem. Phys. **102**, 3593 (1995).
14. H.-M. Keller, H. Floethmann, A. J. Dobbyn, R. Schinke, H.-M. Werner, C. Bauer, and P. Rosmus, J. Chem. Phys. **105**, 4983 (1996).
15. T. G. A. Heijmen, R. Moszynski, P. E. S. Wormer, and A. van der Avoird, J. Chem. Phys. **107**, 9921 (1997).
16. P. Jankowski and K. Szalewicz, J. Chem. Phys. **123**, 104301 (2005).
17. J. M. Hutson and S. Green, MOLSCAT computer code, version 14 (1994), distributed by Collaborative Computational Project No. 6 of the Engineering and Physical Sciences Research Council (UK).
18. M. H. Alexander and D. E. Manolopoulos, J. Chem. Phys. **86**, 2044 (1987).

NASA LAW, February 14-16, 2006, UNLV, Las Vegas

Sub-millimeter Spectroscopy of Astrophysically Important Molecules and Ions: Metal Hydrides, Halides, and Cyanides

L. M. Ziurys, M. A. Flory, & D. T. Halfen

Department of Chemistry, Department of Astronomy, Steward Observatory, University of Arizona, Tucson, AZ 85721

ABSTRACT

With the advent of SOFIA, Herschel, and SAFIR, new wavelength regions will become routinely accessible for astronomical spectroscopy, particularly at sub-mm frequencies (0.5-1.1 THz). Molecular emission dominates the spectra of dense interstellar gas at these wavelengths. Because heterodyne detectors are major instruments of these missions, accurate knowledge of transition frequencies is crucial for their success. The Ziurys spectroscopy laboratory has been focusing on the measurement of the pure rotational transitions of astrophysically important molecules in the sub-mm regime. Of particular interest have been metal hydride species and their ions, as well as metal halides and cyanides. A new avenue of study has included metal bearing molecular ions.

1. Introduction

Over 130 molecular species have been identified in the interstellar medium in a variery of regions, such as circumstellar envelopes, dense clouds, and diffuse gas. These molecules range from diatomics to complex organic species. While much has been learned about the composition of the ISM, a great many spectral features remain unidentified. In order to determine the origin of these emission lines, high resolution, pure rotational laboratory spectroscopy of new metal species has been conducted.

2. Experimental

Three direct absorption, millimeter/sub-mm instruments have been used in the studies of metal containing species, including molecular ions, and they are described in detail elsewhere (Ziurys et al. 1994, Savage & Ziurys 2005). These instruments are all quasi-optical systems employing lenses, grids, and mirrors to propagate the radiation. The radiation

sources are combinations of Gunn oscillators with Schottky diode multipliers, and the detectors used are He-cooled, InSb bolometers. Two systems contain Broida-type ovens for metal vapor production and are employed for studies of neutral molecules, while the third utilizes an ion-selective technique called velocity modulation. Molecules are created *in situ* by reacting specific precursors, often metal vapor and a reactant gas. Organometallic precursors are also used. As molecular constants are generally not available for the species of interest, large regions in frequency space usually need to be searched to identify spectral features.

3. Results and Discussion

The spectra of several small metal-containing molecules of astrophysical interest have been recently measured. A new avenue of research has also been initiated concerning the study of metal-contining molecular ions.

Hydrides - The pure rotational spectra of AlH and CrH have been measured (Halfen & Ziurys 2004, Halfen & Ziurys 2004, Harrison et al. 2006). For AlH, the quadrupole hyperfine structure was accurately determined for the first time in the $N = 1 \leftarrow 0$ transition. Rest frequencies are now available for CrH ($X\ ^6\Sigma^+$). Because of the presence of five unpaired electrons and two nuclear spins, this molecule exhibits complicated fine and hyperfine splittings, as shown in Figure 1. Future laboratory studies are planned for TiH, MnH, and MgH^+.

Halides - Halides are common carriers of metals in the interstellar medium. Therefore, the spectra of several metal halides, including MnCl ($X\ ^7\Sigma^+$) and ZnF ($X\ ^2\Sigma^+$), have been recorded (Halfen & Ziurys 2005, Flory et al. 2006). The work on ZnF represents the first spectroscopic study of this radical in the gas phase. Given the presence of KCl in IRC+10216, ZnF (and ZnCl) may also be present in circumstellar gas.

Cyanides - The rotational spectrum of CrCN ($X\ ^6\Sigma^+$) has been measured. Spectra of three isotopomers of CrCN ($^{52}Cr^{12}C^{14}N$, $^{53}Cr^{12}C^{14}N$, and $^{52}Cr^{13}C^{14}N$) have been recorded in order to determine the ground state structure, which has been established to be the linear metal cyanide rather than the isocyanide. Spectroscopic constants for CrCN are presented in Table 1. Currently, studies of FeNC are being pursued.

Ions - Several metal-containing ions have been studied with the ion-selective spectrometer. The spectra of VCl^+ ($X\ ^4\Sigma^-$), $TiCl^+$ ($X\ ^3\Phi_r$) (Halfen & Ziurys 2005), TiF^+ ($X\ ^3\Phi_r$), and $FeCO^+$ ($X\ ^4\Sigma^-$) have all been observed. $FeCO^+$ has never been studied previously in the gas phase, and it has been found to exhibit a complex spectral pattern, as shown in Figure 2. Plans for future studies include metal hydride ions, such as TiH^+ and CrH^+.

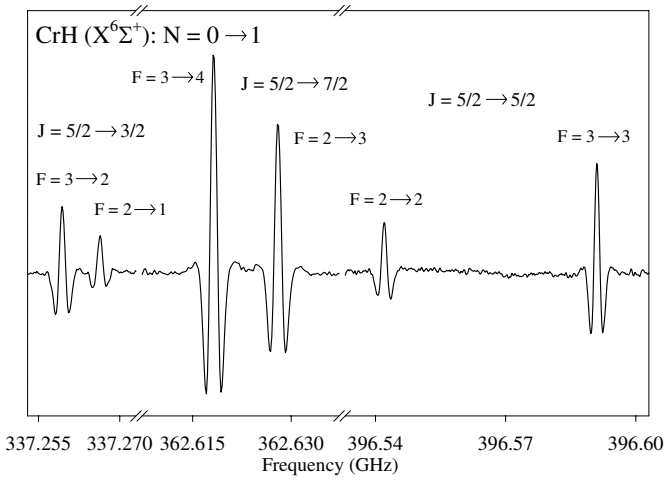

Fig. 1.— Spectrum of CrH N = 0 → 1 showing the fine structure components and proton hyperfine splittings.

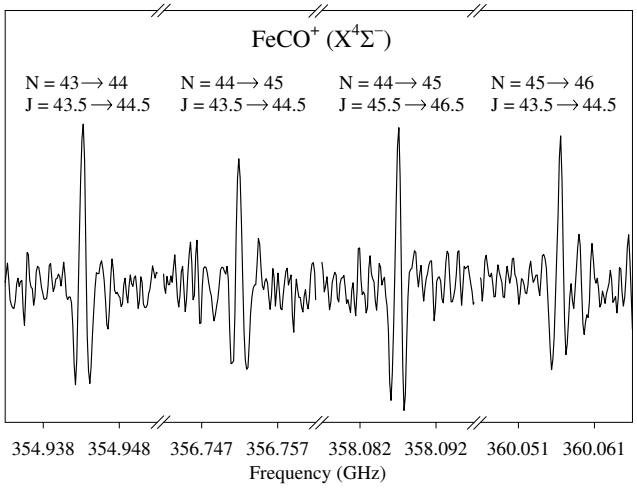

Fig. 2.— The spectrum of $FeCO^+$ near 357 GHz. Four spin components are shown, originating from three rotational transitions. The spin splitting is very large for this ion, resulting in the fine structure overlapping the rotational structure.

Table 1: Spectroscopic Constants for CrCN (X $^6\Sigma^+$) in MHz[a].

Constant	Value	Constant	Value
B	3895.6410(19)	D	0.00144627(26)
γ	36.41(13)	γ_D	-0.000016(11)
λ	633(37)	λ_D	-0.00662(75)
λ_H	0.00000021(10)	rms	0.125

[a]Values in parentheses are 3σ errors.

4. Conclusion

The pure rotational spectra of several metal containing molecules (radicals and ions) have been measured in the laboratory in the millimeter/sub-mm regime. Transition frequencies and molecular constants with accuracy better than 1 in 10^7 are now available for astronomical searches. Such laboratory work is clearly necessary in order to evaluate interstellar spectra, particularly the rich data sets that will be avilable at sub-mm wavelengths.

This work was supported by NASA Grant NAGS-12719 and NSF Grant CHE 04-11551.

REFERENCES

Ziurys, L. M., Barclay, Jr., W. L., Anderson, M. A., Fletcher, D. A., & Lamb, J. W. 1994, Rev. Sci. Instrum., 65, 1517
Savage, C. & Ziurys, L. M. 2005, Rev. Sci. Instrum., 76, 043106/1
Halfen, D. T. & Ziurys, L. M. 2004, Astrophys. J., 607, L63
Halfen, D. T. & Ziurys, L. M. 2004, Astrophys. J., 611, L65
Harrison, J. J., Brown, J. M., Halfen, D. T., & Ziurys, L. M. 2006, Astrophys. J., 637, 1143
Halfen, D. T. & Ziurys, L. M. 2005, J. Chem. Phys., 122, 054309
Flory, M. A., McLamarrah, S. K., & Ziurys, L. M. 2006, J. Chem. Phys., submitted
Halfen, D. T. & Ziurys, L. M. 2005, J. Mol. Spec., 234, 34

NASA LAW, February 14-16, 2006, UNLV, Las Vegas

Spin Changing Collisions of Hydrogen

B. Zygelman

Dept of Physics, University of Nevada Las Vegas, Las Vegas, NV 89154

bernard@physics.unlv.edu

ABSTRACT

We discuss spin changing collisions of hydrogen atoms. Employing a fully quantal theory we calculate and present new collision data. We discuss the respective roles of spin exchange and long range magnetic interactions in collisonal redistribution of sub-level populations. The calculated atomic data is needed for accurate modeling of 21 cm line emission/absorption by primordial hydrogen in the early universe.

1. Introduction

The 21 cm line of atomic hydrogen was first observed by Ewen & Purcell (1951) in 1951. This discovery hastened the development of radio astronomy (Stephan 1999) and observation of the 1420 Mhz transition in interstellar hydrogen allowed the first maps of large scale structures, obscured in the visible bands, in our galactic neighborhood. A new generation of radio observatories, such as the LOFAR array (LOFAR 2006), the proposed Square Kilometer Array (SKA 2006) as well as possible future lunar based arrays, promise capabilities that will allow "transformational" observations of the early universe. By detection of the red shifted 21 cm line from environments at and before the epoch of re-ionization, such instruments could provide unprecedented information on primordial matter density fluctuations and provide insight into the nature of dark matter. Loeb & Zaldarriaga (2004) recently proposed application of 21 cm tomography (Madau et al. 1997) of the dark age universe. Accurate modeling of emission and/or absorption of the 21 cm line in primordial hydrogen depends crucially on the values of spin exchange collision rates. In this abstract we present the results of a multichannel collision theory using state-of-the-art molecular potentials to calculate the spin exchange rate coefficients. We discuss the respective roles of spin exchange and long range magnetic interactions in collisonal redistribution of sub-level populations. Atomic units are used throughout, unless otherwise stated.

2. Discussion

The internal states of the atoms are represented by the kets, $|f_a m_a f_b m_b>$ where $f_a m_a$ are hyperfine quantum numbers of atom A, and $f_b m_b$ that of atom B. We consider a transition from state $|j> \equiv |f_a m_a f_b m_b>$ to $|i> \equiv |f'_a m'_a f'_b m'_b>$, the cross section is given by

$$\begin{aligned} \sigma(j \to i) &= \frac{\pi}{2k_j^2} \sum_L (2L+1) \, |T_{[ij]}(L) + (-1)^L T_{[\tilde{i}j]}(L)|^2 \\ T_{[ij]}(L) &\equiv \delta_{[ij]} - S_{[ij]}(L) \end{aligned} \tag{1}$$

where $k_j^2/2\mu$ is the kinetic energy in the entrance channel, μ is the reduced mass, $S_{[ij]}$ is the S-matrix and the notation $\tilde{i}$ implies that if $i = \{f_b m_b f_a m_a\}$ then $\tilde{i} = \{f_a m_a f_b m_b\}$. The cross sections defined in Eq. (1) take into account the quantum symmetry of two identical bosons (hydrogen atoms). A detailed discussion of the theory and calculations was given elsewhere (Zygelman 2005), here we present the effective rate coefficients for a hydrogen atom to undergo an $F = 1$ to $F = 0$ hyperfine transition as a function of collision temperature. The rates are tabulated in Table 1. For higher temperatures we recommend the rates tabulated by Allison & Dalgarno (1969) multiplied by a factor of 4/3 (Zygelman 2005).

Using these rates, as well as radiation induced transition frequencies, one can model the spin temperature T_s (Purcell & Field 1956) of the hydrogen gas. It is an essential parameter that determines, in part, the observed brightness temperature. The former is defined by the relation

$$\frac{N_{F=1}}{N_{F=0}} = 3 \exp(-\Delta E / k T_s), \tag{2}$$

and implicitly assumes that the $F = 1$ sub-levels are equally populated. In a discussion of processes that populate the magnetic sub-levels (Zygelman 2005), we pointed out that collisions do not necessarily bring those populations into statistical equilibrium. This conclusion follows from selection rules for spin exchange, that two hydrogen atoms must conserve the sum of the two spin components along the quantization axis. Collisional relaxation of the gas requires, in addition to spin exchange, the dipolar spin relaxation (Zygelman 2005) mechanism. The rates for the latter process where estimated to have values that are a factor 10^{-4} smaller than spin exchange rates. For conditions that existed in the dark age universe, we conclude that dipolar spin relaxation processes do not play a role. This could allow a scenario where the hydrogen could acquire distinct sub-level spin temperatures. Full understanding of the kinetic processes that bring the hydrogen gas into equilibrium will require knowledge of all hyperfine level collision transition rates in addition to elastic scattering rates. We are presently pursuing a program that involves an accurate calculation of all state-state collision rates for a range of collision temperatures.

This work was supported in part by a grant from the Department of Energy under Award Number DE-FG36-05GO85028.

Table 1: Rate coefficient $\kappa(1-0)$ for the effective $F = 1 \rightarrow F = 0$ collision induced spin changing transition as a function of temperature. The rates are expressed in units of $cm^3\, s^{-1}$

$T(K)$	$\kappa(1-0)$
1	1.38×10^{-13}
2	1.43×10^{-13}
4	2.71×10^{-13}
6	6.60×10^{-13}
8	1.47×10^{-12}
10	2.88×10^{-12}
15	9.10×10^{-12}
20	1.78×10^{-11}
25	2.73×10^{-11}
30	3.67×10^{-11}
40	5.38×10^{-11}
50	6.86×10^{-11}
60	8.14×10^{-11}
70	9.25×10^{-11}
80	1.02×10^{-11}
90	1.11×10^{-10}
100	1.19×10^{-10}
200	1.75×10^{-10}
300	2.09×10^{-10}

REFERENCES

Ewen, H. I., and Purcell, E. M. 1951, Nature, 168, 356; Muller, C. A., & Oort J. H. 1951, Nature, 168, 357

Stephan, K. D. 1999, IEEE Antennas and Propagation Magazine, 41, 7

LOFAR, http://www.lofar.org

SKA, http://www.skatetelescope.com

Loeb, Abraham, and Zaldarriaga, Matias 2004, Phys. Rev. Lett., 92, 211301-1

Madau, Piero, Meiskin, Avery, and Rees, J., Martin 1997, ApJ, 475, 429

Purcell, Edward M., and Field, George 1956, ApJ, 124, 542

Zygelman, B. 2005, ApJ, 622, 1356

Allison, A. C., and Dalgarno, A. 1969, ApJ, 158, 423

NASA LAW, February 14-16, 2006, UNLV, Las Vegas

Isotope effects in collisional VT relaxation of molecular hydrogen

R. J. Bieniek

Physics Department, University of Missouri-Rolla, Rolla, MO 65409-0640

bieniek@umr.edu

ABSTRACT

A simple exponential-potential model of molecular collisions leads to a two-parameter analytic expression for rates of collisionally induced vibrational-translation (VT) energy exchange that has been shown to be accurate over variations of orders of magnitude as a function of temperature in a variety of systems. This includes excellent agreement with reported experimental and theoretical results for the fundamental self-relaxation rate of molecular hydrogen $H_2(v = 1) + H_2 \rightarrow H_2(v = 0) + H_2$. The analytic rate successfully follows the five-orders-of-magnitude change in experimental values for the temperature range 50-2000 K. This approach is now applied to isotope effects in the vibrational relaxation rates of excited HD and D_2 in collision with H_2: $HD(v = 1) + H_2 \rightarrow HD(v = 0) + H_2$ and $D_2(v = 1) + H_2 \rightarrow D_2(v = 0) + H_2$. The simplicity of the analytic expression for the thermal rate lends itself to convenient application in modeling the evolving vibrational populations of molecular hydrogen in shocked astrophysical environments.

1. VT transitions in shocked environments

In many astrophysical environments, shock fronts can significantly disturb the thermodynamic equilibrium between the kinetic and vibrational motion of quiescent molecular species present (as in cold molecular clouds). Although kinetic energies can rise rapidly in response to the shock, vibrational populations are slower to respond, producing non-LTE situations. Molecular collisions drive the vibrational populations to become equilibrated with thermal kinetic energy by inducing energy exchange between vibrational and translational (VT) forms. The VT rate will determine the evolution of relative populations of vibrational levels in such disturbed environments where the vibrational and translational temperatures are not equilibrated. This will affect an astrophysical systems spectroscopy, energetics, reactions, and radiative signatures.

The evolution of vibrational populations can be calculated if state-to-state rates for vibrational-rotational transitions are available for the species desired. However, these are often hard to come by. Yet, much modeling and analysis can be done by lumping all the rotational states together by envisioning a spherically symmetric molecule whose radius can vibrate (or breathe). By further assuming that the interaction of the target molecule with the collider is exponential with collisional separation, Bieniek & Lipson (1996) showed how a very simple expression for VT rates can be obtained by analytically summing over collisional partial waves and evaluating the thermal average over collisional energies by the method of steepest descent. The resulting mathematical expression has been shown to be highly accurate in predicting VT rates for vibrationally excited N_2, NO, and OH over large temperature ranges and levels of activation with just two fitting parameters. The astrophysically interesting molecule of H_2 and its isotopes is actually the hardest test for the breathing-sphere idea because of the large rotational spacing relative to the vibrational energies. This paper presents numerical results for the fundamental vibrational quenching $v = 1 \rightarrow 0$ of H_2, HD, and D_2 in collision with H_2. The predictions are in impressive agreement with experimental results for molecular hydrogen from 50-2000 K.

2. Analytic VT Rate Constant

The underlying assumption of the collisional model is a breathing sphere comprised of Morse oscillator states for the target molecular coordinate r perturbed by an exponential interaction in the collision coordinate R. Morse oscillators are used to model the diatomic because the vibrational eigenenrgies are $E_v = \hbar\omega_e(v + \frac{1}{2})[1 - \chi_e(v + \frac{1}{2})]$ nicely incorporate the important anharmonicity χ_e into the calculation of the change in vibrational energy $\Delta E_v = E_v - E_{v-1}$ that is transferred to translational motion. The perturbing collider will be represented as a structureless particle of mass M here (although there are methods of allowing for it to change vibrational state). Consequently, the potential operator is $V(R, r) = h_{mo}(r) + Ae^{(-\alpha R - \gamma \Delta r)}$, where A is the strength of the perturbation interaction, α is the exponential slope of the collisional perturbation, and γ is the transitional perturbation between the Morse oscillator states in the molecular stretch Δr. Because the perturbation is fundamentally caused by the collider, we can relate the α and γ by a simple proportion involving the masses (m_1 and m_2) of the two atoms in the target diatomic: $\gamma = \frac{\min(m_1, m_2)}{m_1 + m_2}\alpha$. The transitional coupling between the Morse oscillator states $U_{v,v'} =< v|e^{-\gamma \Delta r}|v' >$ needed here can be analytically evaluated with known properties of these oscillators. It turns out the strength A cancels out in the expression for the rate, so its value need not be not be known. The only other parameter besides α that is needed in the model is the characteristic collisional radius R_c of the interaction, which should be on the order of molecular diameters. All other needed quantities such as molecular masses and vibrational energy spacing can be readily obtained from standard data tables.

The analytic expression for the VT rate constant has been derived elsewhere. Although

it can be modified to incorporate the effects of multi-quantum transitions, we are only dealing with the fundamental single-quantum quenching transitions $v = 1 \rightarrow v = 0$ transition here. For single-quantum transitions $v \rightarrow v-1$, the analytic expression for the thermally averaged rate constant (in units of $length^3/time$) is:

$$k_{v\rightarrow v-1}(T) = \frac{16\pi^3\sqrt{2\pi}}{3\hbar\Gamma(\frac{3}{2})}\left(\frac{2\mu}{\hbar^2}\right)^{\frac{3}{2}}\frac{R_c^2}{\alpha^4}\frac{\Delta E_v^4}{(k_BT)^{\frac{3}{2}}}|U_{v,v-1}|^2|_2F_1(z(X_v))|^2\frac{e^{g_v(X_v)}}{\sqrt{|g_v{}''(X_v)|}} \quad (1)$$

where

$$g_v(x) = \beta_v[\sqrt{ax} - \sqrt{1+ax}] - \frac{\Delta E_v}{k_BT}x + ln(x) \quad (2)$$

$$\beta_v = 2\pi\frac{\sqrt{2\mu\Delta E_v}}{\hbar\alpha} \quad (3)$$

and X_v is the root of the equation

$$X_v g_v{}'(X_v) = \tfrac{1}{2}\sqrt{aX_v} - \tfrac{1}{2}\frac{aX_v}{\sqrt{1+aX_v}} - \frac{\Delta E_v}{\beta_v kT}X_v + \frac{1}{\beta_v} = 0 \quad (4)$$

where $a = 0.85$ and $z(x)$ is the argument of the hypergeometric function ${}_2F_1$:

$$z(x) = 1 + i\frac{\beta_v}{2\pi}(\sqrt{x} + \sqrt{1+x}), 1 - i\frac{\beta_v}{2\pi}(\sqrt{x} - \sqrt{1+x}), 2, 1 - \frac{|U_{v,v}|^2}{|U_{v-1,v-1}|^2} \quad (5)$$

Although all this expression may *seem* daunting, it is actually very easy to use, once one recognizes that 1) there are only two adjustable parameters: α and R_c; 2) the hypergeometric function is straightforward to calculate using a standard series expansions 3) the hypergeometric function is very nearly 1.0 for all reasonable values of its argument encountered in molecular collisions (and can just be set to one); 4) the important equation for X_v has only a single root and it can be found easily using any root-solving iterative process (even the simple Newton-Raphson method).

3. Vibrational relaxation rates for molecular hydrogen and its isotopes

The vibrational relaxation rates for $H_2(v = 1 \rightarrow 0)$ in collision with ground state H_2 have been experimentally measured by Audibert, Joffrin & Ducuing (1974) in the temperature range T=50-400 K, and by Dove & Teitelbaum (1974) for T=1350-2000 K . This experimental data was to determine the two parameters of the analytic rate constant, α and R_c. One first adjust α until the rate shape of the $k_{1\rightarrow 0}$ *vs.* T curve is found, and then R_c is simply adjusted to agree with the absolute value of the rate. The values producing the best fit are: $\alpha = 2.02\text{bohr}^{-1} = 38.2\text{nm}^{-1}$ and $R_c = 5.4$ bohr $= 0.29$ nm. These same values can be used for the interaction of electronically identical HD and D_2 in isotopic substitution.

The resulting temperature dependence of quenching rates is shown in the Figure 1. Note the excellent agreement with experimental results from 100-2000 K with this two-parameter model.

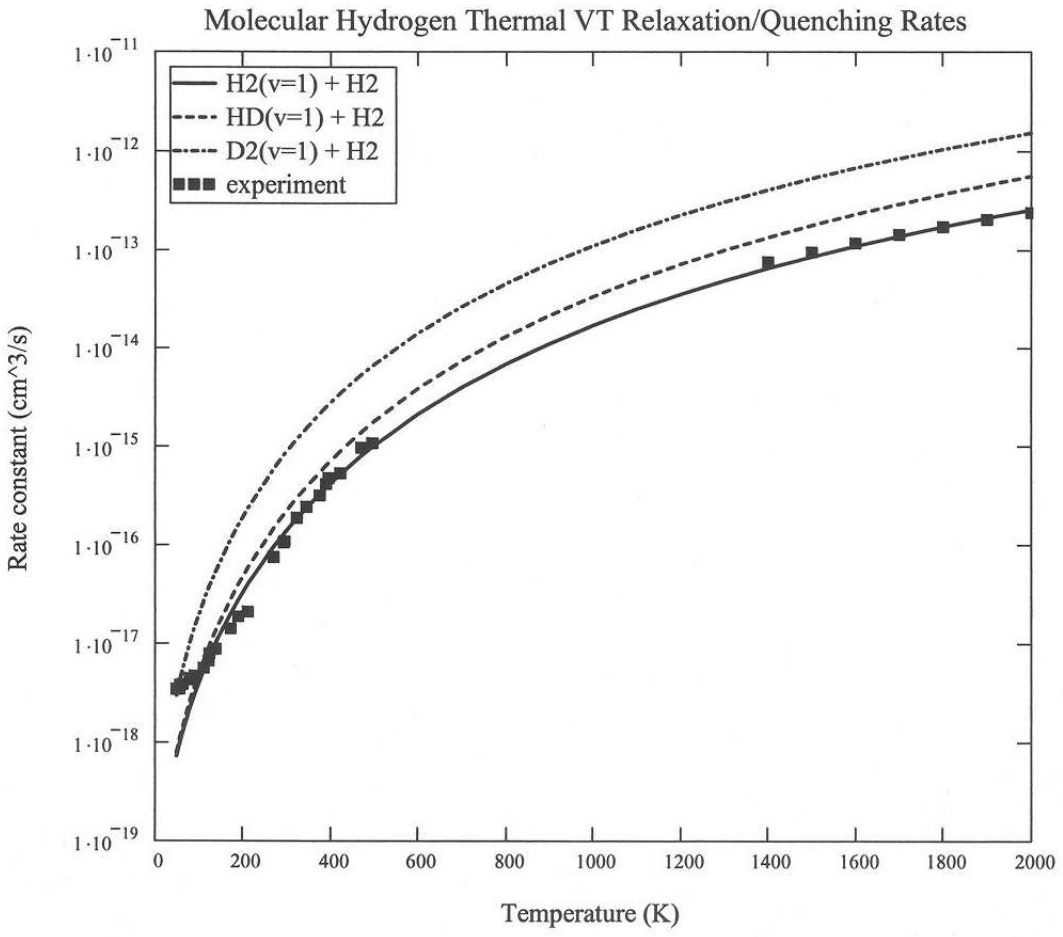

Fig. 1.— Collisional rates for vibrational relaxation of isotopes of molecular hydrogen

The author gratefully acknowledges the support of the University of Nevada, Las Vegas, while he was on sabbatical leave there for the academic year 2005-2006.

REFERENCES

Bieniek, R. J., & Lipson, S. J. 1996, Chemical Physics Letters, 263, 276
Audibert, M. M., Joffrin, C. & Ducuing, J. 1974, Chemical Physics Letters, 25, 158
Dove, J. E. & Teitelbaum, H. 1974, Chemical Physics, 6, 431

APPENDIX A: AGENDA DAY 1

Tuesday, February 14, 2006

Opening Remarks: Chair-Victor Kwong
8:30 Welcome: Carol Harter & Ron Yasbin
8:45 Introduction: Hashima Hasan

Session I (Plenary and Cold Universe): Chair-Steve Federman
9:00 Kate Kirby, *Laboratory Astrophysics: Enabling Scientific Discovery and Understanding*
9:45 Steve Charnley, *Astrochemistry in Sites of Star Formation*

Session II (Cold Universe and Missions): Chair-Victor Kwong
10:30 Al Glassgold, *Circumstellar Disks Around Young Stars*
11:00 Eric Herbst, *Astrochemistry*
11:30 Chas Beichman, *NASA's Search for Habitable Environments and Life: The Role of Laboratory Astrophysics*
12:00 Xander Tielens, *Herschel*

Session III (Cold Universe and Missions): Chair-Lucy Ziurys
2:00 Nick Woolf, *Lab Studies and the Pyramid of Science*
2:30 Paul Feldman, *Comets*

Session IV (Missions and Contributed Talks): Chair-Farid Salama
3:15 Eric Wilson, *Laboratory Analysis for Planetary Science Research: Application for Cassini-Huygens*
3:45 Tom Greene, *SOFIA: The Next Airborne Observatory*
4:15 Raul Baragiola, *Laboratory Simulations in Ices and Minerals*
4:30 Friedrich Huisken, *Spectroscopic Studies of PAHs in Supersonic Jets and Liquid Helium Droplets*
4:45 Ralf Kaiser, *Laboratory Studies on the Formation of Carbon-Bearing Molecules in Extraterrestrial Environments from the Gas Phase to the Solid*
5:00 Guido Fuchs, *Sticking and Desorption of Small Physisorbed Molecules: Laboratory Experiments and Astrophysical Applications*
5:15 Gianfranco Vidali, *Use of Laboratory Data to Model Interstellar Chemistry*

5:30-7:00 Posters

APPENDIX A: AGENDA DAY 2

Wednesday, February 15, 2006

Session V (Hot Universe and Missions): Chair-Nancy Brickhouse
8:30 John Cowan, *Nucleosynthesis*
9:00 Ian Short, *Physical Data Needs for Select Problems in Stellar Atmospheres*
9:30 Frits Paerels, *Laboratory Astrophysics for High Resolution Astrophysical X-ray Spectroscopy*

Session VI (Hot Universe and Missions): Chair-Daniel Savin
10:15 Randall Smith, *X-ray Plasma Models: Current Achievements and Future Needs*
10:45 Todd Tripp, *Ultraviolet and X-ray Spectroscopy of Multiphase Hot Gas in the Interstellar Medium and the IGM*
11:15 Chris Howk, *NASA's Ultraviolet Spectrographs: Science and Atomic Data Needs*
11:45 Evelyne Roueff, *Laboratory Astrophysics in Europe and the Ties to Various Missions*

Session VII (Contributed Talks): Chair-Joe Weingartner
2:00 Michael Flory, *Sub-millimeter Spectroscopy of Astrophysically Important Molecules*
2:15 John Pearson, *Laboratory Spectroscopy of CH^+ and Isotopic CH*
2:30 Douglas Jackson, *Recent Selected Ion Flow Tube (SIFT) Studies Concerning the Formation of Amino Acids in the Gas Phase*
2:45 Timothy Lee, *Calculation of Ro-vibrational Spectra: State-of-the Art*
3:00 Hantao Ji, *Laboratory Study of Magnetorotational Instability and Hydrodynamic Stability at Larger Reynolds Numbers*

Session VIII (Contributed Talks): Chair-Phillip Stancil
3:30 Krister Nielsen, *Targeting Inaccurate Atomic Data in the η Car Ejecta Absorption*
3:45 James Lawler, *A Spatial Heterodyne Spectrometer for Laboratory Astrophysics; First Interferogram*
4:00 Peter Beiersdorfer, *Magnetic Field Sensitive Line Ratios in EUV and X-ray Spectra*
4:15 Tim Kallman, *Sensitivity Analysis Applied to Atomic Data Used for X-ray Spectrum Synthesis*
4:30 David Schultz, *The Southeast Laboratory Astrophysics Community: Our Experience and Outlook*
4:45 Ara Chutjian, *Recent Excitation, Charge Exchange, and Lifetime Results in Highly Charged Ions Relevant to Stellar, Interstellar, Solar, and Comet Collision*
5:00 William Klemperer - Summary

5:30-7:00 Posters

APPENDIX A: AGENDA DAY 3

Thursday, February 16, 2006

9:00-12:00 Break-out Sessions
2:00-4:00 Summary Reports:
Atomic
Molecular
Dust and Ices
Solar System
Plenary Discussion
4:00-4:30 Final Remarks: Steve Federman and Hashima Hasan
4:30-6:30 SOC Executive Session
6:30 Adjourn Workshop

APPENDIX B: POSTER SESSION

The Poster Session will be held on the evenings of Tuesday, February 14 and Wednesday, February 15 following the afternoon sessions in the lobby (1st floor) of the Bigelow Physics Building. All posters will be on display for both evenings and a Reception will be held each evening in conjunction with the Poster Session.

Information for Presenters

Each poster is to be no larger than 4 x 4 ft (1.2 x 1.2 m). Each poster presenter is responsible for hanging and removing his/her own poster materials. Posters can be hung beginning at 8:00 AM on Tuesday and must be removed by 7:30 PM on Wednesday. Push pins and tape will be provided. Each poster has been assigned a code by topic area. To find the code assigned to your poster, find the last name of the submitting author of the abstract and the title as listed in the table below. Last names of submitting authors are sorted by alphabetical order. Code information will be displayed in the lobby of the Bigelow Physics Building to indicate the location for each poster.

O = Observation
M = Modeling
G = General
T = Theory/Calculation
D = Data
E = Experiments/Measurements

Submitting Author	Code	Title
Nigel Adams	E1	Laboratory Studies of the Stabilities of Heterocyclic Aromatic Molecules and Suggested Gas Phase Ion-Molecule Routes to their Production in Interstellar Gas Clouds, ISC
Alex Aguilar	E2	Visible to near infrared emission spectra of electron-excited H_2
Ashraf Ali	E3	Formation of Silicate Grains in Circumstellar Environments: Experiment, Theory and Observations
John Allen	E4	Low-Temperature Thermodynamic Properties of Some Light Hydrocarbons
Aldo Apponi	E5	Difficulties in Laboratory Studies and Astronomical Observations of Organic Molecules: Hydroxyacetone and Lactic Acid
James Babb	E6	Experimental and Theoretical Studies of Pressure Broadened Alkali-Metal Atom Resonance Lines
Richard Blackwell-Whitehead	E7	Accurate VUV laboratory measurements of Fe III transitions for astrophysical applications
Nancy Brickhouse	M1	Assessing the Requirements for Completeness and Accuracy of Atomic Data for X-ray Spectroscopy

Submitting Author	Code	Title
Eduardo Bringa	E8	Processing of Interstellar Silicate Grains by Cosmic Rays
Greg Brown	E9	Laboratory measurements of the electron impact excitation cross section of Fe XVII x-ray transitions
Paul Bryans	E10	Collisional Ionization Equilibrium for Optically Thin Plasmas
Hui Chen	E11	Excitation Cross Section Measurement for $n = 3$ to $n = 2$ Line Emission in Fe^{17+} to Fe^{23+}
Ara Chutjian	E12	Measurements of Polyatomic Molecule Formation on an Icy Grain Analog Using Fast Atoms
Philip Cosby	E13	Laboratory Measurements of Dissociative Recombination
Steven Federman	T1	Oscillator Strengths and Predissociation Widths for Rydberg Transitions in Carbon Monoxide
Steven Federman	E14	Lifetimes and Oscillator Strengths for Ultraviolet Transitions in P II, Cl II, and Cl III
Mike Fogle	E15	Electron-Impact Ionization of Be-like C, N, and O
Mike Fogle	E16	Dielectronic Recombination of C, N, and O Ions
Larry Gardner	E17	Measurements of Electron Impact Excitation Cross Sections at the Harvard-Smithsonian Center for Astrophysics
Tom Gorczyca	T2	Calculation of Atomic Data for NASA Missions
Ming Gu	E18	Laboratory Measurement and Theoretical Modeling of K-shell X-ray Lines from Inner-shell Excited and Ionized Ions of Oxygen
Ming Gu	E19	Laboratory Survey of Fe L-shell X-ray Emission Lines between 7 and 11 Å
Theodore Gull	O1	The Homunculus: a Unique Astrophysical Laboratory
Stephanie Hansen	E20	Laboratory astrophysics on the ASDEX-Upgrade tokamak: Measurements and analysis of O, F, and Ne spectra in the 8 - 20 Å region
Robert Hinde	T3	Fully-First-Principles Quantum Calculations of Helium-Broadened Metal Resonance Lines
Reggie Hudson	E21	Investigations into the Astrochemistry of H_2O_2, O_2, and O_3 in Ion-Irradiated Ices
David Huestis	G1	Critical Evaluation of Chemical Reaction Rates and Collision Cross Sections of Importance in the Earth's Upper Atmosphere and the Atmospheres of other Planets, Moons, and Comets
Victor Kwong	E22	Metastable State Populations in Laser Induced Plasmas
Stephen Lepp	T4	Astrochemistry in the Early Universe
Jaan Lepson	E23	Laboratory measurements of the line emission from mid-Z L-shell ions in the EUV
Chih-Yuan Lin	T5	Quenching of excited Na due to He collisions
Dragan Lukic	E24	Dielectronic Recombination In Active Galactic Nuclei
Steven Manson	T6	The Atomic and Ionic Data for Astrophysics (AIDA) Project at Georgia State University

Submitting Author	Code	Title
Balakrishnan Naduvalath	T7	The Effect of non-equilibrium kinetics on oxygen chemistry in the interstellar medium
Gillian Nave	E25	Atomic Oscillator Strengths in the Vacuum Ultraviolet
Joe Nuth	E26	Circumstellar Silicates Do Nucleate: New Vapor Pressure Data for SiO
John Pearson	E27	THz Spectroscopy and Spectroscopic Database for Astrophysics
Karly Pitman	O2	Challenging the Identification of Silicon Nitride Dust in Extreme Carbon Stars
Scott Porter	E28	Diagnostics of laboratory plasmas with the high resolution XRS instrument at the EBIT-I facility: a critical tool for understanding spectral signatures of x-ray emitting astrophysical sources
Joseph Reader	D1	Atomic Spectroscopic Databases at NIST
Young Rhee	E29	Quantum chemical characterization of dimeric polyaromatic hydrocarbons
Farid Salama	T8	Computational Spectroscopy of Polycyclic Aromatic Hydrocarbons In Support of Laboratory Astrophysics
Farid Salama	E30	Laboratory Spectroscopy of Large Carbon Molecules and Ions in support of Space Missions. A New Generation of Laboratory & Space Studies
Daniel Savin	M2	Cosmological Implications of the Uncertainty in Astrochemical Rate Coefficients
Brian Sharpee	O3	Studying Atomic Physics Using the Nighttime Atmosphere as a Laboratory
Darren Smillie	E31	New Measurements of Doubly Ionized Iron Group Spectra by Fourier Transform and Grating Spectroscopy
Phillip Stancil	T9	Collisional De-excitation of Molecular Hydrogen in the Interstellar Medium
Glenn Stark	E32	Molecular nitrogen photoabsorption cross sections and line widths in support of analyses of planetary atmospheres
Joseph Tan	E33	X-ray Spectroscopy of Neon-like Ions at the NIST EBIT Facility
Swaraj Tayal	T10	Cross Sections for Electron Impact Excitation of Astrophysically Abundant Atoms and Ions
Joshua Thomas	E34	Fluorescence Spectroscopy of Gas-phase Polycyclic Aromatic Hydrocarbons
Richard Thomas	E35	Intra-molecular interactions during the fragmentation of small systems
Brad Wargelin	E36	Charge Exchange Spectra of H-like and He-like Iron
Philippe Weck	T11	Metal Hydride and Alkali Halide Opacities in Extrasolar Giant Planets and Cool Stellar Atmospheres
Joseph Weingartner	E37	Photoelectric Emission from Dust Grains Exposed to Extreme Ultraviolet and X-ray Radiation

Submitting Author	Code	Title
Wolfgang Wiese	D2	New Critical Compilations of Atomic Transition Probabilities for Neutral and Singly Ionized Carbon, Nitrogen and Iron
Robert Wu	E38	EUV-VUV Photolysis of Molecular Ice Systems of Astronomical Interest
Robert Wu	E39	The Temperature-Dependent Photoabsorption Cross Section Measurements Program at the Space Sciences Center, USC
Benhui Yang	T12	Vibrational and rotational quenching of CO by collisions with H, He, and H_2
Libo Zhao	T13	Charge transfer between S^{2+} and He: A comparative study of quantal and semiclassical approaches
Lucy Ziurys	E40	Sub-millimeter Spectroscopy of Astrophysically Important Molecules
Bernard Zygelman	T14	Hydrogen Atom Collisions and Tomography of the Dark Age Universe
Ron Bieniek	PD[1]	Collisional relaxation of isotopic molecular hydrogen

[1]PD: Post-deadline submission

APPENDIX C: BREAK-OUT GROUPS

Group #1: Atomic Astrophysics - Chairs: Nancy Brickhouse & Daniel Savin
Group #2: Molecular Astrophysics - Chairs: Lucy Ziurys & Phillip Stancil
Group #3: Dust & Ices in Astrophysics - Chairs: Farid Salama & Joe Weingartner
Group #4: Solar System - Chair: Steve Federman

Group # 1	Group # 2	Group # 3	Group # 4
R. Blackwell-Whitehead	N. Adams	A. Ali	P. Beiersdorfer
N. Brickhouse	A. Aguilar	J. Allen	P. Crane
G. Brown	A. Apponi	R. Baragiola	S. Federman
P. Bryans	J. Babb	S. Charnley	P. Feldman
S. Cheng	P. Cosby	G. Fuchs	J. Lepson
A. Chutjian	M. Flory	P. Gerakines	K. Pitman
J. Cowan	A. Glassgold	E. Herbst	S. Wilde
M. Fogle	E. Herbst	D. Hudgins	
L. Gardner	R. Hinde	F. Huisken	
M. Gu	D. Jackson	F. Salama	
S. Hansen	R. Kaiser	J. Thomas	
H. Hasan	T. Lee	G. Vidali	
C. Howk	B. McCall	J. Weingartner	
H. Ji	J. Pearson	A. Witt	
K. Kirby	E. Roueff		
C. Kyriakides	D. Schultz		
J. Lawler	P. Stancil		
D. Lukic	R. Thomas		
S. Manson	L. Ziurys		
G. Nave			
K. Nielsen			
F. Paerels			
J. Reader			
D. Savin			
B. Sharpee			
I. Short			
R. Smith			
J. Tan			
S. Tayal			
W. Ward			
B. Wargelin			
W. Wiese			
Z. Yasin			
B. Zygelman			

APPENDIX D: PARTICIPANTS ROSTER

Nigel Adams
University of Georgia
Cedar Street
Athens, GA 30602
tel: 706-542-3722
fax: 706-542-9454
adams@chem.uga.edu

Alejandro Aguilar
Jet Propulsion Laboratory
Earth and Space Science Division 320
Pasadena, CA 91109
tel: 818-354-0120
fax: 818-354-9476
alex.aguilar@jpl.nasa.gov

Joseph Ajello
Jet Propulsion Laboratory
4800 Oak Grove Drive
Pasadena, CA 91109
tel: 818-354-2457
fax: 818-354-9476
jajello@mail.jpl.nasa.gov

Ashraf Ali
Goddard Space Flight Center
Astrochemistry Lab, Code 691
Greenbelt, MD 20771
tel: 301-286-1553
ashraf.ali@ssedmail.gsfc.nasa.gov

John Allen
Goddard Space Flight Center
Code 691
Greenbelt, MD 20771
301-286-5896
301-286-1683
john.e.allen@nasa.gov

Aldo Apponi
University of Arizona
Radio Astronomy Observatory
933 N. Cherry Ave.
Tucson, AZ 85721-0065
tel: 520-621-2553
fax: 520-621-5554
aapponi@as.arizona.edu

David Archer
University of Nevada, Las Vegas
Department of Physics
4505 Maryland Pkwy.
Las Vegas, NV 89154
tel: 702-895-4455
fax: 702-895-3847
dmadance@physics.unlv.edu

James Babb
Harvard-Smithsonian Center
for Astrophysics
60 Garden Street, MS 14
Cambridge, MA 2138
tel: 617-496-7612
fax: 617-496-7668
jbabb@cfa.harvard.edu

Raul Baragiola
University of Virginia
Thornton Hall, 351 McCormick Rd.
Charlottesville, VA 22904
tel: 434-982-2907
fax: 434-924-1353
raul@virginia.edu

Charles Beichman
Michelson Science Center
California Inst. of Technology/JPL

Pasadena, CA 91109
tel: 626-395-1996
fax: 626-397-7018
chas@ipac.caltech.edu

Peter Beiersdorfer
Lawrence Livermore National Laboratory
7000 East Ave., L-260
Livermore, CA 94550
tel: 925-423-3985
fax: 925-423-2302
beiersdorfer@llnl.gov

Ronald Bieniek
University of Missouri-Rolla
Physics Department
1870 Miner Circle
Rolla, MO 65409-0640
tel: 573-341-4781
fax: 573-341-4715
bieniek@umr.edu

Richard Blackwell-Whitehead
Imperial College
Blackett Laboratory
Prince Consort Road
London, England, UK W2 4DX
tel: 44-207-5948184
fax: 44-207-5947772
r.blackwell@imperial.ac.uk

Nancy Brickhouse
Harvard-Smithsonian Center
for Astrophysics
60 Garden St., MS 15
Cambridge, MA 2138
tel: 617-495-7438
fax: 617-495-7049
nbrickhouse@cfa.harvard.edu

Gregory Brown
Lawrence Livermore National Laboratory
7000 East Avenue
Livermore, CA 94550
tel: 925-422-6879
fax: 925-423-2302
gregbrown@llnl.gov

Paul Bryans
Columbia Astrophysics Laboratory
550 West 120th St.
New York, NY 10027
tel: 212-854-1449
fax: 212-854-8121
bryans@astro.columbia.edu

Anthony Calamai
Appalachian State University
Dept. of Physics and Astronomy
Boone, NC 28608
tel: 828-262-4956
fax: 828-262-2049
calamaiag@appstate.edu

Steven Charnley
SETI Institute/NASA Ames
Space Science and Astrobiology Division
MS 245-3
Moffett Field, CA 94035-1000
tel: 650-604-5910
fax: 650-604-6779
charnley@dusty.arc.nasa.gov

Hui Chen
Lawrence Livermore National Laboratory
7000 East Avenue
Livermore CA 94550
chenhui@llnl.gov

Song Cheng
University of Toledo
2801 West Bancroft Street

Toledo, OH 43606
tel: 419-530-4788
fax: 419-530-2723
scheng@physics.utoledo.edu

Ara Chutjian
Jet Propulsion Laboratory and California Institute of Technology
4800 Oak Grove Drive, MS 121-114
Pasadena, CA 91109-8099
tel: 818-354-7012
fax: 818-393-1899
ara.chutjian@jpl.nasa.gov

Philip Cosby
SRI International
Molecular Physics Laboratory
333 Ravenswood Ave.
Menlo Park, CA 94025
tel: 650-859-5128
fax: 650-859-6196
philip.cosby@sri.com

John Cowan
University of Oklahoma
440 W. Brooks
Norman, OK 73019
tel: 405-325-3961
fax: 405-325-7557
cowan@hhn.ou.edu

Philippe Crane
NASA Headquarters Washington, DC 20546-0001
tel: 202-358-0377
fax: 202-358-3097
Philippe.Crane@hq.nasa.gov

Steven Federman
University of Toledo
Dept. of Physics and Astronomy, MS 113
Toledo, OH 43606
tel: 419-530-2652
fax: 419-530-2723
steven.federman@utoledo.edu

Paul Feldman
Johns Hopkins University
Dept. of Physics and Astronomy
Baltimore, MD 21218
tel: 410-516-7339
fax: 410-516-5494
pdf@pha.jhu.edu

Michael Flory
University of Arizona,
Radio Astronomy Observatory
933 N. Cherry Ave.
Tucson, AZ 85721-0065
tel: 520-626-5256
fax: 520-621-5554
mflory@as.arizona.edu

Michael Fogle
Oak Ridge National Laboratory
Physics Division, Bldg. 6010, MS 6372
Oak Ridge, TN 37831
tel: 865-241-1479
fax: 865-574-1118
foglemr@ornl.gov

Guido Fuchs
Leiden Observatory
Niels Bohr Weg 2
Leiden, NL-2333 CA
Netherlands
tel: +31 71 257 8439
fax: +31 71 257 5819
fuchs@strw.leidenuniv.nl

Larry Gardner
Harvard-Smithsonian Center

for Astrophysics
60 Garden St., MS 50
Cambridge, MA 2138
tel: 617-495-7286
fax: 617-495-7455
lgardner@cfa.harvard.edu

Perry Gerakines
University of Alabama at Birmingham
Dept. of Physics
1300 University Blvd., Room CH 310
Birmingham, AL 35294-1170
tel: 205-934-8064
fax: 205-934-8042
gerak@uab.edu

Alfred Glassgold
University of California Berkeley
601 Campbell Hall
Berkeley, CA 94720
tel: 510-642-6708
fax: 510-642-3411
aglassgold@astron.berkeley.edu

William Goldstein
Lawrence Livermore National Laboratory
7000 East Avenue
Livermore, CA 94550
tel: 925-422-2515
fax: 925-423-9307
goldstein3@llnl.gov

Thomas Gorczyca
Western Michigan
Dept. of Physics
1903 West Michigan Ave.
Kalamazoo, MI 49008-5252
tel: 269-387-4913
fax: 269-387-4939
gorczyca@wmich.edu

Tom Greene
NASA Ames Research Center
MS 245-6
Moffett Field, CA 94035
tel: 650-604-5520
fax: 650-604-6779
tgreene@mail.arc.nasa.gov

Ming Gu
Stanford University
382 Via Pueblo Mall, Varian 334
Stanford, CA 94305
mfgu@stanford.edu
Stephanie Hansen
Lawrence Livermore National Laboratory
7000 East Avenue
Livermore, CA 94550
hansen50@llnl.gov

Hashima Hasan
NASA Headquarters
300 E St., SW
Washington, DC 20546
tel: 202-358-0692
fax: 202-358-3096
hhasan@nasa.gov

Eric Herbst
Ohio State University
Department of Physics
Columbus, OH 43210
tel: 614-292-6951
fax: 614-292-7557
herbst@mps.ohio-state.edu

Robert Hinde
University of Tennessee
Department of Chemistry
Knoxville, TN 37996
tel: 865-974-3141
fax: 865-974-3453

rhinde@utk.edu

Christopher Howk
University of Notre Dame
Department of Physics
225 Nieuwland Science Hall
Notre Dame, IN 46556
tel: 574-631-8594
fax: 574-631-5952
jhowk@nd.edu

Douglas Hudgins
NASA Headquarters
300 E St., SW
Washington, DC 20546
Douglas.M.Hudgins@nasa.gov

David Huestis
SRI International Molecular
Physics Laboratory
Menlo Park, CA 94025
tel: 650-859-3464
fax: 650-859-6196
david.huestis@sri.com

Friedrich Huisken
Friedrich-Schiller-Universitaet
Jena Institut fuer Festkoerperphysik
Helmholtzweg 3
Jena, Germany D-07743
tel: 03641/9-47354
fax: 03641/9-47308
friedrich.huisken@uni-jena.de

Douglas Jackson
University of Georgia
Cedar Street
Athens, GA 30602
tel: 706-542-3722
fax: 706-542-9454
kingly1@uga.edu

Hantao Ji
Princeton Plasma Physics Laboratory
P.O. Box 451
Princeton, NJ 08543
tel: 609-243-2162
fax: 609-243-2418
hji@princeton.edu

Ralf Kaiser
University of Hawaii
Department of Chemistry
2545 The Mall
Honolulu, GHI 96822
tel: 808-956-5731
fax: 808-956-5908
kaiser@gold.chem.hawaii.edu

Tim Kallman
NASA/GSFC
Code 662
Greenbelt, MD 20771
tel: 301-286-3680
fax: 301-286-1684
tim@xstar.gsfc.nasa.gov

Kate Kirby
Harvard-Smithsonian Center
for Astrophysics
60 Garden St.
Cambridge, MA 2138
tel: 617-495-7237
fax: 617-495-5970
kkirby@cfa.harvard.edu

William Klemperer
Harvard University
Department of Chemistry
12 Oxford Street
Cambridge, MA 2138
tel: 617-495-4094
klemperer@chemistry.harvard.edu

Victor Kwong
University of Nevada, Las Vegas
Department of Physics
4505 Maryland Pkwy.
Las Vegas, NV 89154
tel: 702-895-1700
fax: 702-895-3847
vhs@physics.unlv.edu

Chrysanthos Kyriakides
University of Nevada, Las Vegas
Department of Physics
4505 Maryland Pkwy.
Las Vegas, NV 89154
tel: 702-895-1890
fax: 702-895-3847
athos@physics.unlv.edu

James Lawler
University of Wisconsin
1150 University Avenue
Madison, WI 53705
tel: 608-262-2918
fax: 608-265-2334
jelawler@wisc.edu

Timothy Lee
NASA Ames Research Center
MS 245-6
Moffett Field, CA 94035
tel: 650-604-5208
fax: 650-604-6799
tjlee@mail.arc.nasa.gov

Stephen Lepp
University of Nevada, Las Vegas
Department of Physics
4505 Maryland Pkwy.
Las Vegas, NV 89154
tel: 702-895-4455
fax: 702-895-3847
lepp@physics.unlv.edu

Jaan Lepson
University of California
Space Sciences Laboratory
7 Gauss Way
Berkeley, CA 94720-7450
tel: 510-643-0794
fax: 510-642-0075
lepson@ssl.berkeley.edu

Chin-Yuan Lin
The University of Georgia
Department of Physics and Astronomy
and Center for Simulational Physics
Athens, GA 30602-2451
tel: 706-583-8225
fax: 706-542-2492
cylin@hal.physast.uga.edu

Dragan Lukic
Columbia Astrophysics Laboratory
550 West 120th St., Mail Code 5247
New York, NY 10027
tel: 212-854-1449
fax: 212-854-8121
lukic@astro.columbia.edu

Steven Manson
Georgia State University
Department of Physics and Astronomy
Atlanta, GA 30303
tel: 404-651-3082
fax: 404-651-1427
smanson@gsu.edu

Pamela Marcum
NASA Headquarters
300 E St., SW
Washington, DC 20546
Pamela.M.Marcum@nasa.gov

Benjamin McCall
University of Illinois at Urbana-Champaign
Departments of Chemistry and Astronomy
600 S. Mathews Ave.
Urbana, IL 61801
tel: 217-244-0230
fax: 217-244-3186
bjmccall@uiuc.edu

Balakrishnan Naduvalath
University of Nevada, Las Vegas
Department of Chemistry
4505 Maryland Pkwy.
Las Vegas, NV 89154
tel: 702-895-2907
fax: 702-895-4072
naduvala@unlv.nevada.edu

Gillian Nave
National Institute of Standards
and Technology
100 Bureau Drive
Gaithersburg, MD 20899-8422
tel: 301-975-4311
fax: 301-975-3038 gnave@nist.gov

Krister Nielsen
The Catholic University of America/GSFC
Washington, DC 20064
tel: 301-286-4533
fax: 301-286-1752
nielsen@milkyway.gsfc.nasa.gov

Frits Paerels
Columbia University
Columbia Astrophysics Laboratory
550 West 120th St.
New York, NY 10027
tel: 212-854-0181
fax: 212-854-8121
frits@astro.columbia.edu

John Pearson
NASA/JPL
4800 Oak Grove Drive, MS 301-429
Pasadena, CA 91109-8099
tel: 818-354-6822
fax: 818-393-6984
John.C.Pearson@jpl.nasa.gov

Karly Pitman
Washington University, St. Louis
Dept. of Earth and Planetary Science
Campus Box 1169, One Brookings Dr.
St. Louis, MO 63130-4862
tel: 314-935-5021
fax: 314-935-5610
kpitman@levee.wustl.edu

Daniel Proga
University of Nevada Las Vegas
Department of Physics
4505 Maryland Pkwy, Box 454002
Las Vegas, NV 89154-4002
tel: 702-895-3507
fax: 702-895-0804
dproga@physics.unlv.edu

Joseph Reader
National Institute of Standards
and Technology
100 Bureau Drive, MS 8422
Gaithersburg, MD 20899
tel: 301-975-3222
fax: 301-975-3038
joseph.reader@nist.gov

Young Rhee
University of California Berkeley
Department of Chemistry
Berkeley, CA 94720
tel: 510-642-9304
ymrhee@berkeley.edu

Evelyne Roueff
Observatoire de Paris
Place J. Janssen
Meudon, France 92190
tel: 33-1-45077435
fax: 33-1-45077123
evelyne.roueff@obspm.fr

Farid Salama
NASA Ames Research Center
MS 245-6
Moffett Field, CA 94035
tel: 650-604-3384
Farid.Salama@nasa.gov

Wilton Sanders
NASA Headquarters
300 E St., SW
Washington, DC 20546
tel: 202-358-1319
fax: 202-358-3096
wsanders@hq.nasa.gov

Daniel Savin
Columbia Astrophysics Laboratory
550 W. 120th St., MC 5247
New York, NY 10027
tel: 212-854-4124
fax: 212-854-8121
savin@astro.columbia.edu

David Schultz
Oak Ridge National Laboratory
Physics Division
MS 6372, Bldg. 6000
Oak Ridge, TN 37831-6372
tel: 865-576-9461
schultzd@ornl.gov

Brian Sharpee
SRI International Molecular
Physics Laboratory
333 Ravenswood Ave.
Menlo Park, CA 94025
tel: 650-859-2975
fax: 650-859-6196
brian.sharpee@sri.com

David Shelton
University of Nevada Las Vegas
Department of Physics
4505 Maryland Pkwy, Box 454002
Las Vegas, NV 89154-4002
tel: 702-895-3564
fax: 702-895-0804
shelton@physics.unlv.edu

Francois Shindo
Smithsonian Harvard Observatory
60 Garden St., MS 14
Cambridge, MA 2138
tel: 617-495-7386
fax: 617-496-7668
fshindo@cfa.harvard.edu

Ian Short
Saint Mary's University
Mc Nally Main 301A
Halifax, Nova Scotia, Canada
tel: 902-496-8194
fax: 902-496-8218
ishort@ap.stmarys.ca

Randall Smith
JHU and NASA/GSFC
Code 662, NASA/GSFC
Greenbelt, MD 20771
tel: 301-286-1155
fax: 301-286-1684
rsmith@milkyway.gsfc.nasa.gov

Phillip Stancil

University of Georgia
Department of Physics and Astronomy
Athens, GA 30602-2451
tel: 706-583-8226
fax: 706-542-2492
stancil@physast.uga.edu

Glenn Stark
Wellesley College
106 Central Street
Wellesley, MA 2481
tel: 781-283-3156
gstark@wellesley.edu

Joseph Tan
National Institute of Standards
and Technology
100 Bureau Drive, Mail Stop 8421
Gaithersburg, MD 20899-8421
tel: 301-975-8985
fax: 301-975-5485
joseph.tan@nist.gov

Swaraj Tayal
Clark Atlanta University
223 James P. Brawley S.W.
Atlanta, GA 30314
tel: 404-880-6877
fax: 404-880-6258
stayal@cau.edu

Joshua Thomas
University of Toledo
2801 West Bancroft Street
Toledo, OH 43606
tel: 419-530-2050
jthomas@physics.utoledo.edu

Richard Thomas
Stockholm University
Molecular Physics AlabNova
University Center, Fysikum
Stockholm, Sweden SE106 91
tel: 46-8-55378487
fax: 46-8-55378601
rdt@physto.se

Xander Tielens
NASA Ames Research Center
MS 245-3
Moffett Field, CA 94035-1000
tel: 650-604-2016
fax: 650-604-6779
atielens@mail.arc.nasa.gov

Todd Tripp
UMass Amherst
Department of Astronomy
710 N. Pleasant St.
Amherst, MA 01003-9305
tel: 413-545-3070
fax: 413-545-4223
tripp@fcrao1.astro.umass.edu

Zlatan Tsvetanov
NASA Headquarters 300 E St., SW
Washington, DC 20546
tel: 202-358-0810
fax: 202-358-3096
zlatan.tsvetanov@nasa.gov

Willem van Breugel
Lawrence Livermore National Laboratory
7000 East Avenue
Livermore, CA 94450
wil@igpp.llnl.gov

Gianfranco Vidali
Syracuse University
337 Tecumseh Rd.
Syracuse, NY 13224
tel: 315-443-9115

gvidali@syr.edu

Wayne Ward
University of Nevada, Las Vegas
Department of Physics
4505 Maryland Pkwy.
Las Vegas, NV 89154
tel: 702-895-1890
fax: 702-895-3847
wward@physics.unlv.edu

Bradford Wargelin
Harvard-Smithsonian Center
for Astrophysics
60 Garden St., MS 70
Cambridge, MA 2138
tel: 617-496-7702
fax: 617-495-7356
bwargelin@cfa.harvard.edu

Philippe Weck
University of Nevada, Las Vegas
Department of Chemistry
4505 Maryland Pkwy.
Las Vegas, NV 89154
tel: 702-895-1710
fax: 702-895-4072
weckp@unlv.nevada.edu

Joseph Weingartner
George Mason University
Department of Physics and Astronomy
4400 University Drive, MSN 3F3
Fairfax, VA 22030
tel: 703-993-4596
fax: 703-993-1269
joe@physics.gmu.edu

Wolfgang Wiese
National Institute of Standards
and Technology
100 Bureau Drive
Gaithersburg, MD 20899-8420
tel: 301-975-3201
fax: 301-990-1350
wiese@nist.gov

Eric Wilson
Jet Propulsion Laboratory
4800 Oak Grove Drive
MS 169-237
Pasadena, CA 91109
tel: 818-354-9971
fax: 818-393-4619
Eric.Wilson@jpl.nasa.gov

Adolf Witt
University of Toledo
2801 West Bancroft Street
Toledo, OH 43606
tel: 419-530-2709
fax: 419-530-2723
awitt@dusty.astro.utoledo.edu

Neville Woolf
University of Arizona
Department of Astronomy and
Steward Observatory
Steward N440
tel: 520-621-3234
fax: 520-621-1532
nwoolf@as.arizona.edu

Robert Wu
University of Southern California
Space Sciences Laboratory, SHS 274
Los Angeles, CA 90089-1341
tel: 213-740-6332
fax: 213-740-6342
robertwu@usc.edu

Benhui Yang

University of Georgia
1055 Baxter St.
Athens, GA 30606
tel: 706-583-8225
fax: 706-542-2492
yang@physast.uga.edu

Zafar Yasin
University of California Riverside
Department of Physics
Riverside, CA
zafar.yasin@email.ucr.edu

Libo Zhao
University of Georgia
Department of Physics & Astronomy
Athens, GA 30602-2451
zhao@physast.uga.edu

Lucy Ziurys
University of Arizona
Radio Astronomy Observatory
933 N. Cherry Ave.
Tucson, AZ 85721-0065
tel: 520-626-8202
fax: 520-621-5554
lziurys@as.arizona.edu

Bernard Zygelman
University of Nevada, Las Vegas
Department of Physics
4505 Maryland Pkwy.
Las Vegas, NV 89154
tel: 702-895-1321
fax: 702-895-3847
bernard@physics.unlv.edu

APPENDIX E: SOC ROSTER

Nancy Brickhouse
Harvard-Smithsonian Center for Astrophysics
60 Garden St., MS 15
Cambridge, MA 2138
tel: 617-495-7438
fax: 617-495-7049
nbrickhouse@cfa.harvard.edu

Steven Federman
University of Toledo
Dept. of Physics & Astronomy, MS 113
Toledo, OH 43606
tel: 419-530-2652
fax: 419-530-2723
steven.federman@utoledo.edu

Victor Kwong
University of Nevada, Las Vegas
Department of Physics
4505 Maryland Pkwy.
Las Vegas, NV 89154
tel: 702-895-1700
fax: 702-895-3847
vhs@physics.unlv.edu

Farid Salama
NASA Ames Research Center
MS 245-6
Moffett Field, CA 94035
tel: 650-604-3384
Farid.Salama@nasa.gov

Daniel Savin
Columbia Astrophysics Laboratory
550 W. 120th St., MC 5247
New York, NY 10027
tel: 212-854-4124
fax: 212-854-8121
savin@astro.columbia.edu

Phillip Stancil
University of Georgia
Department of Physics and Astronomy
Athens, GA 30602-2451
tel: 706-583-8226
fax: 706-542-2492
stancil@physast.uga.edu

Joseph Weingartner
George Mason University
Department of Physics and Astronomy
4400 University Drive, MSN 3F3
Fairfax, VA 22030
tel: 703-993-4596
fax: 703-993-1269
joe@physics.gmu.edu

Lucy Ziurys
University of Arizona
Radio Astronomy Observatory
933 N. Cherry Ave.
Tucson, AZ 85721-0065
tel: 520-626-8202
fax: 520-621-5554
lziurys@as.arizona.edu

APPENDIX F: AUTHOR INDEX

REPORT DOCUMENTATION PAGE

Form Approved
OMB No. 0704-0188

1. REPORT DATE *(DD-MM-YYYY)*	2. REPORT TYPE	3. DATES COVERED *(From - To)*
31-08-2006	Conference Proceedings	

4. TITLE AND SUBTITLE
Proceedings of the 2006 NASA Laboratory Astrophysics Workshop

5a. CONTRACT NUMBER

5b. GRANT NUMBER
NNG06GB72G

5c. PROGRAM ELEMENT NUMBER

6. AUTHOR(S)
Philippe Weck, Victor Kwong, Farid Salama, Editors

5d. PROJECT NUMBER

5e. TASK NUMBER

5f. WORK UNIT NUMBER

7. PERFORMING ORGANIZATION NAME(S) AND ADDRESS(ES)

Ames Research Center
Moffett Field CA 94035-1000

8. PERFORMING ORGANIZATION REPORT NUMBER
A-0600013

9. SPONSORING/MONITORING AGENCY NAME(S) AND ADDRESS(ES)

National Aeronautics and Space Administration
Washington, D.C. 20546-0001

10. SPONSORING/MONITOR'S ACRONYM(S)
NASA

11. SPONSORING/MONITORING REPORT NUMBER
NASA/CP-2006-214549

12. DISTRIBUTION/AVAILABILITY STATEMENT
Unclassified-Unlimited Distribution: Standard
Subject Category 88
Availability: NASA CASI (301)

13. SUPPLEMENTARY NOTES

Point Of Contact: Dr. Farid Salama, Ames Research Center, MS: 245-6, Moffett Field, California 94035-1000

14. ABSTRACT

This document is the proceedings of the NASA Laboratory Astrophysics Workshop, convened February 14-16, 2006 at the University of Nevada, Las Vegas (UNLV). Sponsored by the Astrophysics Division of the NASA Science Mission Directorate (SMD), this programmatic workshop is held periodically by NASA to discuss the current state of knowledge in the interdisciplinary field of laboratory astrophysics and to identify the science priorities ('needs') in support of NASA's space missions. An important role of the workshop is to provide input to NASA SMD in the form of a white paper for incorporation in its strategic planning. This report comprises a record of the complete proceedings of the workshop and the NASA Laboratory Astrophysics White paper drafted at the workshop.

15. SUBJECT TERMS

Laboratory Astrophysics; White Paper

16. SECURITY CLASSIFICATION OF:			17. LIMITATION OF ABSTRACT	18. NUMBER OF PAGES	19b. NAME OF RESPONSIBLE PERSON
a. REPORT	b. ABSTRACT	c. THIS PAGE			Dr. Farid Salama
					19b. TELEPHONE NUMBER *(Include area code)*
Uncl.	Uncl.	Uncl.	Uncl.	338	(650) 604-3384